PUSHOVER ANALYSIS FOR SEISMIC ASSESSMENT AND DESIGN OF STRUCTURES

SPYRIDON THEMELIS

A dissertation submitted for the partial fulfilment of the requirements for the degree of Doctor of Philosophy

HERIOT-WATT UNIVERSITY
School of the Built Environment
October 2008

ABSTRACT

The earthquake resistant design of structures requires that structures should sustain, safely, any ground motions of an intensity that might occur during their construction or in their normal use. However ground motions are unique in the effects they have on structural responses. The most accurate analysis procedure for structures subjected to strong ground motions is the time-history analysis. This analysis involves the integration of the equations of motion of a multi-degree-of-freedom system, MDOF, in the time domain using a stepwise solution in order to represent the actual response of a structure. This method is time-consuming though for application in all practical purposes. The necessity for faster methods that would ensure a reliable structural assessment or design of structures subjected to seismic loading led to the pushover analysis.

Pushover analysis is based on the assumption that structures oscillate predominantly in the first mode or in the lower modes of vibration during a seismic event. This leads to a reduction of the multi-degree-of-freedom, MDOF system, to an equivalent single-degree-of-freedom, ESDOF system, with properties predicted by a nonlinear static analysis of the MDOF system. The ESDOF system is then subsequently subjected to a nonlinear time-history analysis or to a response spectrum analysis with constant-ductility spectra, or damped spectra. The seismic demands calculated for the ESDOF system are transformed through modal relationships to the seismic demands of the MDOF system.

In this study the applicability of the pushover method as an alternative mean to general design and assessment is examined. Initially a series of SDOF systems is subjected to two different pushover methods and to nonlinear-time-history analyses. The results from this study show that pushover analysis is not able to capture the seismic demands imposed by far-field or near-fault ground motions, especially for short-period systems for which it can lead to significant errors in the estimation of the seismic demands. In the case of near-fault ground motions the results suggest that pushover analysis may underestimate the displacement demands for systems with periods lower than half the dominant pulse period of the ground motion and overestimate them for systems with periods equal or higher than half the dominant pulse period of the ground motion. Subsequently a two-degree-of-

freedom, 2-DOF, is studied in the same manner with specific intention to assess the accuracy of the different load patterns proposed in the literature. For this system pushover analysis performed similarly as in the SDOF study. Finally the method is applied on a four-storey reinforced concrete frame structure. For this study pushover analysis was not effective in capturing the seismic demands imposed by both a far-field and a near-fault ground motion. Overall pushover analysis can be unconservative in estimating seismic demands of structures and it may lead to unsafe design.

ACKNOWLEDGEMENTS

I would like to express my gratitude to my supervisor Professor Ian M May for believing in me and for providing me with invaluable advice throughout the duration of this research. I am also thankful to him for his patient and constructive reviews of the thesis.

I would also like to thank Dr Omar Lagrouche and Dr. James Balfour for their advice and stimulating discussions, technical or not, throughout this period.

This thesis would not have been possible to produce without the support of my parents, Dimitris and Pagona, and my sister, Eleni. I owe very much to them, in fact everything. This thesis is fully dedicated to them.

Finally I would like to express my sincerest thanks to Monica Del Campo, and to all my friends for their encouragement, belief in me and for their good spirit. Special thanks go to Amin Abdulmajid, Meysam Banihmad, Vivienne Dell, Laura Pronk, Nikos and Iro Tsourti. You all deserve the best!

To

Dimitris, Pagona, Eleni

TABLE OF CONTENTS

LIST OF FIGURES

LIST OF TABLES

NONMECLATURE

[M]	mass matrix of MDOF system
[C]	damping matrix of MDOF system
{F}	storey force vector of MDOF system
$\ddot{u}_g$	ground acceleration history
$\{\ddot{U}\}$	relative acceleration vector of MDOF system
$\{\dot{U}\}$	relative velocity vector of MDOF system
{1}	influence vector
{Φ}	mode shape vector
ϕ_n	mode shape at the roof
ϕ_i	mode shape at the i^{th} -storey
U	relative displacement vector of MDOF system
u_t	roof/top displacement of MDOF
$\ddot{u}_t$	relative acceleration of roof
$\dot{u}_t$	relative velocity of roof
u^*	reference displacement of ESDOF system
$\ddot{u}^*$	reference acceleration of ESDOF system
$\dot{u}^*$	reference velocity of ESDOF system
M^*	mass of ESDOF system
C^*	damping of ESDOF system
F^*	force relationship of ESDOF system
V_b	base shear of MDOF system
V_y	yield strength of MDOF
K_e	effective elastic stiffness of MDOF
u_y	yield displacement of MDOF system
K_s	hardening/softening stiffness
α	strain-hardening ratio
T_{eq}	elastic period of ESDOF system
K^*	elastic stiffness of ESDOF system

F_y^*	yield force of ESDOF system
u_y^*	yield displacement of ESDOF system
i	storey number
j	mode number
POA	pushover analysis
MPA	modal pushover analysis
CSM	capacity spectrum method
DCM	displacement coefficient method
ADRS	acceleration-displacement spectra
AMP	adaptive modal pushover analysis
AMC	adaptive modal combination procedure
F_i	applied force at i^{th} storey
W_i	weight of i^{th} storey
ϕ_{ij}	i^{th} storey element of the mode shape vector for mode j
h_i	height of the i^{th} storey
n	total number of modes, total number of storeys
$S_d(T_n)$	acceleration ordinate of the design spectrum at the fundamental period T_n
T_n	fundamental period of vibration
W	weight of structure
k	coefficient dependent on the fundamental period T_n
a_{mr}	modification factor in Kunnath load pattern
Γ_j	participation factor for mode j
M_i	mass of the i^{th}-storey
$S_a(\zeta_j, T_j)$	spectral acceleration for a given earthquake at period T and damping ratio ζ for mode j
H	height of building
η	characteristic parameter for different types of buildings
x	distance from ground to floor
k	increment number

k	stiffness of SDOF system
ΔF_i	incremental load
ΔV_b	incremental base shear
$\varphi_{i,j}$	mass-normalised mode shape of i^{th} storey for j^{th} mode
V_{pi},	initial base shear estimate at maximum displacement
u_{pi}	initial maximum displacement estimate
A_1, A_2	areas
S_a	spectral acceleration of inelastic ESDOF
S_d	spectral displacement of inelastic ESDOF
ζ	damping ratio
PF_1	participation factor in CSM method
α_m	modal mass coefficient
M	total mass of structure
a_{pi}	initial performance acceleration of ESDOF for CSM method
d_{pi}	initial performance point of ESDOF for CSM method
α_y	yield acceleration of SDOF
d_y	yield displacement of SDOF for CSM method
β_{eq}	equivalent viscous damping of inelastic ESDOF system
β_o	equivalent viscous damping due to hysteresis
E_D	energy dissipated by damping
E_{So}	elastic strain energy
R_μ	strength reduction factor
S_{ae}	pseudo-acceleration ordinate from the response spectrum
S_v	pseudo-velocity ordinate from the response spectrum
S_{de}	elastic displacement ordinate from the response spectrum
S_d	target displacement of ESDOF from N2 method
S_{ay}	yield acceleration from the capacity spectrum
T_c	characteristic period of the ground motion
T	period of vibration
C_0	modification factor to relate the SDOF spectral

	displacement to MDOF roof displacement
C_1	modification factor to relate the expected maximum inelastic SDOF displacement divided by the elastic SDOF displacement
C_2	modification factor to represent the effect of hysteresis shape on the maximum displacement response
C_3	modification factor to represent increased displacements due to second-order effects
T_e	effective fundamental period
R	ratio of inelastic strength demand to calculated yield strength coefficient
μ	ductility factor
s_j	lateral force distribution for mode j
M_j^*	effective modal mass of j^{th}-mode SDOF system
V_{bjy}	yield base shear of the MDOF system for mode j
F_{sjy}	yield force of j^{th}-mode ESDOF system
u_{tjy}	MDOF roof displacement of j^{th}-mode
φ_{rj}	j^{th} – mode shape value at the roof
D_{jy}	yield deformation for the j^{th} – mode inelastic SDOF
D_j	peak deformation for the j^{th} – mode inelastic SDOF
V_j	modal base shear
r_{MPA}	total response demand
r_j	peak 'modal' response of mode j
F_{ij}	lateral storey force at the i^{th} level for the j^{th} mode
S_n	scaling factor
$\overline{V}_j$	scaled modal base shear
N_s	number of uniform steps
V_B	base shear estimate
$\overline{\phi}_i$	equivalent fundamental mode

v	initial velocity profile
du	incremental displacement du
dE	incremental energy
δ	reference displacement of MDOF model
$\Delta\delta^*$	incremental displacement of MDOF model
EPP	elastic-perfectly-plastic SDOF
EPSH	elastoplastic with strain hardening SDOF
δ_{inel}	inelastic displacement demand of SDOF systems
δ_{el}	elastic displacement demand of SDOF systems
T_p	predominant period of the ground motion
T_m	mean period of the ground motion
C_i	Fourier amplitudes
f_i	discrete Fourier Transform frequency
E_H	hysteretic energy
ω_n	natural frequency
m	mass of SDOF system
c	viscous damping constant of SDOF system
$f_s(u,\dot{u})$	resisting force relationship of an elastoplastic SDOF system
y(t)	acceleration signal of an earthquake
$F(\overline{\omega})$	Fourier amplitude spectrum
$\overline{\omega}$	circular frequency of excitation force
f_y	yield force of SDOF system
$\bar{f}_y$	normalised yield strength of an elastoplastic SDOF system
$\tilde{f}_s(\mu,\dot{\mu})$	force-deformation relationship in dimensionless form
f_e	elastic strength of linear SDOF system
u_e	elastic displacement of linear SDOF system

CHAPTER 1
INTRODUCTION

1.1 INTRODUCTION

The seismic assessment and design of structures is required because of the occurrence of earthquakes. Earthquakes are caused by differential movements of the earth's crust (Kramer 1996). The result of these movements is the well known 'ground shaking' that can lead to significant damage and/or collapse of buildings, infrastructure systems (e.g. dams, roads, bridges, viaducts etc), landslides, when soil slopes loose their cohesion, liquefaction in sand and destructive waves or 'tsunamis' in the maritime environments.

The aforementioned actions have called for the development of design and/or assessment procedures in order to quantify the damage to both structural elements and the entire structure, and also to reduce any loss of life. Seismic assessment is also important for designing retrofit schemes for the strengthening and repair of existing structures.

Bertero *et al.* (1997) discussed from a macroscopic point of view the factors and problems involved in the earthquake-resistant design of structures. The same difficulties apply to seismic assessment. These are illustrated in Figure 1.1, where X1 represents the problem associated with the accurate estimation of base rock motion, X2 represents the problem associated with the correct evaluation of motion transmission from the rock base to the free ground surface, X3 represents the problem of accurately estimating the ground motion at the foundation of the building and X4 is the problem associated with the estimation of the deformation of the top storey of the structure. The parameters A, I, and D represent respectively an attenuation or amplification factor, a factor that relates the interaction between the soil and the structure and a dynamic operator that predicts the top displacement from the foundation displacement. The estimation of these factors has proven to be very difficult in the sense that there exist large uncertainties in their estimation, Bertero *et al.* (1997).

The above qualitative approach shows that those involved with seismic assessment and design practices have realised and rationalised the problems that surround it. However destructive earthquakes such as the 1995 Hyogo-ken-Nanbu earthquake in Japan, the 1999 Kocaeli earthquake in Turkey, and the 2005 Kashmir earthquake in Pakistan have shown that there is still much to do to ensure better practice in the earthquake-resistant design and assessment of structures.

A recent approach to tackle the design and/or assessment problems mentioned above that has been introduced is performance-based earthquake engineering. In brief, performance-based engineering deals with the estimation of quantities such as seismic capacity and seismic demands for different performance levels of the structure. Further details on this approach will be presented in Chapter 2. Generally, the methods available to the design engineer to calculate seismic demands are either dynamic time history analyses or pushover analyses.

Dynamic time history analysis requires as much as possible detailed mathematical models of multi-degree-of-freedom systems, MDOF, i.e. structures, together with information on ground motion characteristics, rendering it quite impractical for everyday use, especially when overly complex structures need to be considered. Additionally the response derived from such an analysis is generally very sensitive to the characteristics of the ground motions as well as the material models used.

A simpler option to assess the performance of structures is pushover analysis or simplified nonlinear static analysis, even though this also requires as much as possible detailed mathematical models of MDOF systems. The method's applicability is increasing continuously in practice because of its relative simplicity. This method assumes that the response of a structure can be predicted by the first, or the first few modes of vibration, which remain constant throughout its response time. It involves the incremental application of loading that follows some predetermined pattern, until the failure modes of the structure can be identified, thus producing a force-displacement relationship or capacity curve, which gives a clear indication of the nonlinear response. The resulting displacement demands from the preceding analysis are then checked and the structural performance of the elements is assessed.

Although the method in relation to a time-history analysis manages to calculate important seismic demands faster, the concepts it adopts lack a strong theoretical background and therefore produce approximate results. Therefore further research is needed to assess its true potential as a general design and assessment tool.

1.2 SUMMARY

The major objective of this thesis is to provide a description of the various pushover analysis methods and assess their efficiency on a number of structural systems.

In Chapter 2 the application of pushover analysis to steel and reinforced concrete buildings as part of performance-based earthquake engineering is explained. The theoretical background of the method is given and a description of the different pushover approaches is presented. The conclusions drawn from the findings of previous researchers are summarised.

Chapter 3 describes and discusses the ground motions used in the research described in this thesis. Fourier spectrum analyses are carried out for each of the ground motions. A description of the elastic and inelastic response spectra calculated using Seismosoft - Seismosignal, (2004), is presented and some implications of the individual ground motions are discussed with an emphasis on strength reduction factors and normalized displacement demands.

In Chapter 4, results from pushover analyses on single, and two-degree-of-freedom systems, SDOF and 2-DOF, are described through a deterministic approach, in order to assess the method's potential within a strict theoretical basis. The results from the pushover analyses are compared to the 'exact' results derived from nonlinear dynamic analyses.

In Chapter 5, a four-storey reinforced concrete frame structure designed according to EC8 is studied. A series of pushover analyses and nonlinear dynamic analyses are carried out

and the important seismic demands derived from both approaches are compared. Some recommendations for the Eurocode are included.

In Chapter 6, general conclusions are drawn regarding the overall results from all chapters. Some recommendations for future research are also provided.

Appendix A reminds the reader on the theoretical background for computing constant-ductility spectra, as presented in Chopra 2005.

Appendix B presents the nonlinear time-history analysis results from the SDOF study. These are the displacement time-histories, the force-displacement responses, and the energy time-histories.

Appendix C illustrates a detailed example of the application of pushover analysis to a SDOF system.

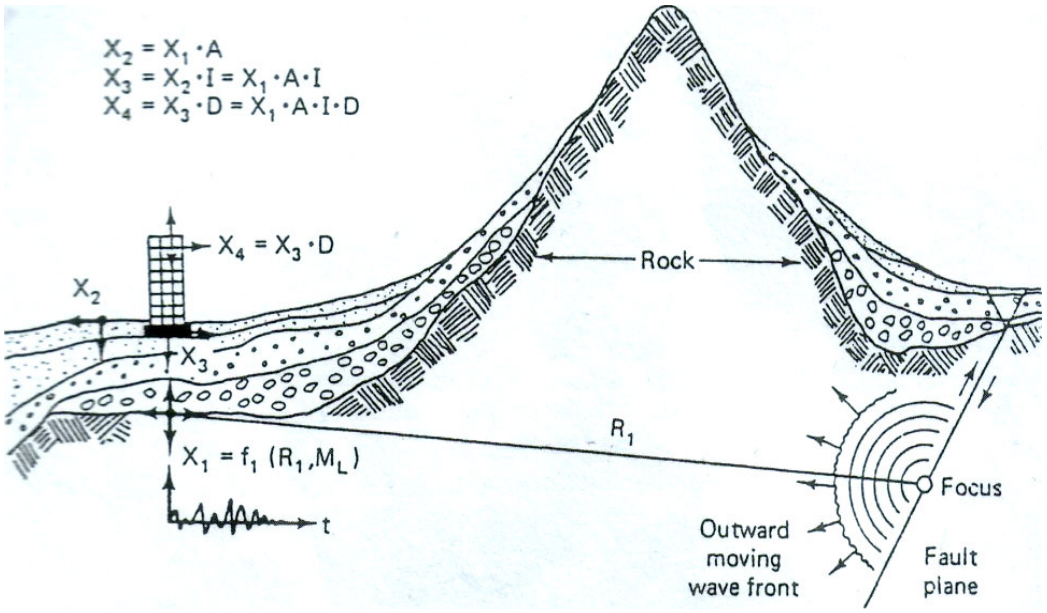

Figure 1-1 General problems and factors involved in the earthquake-resistant design of structures (taken from Bertero *et al.* 1997)

CHAPTER 2
PUSHOVER ANALYSIS IN THE SEISMIC ASSESSMENT AND DESIGN OF STRUCTURES – A REVIEW

2.1 INTRODUCTION

Earthquake engineering is a sector of civil engineering that deals with the mitigation of earthquake-induced damage on structures and the minimization of loss of life. During the last forty years this sector has advanced considerably due to the rapid developments of computers and computing, the improved experimental facilities, and the development of new methods of seismic design and assessment of structures. This advancement though has not been enough to resist the catastrophic consequences that earthquakes impose. However, it has led to some improvement of design and assessment procedures with a shift from traditional force-based procedures to displacement-based procedures (Antoniou 2002), as inelastic displacements have been deemed to be more representative of different structural performance levels. However it is still difficult to physically 'separate' these procedures since forces and displacements are strongly related to each other. Nevertheless, the characterization of the various performance levels has led to performance-based earthquake engineering; the most recent path of seismic design and assessment.

This Chapter provides a short description of the nature of performance-based earthquake engineering and its goals in seismic assessment and design. The procedures that are recommended for seismic design and assessment purposes are briefly described and their shortcomings are addressed. The theoretical background of the nonlinear static 'pushover' analysis method, POA, is then described together with the various pushover analysis procedures. Finally, a review of the state-of-the-art of research on pushover analysis is presented together with general conclusions on the efficiency of the method derived from the literature.

2.2 PERFORMANCE-BASED EARTHQUAKE ENGINEERING

Performance-based earthquake engineering practice arose from the realisation that the problems in the seismic behaviour of structures had to do with the approach of designing them explicitly for life safety, Table 2.1, thus not attempting to reduce damage in a structure, and minimise economic losses. The Structural Engineers Association of California, SEAOC Vision 2000 (1995) and the US National Earthquake Hazard Reduction Program Guidelines NEHRP (1997) recommended a different approach. It was suggested that performance goals should be defined in order to account for all the three previously mentioned factors, Table 2.1: structural damage, loss of life and economic losses. Table 2.1 shows that there has been an attempt to define in a clear manner the performance objectives.

The Vision 2000 document suggests that buildings should be constructed, based on their intended use, to meet the performance objectives shown in Figure 2.1. In the figure, each combination of an earthquake return period and performance level, indicated by a red diamond, represents a specific design performance objective (Hamburger, 1997). For example ordinary buildings should be constructed so that frequent earthquakes do not render them non-functional and or do not cause damage that needs extensive repairs. Essential buildings should be designed such as to avoid damage that will not permit their use, while hazardous facilities should be able to resist even earthquakes of low probability of occurrence and still be fully operational. These performance levels are in contrast to the approach taken by current building code provisions, wherein a single performance evaluation is required, for the Life Safety performance level at a specified level of ground motion, termed the Design Basis Earthquake (Hamburger, 1997).

EC8 (2003) and the International Workshop on Performance-Based Seismic Design Concepts and their Implementation, (Fajfar and Krawinkler, 2004), have shown that performance-based seismic methodology has started gaining ground in Europe. The different performance levels are shown in Figure 2.2 as adapted from Fajfar *et al.* (2004).

Performance Level		Description
NEHRP Guidelines	Vision 2000	
Operational	Fully Functional	No significant damage has occurred to structural and non-structural components. Building is suitable for normal intended occupancy and use.
Immediate Occupancy	Operational	No significant damage has occurred to structure, which retains nearly all its pre-earthquake strength and stiffness. Nonstructural elements are secure and most would function, if utilities were available. Building may be used for intended purpose, albeit in an impaired mode.
Life Safety	Life Safe	Significant damage to structural elements with substantial reduction in stiffness, however margin remains against collapse. Nonstructural elements are secured but may not function. Occupancy may be prevented until repairs can be instituted.
Collapse Prevention	Near Collapse	Substantial structural and nonstructural damage. Structural strength and stiffness substantially degraded. Little margin against collapse. Some falling debris hazards may have occurred.

Table 2-1Structural performance levels definition (taken from Antoniou 2002)

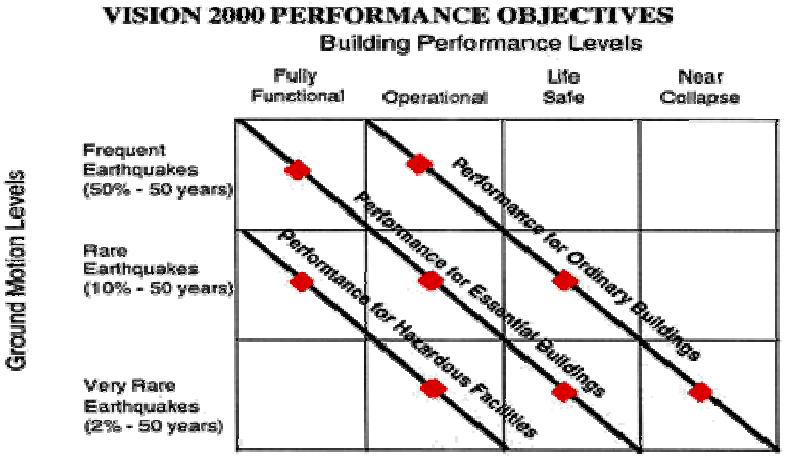

Figure 2-1 Vision 2000 Performance objectives (taken from Hamburger, 1997)

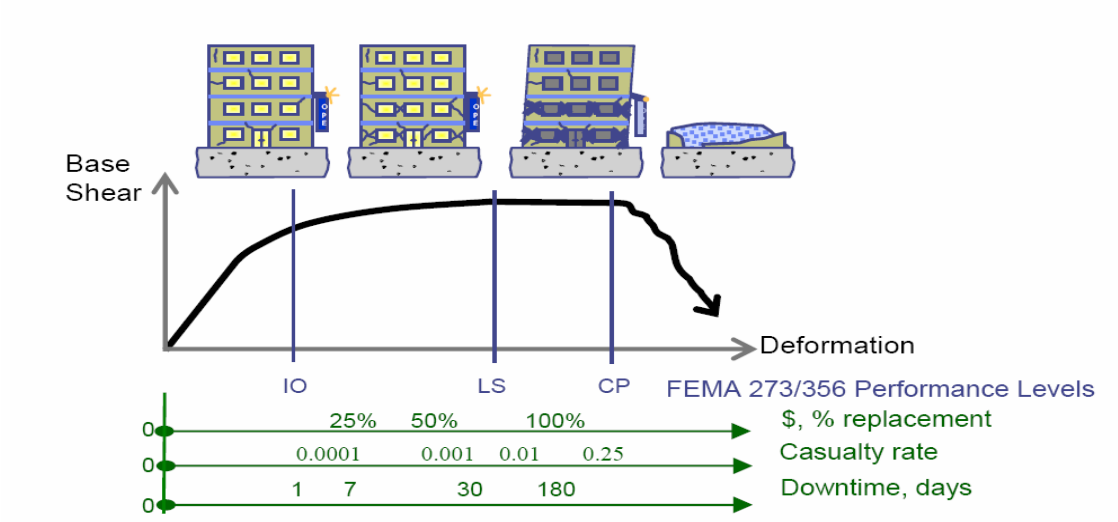

Figure 2-2 FEMA 356 Performance levels (taken from Fajfar *et al.* 2004)

2.2.1 Performance-Based Methodology Tools

The performance-based methodology necessitates the estimation of two quantities for assessment and design purposes. These are the seismic capacity and the seismic demand. Seismic capacity signifies the ability of the building to resist the seismic effects. Seismic demand is a description of the earthquake effects on the building. The performance is evaluated in a manner such that the capacity is greater than the demand (ATC-40, 1996). These quantities can be determined by performing either inelastic time-history analyses or nonlinear static 'pushover' analyses. The former is the most realistic analytical approach for assessing the performance of a structure, but it is usually very complex and time consuming mainly because of the complex nature of strong ground motions. This complexity has led to the adaptation of nonlinear static analysis methods as necessary assessment and design tools.

There are four analytical procedures for design and assessment purposes recommended in the guidelines of FEMA, ATC, and EC8. These are the Linear Static Procedure, LSP, Linear Dynamic Procedure, LDP, Nonlinear Static Procedure, NSP, and the Nonlinear Dynamic Procedure, NDP, with ascending order of complexity.

2.2.1.1 Linear Static Analysis Procedure, LSP

The LSP procedure uses a pseudo-lateral static load pattern in order to compute the force and displacement demands on each element of the structure resulting from strong ground motion. These demands are compared with the capacities of the structural elements. The LSP however cannot be used if the structure is irregular, in terms of stiffness, strength, mass distribution, etc, if the elements have large ductility demands or the lateral force resisting system is non-orthogonal (Gupta 1998).

2.2.1.2 Linear Dynamic Analysis Procedure, LDP

The LDP procedure involves the computation of force and displacement demands using a modal analysis, a response spectrum analysis, or a time-history analysis. Usually the response spectrum analysis is favored compared to the modal analysis because it avoids the time-history analysis of a number of SDOF systems that correspond to each mode of vibration of interest. Instead the demands are computed directly by obtaining the maximum ground acceleration from the response spectrum of the ground motion or from the response spectrum of the ensemble of the ground motions.

2.2.1.3 Nonlinear Static Analysis Procedure, NSP, or Pushover Analysis, POA

The NSP procedure normally called Pushover Analysis, POA, is a technique in which a computer model of a structure is subjected to a predetermined lateral load pattern, which approximately represents the relative inertia forces generated at locations of substantial mass. The intensity of the load is increased, i.e. the structure is 'pushed', and the sequence of cracks, yielding, plastic hinge formations, and the load at which failure of the various structural components occurs is recorded as function of the increasing lateral load. This incremental process continues until a predetermined displacement limit. This method will be explained in more detail later in this Chapter.

2.2.1.4 Nonlinear Dynamic Analysis Procedure, NDP

The NDP procedure is the most sophisticated analysis method because it eliminates the shortcomings of the methods discussed in sections 2.2.1.1 – 2.2.1.3. It is usually considered to provide 'exact' solutions to assessment or design problems. The accuracy of the method depends on the modeling of the structure, the ground motion characteristics and the nonlinear material models used in the analyses, something that is true for any method of analysis.

2.3 PUSHOVER ANALYSIS

2.3.1 Background to pushover analysis method

The static pushover analysis method, POA, has no strict theoretical base. It is mainly based on the assumption that the response of the structure is controlled by the first mode of vibration and mode shape, or by the first few modes of vibration, and that this shape remains constant throughout the elastic and inelastic response of the structure. This provides the basis for transforming a dynamic problem to a static problem which is theoretically flawed. Furthermore, the response of a MDOF structure is related to the response of an equivalent SDOF system, ESDOF. This concept is illustrated in Figure 2.3.

The earthquake induced motion of an elastic or inelastic MDOF system can be derived from its governing differential equation:

$$[M]\{\ddot{U}\}+[C]\{\dot{U}\}+\{F\}=-[M]\{1\}\ddot{u}_g \qquad (2.1)$$

where [M] is the mass matrix, [C] is the damping matrix, {F} is the storey force vector, $\{1\}$ is an influence vector characterising the displacements of the masses when a unit ground displacement is statically applied, and $\ddot{u}_g$ is the ground acceleration history.

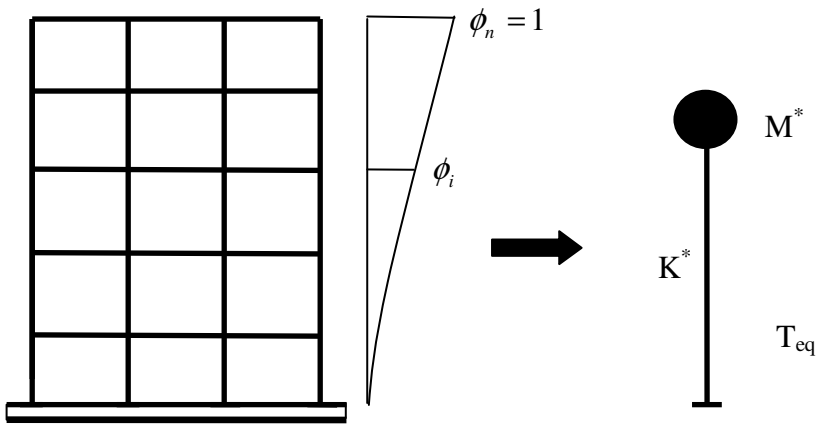

Figure 2-3 Conceptual diagram for transformation of MDOF to SDOF system

By assuming a single shape vector, $\{\Phi\}$, which is not a function of time and defining a relative displacement vector, U, of the MDOF system as $U = \{\Phi\}u_t$, where u_t denotes the roof/top displacement, the governing differential equation of the MDOF system will be transformed to:

$$[M]\{\Phi\}\ddot{u}_t + [C]\{\Phi\}\dot{u}_t + \{F\} = -[M]\{1\}\ddot{u}_g \qquad (2.2)$$

If the reference displacement u^* of the SDOF system is defined as

$$u^* = \frac{\{\Phi\}^T [M]\{\Phi\}}{\{\Phi\}^T [M]\{1\}} u_t \qquad (2.3)$$

Pre-multiplying equation (2.2) by $\{\Phi\}^T$ and substituting for u_t using equation (2.3) the following differential equation describes the response of the ESDOF system:

$$M^*\ddot{u}^* + C^*\dot{u}^* + F^* = -M^*\ddot{u}_g \qquad (2.4)$$

where $M^* = \{\Phi\}^T [M]\{1\}$ (2.5)

$$C^* = \{\Phi\}^T [C]\{\Phi\} \frac{\{\Phi\}^T [M]\{1\}}{\{\Phi\}^T [M]\{\Phi\}} \quad (2.6)$$

$$F^* = \{\Phi\}^T \{F\} \quad (2.7)$$

A nonlinear incremental static analysis of the MDOF structure can now be carried out from which it is possible to determine the force-deformation characteristics of the ESDOF system. The outcome of the analysis of the MDOF structure is a Base Shear, V_b, - Roof Displacement, u_t, diagram, the global force-displacement curve or *capacity curve* of the structure, Fig.2.4a. This capacity curve provides valuable information about the response of the structure because it approximates how it will behave after exceeding its elastic limit. Some uncertainty exists about the post-elastic stage of the capacity curve and the information it can provide since the results are dependent on the material models used (Pankaj *et al.* 2004) and the modelling assumptions (Dieirlein *et al.* 1990, Wight *et al.* 1997).

For simplicity, the curve is idealised as bilinear from which the yield strength V_y, an effective elastic stiffness $K_e = V_y/u_y$ and a hardening/softening stiffness $K_s = \alpha K_e$ are defined. The idealised curve can then be used together with equations (2.3) and (2.7) to define the properties of the equivalent SDOF system, Figure 2.4b.

Thus the initial period T_{eq} of the equivalent SDOF system will be:

$$T_{eq} = 2\pi \sqrt{\frac{M^*}{K^*}} \quad (2.8)$$

where K^* defines the elastic stiffness of the equivalent SDOF system and is given by:

$$K^* = \frac{F_y^*}{u_y^*} \quad (2.9)$$

The strain-hardening ratio, α, of the base shear – roof displacement relationship of the ESDOF system is taken as the same as for the MDOF structure.

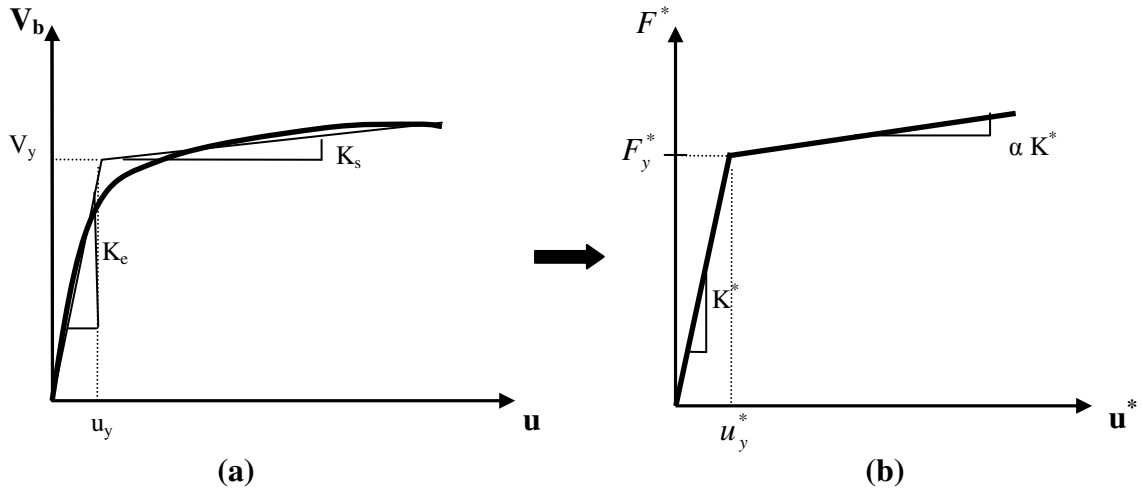

Figure 2-4 (a) Capacity curve for MDOF structure, (b) bilinear idealization for the equivalent SDOF system.

The maximum displacement of the SDOF system subjected to a given ground motion can be found from either elastic or inelastic spectra or a time-history analysis. Then the corresponding displacement of the MDOF system can be estimated by re-arranging eq. 2.3 as follows:

$$u_t = \frac{\{\Phi\}^T [M]\{1\}}{\{\Phi\}^T [M]\{\Phi\}} u^* \qquad (2.10)$$

The formulation of the equivalent SDOF system should not introduce much sensitivity in the results (Krawinkler *et al.* 1998) unless the design spectrum is sensitive to small period variations. It is also common in the pushover method that the deflected shape of the MDOF system can be represented by a single and constant shape vector $\{\Phi\}$ regardless of the level of deformation (Krawinkler *et al.* 1998).

The target displacement u_t is dependent on the choice of the mode shape vector $\{\Phi\}$. Previous studies of pushover analysis have shown that the first mode-shape can provide accurate predictions of the target displacement if the response of the structure is dominated by its fundamental mode (Lawson 1994, Fajfar *et al.* 1996, Krawinkler *et al.* 1998, Antoniou 2002, and many others).

The Capacity Curve according to Reinhorn (1997) can be approximated by a set of bilinear curves according to the following relationship:

$$V(u) = V_y \times \{u/u_y - (1-a)(u/u_y - 1)U(u/u_y - 1)\} \quad (2.11)$$

in which V_y and u_y are the yield strength and displacement respectively, $\alpha = K_s/K_e$ is the post-yield stiffness ratio, and $U(u/u_y - 1)$ is a step function that equals 0 for $u/u_y < 1$ or 1 for $u/u_y > 1$. However, the special case of $K_s = 0$ was not addressed by the author.

Simplifying Equation 2.11 the Capacity Curve is expressed as follows:

$$V(u) = \begin{cases} K_e u & u < u_y \\ V_y + aK_e(u - u_y) & u > u_y \end{cases} \quad (2.12)$$

Reinhorn's approximation seems quite simple for everyday design purposes. It would be of interest to check if higher degree polynomials could serve some purpose in the 'rapid' seismic evaluation of structures.

2.3.2 Lateral Load Patterns

In order to perform a pushover analysis for a MDOF system, a pattern of increasing lateral forces needs to be applied to the mass points of the system. The purpose of this is to represent all forces which are produced when the system is subjected to earthquake excitation. By incrementally applying this pattern up to and into the inelastic stage, progressive yielding of the structural elements can be monitored. During the inelastic stage the system will experience a loss of stiffness and a change in its vibration period. This can be seen in the force-deformation relationship of the system.

The choice of the load pattern to capture a dynamic phenomenon through a static analysis is of much importance because it has been recognized, Lawson *et al.* (1994), Naeim *et al.*

(1998), Gupta *et al.* (1999), Mwafy *et al.* (2001), Lew *et al.* (2001), İnel *et al.* (2003), Moghadam *et al.* (2005), that it can affect the results significantly.

It has been agreed that the application of a single load pattern would not be able to capture the dynamic response of any system due to a seismic event. This is reflected in FEMA 356 and EC8 which recommend that at least two load patterns should be used in order to envelope the responses.

For pushover analyses the following load patterns have been used:

1. Mode Shape distribution based on the fundamental mode or other mode shapes of interest

$$F_i = W_i \phi_{ij} \qquad (2.13)$$

where W_i is the weight of the '*i*' storey, and ϕ_{ij} is the i^{th} element of the mode shape vector corresponding to the '*i*' storey for mode *j*.

2. An Inverted Triangular Distribution

$$F_i = \frac{W_i h_i}{\sum_{l=1}^{n} W_l h_l} \cdot V_b \qquad (2.14)$$

where h_i is the height of the '*i*' storey, *n* is the total number of the storeys, and V_b is the base shear given by the following equation:

$$V_b = S_d(T_n) W \qquad (2.15)$$

where $S_d(T_n)$ is the acceleration ordinate of the design spectrum at the fundamental period T_n, and *W* is the total weight of the structure.

3. The FEMA Load distribution

$$F_i = \frac{W_i h_i^k}{\sum_{l=1}^{n} W_l h_l^k} \cdot V_b \qquad (2.16)$$

where k is a coefficient which can be assumed to be dependent on the fundamental period T_n of the structure. It can be set equal to 1.0 for structures that have period shorter than 0.5 seconds and equal to 2.0 for T >2.5 seconds. A linear variation between 1 and 2 can be used to obtain a simple transition between the two extreme values (FEMA 2000).

4. A Uniform Load distribution

$$F_i = W_i \qquad (2.17)$$

5. Kunnath's Load distribution (Kunnath, 2004)

$$F_i = \sum_{j=1}^{n} a_{mr} \Gamma_j M_i \varphi_{ij} S_a(\zeta_j, T_j) \qquad (2.18)$$

where a_{mr} is a modification factor that can control the relative effects of each included mode and which can take positive or negative values; usually positive or negative unity, Γ_j is the participation factor for mode *j*, M_i is the mass of the i^{th}-storey, φ_{ij} is the mode shape of the i^{th}-storey for mode *j*, $S_a(\zeta_j, T_j)$ is the spectral acceleration for a given earthquake loading at frequency corresponding to the period *T* and damping ratio ζ for mode *j*.

6. Two-phase load pattern (Jingjiang *et al.* 2003): Initially an inverted triangular load distribution is applied up to the performance level of interest and the maximum value of the base shear is obtained. Subsequently a second pushover analysis is performed using again the inverted triangular load pattern until the base shear reaches some fraction β of its maximum value followed by an exponential form pattern defined as $(x/H)^{\eta}$ where x is the distance from the ground to the floor, H is height of the building and η is a characteristic parameter for different types of buildings. No clear justification on the estimation of parameter η was provided.

7. Adaptive force patterns that are updated according to the instantaneous dynamic properties of the system under study. As an example, Bracci *et al.* (1997) assumed an initial load pattern (F_i), and calculated the incremental loads according to the following equation:

$$\Delta F_i^{k+1} = V_b^k \left(\frac{F_i^k}{V_b^k} - \frac{F_i^{k-1}}{V_b^{k-1}} \right) + \Delta V_b^{k+1} \left(\frac{F_i^k}{V_b^k} \right) \quad (2.19)$$

where *i* is the storey number, *k* is the increment number, V_b is the base shear, ΔV_b is the incremental base shear. This was later modified by Lefort (2000) – as suggested by Antoniou (2002) - to account for higher mode contributions:

$$F_i = \frac{W_i \sqrt{\sum_{j=1}^{n} (\varphi_{i,j} \Gamma_j)^2}}{\sum_{L=1}^{N} W_L \sqrt{\sum_{j=1}^{n} (\varphi_{L,j} \Gamma_j)^2}} \cdot \Delta V_b + F_i^{old} \quad (2.20)$$

where *i* is the storey number, *j* is the mode number, Γ_j is the modal participation factor of mode *j*, $\varphi_{i,j}$ is the mass-normalised mode shape for the i^{th} storey and the j^{th} mode, n is the number of modes considered in the analysis, and ΔV_b is the incremental base shear.

2.4 PUSHOVER ANALYSIS METHODS

The POA methods that are used can be divided into three general groups: the Conventional POA methods, the Adaptive POA methods, and the Energy-Based POA methods. Some other pushover procedures exist in the literature. The Conventional POA methods are the following:

1. Capacity Spectrum Method , CSM
2. Improved Capacity Spectrum Method, ICSM

3. N2 method
4. Displacement Coefficient Method, DCM
5. Modal Pushover Analysis, MPA

The CSM and N2 methods differ in the use of appropriate inelastic spectra to calculate the ESDOF maximum displacement, as will be explained in the following sections. The ICSM method is a modification of the CSM procedure, and resembles the N2 method in the use of inelastic spectra. The Adaptive POA methods are more recent sophisticated variations of the Conventional POAs. The Adaptive and Energy-Based POA methods will also be presented even though they are not utilized in this research.

2.4.1 Capacity Spectrum Method, CSM, (ATC 40, 1996)

The Capacity Spectrum Method, CSM, was first presented by Freeman *et al.* (1975) as a rapid seismic assessment tool for buildings. Subsequently, the method was accepted as a seismic design tool. The steps in the method are as follows:

2.4.1.1 Nonlinear static pushover analysis of the MDOF model

A vertical distribution of the lateral loading to be applied to the structure is assumed based on the fundamental mode of vibration. Other lateral load patterns can also be used instead, section 2.3.2. A nonlinear static analysis is then carried out to give a Base Shear – Roof Displacement Curve, the Capacity Curve.

2.4.1.2 Definition of Inelastic Equivalent SDOF system, ESDOF

The capacity curve is then approximated as a bilinear relationship with the choice of a global yield point (V_y, u_y) of the structural system and a final displacement (V_{pi}, u_{pi}). The yield point (V_y, u_y) is defined such that the area A_1 in Figure 2.5 is approximately equal to the area A_2 in order to ensure that there is equal energy associated with each curve.

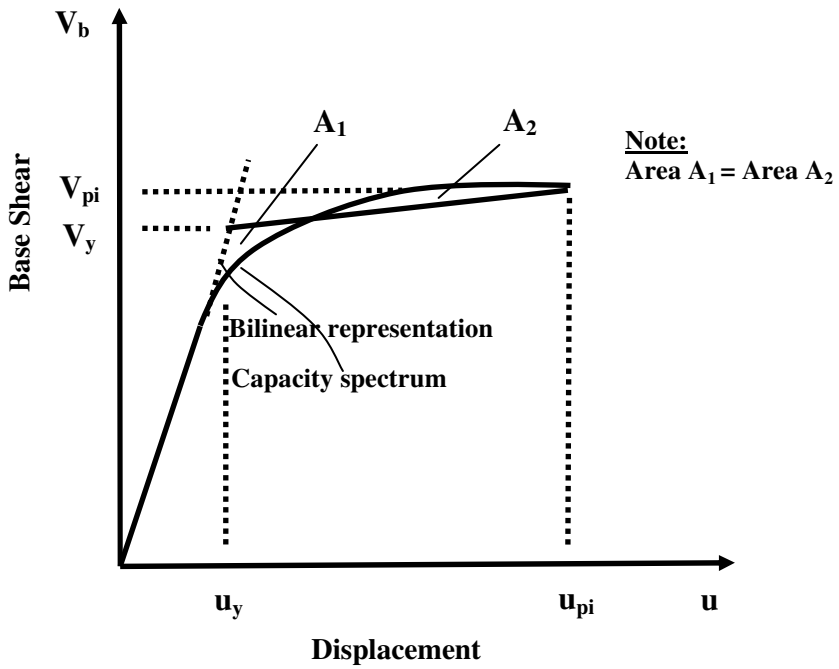

Figure 2-5 Bilinear approximation of the capacity curve

Utilising equations 2.8 and 2.9, the properties of the inelastic equivalent SDOF system, ESDOF, can be defined.

2.4.1.3 Conversion of Capacity Curve to Capacity Spectrum

The Capacity Curve is then converted to a Capacity Spectrum relationship using the following equations:

$$S_a = \frac{V_b}{\alpha_m \cdot M} \quad (2.21)$$

$$S_d = \frac{u}{PF_1 \phi_{ij}} \quad (2.22)$$

where M is the total mass of the building, ϕ_{ij} is the modal amplitude at storey level 'i' for mode j, PF_1 is a participation factor and α_m is the modal mass coefficient which are given by:

$$PF_1 = \frac{\{\Phi\}^T [M]\{1\}}{\{\Phi\}^T [M]\{\Phi\}} \quad (2.23)$$

$$\alpha_m = \frac{\left[\sum_{j=1}^{n} m_i \phi_{ij}\right]^2}{\sum_{i=1}^{n} m_i \sum_{j=1}^{n} m_i \phi_{ij}^2} \quad (2.24)$$

2.4.1.4 Elastic Response Spectrum and Acceleration-Displacement Spectrum, ADRS format

The conversion of the capacity curve to the capacity spectrum necessitates that the elastic response or design spectrum is plotted in acceleration-displacement format, ADRS, rather than acceleration-period format, Figure 2.6. The ADRS spectrum is also denoted as the demand spectrum. This has been the first improvement of the CSM method, by Mahaney *et al.* (1993).

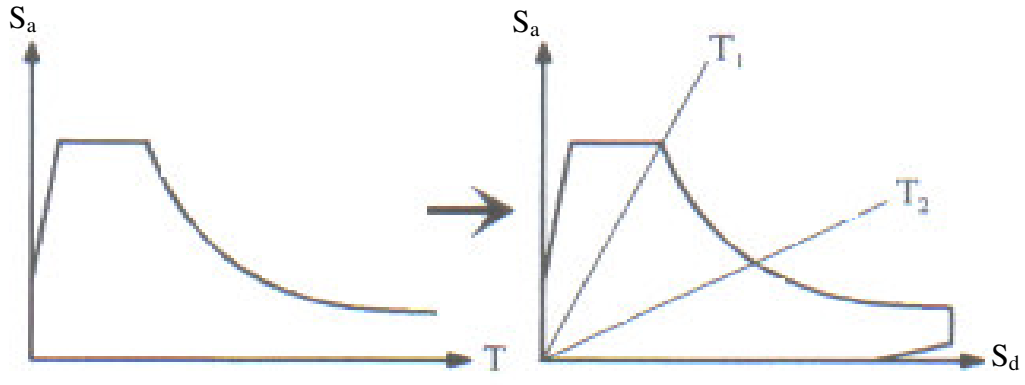

Figure 2-6 Conversion of elastic spectrum to ADRS spectrum

2.4.1.5 Superposition of the Capacity Spectrum on the Elastic Damped Demand Spectrum

Once the capacity spectrum and the 5% damped elastic demand spectrum are plotted together in the ADRS format, Figure 2.7, an initial estimate of the performance point (a_{pi}, d_{pi}) using the equal displacement rule can be obtained by extending the linear part of the capacity spectrum until it intersects the 5% damped demand spectrum. Alternatively, the performance point can be assumed to be the end point of the capacity spectrum, or it might be another point chosen on the basis of engineering judgment, as ATC-40 has suggested.

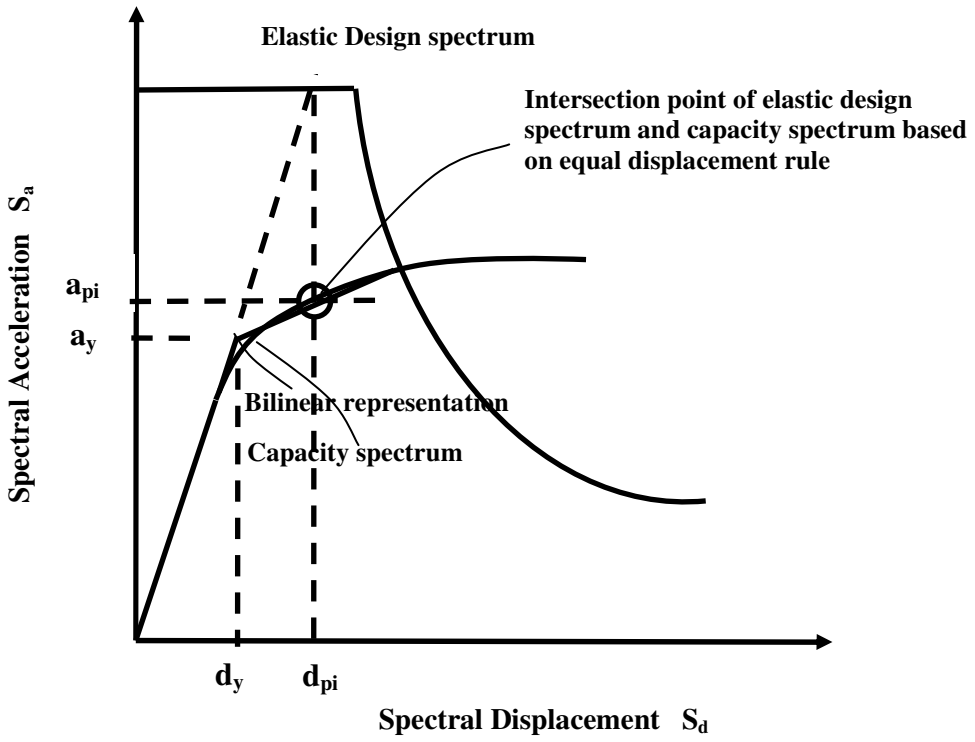

Figure 2-7 Initial estimation of performance point using the Equal Displacement rule

2.4.1.6 Equivalent Viscous Damping

When structures enter the nonlinear stage during a seismic event they are subjected to damping which is assumed to be a combination of viscous damping and hysteretic damping. Viscous damping is generally accepted that is an inherent property of structures. Hysteretic damping is the damping associated with the area inside the force-deformation relationship of the structure and is represented by equivalent viscous damping. The

equivalent viscous damping is therefore associated with a specific maximum displacement d_{pi} and is estimated using the following equation:

$$\beta_{eq} = \beta_o + 0.05 \quad (2.25)$$

Chopra (1995) has defined β_0 by equating the energy dissipated in a vibration cycle of the inelastic system and of its equivalent linear system, Figure 2.8. This is provided by the following equation:

$$\beta_0 = \frac{1}{4\pi}\frac{E_D}{E_{So}} \quad (2.26)$$

where E_D is the energy dissipated by damping, and E_{So} is the maximum elastic strain energy.

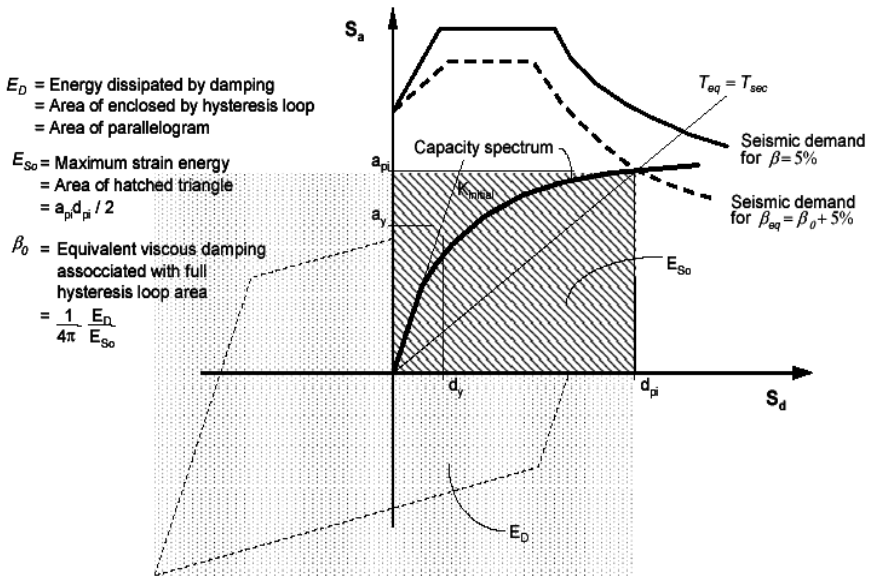

Figure 2-8 Estimation of equivalent viscous damping using CSM method (ATC-40, 1996)

Once the maximum displacement, d_{pi}, has been assumed equation 2.26 becomes:

$$\beta_0 = \frac{200(a_y d_{pi} - \alpha_{pi} d_y)}{\pi \alpha_{pi} d_{pi}} \quad (2.27)$$

The reader is referred to ATC-40, for the derivation of equation 2.27. Other relationships have also been proposed based on ductility, μ, and strain hardening ratio, α, Chopta *et al.* 2000.

Using equation 2.25 the amount of damping for which the demand spectrum needs to be computed can be calculated.

2.4.1.7 Performance point of equivalent SDOF system

The new demand spectrum should then be checked if it intersects the capacity spectrum at or close enough to the estimate of performance point, Figure 2.9. If the demand spectrum intersects the capacity spectrum within an acceptable tolerance then the estimate is accepted. Otherwise the performance point is re-estimated and the procedure repeated from the step of superimposing the capacity spectrum on the ADRS spectrum, section 2.4.1.4.

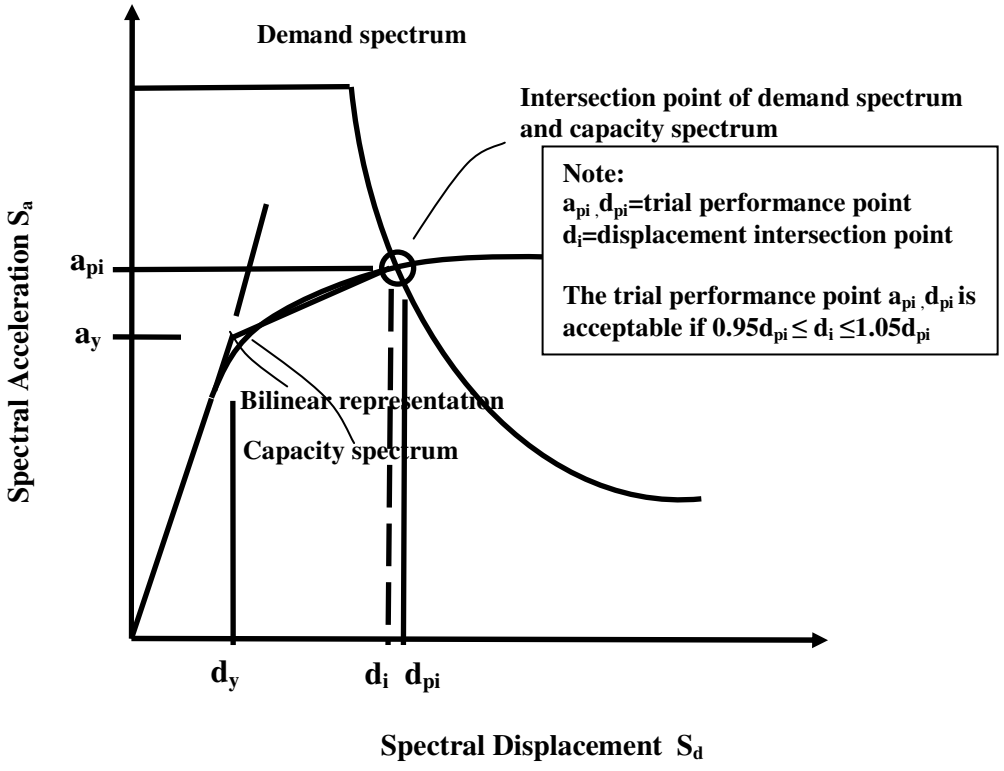

Figure 2-9 Estimation of target displacement using CSM method

2.4.1.8 Performance Point of MDOF system

When the performance point has been calculated it is converted to the target displacement of the MDOF system using:

$$u_t = PF_1 \phi_{ij} S_d \qquad (2.28)$$

where PF_1 is the participation factor defined in eq. 2.23 and S_d is the spectral displacement of the equivalent SDOF system defined in eq. 2.22.

The strength of structural elements and storey drifts can now be checked for the target displacement.

The notion of the CSM method can also be summarized as follows (Paret *et al.*, 1996):

If the capacity curve can extend through the envelope of the demand curve, the structure survives the earthquake. The intersection of the capacity and demand curve represents the force and displacement of the structure for that earthquake.

An improvement of the CSM method in order to identify higher –mode effects was proposed by Paret *et al.* (1996), called Modal Pushover Procedure, MPP. It required several nonlinear static analyses to be carried out based on the number of modes of vibration of interest. In this way the influence of each individual mode could be observed when the individual capacity spectra were superimposed on the damped demand spectrum. However, the effects of higher modes cannot be quantified in this way since the method does not provide estimation of response, Antoniou (2002).

2.4.2 Improved Capacity Spectrum Method, ICSM

The ICSM method was proposed by Chopra *et al.* (2000) with the purpose of introducing the constant-ductility inelastic design spectra in the CSM method instead of the elastic damped spectra. The method is different from the CSM method from the step of estimating the seismic demands of the equivalent SDOF system, section 2.4.1.7. At this point when

the capacity spectrum of the system under study is superimposed on the inelastic spectrum it will intersect it at several ductility μ values, Figure 2.10. One of the intersection points will provide the deformation demand. The criterion for this decision is that the ductility factor μ obtained from the capacity diagram should match the ductility value associated with the intersecting demand curve. This procedure requires iterations as the CSM method.

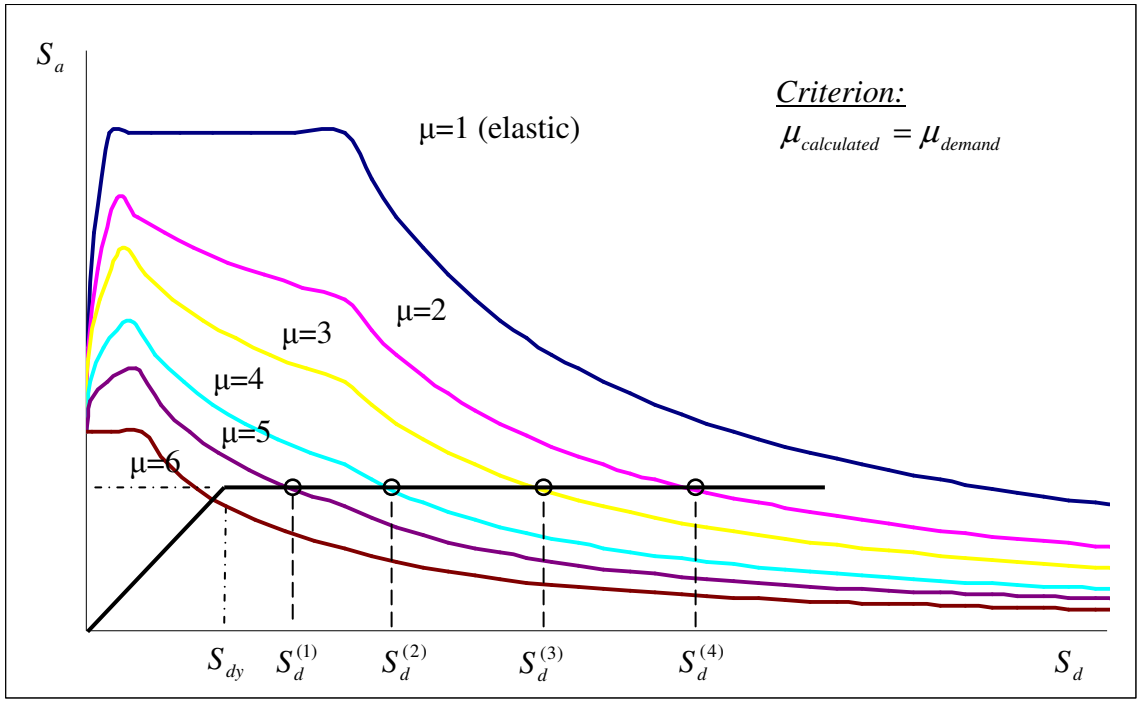

Figure 2-10 Application of ICSM method

2.4.3 N2 Method

The N2 method was firstly presented by Fajfar *et al.* (1988) as an alternative to the CSM method. The basic idea of the N2 method stems from the Q-model developed by Saiidi *et al.* (1981) which in turn is based on the work of Gulkan *et al.* (1974). The main difference of the method with respect to the CSM method is the type of demand spectra used for the estimation of the target displacement. The steps of the method are given in the following sections.

2.4.3.1 Nonlinear static pushover analysis of the MDOF model

This step is the same as for the Capacity Spectrum Method, section 2.4.1.2**.**

2.4.3.2 Determination of the equivalent SDOF model

The pushover curve is converted to a Capacity Spectrum relationship for the equivalent SDOF system using the following equations:

$$S_a = \frac{V_b}{\Gamma_j \cdot M^*} \quad (2.29)$$

$$S_d = \frac{u}{\Gamma_j \cdot \phi_n} \quad (2.30)$$

where $M^* = \sum M_i \phi_{ij}$ is the effective mass of the building, ϕ_n is the roof element of the mode shape vector, and Γ_j is the participation factor for mode *j*.

The capacity spectrum is then plotted in the ADRS format, section 2.4.1.2.

An approximate bilinear idealisation of the capacity spectrum is performed in order to determine the yield strength F_y^*, yield displacement u_y^* from the bilinear capacity curve and effective period T_{eq} of the ESDOF system using Eq.(2.8).

It should be noted that equations 2.29 and 2.30 are practically the same as equations 2.21 and 2.22 respectively.

2.4.3.3 Seismic Demand

The damped elastic acceleration spectrum to be used is defined in the ADRS format. The inelastic spectra are then computed in terms of the ductility reduction factor R_μ, and ductility factor μ. The ductility dependent reduction factor R_μ is defined as:

$$R_\mu = \frac{S_{ae}}{\alpha_y} \quad (2.31)$$

where S_{ae} is the pseudo-acceleration ordinate from the response spectrum and α_y is the yield acceleration from the capacity spectrum. The acceleration ordinate S_a, and the spectral displacement S_d of an inelastic SDOF system can be calculated as follows, Vidic *et al.* (1994):

$$S_a = \frac{S_{ae}}{R_\mu} \quad (2.32)$$

$$S_d = \frac{\mu}{R_\mu} S_{de} \quad (2.33)$$

The ductility dependent reduction factor R_μ is usually expressed in terms of ductility μ and period T, through the so called $R_\mu - \mu - T$ relationships. An example bilinear $R_\mu - \mu - T$ relationship as presented in Vidic *et al.* (1994), is shown below and graphically in Figure 2.11.

$$R_\mu = \begin{cases} (\mu - 1)\dfrac{T}{T_C} + 1 & T < T_C \\ \mu & T \geq T_C \end{cases} \quad (2.34)$$

where T_C is the characteristic period of the ground motion, defined as the transition period from the constant acceleration domain to the constant velocity domain of the spectrum.

2.4.3.4 Seismic Demand for the equivalent SDOF system

The displacement demand S_d of the ESDOF system can be determined by substituting eq. 2.34 into eq. 2.33. This leads to:

$$S_d = \begin{cases} \dfrac{S_{de}}{R_\mu} \cdot \left(R_\mu - 1 \right) \dfrac{T_C}{T} + 1 \right) & T < T_C \\ S_{de} & T \geq T_C \end{cases} \quad (2.35)$$

Equation 2.35 implies that the displacement estimate will always be larger than the initial elastic displacement for short-period structures, or structures that have fundamental period lower than the characteristic period of the ground motion T_C. This is shown in Figure 2.12. Figure 2.13 applies for medium- and long-period structures.

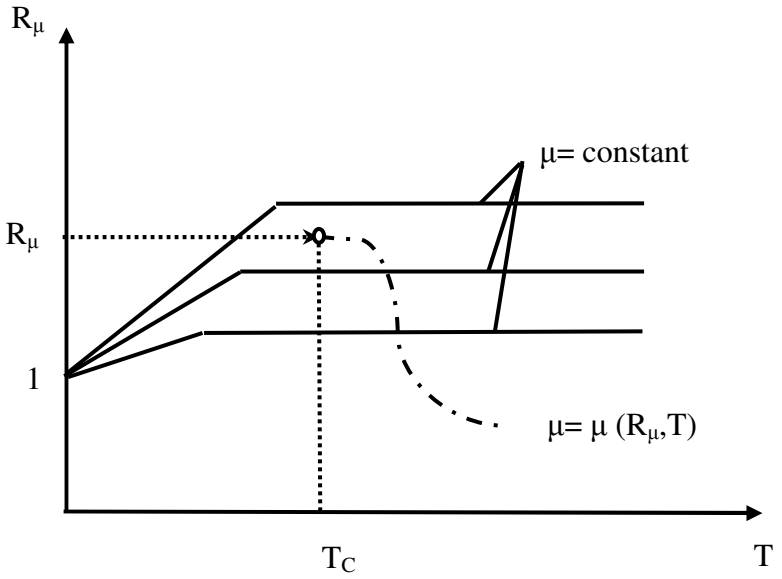

Figure 2-11 R_μ –μ-T relationship, Vidic *et al.* (1994)

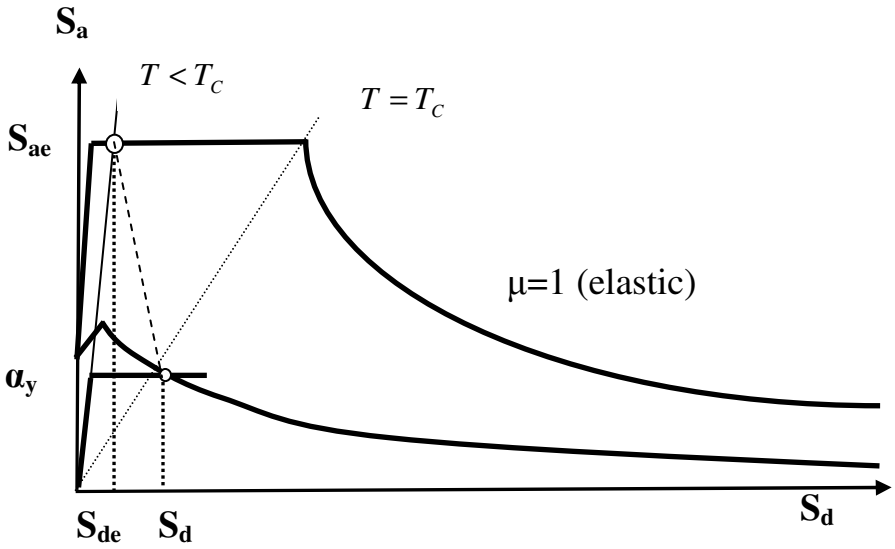

Figure 2-12 Estimation of target displacement from N2 method for $T < T_C$.

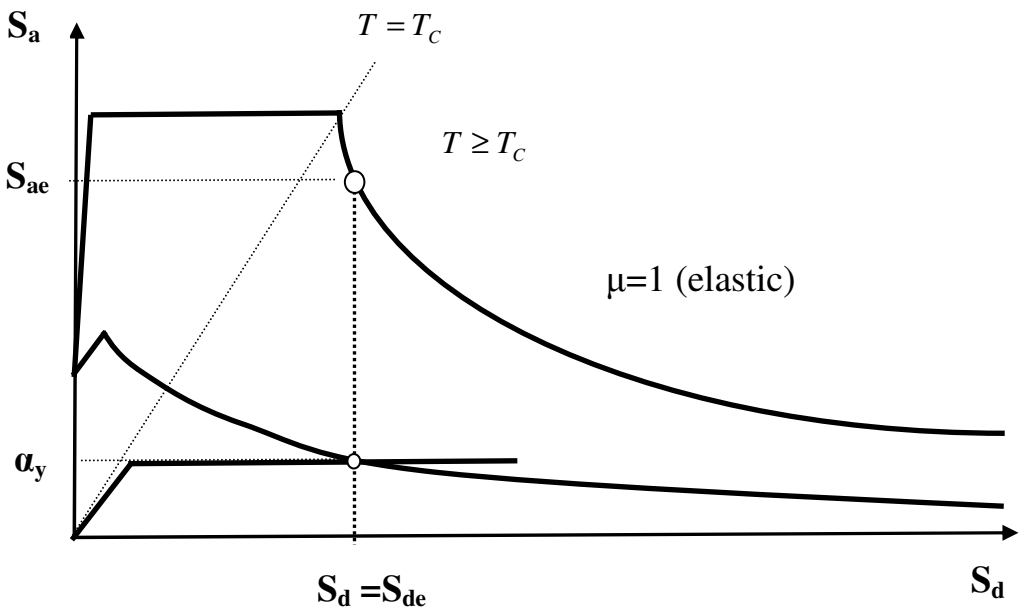

Figure 2-13 Estimation of target displacement from N2 method for $T \geq T_C$.

2.4.3.5 Global Seismic Demand for MDOF model

The displacement S_d of the equivalent SDOF can be transformed to the top displacement u_t of the MDOF model using the following equation:

$$u_t = \Gamma_j S_d \quad (2.36)$$

2.4.3.6 Local Seismic Demand for MDOF model

Local quantities of interest such as rotations, storey drifts, energy demands, corresponding to u_t, can then be determined.

2.4.4 Displacement Coefficient Method, DCM

The DCM method differs to the CSM and N2 methods in the estimation of the target displacement, which does not require the conversion of the capacity curve to a capacity

spectrum. The step described in sections 2.4.1.1 and 2.4.3.1 can be used to calculate the force-deformation relationship of the structure. The target displacement is then calculated using the following relationship:

$$u_t = C_0 C_1 C_2 C_3 S_a \frac{T_e^2}{4\pi^2} \quad (2.37)$$

where C_0 = modification factor to relate the SDOF spectral displacement to MDOF roof displacement.

C_1 = modification factor to relate the expected maximum inelastic SDOF displacement divided by the elastic SDOF displacement.

$$C_1 = \begin{cases} 1.0 & for \quad T_e \geq T_C \\ [1.0 + (R-1)T_C / T_e] / R & for \quad T_e < T_C \end{cases} \quad (2.38)$$

where T_C is the characteristic period of the response spectrum, defined as the period associated with the transition from the constant acceleration domain of the spectrum to the constant velocity domain, T_e is the effective fundamental period, and R is the ratio of inelastic strength demand to calculated yield strength coefficient calculated as follows:

$$R = \frac{S_a / g}{V_y / W} \cdot \frac{1}{C_o} \quad (2.39)$$

C_2 = modification factor to represent the effect of hysteresis shape on the maximum displacement response.

C_3 = modification factor to represent increased displacements due to second-order effects. For buildings that have positive post-yield stiffness, C_3 should be equal to 1.0. For buildings that have negative post-yield stiffness C_3 should be calculated as:

$$C_3 = 1 + \frac{|\alpha|(R-1)^{3/2}}{T_e} \quad (2.40)$$

where α is the ratio of post-yield stiffness to elastic stiffness when the nonlinear force-deformation relationship is bilinear.

S_a = spectral acceleration

V_y = is the yield strength calculated from the bilinear representation of the

capacity curve.

W= Total dead load and anticipated live load

The displacements and forces at sections of interest can be calculated for the target displacement.

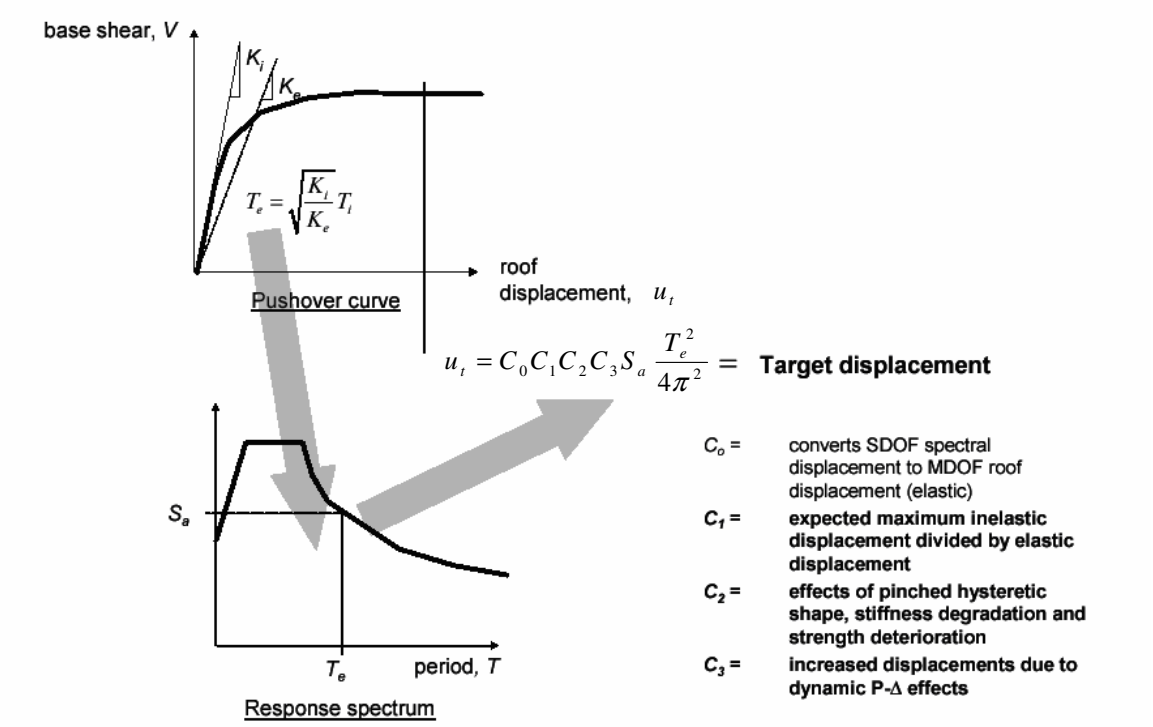

Figure 2-14 Procedure of DCM method (ATC 40, 1996)

2.4.5 Modal Pushover Analysis, MPA

The Modal Pushover analysis, MPA, was developed by Chopra and Goel (2001, 2002), as a generalization of the Modal Pushover Procedure by Paret *et al.* (1996). The steps of the method are as follows:

2.4.5.1 Calculation of Dynamic Properties

The natural periods T_n, and modes of vibration φ_j, characterizing the elastic vibration of the structure are calculated. The fundamental mode shape and other mode shapes that are

expected to influence the response of the structure are then used to form the distribution of horizontal forces to be applied to the structure. The influence of each mode can be observed in the elastic dynamic analysis of the MDOF structure. The distributions of the lateral forces for each mode *j* are calculated using:

$$s_j = [M]\phi_j . \quad (2.41)$$

where [M] is the mass matrix of the structure.

2.4.5.2 Nonlinear static pushover analysis of the MDOF model

This step is similar to that used for the Capacity Spectrum Method, CSM, and the N2 method. The base shear – roof displacement pushover curve of the j^{th} – mode force distribution is developed in this analysis for the selected number of modes *n*.

2.4.5.3 *J* th – mode inelastic SDOF system

The j^{th}-mode pushover curve is then idealised as a bilinear curve and is converted to the force-deformation relation for the j^{th} – mode inelastic SDOF system by utilising the following relationships, Figure 2.13:

$$\frac{V_{bjy}}{M_j^*} = \frac{F_{sjy}}{L_j} \quad (2.42)$$

$$D_{jy} = \frac{u_{tjy}}{\Gamma_j \phi_{nj}} \quad (2.43)$$

where M_j^* is the effective modal mass of mode *j*, V_{bjy} is the base shear of the MDOF system for mode *j*, F_{sjy} is the force of the ESDOF system for mode *j*, u_{tjy} is the j^{th} – mode MDOF roof displacement, and φ_{nj} is the j^{th} – mode shape value at the roof.

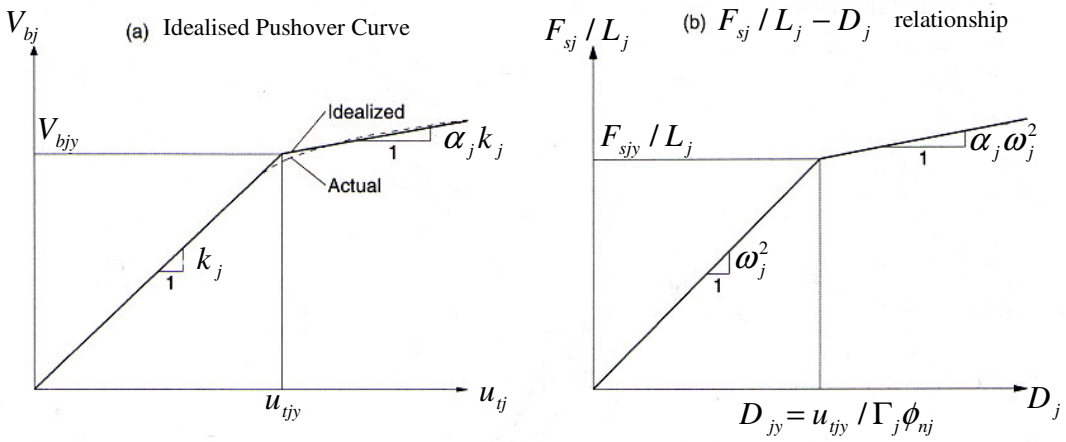

Figure 2-15 MPA procedure (taken from Chopra *et al.* 2001)

2.4.5.4 Peak Deformation of the j^{th} – mode inelastic SDOF system

The peak deformation D_j, for the j^{th} – mode inelastic SDOF system with the above force-deformation relation and damping ratio ζ_j is computed using a nonlinear time-history analysis or directly from the available inelastic design or response spectrum.

2.4.5.5 MDOF peak displacement

The peak roof displacement u_{tj} associated with the j^{th} – mode inelastic SDOF system is then obtained from:

$$u_{tj} = \Gamma_j \varphi_{nj} D_j \quad (2.44)$$

Floor displacements, story drifts, and plastic hinge rotations can be calculated for the roof displacement u_{rn}.

The procedure should be repeated for as many 'modes' as required for sufficient accuracy; usually the first two or three 'modes' will suffice.

Finally the total response demand r_{MPA} can be determined by combining the peak 'modal' responses r_j using an appropriate modal combination rule, e.g., the square root of the sum of the squares, SRSS combination rule:

$$r_{MPA} = \left(\sum_{j=1}^{n} r_j^2 \right)^{1/2} \quad (2.45)$$

where n is the number of modes included.

Chopra et al. (2004) proposed a Modified Modal Pushover Analysis, MMPA, in which the higher modes were assumed to cause only elastic behaviour of the structure. The application of the MMPA to structures in this study showed that it is not always possible to predict the seismic demands accurately in all cases because even the second mode and the third mode of vibration can lead the structure to the nonlinear stage.

2.4.6 Adaptive Pushover Procedures

Adaptive POA procedures have been developed by Bracci *et al.* (1997), Gupta (1998), Requena *et al.* (2000). They all differ from the conventional POA procedures in the execution of nonlinear static analysis of the MDOF model.

The Adaptive POA procedures are mostly concerned with an appropriate estimation of the force vector that is going to 'push' the structure at each static force increment. The monitoring in the change of the incremental force vector could ensure that the stiffness degradation or strength deterioration of the structure is accounted for more realistically, than conventional nonlinear static analyses. When the new force vector has been determined, the remaining steps of the Adaptive POAs follow those of the Conventional POAs.

Bracci *et al.* (1997) introduced the Adaptive Pushover Analysis, APA, by utilizing an adaptive load pattern given by equation 2.17. The basis of the load pattern was an inverted triangular distribution, however it was stated that any assumed lateral force distribution could be equally used. The nonlinear static analysis in the APA method comprised the identification of four distinct response phases: elastic, first yield, incipient failure mechanism and full failure mechanism. The storey level forces obtained from equation 2.17 were updated for each of these response stages through eigenvalue analyses of the structure and determination of the mode shapes and modal base shears that need be combined

through the SRSS rule and distributed across the floor levels in the next increment. The analysis is performed until the inter-storey drift has reached a specified limit, or the structure has failed.

A similar method, the Adaptive Modal Pushover Analysis, AMP, was presented by Gupta (1998), Kunnath *et al.* (1999), and Gupta *et al.* (2000). This analysis requires the computation of the eigenvalues of the system and hence the modes and periods of vibration prior to the execution of each load increment, thus using the current stiffness state of the system Antoniou (2002). Initially before commencing the nonlinear statsic analysis, the storey forces corresponding to all storey levels and number of modes of interest, n, are calculated using the following expression:

$$F_{ij} = \Gamma_j \phi_{ij} W_i S_a(j) \qquad (2.46)$$

where F_{ij}=lateral storey force at the ith level for the jth mode $(1 \le j \le n)$, and $S_a(j)$=spectral acceleration corresponding to the jth mode, ϕ_{ij}=mass normalized mode shape value at ith level and jth mode, W_i=Weight of ith storey, and Γ_j is the modal participation factor for the jth mode.

The modal participation factors are determined using the following relationship:

$$\Gamma_j = \frac{1}{g} \sum_{i=1}^{i=N} W_i \phi_{ij} \quad (2.47)$$

where g is the acceleration due to gravity, and N is the number of storeys.

Subsequently the modal base shears, V_j, need to be computed and combined using the SRSS rule so as to determine the building base shear, V, as shown below:

$$V_j = \sum_{i=1}^{i=N} F_{ij} \qquad (2.48)$$

$$V = \sqrt{\sum_{j=1}^{n} V_j^2} \qquad (2.49)$$

The storey forces are then uniformly scaled using a scaling factor S_n through the following equation:

$$\overline{V_j} = S_n V_j \qquad (2.50)$$

where

$$S_n = \frac{V_B}{N_s V} \qquad (2.51)$$

and V_B is the base shear estimate of the structure, and N_s is the number of uniform steps to be used for applying the base shear. Note that this is still prior to commencing the nonlinear static analysis.

Nonlinear static analysis of the structure is then performed for storey forces corresponding to each mode independently. Element forces displacements, storey drifts, member rotations, etc., are computed using an SRSS combination of the modal quantities for the current step and added to those from the previous step. At the end of each step, the member forces are compared with their yield values. If any member has yielded, the member and global stiffness matrices are updated and an eigenvalue analysis is performed to compute new modes and periods of vibration. The process is repeated until either the maximum base shear is reached or the global drift has exceeded the specified limit.

This method seems to be quite demanding because each mode is treated separately. Additionally the SRSS combination rule probably suggests that equilibrium cannot be achieved at each step.

Requena and Ayala (2000) proposed two variations of a different Adaptive Pushover Analysis with the aim to consider the contribution of the higher modes of vibration to the seismic response of building structures. These variations - denoted as approaches 2A and 2B- differ in the derivation of the equivalent horizontal forces to be applied in the structure at each static force increment. In approach 2A the distribution of lateral forces was

calculated using the SRSS modal superposition of the modes of vibration of interest. This is given by:

$$F_i = \sqrt{\sum_{j=1}^{N}\left(\left[\frac{\sum_{i=1}^{N} m_i\phi_{ij}}{\sum_{i=1}^{N} m_i\phi_{ij}^2}\right]\phi_{ij} Sa_j m_i\right)^2} \qquad (2.52)$$

where ϕ_{kj} is the modal amplitude of the i^{th}- storey and the j^{th} - mode, and Sa_j is the pseudo-spectral acceleration of the j^{th} mode. In approach 2B, an 'equivalent fundamental mode' $\bar{\phi}_i$ was assumed in which the contribution of higher modes of vibration were included using the SRSS rule. Thus

$$\bar{\phi}_i = \sqrt{\sum_{j=1}^{N}\left(\phi_{ij}\Gamma_j\right)^2} \qquad (2.53)$$

where Γ_j is the participation factor of mode j defined as

$$\Gamma_j = \left[\frac{\sum_{k=1}^{N} m_i\phi_{ij}}{\sum_{k=1}^{N} m_i\phi_{ij}^2}\right] \qquad (2.54)$$

The lateral force distribution to be applied is then calculated as follows:

$$F_i = \frac{m_i\bar{\phi}_i}{\sum_{i=1}^{n} m_i\bar{\phi}_i}\cdot V_b \qquad (2.55)$$

2.4.7 Energy-Based Pushover Analysis

Energy-Based pushover analyses have emerged due to some problems observed on the performance of force-controlled or displacement controlled nonlinear static analyses. For example it has been observed that a force-based method neglects the redistribution of forces in the structure and the energy dissipation of the structure while displacement control method may underestimate any strain localizations at weak points in the structure, Coleman *et al.* (2001), Antoniou (2002), Albanesi *et al.* (2002).

Energy-based pushover analyses have independently been proposed by Albanesi *et al.* (2002), Hernandez – Montes *et al.* (2004), Parducci *et al.* (2006).

Albanesi *et al.* (2002) proposed an Energy-based pushover analysis based on the principle that the force or displacement patterns to be applied in the structure should be taking into account the inertial properties and kinetic energy of the structure. That implies that pushover analyses should be seismic input dependent, since there is not a unique structural response independent of the seismic intensity, Albanesi *et al.* (2002).

The Energy-based pushover analysis uses the fundamental mode shape ϕ or another mode shape considered to be representative of the dynamic behaviour of the structure, an effective damping to which the response spectrum is to be scaled, and a velocity profile based on the assumed mode shape and the damped response spectrum.

The initial velocity profile is calculated as follows:

$$v = \phi_{ij} \cdot \Gamma_j \cdot S_v \qquad (2.56)$$

where Γ_j is the participation factor and S_v is the pseudo-velocity.

This information was used in a nonlinear dynamic analysis of the MDOF model, in which the structure was allowed to deform under its initial velocity (energy) profile. In this way the kinetic energy was dissipated through the plastic behaviour of the structure. However

this explanation was vague in that it is unclear how the force-displacement curve was obtained.

Hernandez-Montes, Kwon, and Aschheim (2004), attempted to use an energy-based formulation for first- and multiple-mode nonlinear static pushover analyses. The authors argued that the roof displacement was a useful index for the first mode response of many structures including structures for which displacements over the height of the structure did not increase proportionately. However, for structures outside this assumption field – for example braced structures-, the roof displacement index was deemed questionable, even for elastic response. Reasons for this argument were not provided. Additionally, higher-mode pushover analyses could reverse the roof displacements, (Chopra *et al.* 2002), leading to capacity curves that implied a violation of the first law of thermodynamics, since for increasing base shear the corresponding roof displacement decreased. Thus, the energy absorbed by the MDOF structure in the pushover analysis was used to derive a displacement that described the work done by the equivalent SDOF system, or else an 'energy-based displacement'. Therefore, in contrast to the conventional view, pushover analysis could be considered equivalently in terms of the work done (or absorbed energy) versus base shear response.

Generally, the work done by the base shear V_b of a MDOF structure in an incremental displacement du is dE assuming both elastic and inelastic response:

$$dE = V_b \cdot du \quad (2.57)$$

The base shear and the incremental displacement for each step of pushover analysis can then be calculated by re-arranging equation 2.57, as follows:

$$du = \frac{dE}{V_b} \quad (2.58)$$

However this analysis did not consider higher-mode effects.

Parducci *et al.* (2006) proposed a different version of Energy-based pushover analysis. In this method a reference displacement δ of the MDOF model is chosen so as to equalize the deformation of both MDOF and SDOF models. In each step of the pushover analysis the horizontal forces F_i applied to the floor levels are incremented by ΔF_i which is proportional to the shape of the force distribution. The application of incremental forces ΔF_i results in the displacements being incremented by Δu_i. Then the sum of the forces F^* and masses M^* of the structure are used to define an energy equivalent SDOF model based on the following relationship:

$$\left(F^* + \frac{1}{2}\Delta F^*\right) \cdot \Delta\delta^* = \sum_i \left(\left(F_i + \frac{1}{2}\Delta F_i\right) \cdot \Delta u_i\right) \quad (2.59)$$

Re-arranging equation 2.59 provides the incremental displacements produced by F_i. That is:

$$\Delta\delta^* = \frac{\sum_i \left(\left(F_i + \frac{1}{2}\Delta F_i\right) \cdot \Delta u_i\right)}{\left(F^* + \frac{1}{2}\Delta F^*\right)} \quad (2.60)$$

The total equivalent displacement δ* is then calculated using all the incremental $\Delta\delta^*$ values. The general notion of this method is illustrated in Figure 2.16.

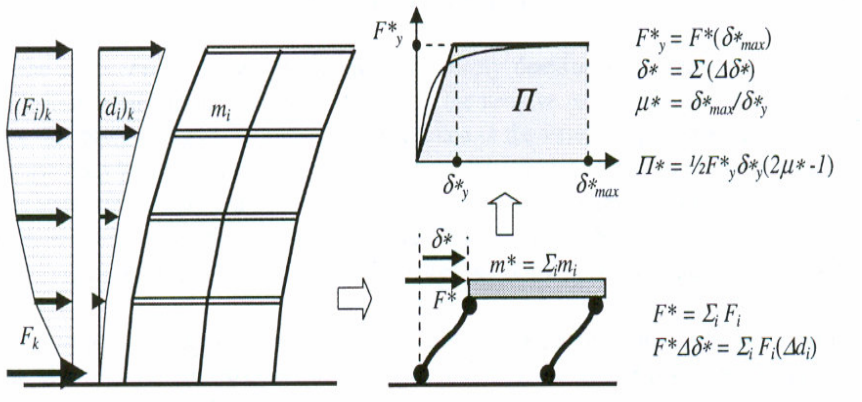

Figure 2-16 Simplified Energy-Based Pushover analysis (adapted from Parducci *et al.* 2006)

The authors did not apply the method to any structural system so it has not been possible to address its potential as well as its drawbacks.

2.5 OTHER POA METHODS

Other pushover analysis methods exist in the literature such as the upper-bound pushover analysis proposed by Jan *et al.* (2004), and the Adaptive Modal Combination procedure, AMC, proposed by Kalkan *et al.* (2006).

The upper-bound pushover analysis differs from the other methods only in the estimation of the storey forces to be applied for the nonlinear static analysis. The load distribution is a combination of the first mode shape and a factored second mode shape, Kalkan *et al.* (2007).

The AMC procedure is a combination of the CSM method, the AMP method, the MPA method, and the Energy-based pushover analysis of Hernandez *et al.* (2004). The reader is referred to Kalkan *et al.* (2006) and Kalkan *et al.* (2007) for a detailed description of the method. This method seems to be quite demanding in terms of computational effort however it was shown that it could perform generally satisfactorily for tall structures.

2.6 REVIEW OF PREVIOUS RESEARCH ON PUSHOVER ANALYSIS

The following review is concerned with studies of the development and application of pushover analysis. It is provided in order to offer an insight into the attempts that have been made to verify the potential, shortcomings and limitations of the method. The findings of previous researchers are given in chronological order.

The pushover analysis method was firstly introduced by Freeman *et al.* (1975) as the Capacity Spectrum Method. The main purpose of this empirical approach was to use a simplified and quick method to assess the seismic performance of a series of 80 buildings located in a shipyard in the USA. The study combined the use of analytical methods with site-response spectra to estimate values of peak structural response, peak ductility demands, equivalent period of vibration, equivalent percentages of critical damping, and residual

capacities. It was concluded that it could perform, in most of the cases, a worthwhile evaluation of existing structures in a reasonable time-scale and cost.

Freeman (1978) presented the Capacity Spectrum method in a clearer manner together with its application to two instrumented 7-storey reinforced concrete structures. The data obtained from the recorded motions were compared with the analysis results showing reasonable agreement. Freeman cautioned engineers that the elastic modelling assumptions, e.g. the choice between cracked or uncracked sections, the inelastic stiffness degradation, e.g. appropriate reduction of structural elements' stiffnesses in the post-elastic region, and the percentage of critical damping used to construct the demand spectra, and determination of the inelastic capacity needed careful judgment and some experience to be adequately defined and assessed. It was suggested that two levels of equivalent viscous damping should be assumed relating to the initial undamaged state and to the ultimate limit state in order to account for the effect of period lengthening that is usual when the structure enters the nonlinear region. Furthermore, it was concluded that more structures needed to be assessed to validate the method.

Saidi and Sozen (1981) produced a 'low-cost' analytical model which was named the Q-Model for calculating displacement histories of multi-storey reinforced concrete structures subjected to ground motions. The Q-model, which was based on the idea of Gulkan *et al.* (1974), involved two simplifications, the reduction of a MDOF model of a structure to a SDOF oscillator and the approximation of the variation of the stiffness properties of the entire structure by a single spring to take account of the nonlinear force-displacement relationships that characterise its properties. Earthquake-simulation experiments of eight small-scale structures were performed and the displacement histories were compared with the results from nonlinear static analyses based on the Q-model. It was shown that the performance of the Q- Model in the simulation of high- and low- amplitude responses was satisfactory for most of the test structures. It was stated that the model would need to be further validated by more experimental and theoretical analyses.

Fajfar and Fischinger (1988) presented a variation of pushover analysis, the N2 method, and assessed it on a seven-storey RC frame-wall building structure that had been experimentally tested in Tsukuba, Japan as part of the joint U.S. – Japan research project,

Kabeyasawa *et al.* (1983), Okamoto *et al.* (1984), Bertero *et al.* (1984), and Fajfar *et al.* (1984). The authors used the uniform and inverted triangular load distributions to perform nonlinear static analyses of the structure. The pushover curves were compared to the dynamic experimental and analytical results showing considerable differences in their shapes. It was noted that the inverted triangular distribution was unconservative in estimating base shear demands due to the effect of higher modes. It was observed that the uniform distribution seemed more rational when shear strength demand was to be assessed. It was also observed that the nonlinear dynamic analysis of the equivalent SDOF system yielded in general non-conservative shear forces compared with the experimental and theoretical results. However the target displacement at the ultimate limit state and the rotations of the floors were approximated satisfactorily compared with the experimental and theoretical results.

Baik, Lee, and Krawinkler (1988) proposed a simplified analysis model for the seismic response prediction of steel frames that was based on the pushover analysis concept but included cumulative damage parameters using the Park-Ang damage model (Park *et al.* 1985). These parameters accounted for the effects of all inelastic excursions and not only for the maximum excursion. The model was tested on 10- and 20- single bay steel structures and was considered to be acceptable for preliminary design purposes. It was noted, that the prediction of damage using the equivalent SDOF model 'deteriorated' with increasing structure height, and in the presence of irregularities. The authors suggested though that the ESDOF nonlinear model could provide better estimation of damage parameters than an elastic multi-storey model.

Deierlein and Hsieh (1990) utilized the Capacity Spectrum method to compare the experimental and theoretical results for the seismic response of a single storey single bay steel frame with the analytical results of a 2D pushover analysis. The frame was modeled with semi-rigid connections. The results showed differences of the order of 10% to 20% between the compared quantities such as the period of vibration, maximum displacement and maximum acceleration. It was concluded that the Capacity Spectrum method could provide reasonably accurate lower and upper bounds on the inelastic response of a structure subjected to strong ground motion.

Gaspersic, Fajfar, and Fischinger (1992), extended the N2 method by attempting to include cumulative damage; a characteristic resulting from numerous inelastic excursions. The test structure was the seven-storey reinforced concrete building tested in the U.S. – Japan research project. The seismic demands for each element were computed in terms of the dissipated hysteretic energy using the Park-Ang model (Park *et al.* 1985). The conclusions drawn were that the dissipated hysteretic energy increased with increasing duration of ground motion, and it was significantly affected by the reduction of strength of the structural elements. They also concluded that when the fundamental period of the structure was much larger than the dominant period of the ground motion, the higher mode effects became an important issue. In this case the input energy and dissipated hysteretic energy of a MDOF system were generally larger than the corresponding quantities in the equivalent SDOF system. The authors suggested that the N2 method was likely to underestimate quantities which governed damage in the upper part of a structure.

Mahaney, Paret, Kehoe and Freeman (1993), utilized the Capacity Spectrum Method in four case studies of structures to evaluate their seismic response after the Loma Prieta Earthquake. The structures analysed included one-storey and two-storey wood-frame residences, an eleven-storey reinforced concrete shear wall building and several framed buildings with brick infilled walls. In that study the ADRS spectra format was firstly introduced. The results indicated that the damped elastic earthquake displacement demands did not necessary equal the actual inelastic displacement demands as had been assumed. This can be attributed to the short predominant period of some of the structures which were not in the permissible region of applicability of the equal displacement rule. However it was stated that the damage predicted by the Capacity Spectrum Method was in good agreement with the observed damage for the eleven-storey reinforced concrete shear wall building. Details for the other buildings were not provided.

Lawson, Vance and Krawinkler (1994) carried out a general assessment of pushover analysis on 2-, 5-, 10-, and 15- storey steel moment resisting frames. The pushover analysis results were compared to nonlinear dynamic analyses results using seven ground motions. Storey deflections calculated from the pushover analyses correlated well with those derived from nonlinear dynamic analyses for the short structures. Additionally, pushover analysis could identify weak stories that led to concentration of inelastic

deformations. For the tall structures large differences between nonlinear static and nonlinear dynamic deflections across the storey levels were observed and the results became sensitive to the applied load pattern indicating that higher mode effects became important. Good correlation of inter-storey drifts from the pushover and nonlinear dynamic analyses results was observed for the short structures while poor correlation was observed in the upper storeys of the tall structures. The accuracy in the evaluation of inter-storey ductility ratios and plastic hinge rotations, decreased with the increasing height of structures especially at the higher storeys. Furthermore, the area under the static load-displacement curve correlated poorly with the dynamic hysteretic energy dissipation and therefore was a poor measure of the cumulative damage demand.

Krawinkler (1996) carried out a general appraisal of pushover analysis. The physical meaning of the modification factors used in the Displacement Coefficient Method was explained in some detail. It was noted that generally the displacement of an inelastic SDOF system will differ from the one of the respective elastic SDOF system. This difference will depend on the extent of yielding and the period of the system. Additionally degradation of the unloading or reloading stiffness could have an effect on the target displacement, though this was found to be only significant for very short-period systems. Strength deterioration was noted to have more adverse effects on the inelastic displacement demands. The magnitude of this effect was said to depend on the strong ground motion duration. P-delta effects were also noted to affect significantly the target displacement of a structure. These effects are dependent on the ratio of the post-yield stiffness to the effective elastic stiffness, the fundamental period of the structure, the strength reduction factor, the hysteretic load deformation characteristics of each storey, the frequency characteristics and duration of the ground motion. Other modification factors would need to be developed to account for different levels of damping, foundation uplift, torsional effects, and semi-rigid floor diaphragms. The effect of load pattern on the sensitivity of the results was acknowledged. The general conclusion about pushover analysis was that the different aspects of structural response that could affect the displacement response should be considered explicitly.

Fajfar and Gašperšič (1996) applied the N2 method to the standard seven-storey reinforced concrete building tested in Tsukuba, Japan in the joint U.S. – Japan collaboration, which had been tackled in previous studies, Fajfar *et al.* (1988), and Gaspersic *et al.* (1992). Three

case studies were carried out. The first corresponded to the actual structure without any modeling modifications. Two additional variants of this model were considered. The first variant considered only the frame structure without the structural wall, and was denoted as Model 1. The second variant, Model 2, considered a weak first storey. These modifications however did not change the initial natural period of the structures. The conclusions drawn from the study were that for structures which vibrated primarily in the fundamental mode the method could provide reliable estimates of global seismic demand. In most cases the demands at the local level in terms of deformation, dissipated energy and damage indices could be adequate enough to be used in practice. The method could detect weaknesses such as storey mechanisms or excessive demands. However, it was also concluded that if higher mode effects became important, some demand quantities determined by the N2 method would be underestimated. Therefore an appropriate magnification of selected quantities could be advantageous. No such recommendations were provided. Additionally, the authors claimed that the N2 method appeared to be not very sensitive to changes in the assumed displacement shape and the corresponding vertical distribution of the loads, as well as the bilinear force-displacement idealisation, which is not in agreement with other studies (Antoniou 2002). The largest uncertainty on the interpretation and comparison of results was thought to have been introduced by the characteristics of the each ground motion. Finally it was acknowledged that bidirectional input and the influence of the coupling of the fundamental translational and torsional modes needed to be incorporated before the N2 method could be extended to the analysis of three-dimensional models of buildings.

Paret, Sasaki, Eilbeck and Freeman (1996) studied the seismic response of two 17-storey steel frame buildings with the purpose of identifying failure mechanisms caused by higher-mode effects. A modal pushover procedure was used which involved several pushover analyses using lateral load patterns based on different elastic mode shapes. The results indicated that the first mode was not critical while the second mode was, thus showing the deficiency in the assumption of pushover analysis that the first mode is dominant in the seismic response of structures. The authors proposed a Modal Criticality Index, being the demand divided by the capacity, in order to assess the importance of modes of vibration other than only the fundamental mode. These values can be directly extracted from the superimposed curves of pushover analyses and of the acceleration-displacement spectra.

Kilar and Fajfar (1996) extended the N2 method with the development of a pseudo three-dimensional model of the structure that could be analysed into the inelastic range. The model consisted of assemblages of two-dimensional macroelements/substructures such as frames, walls and coupled walls. Using a step by step analysis, an approximate base shear-roof displacement curve was computed and the formation of plastic hinges could be monitored. The conclusions of this study were that the proposed use of macro-elements was quite simple in concept and gave satisfactory results. Several important characteristics of nonlinear structural behaviour, especially the strength and the global plastic mechanism were identified.

Faella (1996) carried out both nonlinear static and nonlinear dynamic analyses using artificial and natural earthquake records on 3-, 6-, and 9-storey symmetrical reinforced concrete structures, designed to EC8, which were characterized as high ductility structures standing on stiff soil. Results showed that pushover analysis could identify collapse mechanisms, critical regions that would need particular detailing, and also inter-storey drifts and structural damage. It was suggested that for design purposes, inter-storey drifts and structural damage had to be computed for a top displacement larger than the target displacement calculated from a POA. This could be achieved by the use of a coefficient which numerically increased as the number of storeys increased. However Faella suggested that when carrying out pushover analyses it is necessary to compute the pushover curve at a target displacement higher than the one obtained from a nonlinear dynamic analysis. This would mean that a nonlinear dynamic analysis would be needed before conducting a pushover analysis. In this way though pushover analysis would not be needed therefore this approach is questionable. Finally, it was suggested that further analyses needed to be carried out to verify if this method could be an efficient tool for a range of input ground motion characteristics and for soft soil conditions.

Kunnath, Valles-Matox and Reinhorn (1996) performed a seismic evaluation of a 4-storey reinforced concrete building subjected to five strong ground motions. The prediction of displacements from pushover analyses and nonlinear time-history analyses showed fairly good agreement – with a tendency for pushover analyses to be on the unconservative side. The authors recognized the considerable differences in the time and computational effort

required, for the types of analyses. In terms of time management pushover analysis appeared to be superior.

Reinhorn (1997) studied the response of a three-storey reinforced concrete building that had been retrofitted with visco-elastic dampers. Comparison of results from nonlinear static pushover analysis and nonlinear dynamic analysis suggested fairly good agreement thus showing the effectiveness of the method when the target displacement needs to be estimated.

Fajfar, Gaspersic, and Drobnic (1997), utilised the N2 method to analyse the seismic response of light masonry-infilled frame structures. A series of physical pseudo-dynamic tests were carried out on a full scale four-storey reinforced concrete structure. Pseudo-dynamic seismic tests were conducted first on the bare structure. Then some of the bare frames were infilled and the new structure was subjected to subsequent pseudo-dynamic tests using one artificial ground motion. The results showed that the presence of infilled frames changed the response of the structure significantly. The authors concluded that the N2 method was able to predict adequately the seismic demand and seismic damages since the predicted results were similar to the results obtained by nonlinear dynamic analyses for different accelerograms for all the test structures. The displacement and storey drift demands, and the hysteretic energy dissipation were generally overestimated by the N2 method. This was attributed to the slippage of the reinforcing bars during the dynamic tests which caused relatively slow energy dissipation. It is unclear though if this slippage had been accounted for in the pushover analyses conducted.

Tso and Moghadam (1997) proposed an extension of pushover analysis that included torsional effects, to compute the seismic response of two 7-storey reinforced concrete structures; one being symmetrical and the other asymmetrical. The method included the use of 3D elastic dynamic analyses of the models in order to provide the maximum target displacements for the lateral-load resisting elements. The force distributions across the structures derived from the dynamic analyses were used as static force distributions to carry-out a series of 2D pushover analyses. The results showed good estimates of floor displacements, inter-storey drifts and ductility demands for both types of structures.

Kilar and Fajfar (1997) tested the effectiveness of their proposed method (Kilar *et al.*, 1996) on an asymmetric 21-storey reinforced concrete structural wall building. Some additional results for the symmetric and asymmetric 7-storey structures discussed in Kilar *et al.*, (1996), were also provided. These indicated that generally, a larger ductility is required in an asymmetrical structure in order to develop the same strength as a symmetrical structure. It was concluded that the procedure was an effective tool to estimate the ultimate strength and global plastic mechanism, and provided information on the sequence of plastic yield formation across the structure. It is difficult to draw more substantial conclusions regarding the effectiveness of the procedure because only a few results were presented and the discussion is vague.

Bracci, Kunnath and Reinhorn (1997) introduced an adaptive pushover analysis and tested its effectiveness on a three-storey reinforced concrete frame building by comparing the analytical results with experimental. The target displacement was found to be in agreement with the experimental displacement. The study focused mainly on identification of the failure modes of the structure by inspecting the force-deformation relationships obtained from both experimental and analytical approaches.

Naeim and Lobo (1998) attempted to identify some potential pitfalls when carrying out a pushover analysis and summarised ten important aspects which should be considered preceding the analysis. These were:

- The importance of the loading shape function should not be underestimated. The effect of three load patterns, Uniform, Triangular, FEMA, was checked on a two-storey reinforced concrete frame. The pushover curves showed differences in the global base shear- roof displacement response of about 10%, which do not seem particularly significant
- Performance objectives should be known before the building is 'pushed'.
- If the building is not designed, it cannot be pushed.
- Gravity loads should not be ignored.
- The structure should not be pushed beyond failure unless the engineer can model failure. This has to do mainly with the available computer codes being incapable of

modelling post-failure behaviour of structural components. It was suggested that the pushover analysis should be stopped at the onset of the first failure mechanism.

- Attention to rebar development and lap lengths should be given.
- Shear failure mechanisms should not be ignored.
- P-Delta effects should be adequately included; otherwise the results obtained could be unconservative. An example of the base shear-roof displacement responses of a ten-storey frame model with and without P-Delta effects showed a difference of the order of 10% for the base shear.
- The pushover loading should not be confused with the real earthquake loading.
- Three-dimensional buildings may require more than a planar 'push'.

Krawinkler, Seneviratna (1998) carried out a study of a four-storey steel perimeter frame structure in order to assess the effectiveness of pushover analysis. Comparison of pushover inter-storey drifts with the nonlinear dynamic inter-storey drifts showed good agreement. It was concluded that for regular-low rise structures where higher modes are not important and in which the effect of inelasticity is distributed approximately uniformly the method could give good predictions. It was suggested that pushover analysis could be implemented for all structures but it should be complemented with other evaluation procedures if higher modes were judged to be important. Furthermore, the importance of higher mode effects was thought to depend on the number of storeys and on the relative position of the modal periods of the structure regarding the design spectrum.

Satyarno, Carr, and Restrepo (1998), attempted to refine pushover analysis by introducing a compound spring element in the computer program RUAUMOKO capable of modelling plastic hinge regions that could take into account the flexural and shear properties of typical beam-column joints of existing reinforced concrete frame structures. The idea behind this element was that shear and/or flexural failure modes can occur after certain critical regions of the structure sustain significant inelastic flexural rotations. The authors argued that there can be a shift in the structures' response from a flexural failure mode to a shear failure mode and this feature needs to be properly accounted for in pushover analyses. Additionally the authors suggested an adaptive pushover method that utilised Rayleigh's equation for calculating the period of vibration of the structure at every force increment.

The authors tested the spring model on a typical beam-column joint and compared the results with experimental values. The agreement between these two approaches seemed reasonable. Then the authors applied four different load patterns - named as uniform, outward parabolic, code and inward parabolic- to a six-storey reinforced concrete frame and studied the effect of excluding and including shear-flexure interaction for modelling plastic hinge regions on the capacity curves. Results showed that shear failure can cause a significant different pushover curve than that just considering flexural characteristics especially in the post-elastic stage of response. However results of maximum displacement estimates or other seismic demands of interest were not provided and no comparison was carried out with nonlinear dynamic analyses results.

Aschheim, Maffei, and Black (1998), performed a comparison of the Capacity Spectrum Method and the Displacement Coefficient Method with results from nonlinear dynamic analyses for a large number of SDOF systems with various periods, strengths, and hysteretic models and on a three-storey reinforced concrete building. For the SDOF systems the authors concluded that the displacement estimates from the pushover methods could be either conservative or unconservative, and showed great variability. None of these methods was reported to show any superiority on the accuracy of these estimates. Additionally, for the three-storey structure the authors concluded that the pushover methods could both underestimate and overestimate significantly the displacement demands caused by various ground motions. In the case of short period structures the displacement estimates were most probably overestimated. The main factor causing these differences was the variability of the individual ground motions used.

Kim and D'Amore (1999) performed a case study of a six-storey building structure to illustrate that the distribution of damage in the structure during earthquakes predicted by the pushover analysis procedure could not be adequately monitored. Their case study demonstrated that the use of maximum roof drift as a damage measure was too simplistic and maybe inadequate. In addition the pushover procedure was not satisfactory when the structure was subjected to impulsive earthquakes such as the Kobe earthquake. Lastly it was noted that the pushover analysis procedure could not predict the cyclic hysteretic energy demand and fundamentally ignored the dynamical nature of the building responses

during earthquakes. It was realized though that the pushover analysis was perhaps more realistic than the existing code procedure for evaluating seismic vulnerability of structures.

Gupta and Kunnath (1999) performed an evaluation of pushover analysis on four isolated reinforced concrete walls with 8, 12, 16 and 20- storeys. The authors utilized two conventional load patterns (FEMA and uniform), and a load pattern that changed continuously depending on the instantaneous dynamic properties of the system. The results were compared with the results of the nonlinear dynamic analyses. Two critical issues concerning these types of structures were identified: amplification of base shear demands due to higher mode effects, and progressive yielding. It was shown that the adaptive load pattern was able to capture accurately the base shear amplification and progressive yielding while the other two patterns calculated base amplification demands of less than 50% of the 'exact'.

Iwan (1999) investigated the applicability of the Capacity Spectrum Method for the analysis of structures subjected to near-fault ground motions. The method was applied to SDOF and MDOF bilinear hysteretic systems. Details of these systems were not provided in the paper. The conclusions regarding SDOF systems were that the CSM method did not give satisfactory results except for a very limited short-period range being near the dominant pulse period of the ground motion. Additionally, the performance points obtained using the equivalent viscous damping resulted in underestimation of the true inelastic response of SDOF systems with periods shorter than the predominant period of the earthquake pulse. The author stated that studies of MDOF systems showed that elastic SDOF analyses and elastic MDOF analyses correlated well only for structural periods shorter than the ground pulse duration. It was concluded that the Capacity Spectrum Method provided a reasonable estimation of the maximum roof displacement. However, for taller buildings it proved to be insufficient to predict the demands in the upper storeys.

Kuramoto and Teshigawara (1999) studied the effectiveness of the Capacity Spectrum method for three reinforced concrete buildings of 6, 10 and 19 stories and three steel buildings of 5, 10 and 20 storeys. For each building structure, four variants were considered, one regular and three irregular variants. The irregularities were a soft first storey, a stiff first storey and soft middle storeys. The results showed that the SDOF

approximation of a MDOF system appeared to be satisfactory in most of the cases. For the soft first- and stiff first-storey models the SDOF idealisation resulted in good agreement with nonlinear dynamic MDOF responses for all structural types and numbers of storeys. Regarding soft-middle storey models the responses derived from the SDOF analysis were somewhat smaller than the MDOF responses across the whole height of the buildings. The deficiency of the method to capture higher-mode effects was again pointed out.

Kunnath and Gupta (1999a) introduced a spectrum-compatible pushover analysis method. The main differences between the conventional pushover analysis and the proposed method were that the latter included site-specific ground motion characteristics and secondly the applied load pattern changed depending on the instantaneous dynamic properties of the system. The proposed method was evaluated using a 14-storey moment-resisting frame. The results showed superiority of the method with respect to the conventional ones to capture plastic hinging especially in the upper stories when compared to the nonlinear dynamic analysis results. It was also concluded that the smooth spectra mostly used in the conventional methods were not sufficient to identify hinging at the upper stories. It was proposed that the method should be carried out on a greater number of structures to identify its potential.

Kunnath and Gupta (1999b) compared the responses of an 8-storey building derived from the spectra-compatible pushover method and the conventional pushover method. The superiority of the spectra-compatible method to the conventional pushover method for capturing upper-storey demands was pointed out, when results were compared with nonlinear dynamic analysis results. It was observed that the square root of the sum of the squares (SRSS) combination used, tended to magnify some modal contributions and this resulted in an underestimation of the lower- storey demands.

Matsumori, Otani, and Shiohara (1999) investigated the accuracy of pushover analysis in the estimation of ductilities across the floor levels on two 12-storey and three 18-storey reinforced concrete structures. The authors utilized two new lateral load patterns which were the sum and the difference of the storey shear distributions for the first two modes of vibration. Results showed that the ductility demands obtained were an upper bound when compared to nonlinear dynamic analysis results.

Chopra and Goel (1-2) (2000) suggested an improved capacity-demand-diagram method that used constant ductility design spectra for estimating the deformation of inelastic SDOF systems. The method suggested that the target displacement would be given by the intersection point where the ductility factor calculated from the capacity diagram matched the value associated with the intersecting demand curve. The authors pointed out that the original ATC-40 procedure underestimated significantly the deformation of inelastic systems for a wide range of natural periods T_n and ductilities μ compared to the deformation demands determined from the inelastic design spectrum. Several deficiencies in the ATC-40 procedure A were found since it did not converge for some of the systems analyzed. Also in the cases in which it did converge it yielded deformation estimates and ductility factors that were significantly different to those obtained from a nonlinear time-history analysis. Some of the analyses showed that the above parameters were underestimated with up to a 50% error. Furthermore, the authors concluded that the ATC-40 procedures were deficient relative even to the elastic design spectrum in estimating the peak deformation of an inelastic system with period T_n in the velocity-sensitive or displacement-sensitive regions of the spectrum.

Yang and Wang (2000) applied the pushover method to three frame structures of 8, 12, and 15 storeys and compared the results with nonlinear time-history analyses. The results provided were estimates of roof displacement and floor rotations. In one case a difference of up to 30% could be observed but generally results could be deemed satisfactory. The differences in the results were mainly attributed by the authors to the frequency contents of the ground motions used. Also it was noted that the bilinear representation of the pushover curves introduced errors in the estimation of the base shear and the yield displacement. These in turn resulted in differences in the calculated responses between analyses.

Hosseini and Vayeghan (2000) recognized that some irregular buildings that had been designed using recent seismic codes had shown some vulnerability against earthquakes. Their observations led them to the conclusion that there was some need for further modifications to the design standards. They investigated the three-dimensional response of an existing irregular 8-story steel building designed according to the Iranian National Seismic Code by performing three-dimensional linear dynamic and nonlinear pushover analyses. Time-history analyses were performed by applying accelerograms of some local

earthquakes in different configurations to account for possible cases of seismic response. The response quantities that were investigated and compared were the displacements in different levels of the building, shear and axial forces and also bending moments in some corner, side and middle columns and some bracing elements, and finally the stresses in the critical members. Their numerical results showed that in the case of multi-component excitations the response values could be much higher than those predicted by code recommended loadings. Furthermore, it was observed that by considering geometric and material nonlinearity the ultimate sustained displacement of the building was decreased. Finally it was concluded that the nonlinear behaviour of the building was very different from that assumed in the Code Seismic Analysis. This difference was very obvious for the corner columns. Therefore further modifications would be needed in the code for considering irregular buildings.

Albanesi, Nuti, and Vanzi (2000) proposed the use of variable-damping response spectra in the pushover method proposed in ATC-40 document to evaluate seismic response of nonlinear structures in terms of the maximum displacement and acceleration, given the structural initial elastic period, the yielding acceleration and the hardening ratio in the plastic range. The somewhat improved procedure was used to study elastoplastic and Takeda degrading hysteretic SDOF systems and also a two-storey and a seven-storey existing reinforced structures. The results showed much variation in responses between hysteretic models and not any clear improvement on the effectiveness of the method. The degrading Takeda model was found to be more appropriate for modeling concrete behaviour than the elastoplastic model even though the applicability of the latter was thought to be satisfactory.

Peter and Badoux (2000) applied the capacity spectrum method to a 9-storey reinforced concrete building with reinforced concrete and masonry structural walls. The structure was subjected to two strong ground motions. Three types of lateral load patterns were used to simulate seismic behaviour in a static manner. These were the uniform distribution, the modal distribution and the modal adaptive force distribution. The conclusion the authors drew from their study were that the CSM method was adequate to estimate seismic demands such as inter-storey drifts. Furthermore, the uniform load pattern proved to be quite effective. A need for more reliable structural models was acknowledged.

Magenes (2000) investigated the application of pushover analysis to a two-storey masonry structure and compared the results with experimental data. It was found that pushover analysis was able to capture the overall strength and the failure mechanisms of the structure with a maximum error of 10%. It was pointed out though that more verification work was needed to reinforce these conclusions and generalize the method.

Gupta and Kunnath (2000) investigated the effectiveness of the adaptive-spectra pushover procedure with respect to the other conventional pushover methods and the nonlinear time-history analyses on five reinforced concrete structures of 4, 8, 12, 16, and 20 storeys. The results indicated increasing deviations in inter-storey drift responses for increasing height of buildings, between the conventional pushover methods and the nonlinear time-history analyses. It was also noted that great care should be taken when interpreting results from pushover analyses because they could obscure real deficiencies in a structural system and lead the engineer to recommend retrofitting of the structure when it is not needed while failing to address the real deficiencies. For the taller structures the adaptive method was able to incorporate higher-mode effects and therefore provided reasonable estimates of inter-storey drifts and plastic hinge locations.

Skokan and Hart (2000) carried out nonlinear static pushover analyses on three steel moment-resisting frame buildings – 3-storey, 9-storey and 20-storey - using two different variations of analyses being, the Coefficient Method, the Capacity Spectrum Method and compared the results with those obtained from nonlinear time-history analyses. The quantities of most interest in their research were the maximum roof displacement, and the maximum inter-storey drift. Their results depicted that the Coefficient Method provided estimates of maximum roof displacement and inter-storey drift within 20% of the results from nonlinear time-history analyses. On the other hand the Capacity Spectrum Method tended to underestimate seismic demands. The demand comparisons were found to be relatively insensitive to the analytical model and load pattern. Moreover, maximum inter-storey drift demands were found to be load pattern dependent.

Fajfar (2000) applied the N2 method to a four-storey reinforced concrete frame structure subjected to three ground motions. The results were said to have been compared with experimental data provided from pseudo-dynamic tests of the model. The method was

deemed acceptable for estimating seismic demands in planar structures. It was noted though that the type of spectra used were not adequate for estimating seismic response from near-fault ground motions, for soft soils, for hysteretic loops with significant stiffness or strength deterioration and for systems with low strength. These arguments were provided though as conclusions and were not explained at all.

Requena and Ayala (2000) discussed two variations of adaptive pushover analysis mainly concerned with the estimation of the contribution of the higher modes of vibration in the seismic response of building structures. These variations have been discussed in section 2.4.5, named as approach 2-A, and approach 2-B. The approaches together with the fundamental mode distribution were tested on a 17-storey reinforced concrete frame and results of maximum displacement, inter-storey drifts and plastic hinge locations were compared with results from nonlinear dynamic analyses. Good agreement was achieved by both proposed methods with approach 2-B being slightly more efficient than 2-A. Furthermore, the authors investigated the changes in the first three modes of vibration of the structure when it behaved nonlinearly through a nonlinear static analysis. The authors concluded that stiffness degradation of the structure influenced more the fundamental mode shape than mode shapes corresponding to higher modes. Furthermore it was suggested that the changes in the modes of vibration need to be considered in this type of analysis.

Kunnath and John (2000) and Lew and Kunnath (2001) examined the effectiveness of conventional pushover procedures for seismic response analysis of a 6-storey and a 13-storey steel building and a 7-storey and a 20-storey reinforced concrete building. The results presented showed that the pushover procedures (FEMA 273/356) were generally not effective in predicting inter-storey drift demands compared to nonlinear dynamic procedures. Drifts were generally underestimated at upper levels and sometimes over-estimated at lower levels. The peak displacement profiles predicted by both nonlinear static and nonlinear dynamic procedures were in agreements. This suggested that the estimation of the displacement profile at the peak roof displacement by nonlinear static procedures was reasonable so long as inter-storey drifts at the lower levels were reasonably estimated. Finally they stated that nonlinear static methods did not capture yielding of columns at the upper levels. This inability could be a significant source of concern in identifying local upper story mechanisms.

Kim, Kim, and Kim (2001) dealt with the evaluation of ductility using pushover and nonlinear dynamic analyses. The example structures that have been used were a 7-, 15-, and 25-story building. Two ground motions were considered. The main parameters of interest in the study were the displacement estimates and ductility estimates obtained from pushover and nonlinear dynamic analyses. The results showed that the target displacement from pushover analysis was considerably overestimated compared to the nonlinear dynamic analysis results, especially in the case of the 25-storey building. The estimates of ductility from pushover analysis were generally satisfactory but conservative, something that is not on the safe side. In the case of the 25-story building the ductility was overestimated significantly showing that the nonlinear static analysis did not estimate correctly the higher mode effects. Additionally the authors showed that the plastic hinge rotation from a pushover analysis will gradually increase as the structure is damaged but this is not the case in the nonlinear dynamic analysis where plastic hinge rotations can become zero due to the alternating direction of the seismic loading for the same damage state of the structure. Finally the superiority of the nonlinear dynamic analysis procedure in reflecting more exactly the hysteretic characteristics of seismic behaviour and higher mode effects was noted.

Fuentes, Sakai, and Kabeyasawa (2001) studied the difference in the deformation response of various systems when they were subjected to different ground motions. Their response was primarily influenced by the seismic load pattern used and was a consequence of the presence of higher mode response. The study identified that the gap in the storey drift response from pushover and time-history analysis grew larger as the period of the structure increased. Another observation from the results was the insignificant difference in the global displacement estimates obtained using the three different lateral load patterns. However, it was found that storey drifts and local responses were consistently underestimated by the pushover analyses. The magnitude of the storey drift underestimation grew larger for longer structural periods. Moreover large differences in the ratio of the storey drift from the pushover analysis compared to the dynamic analysis storey drift appeared because of the different ground motions used. It was suggested that further investigation on the causes of these variations due to seismic input was needed.

Memari, Rafiee, Motlagh and Scanlon (2001) performed a comparative evaluation of current seismic assessment methodologies on a 32-storey reinforced concrete building. The authors suggested that pushover analysis is a good tool for approximating seismic demands in the lower storeys of tall structures. The predictions have a better agreement with the nonlinear time-history analyses for larger peak ground acceleration values. The mode of failure though for the structure could not be safely predicted by pushover analysis, something that is worrying since the identification of the failure mode of a structure by pushover analysis has been considered as one of the virtues of the method.

Mwafy and Elnashai (2001) studied the seismic response of twelve reinforced concrete buildings using nonlinear static and nonlinear dynamic analyses. The buildings were divided into three general groups: four 8-storey irregular frames, four 12-storey regular frames and four 8-storey dual frame-wall structures. It was found out that in all cases the responses of the buildings were sensitive to the shape of the lateral load pattern. Also the multi-mode pattern did not appear to provide enhanced results with respect to the other conventional load patterns. Bigger discrepancies in demands were observed for the last group of structures as the amplification of base shear could not be predicted by pushover analyses. The latter conclusion confirmed findings of Krawinkler *et al.* (1998).

Lew and Kunnath (2001) examined the effectiveness of nonlinear static procedures to capture the seismic response of two steel – 6-storey and 13-storey - and two reinforced concrete buildings – 7-storey and 20-storey. The conclusions that were drawn from this study were that nonlinear static procedures were not effective in capturing inter-storey drifts and locations of plastic hinges for any type of the tested structures especially at higher-storeys. The peak displacement profiles calculated from all procedures were in agreement though.

Mostafei and Kabeyasawa (2001) attempted to correlate results between nonlinear time-history analysis and the Capacity-Spectrum method for an eight-storey plane frame-wall reinforced concrete building. Discussion mainly targeted modeling issues such as the choice of hysteretic material models and gave little information on the accuracy of the results obtained. The output of the study was solely the target displacement which was

approximated satisfactorily from the pushover analysis. The authors concluded that a more rationalised version of the method was needed but no suggestions were made.

Chopra and Goel (2001) developed the so-called Modal Pushover Analysis procedure (MPA). Their estimates of the seismic story-drift demands were accurate to a degree that should be sufficient for most building design and retrofit applications. With the inclusion of a few modes, the height-wise distribution of seismic storey drift demands determined by MPA was similar to the 'exact' results from nonlinear RHA. Their procedure was much more accurate compared to the results obtained using the force distribution specified in FEMA-356. Also the computational effort was comparable to the FEMA-356 procedure that required pushover analysis for at least two force distributions. However the procedure was inadequate when local response quantities were estimated.

Albanesi, Biondi, and Petrangeli (2002) suggested an energy-based approach for pushover analysis – presented in section 2.4.5- and studied its efficiency on two reinforced concrete frame structures – a three-storey three-bay frame and a seven-storey two-bay frame. The results were compared with nonlinear dynamic analyses results and with the conventional Capacity Spectrum Method results using both force- and displacement- control incremental analyses. The capacity curves derived using all methods were very similar for the three-storey structure but quite different for the seven-storey structure, showing that deviations in the response can occur due to using either force-controlled or displacement-controlled nonlinear static analyses. The use of force-controlled or displacement-controlled nonlinear static analyses in the Capacity Spectrum method can cause significant differences in the estimation of the seismic demands. Furthermore, the results showed in general underestimation of maximum displacement and base shear from both the conventional and the proposed method with respect to the dynamic analyses results.

Penelis and Kappos (2002) performed a 3D pushover analysis with the purpose of including torsional effects. This was achieved by applying load vectors at the mass centre of two single-storey structures, one being torsionaly restrained and the other torsionaly unrestrained. The load vectors were derived from dynamic elastic spectral analyses. The equivalent SDOF system properties included translational and torsional characteristics,

though the transformation equations were not explained sufficiently. Results were too vague to draw any substantial conclusions on the method.

Williams and Albermani (2003) evaluated the performance of pushover methods in the design of unretrofitted frames or frames fitted with hysteretic and frictional dissipative devices. The structures were 3-, 6- and 10-storey steel moment resisting frames. The results showed good agreement in the demands between pushover analysis methods and nonlinear time-history results for the unretrofitted frames. However the pushover procedures were less effective at determining the seismic demands in retrofitted frames as the additional energy dissipation resulting from the dampers could not be taken into account. Out of the procedures used it was observed that the Modal Analysis procedure appeared to be the most superior.

İnel, Tjhin, and Aschheim (2003) evaluated the accuracy of five different load patterns used in pushover procedures. The load patterns assessed were the Modal, Inverted Triangular, Rectangular, Code, Adaptive First Mode and the Multimodal. The test structures were two steel-moment resisting frames, 3- and 9-storeys and two variants of these to include weak storey behaviour. In general, results of this study showed quite good agreement for all structures and all load patterns in the estimation of the target displacement. However there was a consistent underestimation of the inter-storey drifts even from the Multimodal pattern, even though this underestimation was less than the other load patterns. Storey shears were generally underestimated in the lower storeys and overestimated in the upper storeys. Finally the overturning moment was evaluated satisfactorily for the regular frames from the Multimodal load pattern. The other load patterns could not account for contributions in the response from higher-mode effects.

Jingjiang, Ono, Yangang, and Wei (2003) proposed a two-phase load pattern: an inverted triangular load pattern until the base shear reached some fraction β of its maximum value followed by an exponential form pattern defined as $(x/H)^a$ where x is the distance from the ground to the floor, H is height of the building and a is a characteristic parameter for different types of buildings. The authors performed pushover analyses with two more load patterns –uniform and triangular- for three groups of reinforced concrete buildings. These groups were seven frame buildings of 4-, 4-, 5-, 6-, 6- and 8-storeys, two frame-wall

buildings of 9- and 20-storeys and three shear walls of 6-, 10- and 16-storeys. It was concluded that the inverted triangular and the proposed load patterns were the most effective in estimating the target displacements for the frame buildings. Regarding the second group the uniform and the proposed load patterns were satisfactory for the 9-storey but unsatisfactory for the 20-storey building. The conclusions drawn for the last group were that the uniform and the proposed load patterns produced good results for low-rise shear walls but poor for mid- and high-rise walls. However, vague explanation was provided of the criteria needed to determine at which magnitude of base shear the conventional load pattern should change to the proposed one. For the frame structures the authors changed the load pattern at a half the value of maximum base shear while for the remaining buildings the load pattern was altered at 70-80% of the maximum base shear.

Chopra, Goel and Chintanapakdee (2003) assessed the assumption usually implemented in pushover analyses that the roof displacement of a building could be estimated from the deformation of its equivalent single-degree-of-freedom system. The test structures used were two groups of steel moment-resisting frames. The first group consisted of one-bay frames of six different heights: 3, 6, 9, 12, 15, and 18 storeys. The second group consisted of two buildings of 9, and 20-stories. The most important observation was that the SDOF systems with high ductility overestimated the roof displacement and this overestimation increased for longer-period systems. The above situation was completely reversed for low ductility SDOF systems. Furthermore the authors concluded that sometimes the use of the ESDOF system can lead to wrong conclusions of the collapse state of the structure. In other words, while it may be found that the ESOF system has collapsed the building as whole might have not.

Jan, Liu and Kao (2003) proposed an upper-bound pushover analysis in order to estimate seismic demands in high-rise buildings. The proposed procedure attempted to include higher-mode effects through the use of modal contribution ratios, on a new lateral load pattern for determining the target roof displacement, inter-storey drifts and plastic hinge rotations. Five steel moment-resisting frame buildings of 2-, 5-, 10-, 20-, and 30-storeys were analysed to compare the effectiveness of the proposed procedure with other conventional and modal pushover methods. The pushover analysis results were compared with results from nonlinear dynamic analyses. It was found that the proposed procedure

mostly overestimated seismic demands in the upper storeys and underestimated them at the lower storeys. The conventional procedure predicted the opposite behaviour to the proposed procedure except that plastic hinge rotations could not be identified. The modal pushover analysis procedure behaved similarly to the conventional procedure. However the authors claimed that the inclusion of the first two modes could provide reasonable estimates of target displacements, something that was not reflected in the results of their study.

Almeida and Barros (2003) proposed a multimodal load pattern in order to include the effect of the higher modes of vibration. The proposed load pattern was based on the relative participation of each mode of vibration derived from the elastic response of the structure. The pattern was applied to three-dimensional structure models: a symmetric structure, a stiffness asymmetric structure, and a mass asymmetric structure. Analyses considered also the effect of direction of the ground motion. The results showed that the proposed load pattern was more effective in capturing torsional effects than the load pattern proportional to fundamental mode shape, especially for the mass asymmetric structure.

Makarios (2004) attempted to optimize mathematically the definition of an equivalent single-degree-of-freedom system needed in pushover analysis. This was done by optimizing the capacity curve when it is transformed to a bilinear form. The proposal was evaluated on a nine-storey reinforced concrete regular-frame building. The method could provide with two iterations a reasonable accuracy of the target displacement with an error of 1 to 8%.

Hernandez-Montes, Kwon, and Aschheim (2004), attempted to use an energy-based formulation for first- and multiple-mode nonlinear static pushover analyses. The method was presented in section 2.4.5. The proposed method was compared with the conventional pushover analysis of a three-storey steel frame. It was concluded that the energy-based formulation provided a stronger theoretical basis for establishing the capacity curves of the first and higher mode equivalent SDOF systems by avoiding load reversals of the nonlinear static curves. The results provided a good estimate of target displacement with up to 10% error.

Matsumori and Shiohara (2004) compared results from nonlinear earthquake response analyses and static pushover analyses of two 12-story and three 18-story structures. Their main objective was to estimate member deformation demands, the distribution of storey displacements and member ductility demands across the structures' heights. According to their results the earthquake response analyses of the mentioned structures above, yielded ductility demands that varied significantly with different ground motions and structures. Secondly they concluded that the earthquake responses could be reasonably estimated by the results of pushover analyses by using a story shear distribution corresponding to the sum and the difference of the first two modes.

Chintanapakdee and Chopra (2004) investigated the effects of stiffness, strength and combined stiffness-and-strength irregularity on seismic demands of strong-column-weak-beam frames through MPA and nonlinear time-history analyses. The effects of strength irregularity were found to be larger than stiffness irregularity and the effects of combined-stiffness-and-strength irregularity were found to be the largest among the three on the estimation of the storey drifts across the floors. The authors concluded that the MPA procedure was quite effective in capturing demands independently of the irregularity of the structure. However it was argued that the MPA procedure could give inaccurate results for frames with strong first storey or strong lower half.

Goel and Chopra (2004) carried out an evaluation study of Modal and FEMA pushover procedures on three 9-storey and three 20-storey buildings subjected to twenty ground motions. The 'exact' dynamic response of the buildings was computed using nonlinear time-history analyses. For the FEMA pushover procedure the authors used four different load patterns and for the Modal Pushover method the first three modes of vibration were considered. The results showed that the FEMA load distributions underestimated story drifts by up to 75% and failed to estimate reasonably the plastic rotations at the upper storeys for all buildings. The Uniform Load distribution was considered unnecessary because it grossly underestimated the displacement and rotation demands at the upper storeys and grossly underestimated them in the lower storeys. The MPA procedure showed to be more adequate in identifying the above seismic demands when compared to the nonlinear time-history analyses. The effect of P-Δ effects was also studied. It was observed that P-Δ effects could be significant if the building is deformed much into the

inelastic stage where strength and stiffness degradation lead to negative post-yield stiffness as observed in the some of the pushover curves presented. However P-Δ effects did not seem to affect the behaviour of all the structures studied. No explanation was provided on the cause of this.

Antoniou and Pinho (2004) presented a displacement-based adaptive pushover procedure. The method used monotonic lateral incremental displacements instead of monotonic lateral incremental forces to obtain the capacity curves. The authors applied it to twelve reinforced concrete buildings and compared the results with the force-based method and with nonlinear time-history analysis. It was concluded that the method was able to provide improved predictions of demands with respect to the conventional method but could not reproduce results from the nonlinear time-history analysis. This was appointed to the static nature of the method that was used to the possible incorrect updating of the displacement vector.

Kunnath (2004) proposed a modal combination rule, section 2.3.2, similar to the one proposed by Matsumori *et al.* (1999). The author applied a number of load distributions based on the modal combination rule, to an eight-storey and a sixteen-storey reinforced concrete building. The pushover analyses results provided from the DCM method, were compared with those from nonlinear time-history analyses of a typical ground motion. These indicated quite good agreement in the estimation of the inter-storey drifts in the eight-storey building but inappropriate for the upper levels in the case of the sixteen-storey building.

Lin and Pankaj (2004) and later Pankaj and Lin (2005) examined the influence of strain rate and material modeling on the seismic response of a four-storey reinforced concrete frame structure. Two pushover procedures namely the Displacement Coefficient Method and the Capacity Spectrum Method were utilized and subsequently compared to results from five nonlinear dynamic analyses. The material models used were the Drucker-Prager (DP) and Concrete-Damage Plasticity (CDP) models. The influence of strain rate on the seismic analysis of reinforced concrete structures was found to be small, in agreement with other studies (Bischoff *et al.* 1991). The study showed that the target deformation values at the control node from all analyses were in reasonable agreement; however there were some

differences in the internal force responses. This study showed that material models used could influence the estimation of seismic demands.

Papanikolaou and Elnashai (2005 a & b) evaluated the conventional and adaptive pushover analyses on eight structural building models. These comprised two twelve-storey regular reinforced concrete structures of high and low ductility class, two eight-storey shear wall type structures of high and low ductility class, two eight-storey irregular structures of high and low ductility class, a four-storey reinforced concrete frame structure with irregularity in plan, which had been experimentally tested, Pinho *et al.* (2000), and a three-dimensional three-storey reinforced concrete frame with irregularities in plan and elevation. The results were compared with nonlinear dynamic analyses results. It was shown that pushover analysis can approximate displacement demands for structures that are free of irregularities in plan and elevation. The adaptive pushover procedure did not improve the results much in any of the cases thus not showing any clear advantages over the conventional pushover procedure. This was mainly attributed to the fact that at very high inelastic deformations, or in cases of brittle failure of the structure, the adaptive procedure is compromised because the load vector cannot be updated due to difficulty in solving the eigenvalue problem at every time step. In the case of the three-dimensional structure the authors stressed the need for refinement of pushover analysis to account for torsional effects.

Dolsek and Fajfar (2005) extended the N2 method to approximate the seismic response of two 4-storey infilled reinforced concrete frame structures. The basic differences from the standard N2 method were the multi-linear instead of bilinear idealisation of the pushover curve thus taking into consideration the strength degradation of the infill and the new proposed R-μ-T relationships proposed by Dolsek *et al.* (2004). The results obtained showed an overestimation of storey drifts in the first storey and underestimation in the rest of the storeys with respect to the nonlinear dynamic analysis results. However there was no clear presentation of the load pattern used and no comparison of other seismic demands was carried out.

Goel and Chopra (2005) studied the three-storey steel building presented in Hernandez-Montes *et al.* (2004), in order to explain the reversal of the higher-mode pushover curves and suggest ways that could avoid these reversals. The explanation that was given was that

these occurred after the formation of a mechanism if the resultant force above the mechanism was in the direction that moved the roof in a direction opposite to that prior to formation of the mechanism. It was suggested to always check if the building deformed beyond the elastic stage which would most probably be the case in most buildings for intense ground motions. The higher-mode contributions to the seismic demands could then be estimated from the elastic part of the pushover curve. Finally the study showed again that higher-mode pushover analyses could detect local storey mechanisms that could not be identified by conventional pushover methods.

Tjhin, Aschheim, and Hernandez-Montes (2005, 2006) evaluated the energy-based pushover method proposed by Hernandez-Montes *et al.* (2004) by studying the behaviour of five building models; a three-storey and an eight-storey steel moment-resisting frames, a reinforced concrete wall building and two weak storey variants of the steel frames. The results showed that the proposed method was in general satisfactory to approximate the target displacements and inter-storey drifts. Furthermore, it was pointed out that conventional pushover procedures tended to underestimate the roof displacements. Questionable estimates were obtained for the storey shears and the overturning moments. The authors prompted for more clarification of the cases where these methods could be reliable.

Moghaddam and Hajirasouliha (2006) investigated the accuracy of pushover analysis when seismic demands need to be estimated for braced steel frames. Three steel braced frames of 5-, 10-, and 15- storeys were considered. Three different load patterns were used; the first-mode distribution, the uniform distribution and the inverted triangular distribution. The results showed significant sensitivity to the choice of the load patterns for all the structures and were generally inaccurate. In this study the authors proposed a modified-shear building model that incorporated shear-type and flexural-type characteristics using springs to account for the shear and the additional flexural displacements of the building floors. The results were similar the conventional results and did not show much improvement. However the simplified model they proposed was computationally efficient and could predict the behaviour very similarly to the detailed model.

Kalkan and Kunnath (2006) proposed an Adaptive Modal Combination procedure described previously in section and applied it on a 6- and a 13-storey steel building structures. The results from this procedure were compared to the conventional pushover method using the mode shape load distribution, the MMPA method and the nonlinear dynamic analysis results. The authors performed the nonlinear dynamic analyses using a range of far-field and near-fault strong ground motions. The quantities of interest in this study were the displacement demands, and inter-storey drift demands. The results showed that the MMPA method and the AMC method were satisfactory at estimating seismic demands across the floor levels but not in all cases. Additionally, the conventional pushover procedure was found to underestimate the displacement and inter-storey drift demands.

Kalkan and Kunnath (2007) investigated the accuracy of pushover procedures for the seismic evaluation of buildings. These were the conventional pushover analysis using the Mode Shape load distribution and the Uniform load distribution, the Modified Modal Pushover Analysis, MMPA, the Upper-bound Pushover Analysis, and the Adaptive Modal Combination Procedure, AMC. These were applied to a 6- and 13-storey steel building, and to a 7- and a 20-storey RC moment frame building. The results from these analyses were compared to the results from nonlinear dynamic analyses based on the behaviour of these buildings to far-field and near-fault ground motions. The quantities of interest in this study were the displacement demands, inter-storey drifts and rotation demands. The study found that the conventional pushover analysis overestimated the displacement demands in the low and intermediate storeys for all buildings and ground motions. The upper-bound pushover analysis on the other hand underestimated the displacement demands. The MMPA and the AMC procedures overestimated the displacement demands but with the smallest error. These last two procedures predicted very similar results. Regarding the inter-storey drift demands the conventional pushover procedures significantly underestimated the drifts in the upper storeys and overestimated them in the lower storeys for most of the buildings. The upper-bound pushover analysis on the other hand, overestimated the drifts in the upper storeys and underestimated them in the lower storeys. The MMPA and the AMC methods performed slightly better with reasonable accuracy in the lower storeys but with overestimation in the upper storeys for most of the buildings. Finally the plastic rotation demands were compared between the MMPA, AMC and nonlinear dynamic analyses only.

It was found that that the MMPA was able to capture the rotation demands mostly in the lower storeys. The AMC procedure was the most effective for estimating this quantity across the buildings' floors.

2.7 CONCLUSIONS

A number of conclusions can be drawn from the above review of pushover analysis. Firstly, pushover analysis is becoming a standard seismic assessment and design tool even though its predictions are sometimes not on the safe side. The studies reviewed have concentrated on applying the pushover procedure to moment-resisting frames, structural walls, and wall-frame systems. It has also been applied to bridges and offshore structures though these applications have not been discussed herein.

The review has shown that for structures that vibrate primarily in the fundamental mode the method will provide good information on many of the response characteristics. These include as discussed in Krawinkler *et al.* (1998):

- Realistic estimates of force demands on potentially brittle elements, such as axial forces on columns, forces on bracings, moments on beam-to-column connections, and shear forces on deep beams.
- Estimates of deformation demands for elements that have to deform inelastically in order to dissipate energy imposed to the structure by ground motions.
- The effect of strength deterioration of individual elements on the behaviour of the structural system.
- Identification of critical regions in which the deformation demands are expected to be high and that therefore have to become the focus of careful detailing.
- Identification of strength discontinuities in plan or elevation that will lead to changes in dynamic characteristics in the inelastic range.
- Estimates of inter-storey drifts accounting for strength or stiffness discontinuities which may be used to control damage.
- Estimates of global drift which can be used to assess the potential for pounding of adjacent structures.

- Verification of the adequacy of the load path, considering both structural and non-structural elements, and the foundation system.

The most important, and maybe unsafe, approximation is the fact that pushover analysis does not account directly for the dynamic effects of earthquakes since it is a static procedure. Therefore the method suggests that structural damage is a function of only the lateral deformation of the structure. Thus the effects of strong ground motion duration and cumulative energy dissipation are clearly neglected, rendering the method approximate.

Even though pushover procedures in some of the cases produce satisfactory results in terms of global deformation, local quantities can be underestimated in the case of tall structures where higher-mode effects can dominate the behaviour (Paret *et al.* 1996, Sasaki *et al.* 1998, Fuentes *et al.* 2001, Memari *et al.* 2001, Tjhin *et al.* 2006). It is also difficult to capture the effects of plastic hinge formation for tall structures (Lawson *et al.* 1994, Kim *et al.* 1999), and generally for structural walls (Lawson *et al.* 1994, Gupta 1998). Additionally erroneous responses can be arrived at when near-fault ground motions are considered (Iwan 1999) especially in the upper parts of tall structures. This can be attributed to the fact that the applicability of pushover analysis has not been assessed for near-fault ground motions.

Pushover analysis does not identify the progressive changes in the modal properties of the structure that occur due to yielding and cracking, when it enters the post-elastic domain of response. The constant load patterns used ignore the redistribution of inertial forces thus producing very approximate results. However, studies (Antoniou 2002), have shown that adaptive load patterns are not that superior to the constant load patterns in capturing these changes even though the study by Bracci *et al.* (1997) had appeared promising.

The type of pushover analysis that has proven till now to be most effective is Modal Pushover Analysis, MPA. However, it has been argued that the method of conducting independent modal pushover analyses and combining them in the domain of inelastic response (Chopra *et al.* 2002) may require further study to be adequately assessed (Antoniou 2002, Hernandez *et al.* 2004).

Finally, it has been suggested that pushover procedures imply a separation of structural capacity and earthquake demand, whereas in practice these two quantities appear to be interconnected. The internal force distribution in the post-elastic stage of response of any structure compared to the internal force distribution in the elastic stage, shows that this separation is not justifiable.

CHAPTER 3
ANALYSIS OF GROUND MOTIONS

3.1 INTRODUCTION

Ground motions are mainly characterized by, the intensity, the frequency content and the duration of the ground motion. Factors that are equally as important include the energy release mechanisms in the vicinity of the hypocenter and along the fault interfaces, the geology and any variations in geology along the energy transmission paths, the epicentral distance, the focal depth, the magnitude and the local soil conditions at the recording station (Clough *et al.* 1993).

The appropriate selection of ground motions is a difficult task in earthquake engineering practice because a large number of uncertainties exist on their nature. For this reason, statistical studies of dynamic structural response are usually undertaken for design and assessment purposes. The choice of ground motions is also very likely to affect the drawn conclusions (Seneviratna, 1995).

As stated in Chapter 1 this study is deterministic, not statistical or stochastic. Therefore two ground motions of different nature have been chosen in order to account for near-fault and far-field ground motions. Many studies have been conducted on the accuracy of pushover analysis when far-field motions are of interest. However, few studies of near-fault ground motions (Iwan 1999, McRae *et al.* 2001, Akkar *et al.* 2005) have been performed on structural systems.

In this chapter, information on the nature of the used ground motions is provided, giving emphasis to the factors that seem appropriate when pushover analyses are to be executed.

3.2 GROUND MOTIONS

The ground motions adopted were the Imperial Valley, US (El Centro station, 1940) ground motion and the Kocaeli, Turkey (Sakaria station, 1999) ground motion. The acceleration, velocity and displacement time-histories are shown in Figures 3.1 to 3.6. Table 3.1 summarises basic information on the two ground motions.

The 1940 Imperial Valley (El Centro station) earthquake of moment magnitude 6.3 was a right-lateral strike-slip fault process along the San Andreas Fault. It caused approximately 70 km of surface rupture on the Imperial Fault, part of the San Andreas Fault system. The recorded ground motion was characterised as a far-field ground motion because the site of the recoding station – despite being 8.3 km away from the epicenter- was located in the rear of the fault rupture direction (Phan *et al.* 2005). The recording station was located on an alluvium site.

The 1999 Kocaeli earthquake had a moment magnitude of 7.4 and was a strike-slip rupture process. Multiple ruptures took place in a propagating fashion along three successive segments of the fault. The earthquake caused approximately 140 km of surface rupture and substantial damage to poorly designed structures situated on recent alluvial soil layers (D'Ayala *et al.* 2003). Geotechnical studies after the earthquake indicated that the top soil layers consisted of loose and medium stiff sandy layers of varying amounts of low plasticity clay, silt, and gravel (D'Ayala *et al.* 2003). These soil properties were responsible for the amplification of the response and also for significant damage due to liquefaction.

The Kocaeli ground motion (Sakaria station) was characterised as a near-fault ground motion. The velocity time series of the Kocaeli earthquake in Figure 3.5 shows a large and long period pulse implying a large amount of energy being released, an effect which is observed in near-fault ground motions. Alavi *et al.* (2001) among others explained that when ground shaking occurs near a fault rupture there is a short-duration impulsive motion that exposes structures to high input energy at the beginning of the record. This is attributed to the fact that proximity to the earthquake epicenter does not allow the ground motion to be attenuated significantly. The Kocaeli motion is also linked to the forward directivity phenomenon in which the rupture propagates towards the site and the direction

of the slip on the fault is aligned with the site (Somerville 2002). It should be acknowledged however that forward directivity effects are not evident in every near-fault ground motion. Backward directivity effects can occur when the rupture propagates away from the site. These types of motions exhibit long duration records that have low amplitudes at long periods (Somerville *et al.* 1997). This is the case in the El Centro ground motion.

The ground motions that are therefore studied in this research contain different intensity, frequency content, as will be shown later, and duration characteristics. They are characterized as being near-fault, Kocaeli, and far-field, El Centro, ground motions.

3.3 FREQUENCY CONTENT

Ground motions contain a wide range of frequencies. A good insight into the nature of the earthquake ground motions can be achieved by estimating their frequency content. Among most of the papers discussed in Chapter 2, the frequency content of the used earthquakes has not been assessed, even though this quantity has been widely accepted as providing valuable information about the nature of the ground motions. Since pushover analysis is a predominantly static procedure that attempts to model a dynamic phenomenon it needs other tools to render it efficient and meaningful. These tools need to be dynamic in nature and the Fourier amplitude spectrum could assist in this purpose.

The Fourier amplitude spectrum determines the range of frequencies at which the earthquake could cause the most significant damage. Thus it can be thought of as a dynamic tool that can provide information on the damage potential of earthquakes on structures by identifying the distribution of frequencies. In this way, it is possible to check if the frequency content of the earthquake falls near the fundamental frequencies of the structural systems to be assessed or designed. In practice, frequencies in ground motions above to 40 Hz are thought to have an insignificant effect on the structural response.

Consider that the earthquake input acceleration signal, being a function of time *t,* is denoted as *y(t)*. Then the Fourier Amplitude of the signal can be computed by firstly expressing *y(t)* through a superposition of a full spectrum of harmonics using the following equation:

$$F(\overline{\omega}) = \int_{-\infty}^{\infty} y(t) e^{-i\overline{\omega}t}\, dt \qquad (3.1)$$

where $\overline{\omega}$ is the circular frequency of the excitation force.

Equation 3.1 can only be solved by assuming that the ground motion is nonzero in a finite time range. In this way one can break up Eq. (3.1) into its real and imaginary components as follows:

$$F(\overline{\omega}) = \underbrace{\int_{0}^{t_1} y(t)\cos\overline{\omega}t dt}_{A(\overline{\omega})} - i\underbrace{\int_{0}^{t_1} y(t)\sin\overline{\omega}t dt}_{B(\overline{\omega})} \qquad (3.2)$$

The Fourier Amplitude Spectrum is given by:

$$\left|F(\overline{\omega})\right| = \left[A(\overline{\omega})^2 + B(\overline{\omega})^2\right]^{1/2} \qquad (3.3)$$

It should be noted that the Fourier amplitude spectrum $F(\overline{\omega})$ does not uniquely define a ground motion time-history since the phase angles between the pairs of harmonics are not included (Clough *et al.* 1993).

The Fourier amplitude spectra for both motions were computed using the acceleration time-histories of both ground motions, and the Fast Fourier Transform algorithm (FFT). These are displayed in Figures 3.7 and 3.8 together with Table 3.1 which indicates the frequency at which the Fourier Amplitude is the maximum. The dotted lines in Figures 3.7 and 3.8 indicate the maximum limit of the frequencies of interest for structural systems. It would generally be expected, as mentioned earlier, that systems with fundamental frequencies close to the dominant frequencies of these ground motions will be affected the most.

Other quantities characterising the frequency content of a ground motion exist (Rathje *et al.* 1998). These are the predominant period T_p of the ground motion, and the mean period T_m. The predominant period T_p is defined as the period at which the acceleration response spectrum attains its maximum value. The mean period T_m is defined as:

$$T_m = \frac{\sum_i C_i^2 \cdot \left(\frac{1}{f_i}\right)}{\sum_i C_i^2} \quad \text{for } 0.25Hz \le f_i \le 20Hz \quad (3.4)$$

where C_i are the Fourier amplitudes for the entire accelerogram, and f_i are the discrete Fourier transform frequencies between 0.25 and 20 Hz. It has been found that the mean period T_m is a more consistent characterization for a ground motion than the predominant period T_p because it stems from a more precise representation of the acceleration time history. These additional frequency content quantities are shown in Table 3.2.

3.4 ELASTIC & INELASTIC SPECTRAL CHARACTERISTICS

3.4.1 Elastic & Inelastic Response Spectra

The elastic and inelastic response spectra provide the basis for calculating the target displacements of any structural systems being studied using pushover analysis. The two types of spectra used are spectra for different levels of damping, damped spectra for the CSM method, and constant-ductility spectra for the N2 method. Chopra *et al. (*1999) have presented the constant-ductility spectra as an improvement over the damped spectra.

The use of damped spectra in the CSM method has been questioned by Krawinkler (1995), for two reasons: a) there is no physical principle from which can be derived a stable relationship between energy dissipation of the maximum excursion and equivalent viscous damping and b) the period associated with the intersection of the capacity curve with the highly damped spectrum may have little to do with the dynamic response of the inelastic system.

In view of the above remark, constant-ductility inelastic spectra have been utilized in this study. The constant-ductility spectra have been computed using the Seismosignal software of Seismosoft (2004) developed by Antoniou. The procedure for calculating these spectra is presented in Chopra (1995). The calculation involves the numerical solution of the following equation:

$$\ddot{\mu} + 2\zeta\omega_n\dot{\mu} + \omega_n^2 \tilde{f}_s(\mu, \dot{\mu}) = -\omega_n^2 \frac{\ddot{u}_g(t)}{\alpha_y} \qquad (3.5)$$

where α_y is the acceleration of the mass necessary to produce yield force F_y , $\tilde{f}_s(\mu, \dot{\mu})$ is the dimensionless force-deformation relationship, μ is the ductility factor, ζ is the damping ratio and ω_n is the natural frequency of the SDOF system. The derivation of equation 3.5 is presented in Appendix B, as in Chopra, 1995.

The ductility factors used for deriving the spectra were, μ = 2, 3, 4, 5, 6, 7 and 8. The damping was assumed to be 5%.

Two material models were used to derive the spectra, namely elastic-perfectly-plastic, EPP, and elastoplastic with strain-hardening, EPSH, with strain hardening ratios of α = 0.0 and α = 0.03, respectively, Figure 3.9.

Figures 3.10 and 3.11 show the elastic and constant-ductility spectra for the El Centro ground motion and for the EPP and EPSH models respectively. Figures 3.12 and 3.13 show the ADRS spectra for the El Centro ground motion and for the EPP and EPSH models respectively. In the same manner, Figures 3.14 and 3.15 show the elastic and constant-ductility spectra for the Kocaeli ground motion and for the EPP and EPSH models respectively while Figures 3.16 and 3.17 show the ADRS spectra for the Kocaeli ground motion for the EPP and EPSH models. As explained earlier, Chapter 2, the ADRS spectra are important for estimating the demand target displacements from pushover analyses.

3.4.2 Strength Reduction Factors

The strength reduction factor R_μ is the ratio of the elastic strength to the inelastic strength of a series of SDOF systems for a given ductility factor μ. Figures 3.18 & 3.19 show values of strength reduction factors for the El Centro ground motion, for target ductilities μ = 2, 3, 4, 5, 6, 7 and 8, for the EPP and EPSH hysteretic models respectively. Figures 3.20 to 3.21 are for the Kocaeli ground motion and the EPP and EPSH hysteretic models respectively. Inspecting Figures 3.18-3.19 for the El Centro and 3.20-3.21 for the Kocaeli ground motion, the following observations can be made:

- The R_μ -μ-T curves show a sudden increase in R_μ in the short period range with increasing ductility, μ. As the period, T, approaches zero, R_μ approaches unity for all ductility factors.

- For the intermediate period range of periods of 0.5-2.0 seconds, R_μ decreases uniformly for the El Centro ground motion. For the Kocaeli ground motion R_μ increases as T approaches 2.0 seconds.

- In the long-period range R_μ approaches the value of μ for both ground motions and hysteretic models.

3.4.3 Normalised Displacement Demands

The effects of inelastic behaviour compared to elastic behaviour for SDOF systems with the two imposed ground motions are apparent when normalized displacement demands of the form $\delta_{inel} / \delta_{el}$ are considered. Figures 3.22, 3.23 show these demands for the El Centro ground motion and for the EPP and EPSH hysteretic models, respectively. Figures 3.24 and 3.25 show the normalized displacement demands for the Kocaeli ground motion.

The general characteristics of the normalized displacement demands are similar for both motions. For periods of 0-0.2 seconds, increases in the displacement demand as the period

approaches zero are apparent. These amplifications are higher for the Kocaeli ground motion. The region of significant amplification for the El Centro record is for periods less than approximately 0.4 seconds and for the Kocaeli record for periods less than approximately 0.9 seconds. For longer periods the ratio is virtually independent of both period and ductility. Additionally, the effect of strain hardening in reducing the displacement demands with respect to the EPP systems appears to be quite small for all ductilities and ground motions.

Earthquake	Imperial Valley	Kocaeli
Station	El Centro	Sakaria
Magnitude (M_L)	6.3	7.4
Source Mechanism	lateral strike-slip	lateral strike-slip
Soil Class	alluvium	Thin layer of stiff soil over rock
Acc (g)	0.31882g	0.62822g
Vel (m/sec)	0.36154	0.77418
Disp. (m)	0.21357	0.59655
Duration (sec)	31.18	20

Table 3-1 Information on ground motions used

FREQUENCY CONTENT	El Centro	Kocaeli
Maximum Fourier Amplitude	0.25	0.27
Frequency at max Fourier Amplitude (Hz)	1.2	3.2
T_p (s)	0.5	0.16
T_m (s)	0.52	0.5

Table 3-2 Frequency content characteristics of El Centro and Kocaeli

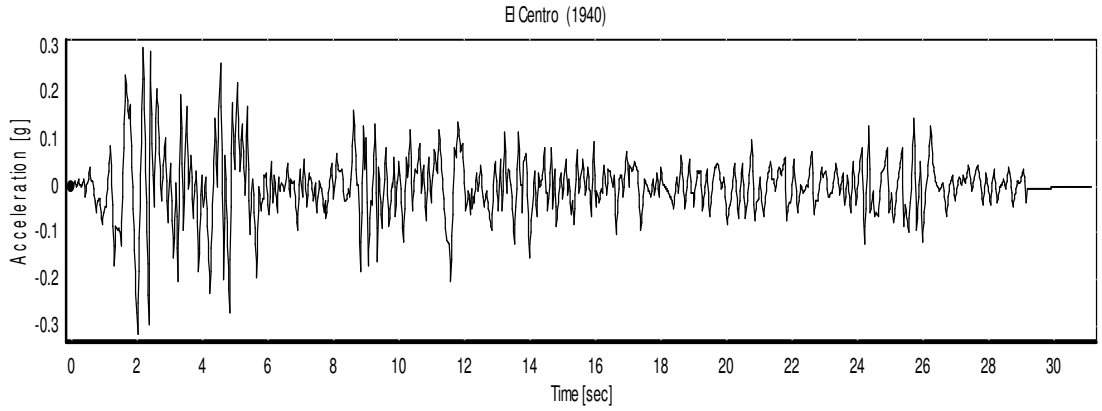

Figure 3-1 Acceleration Time Series of El Centro 1940

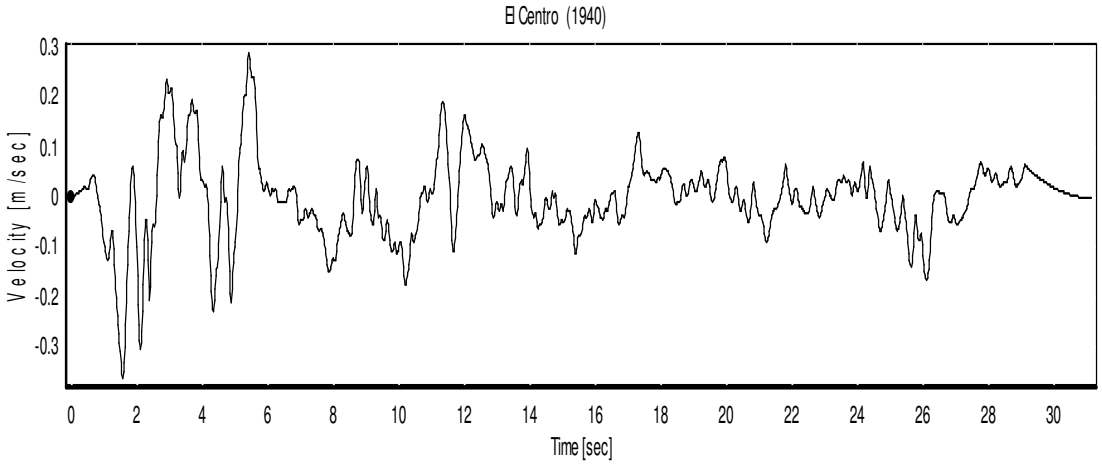

Figure 3-2 Velocity Time Series of El Centro 1940

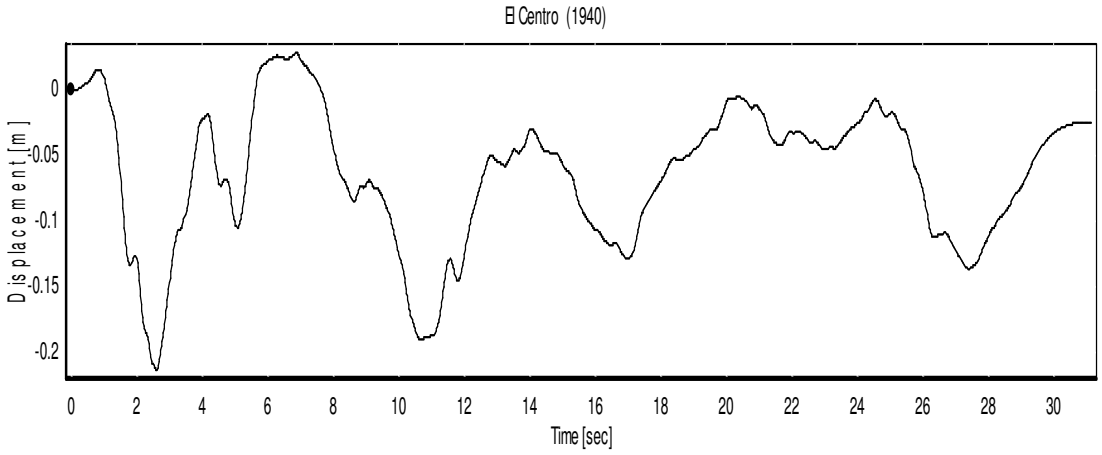

Figure 3-3 Displacement Time Series of El Centro 1940

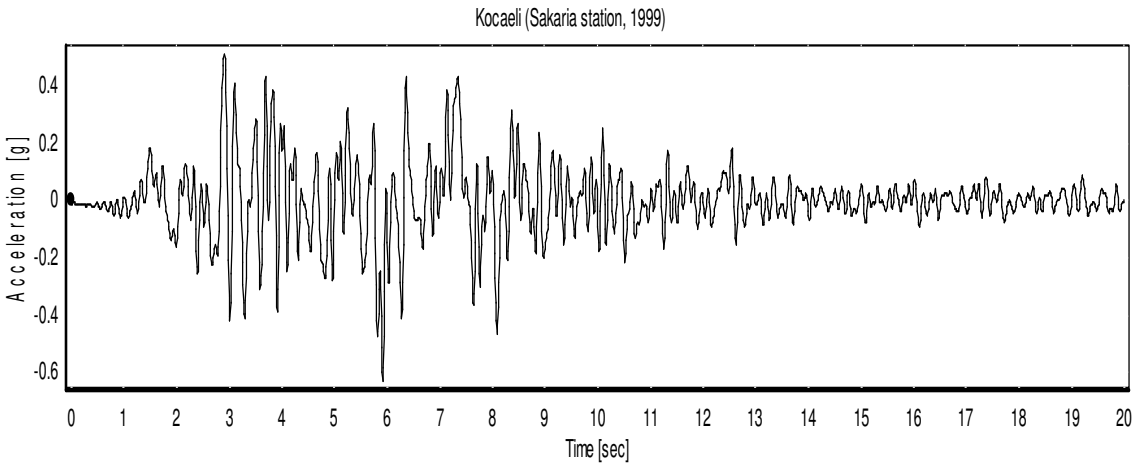

Figure 3-4 Acceleration Time Series of Kocaeli Turkey

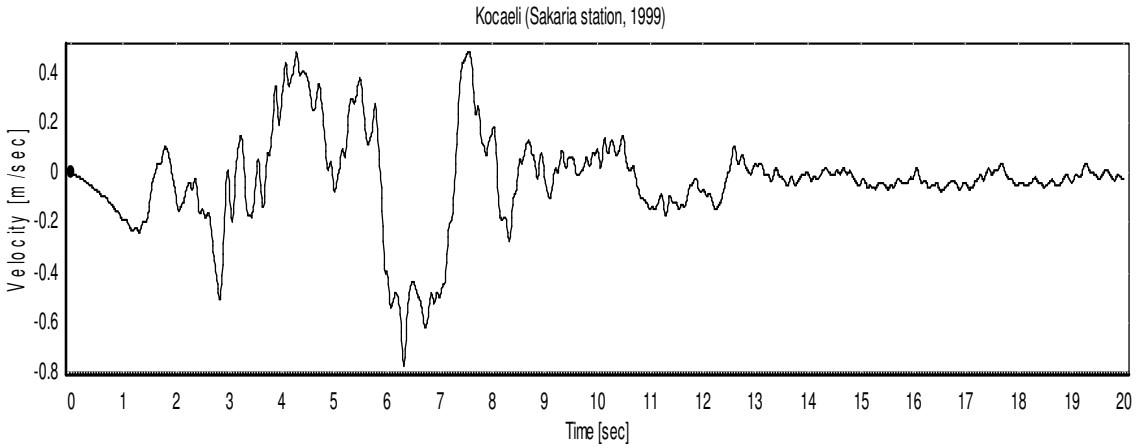

Figure 3-5 Velocity Time Series of Kocaeli Turkey

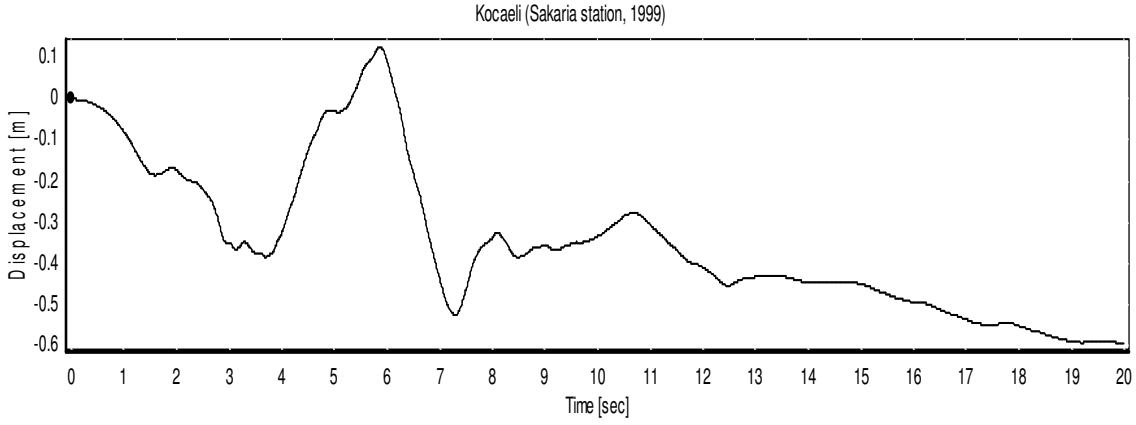

Figure 3-6 Displacement Time Series of Kocaeli Turkey

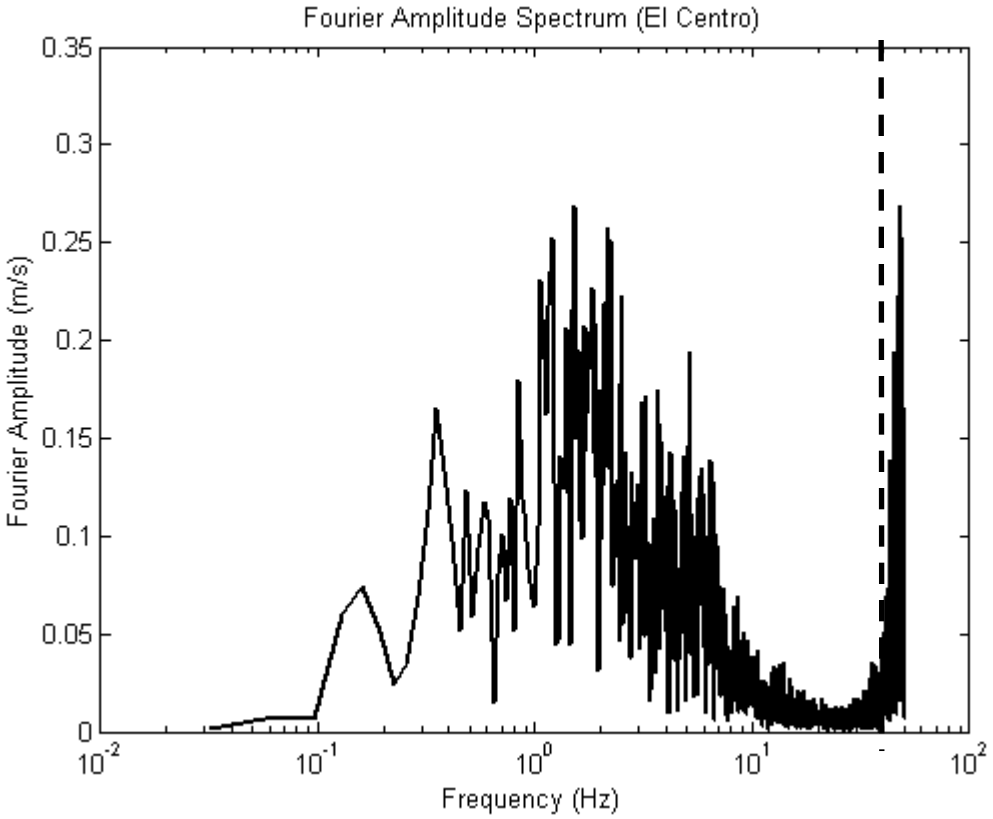

Figure 3-7 Fourier Amplitude Spectrum of El Centro

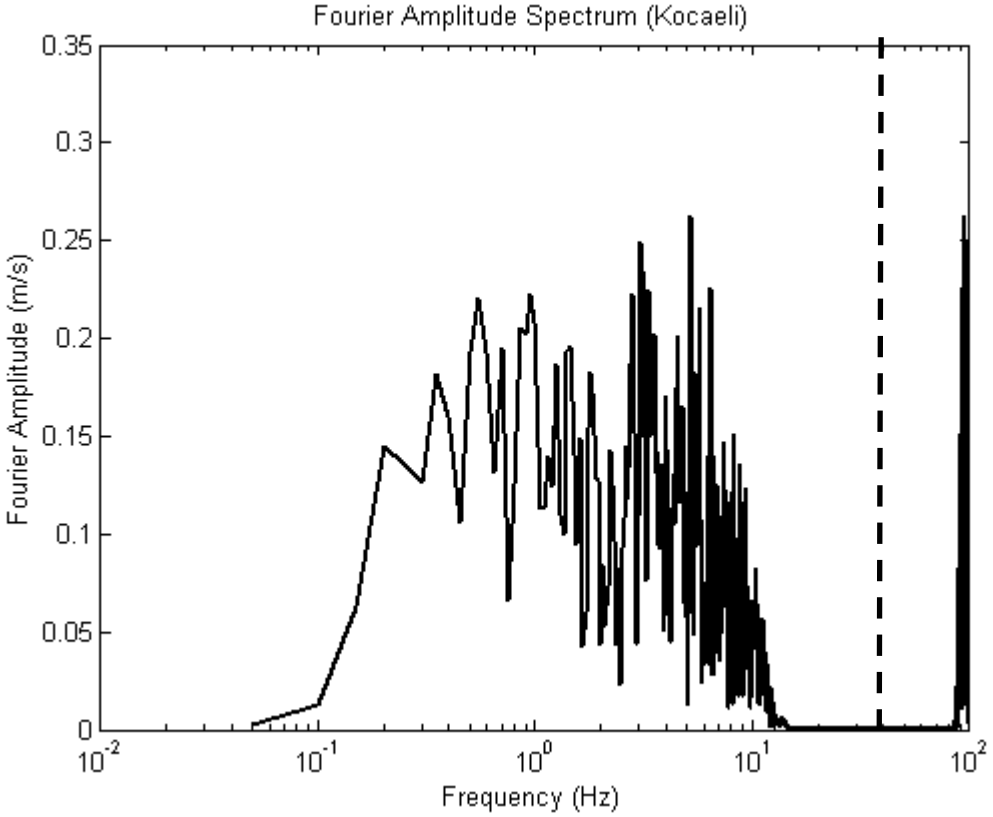

Figure 3-8 Fourier Amplitude Spectrum of Kocaeli

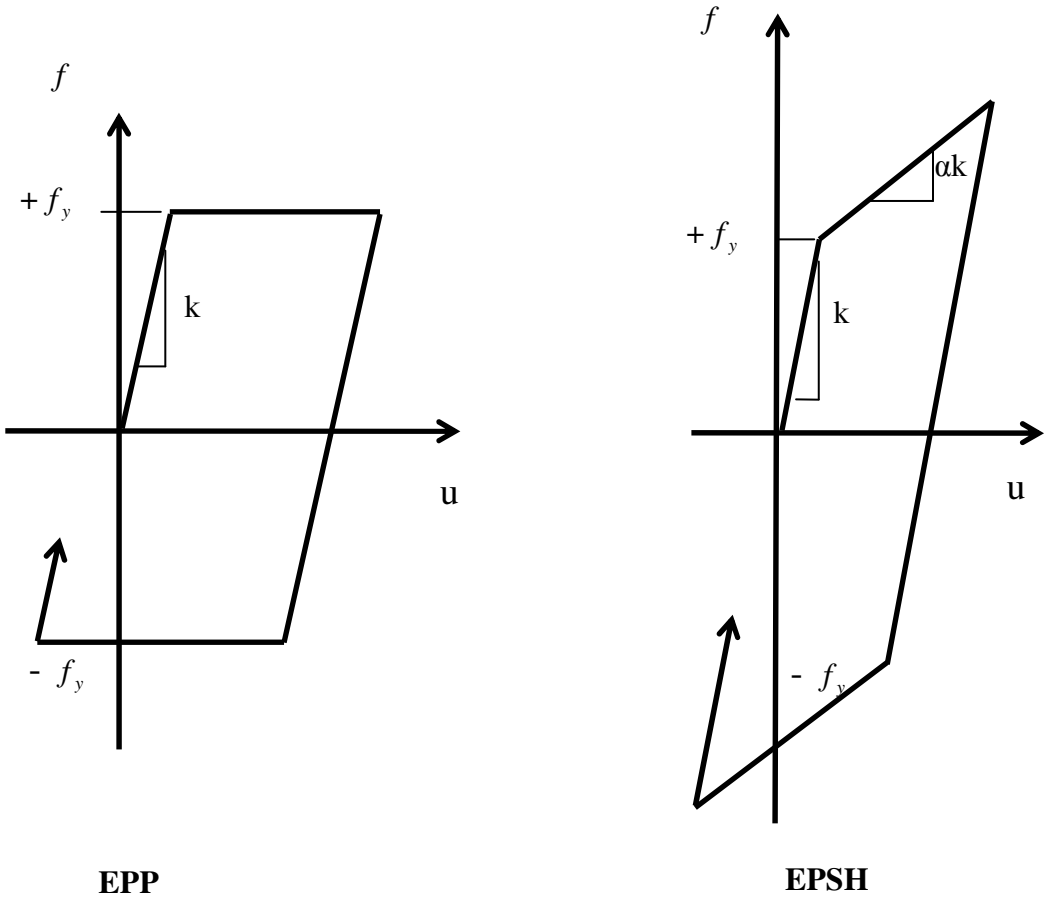

EPP **EPSH**

Figure 3-9 Hysteretic models

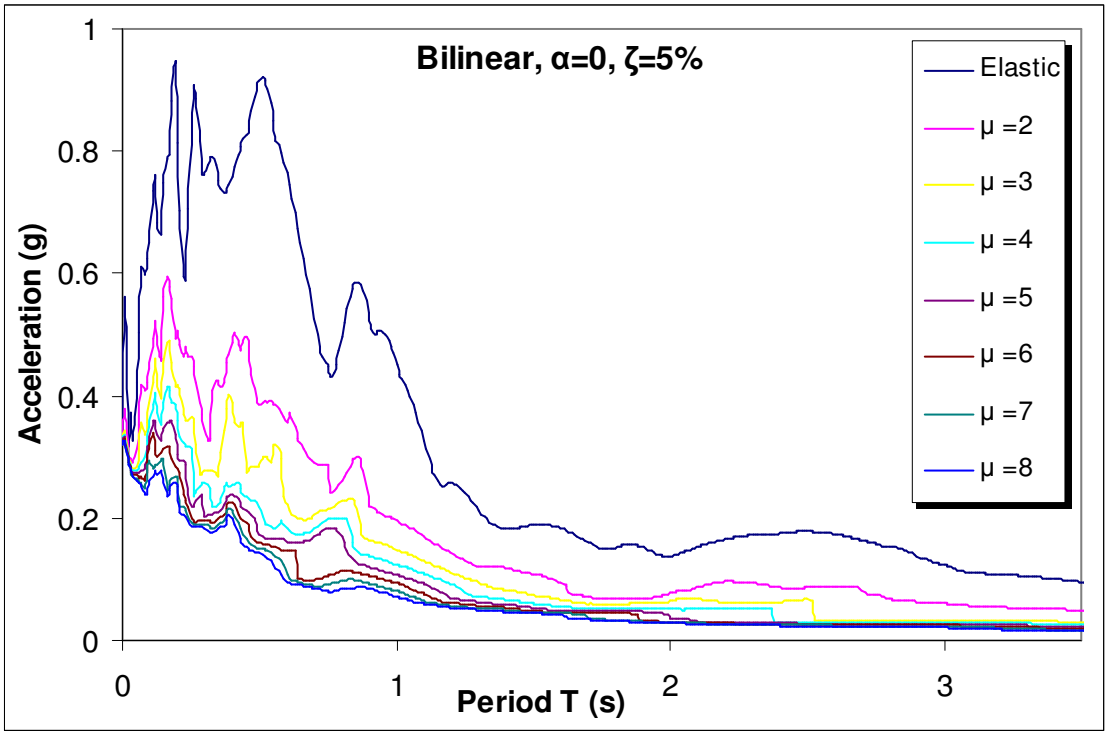

Figure 3-10 Elastic/Inelastic Acceleration Response Spectra of El Centro ground motion for elastic-perfectly plastic systems

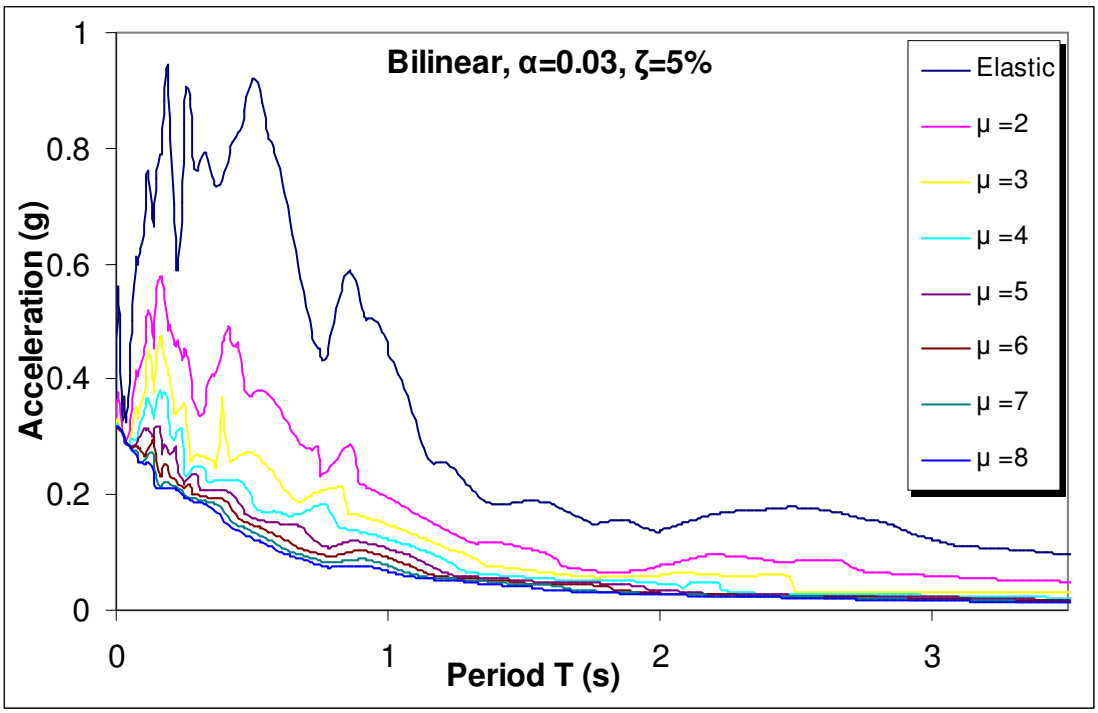

Figure 3-11 Elastic/Inelastic Acceleration Response Spectra of El Centro ground motion for elastoplastic with strain hardening systems

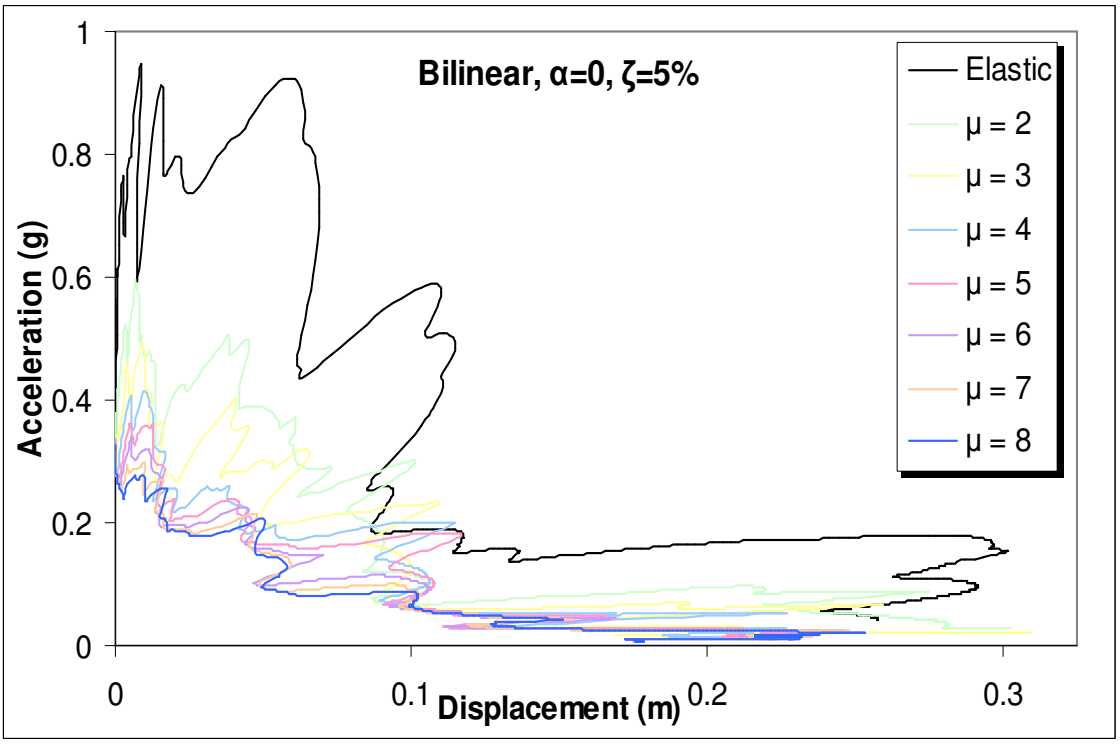

Figure 3-12 Acceleration - Displacement (ADRS) Spectra of El Centro ground motion for elastic-perfectly plastic systems

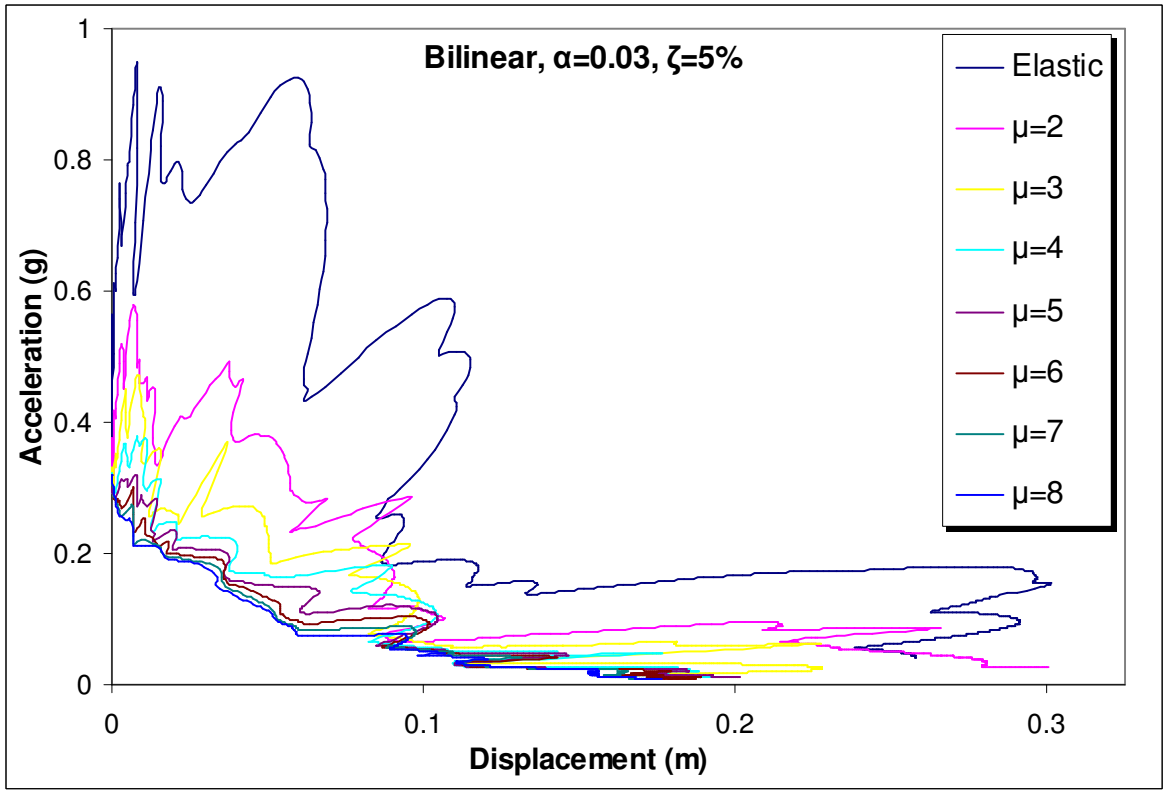

Figure 3-13 Acceleration - Displacement (ADRS) Spectra a of El Centro ground motion for elastoplastic with strain hardening systems

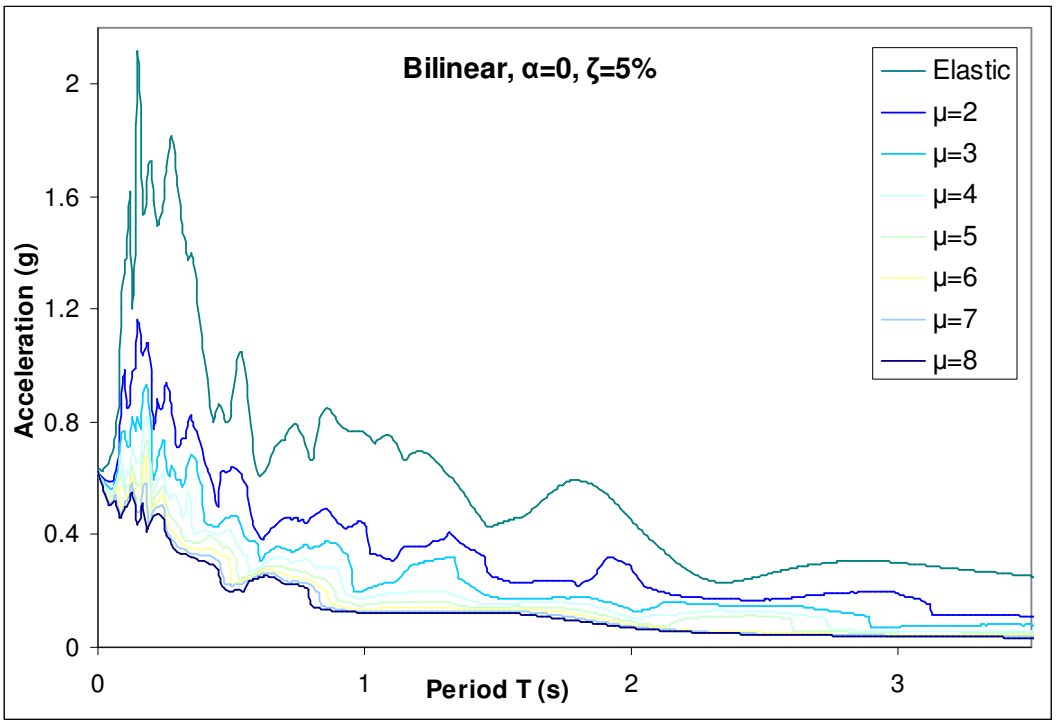

Figure 3-14 Elastic/Inelastic Acceleration Response Spectra of Kocaeli ground motion for elastic-perfectly plastic systems

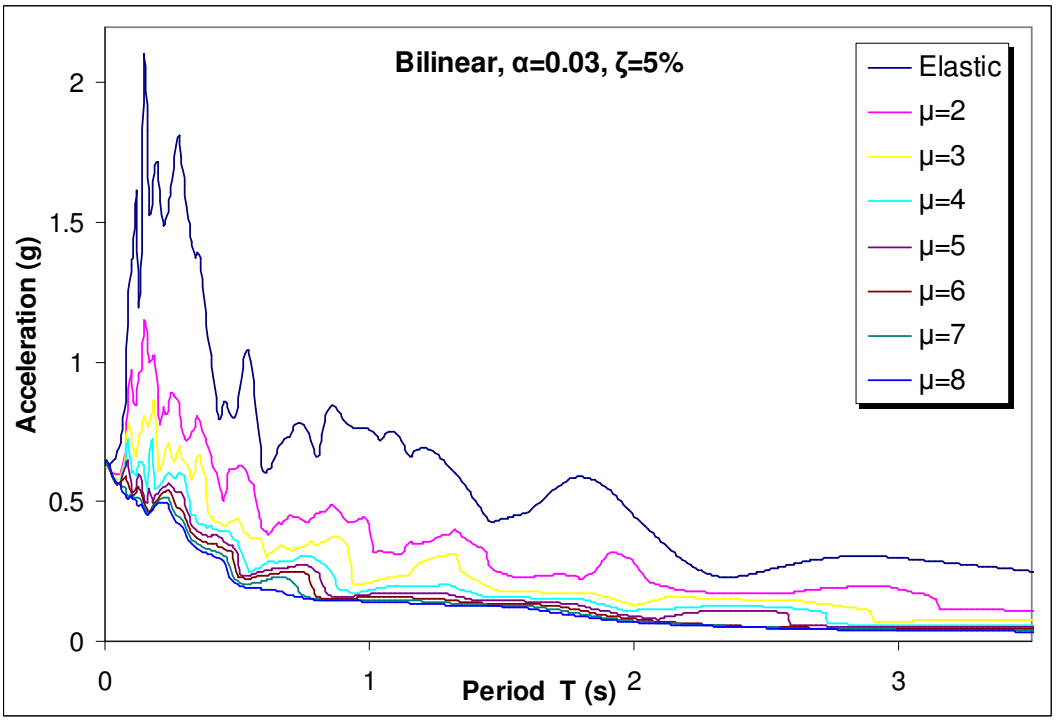

Figure 3-15 Elastic/Inelastic Acceleration Response Spectra of Kocaeli ground motion for elastoplastic with strain hardening systems

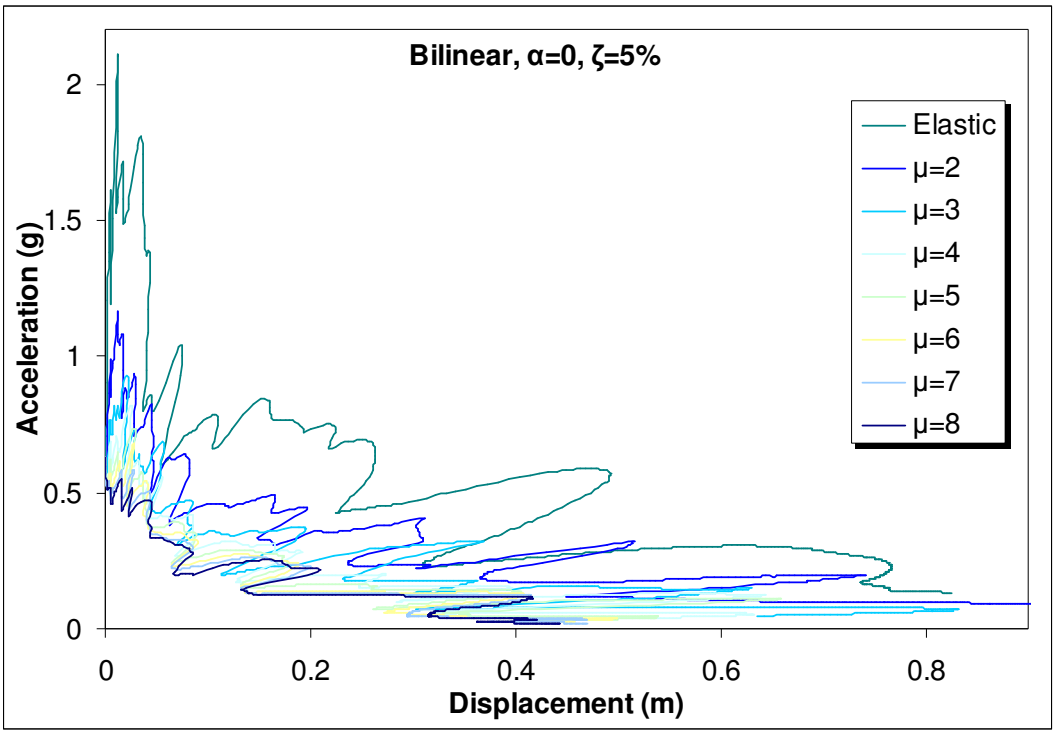

Figure 3-16 Acceleration - Displacement (ADRS) Spectra of Kocaeli ground motion for elastic-perfectly plastic systems

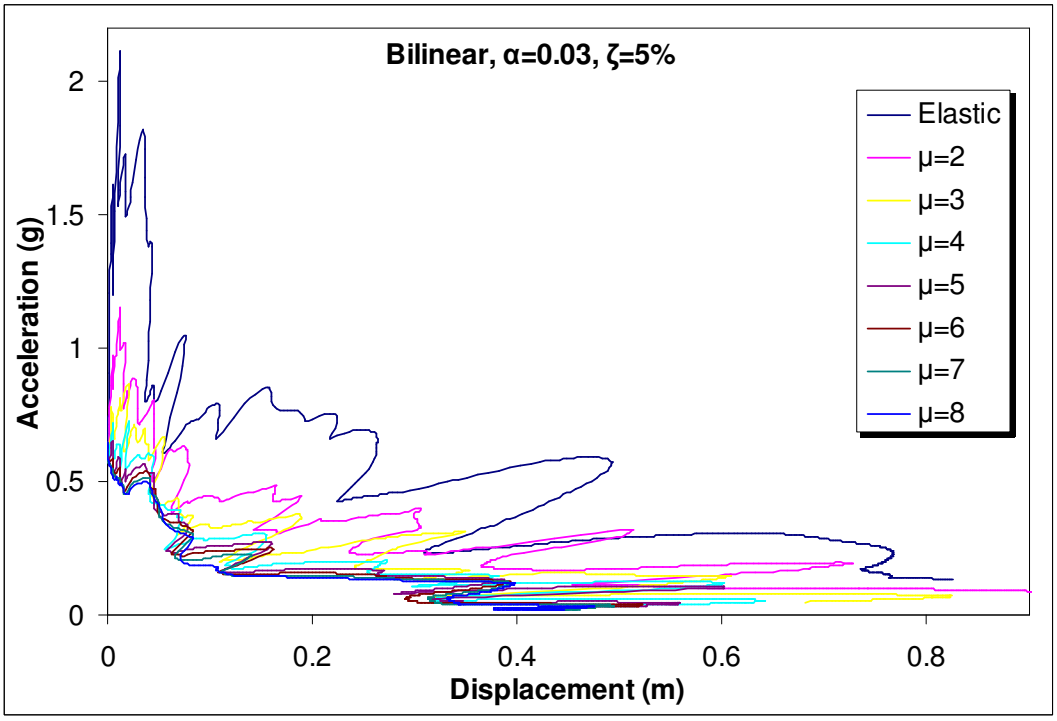

Figure 3-17 Acceleration - Displacement (ADRS) Spectra of Kocaeli ground motion for elastoplastic with strain hardening systems

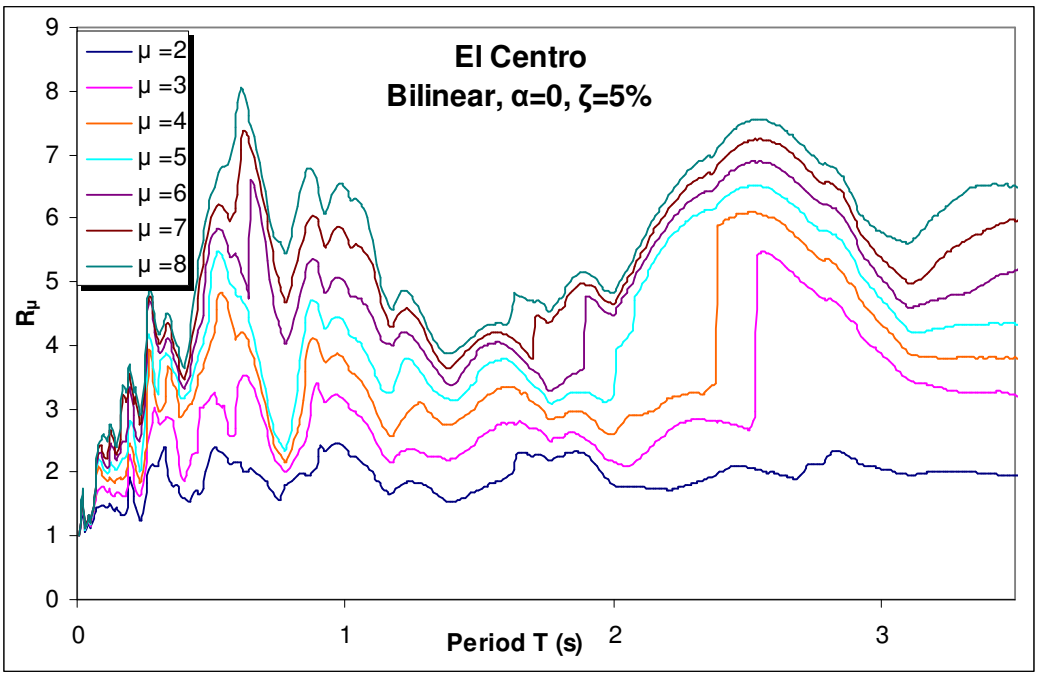

Figure 3-18 Strength Reduction Factors for El Centro, EPP model

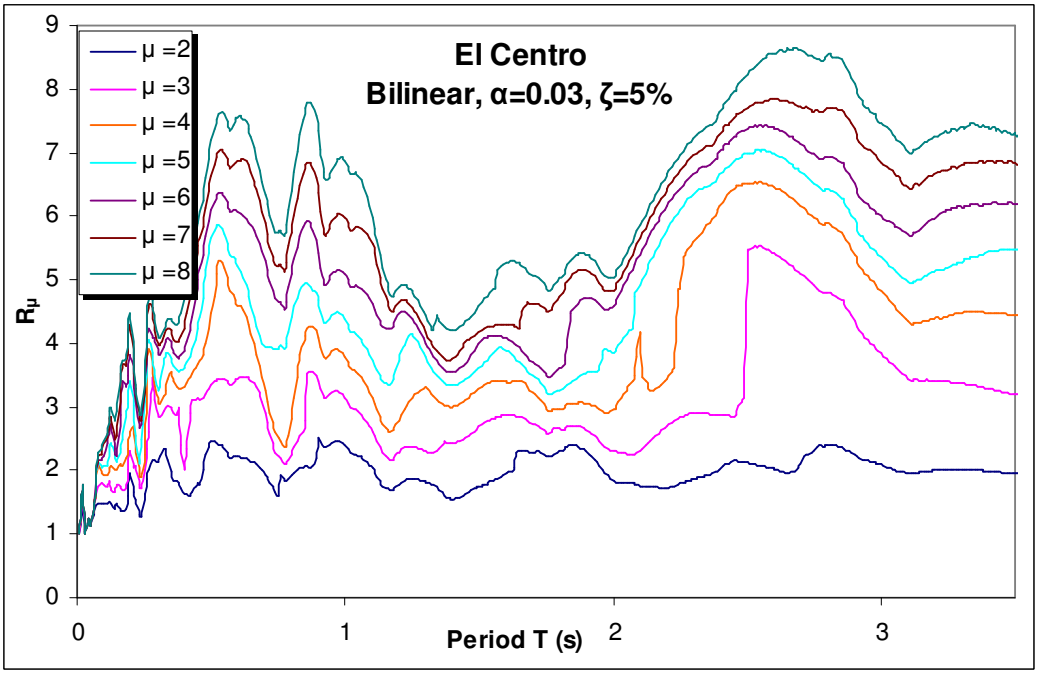

Figure 3-19 Strength Reduction Factors for El Centro, EPSH model

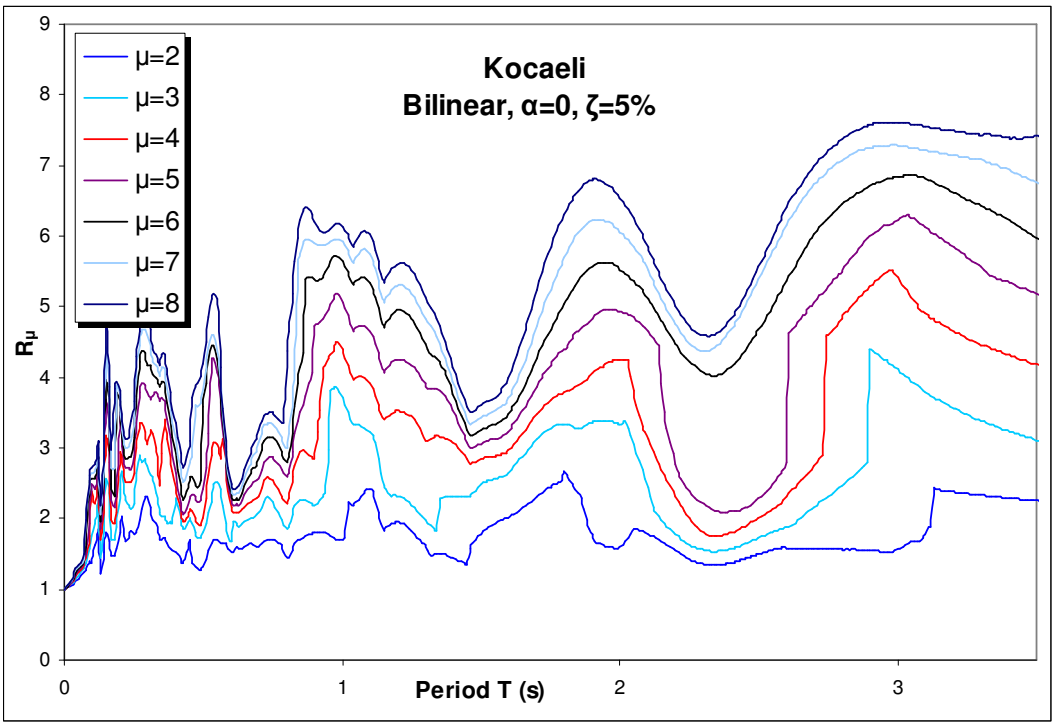

Figure 3-20 Strength Reduction Factors for Kocaeli, EPP model

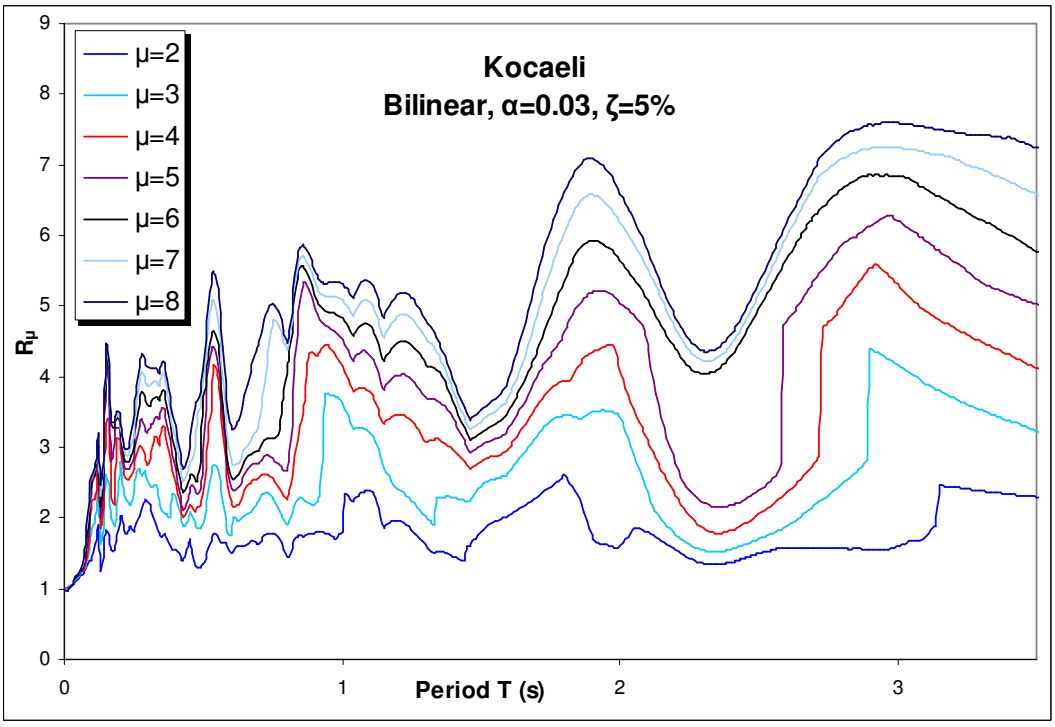

Figure 3-21 Strength Reduction Factors for Kocaeli, EPSH model

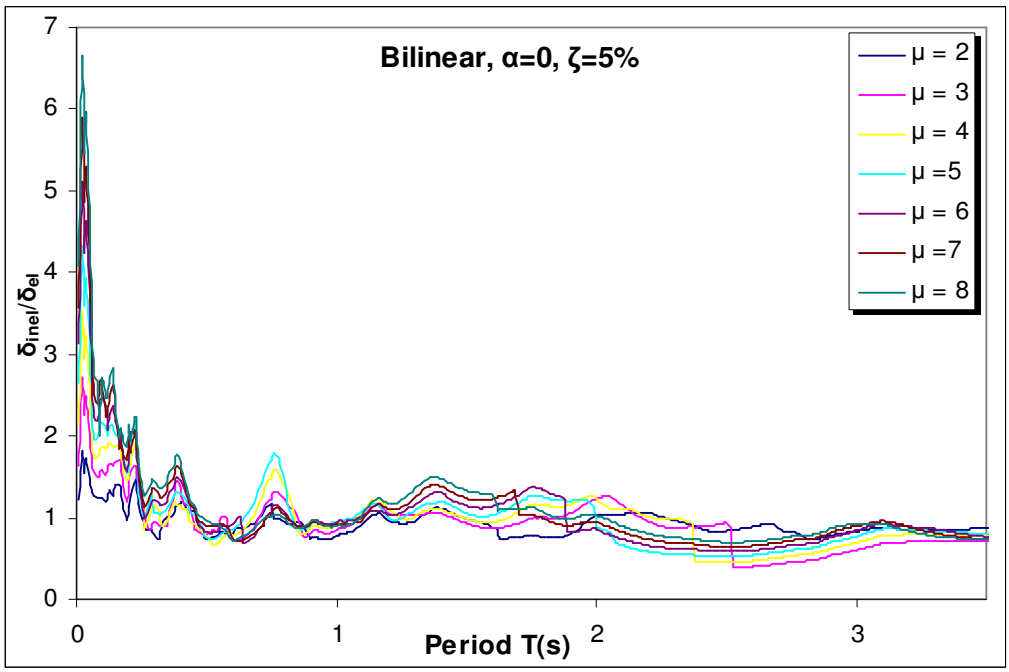

Figure 3-22 Normalised Inelastic Displacement Demands of El Centro ground motion for elastic-perfectly plastic systems

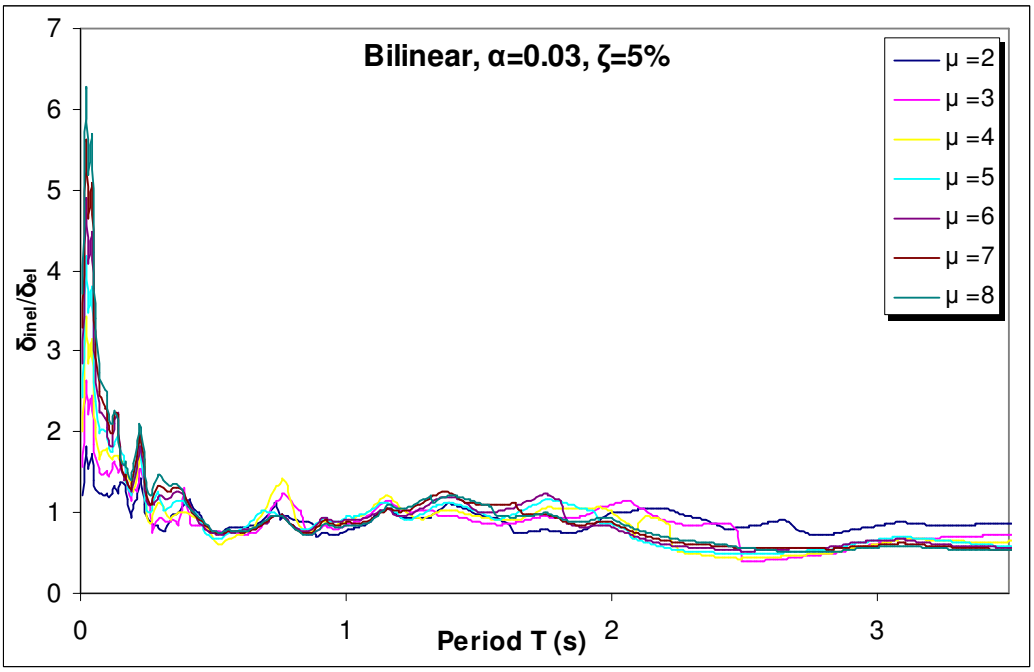

Figure 3-23 Normalised Inelastic Displacement Demands of El Centro ground motion for elastoplastic with strain hardening systems

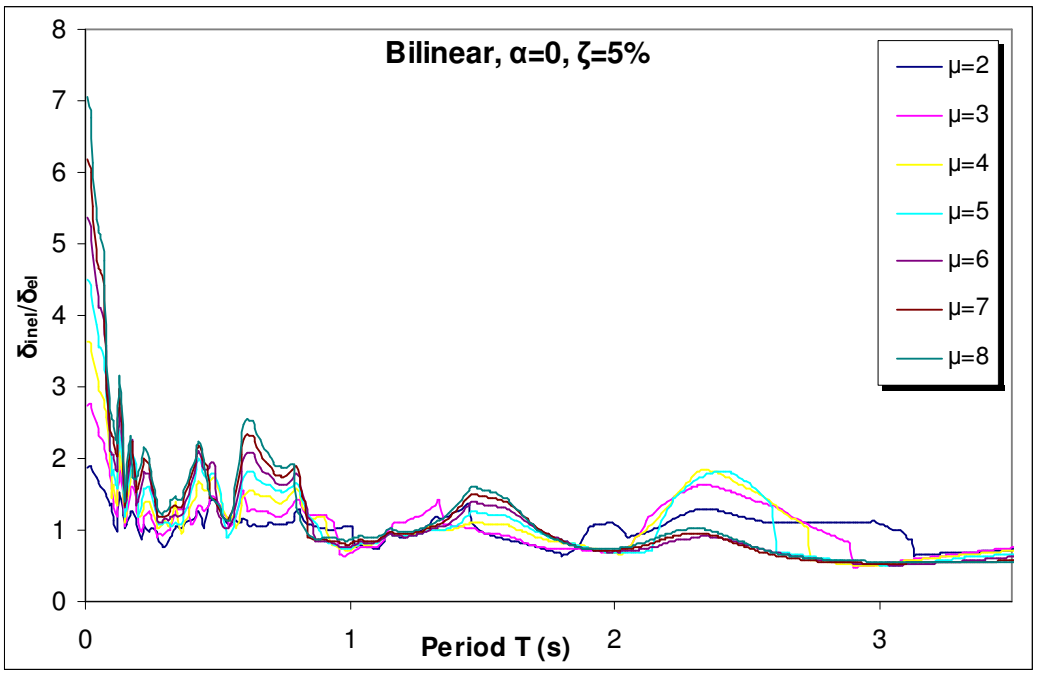

Figure 3-24 Normalised Inelastic Displacement Demands of Kocaeli ground motion for elastic-perfectly plastic systems

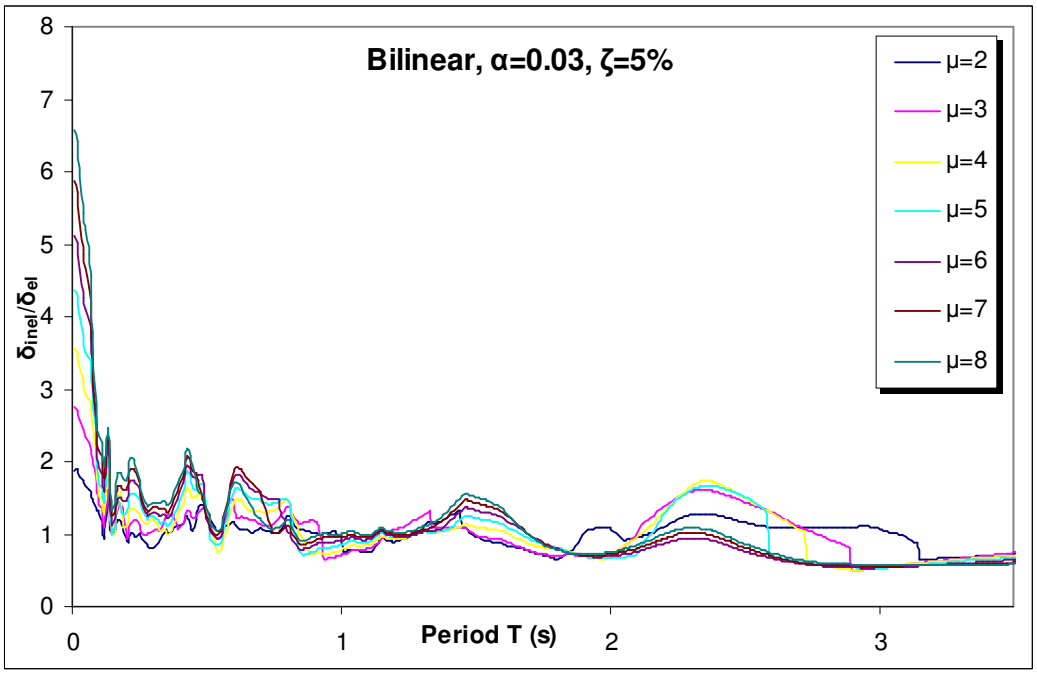

Figure 3-25 Normalised Inelastic Displacement Demands of Kocaeli ground motion for elastoplastic with strain hardening systems

CHAPTER 4
PUSHOVER ANALYSES ON SDOF AND 2-DOF SYSTEMS

4.1 INTRODUCTION

This chapter is divided into two parts: In the first part, the N2 and DCM methods are applied to six SDOF systems using the two ground motions, the Kocaeli and El Centro, discussed in Chapter 3 so as to give an insight into the methods and address their potential and limitations by considering the SDOF system. The SDOF response has been studied independently for each ground motion. In the second part, the N2, DCM, and MPA methods are applied to a 2-DOF system with similar objectives to those for the SDOF systems.

4.2 PUSHOVER ANALYSIS OF SDOF SYSTEMS

4.2.1 Insight into Modelling

SDOF systems with natural vibration periods of T_n = 0.1, 0.3, 0.5, 0.8, 1 and 2 seconds and a damping ratio ζ of 5% were modeled in the LUSAS FEA package using the joint element, JNT3. The systems will be denoted as SDOF 0.1, SDOF 0.3, SDOF 0.5, SDOF 0.8, SDOF 1 and SDOF 2 respectively. The physical model of the systems is shown in Figure 4.1(a). The elastic resistance of each system to displacement was provided by a massless spring *k,* assumed to have only degrees of freedom in the x-direction thus allowing translation to occur. The mass *m* was idealized as being lumped at node 2 of the element, Figure 4.1(b). Rayleigh damping represented by stiffness and mass proportional matrices in order to decouple the equation of motion to simplify the solution process, was used.

For the inelastic analyses the yield strength of each system was assumed to be 0.25 of the maximum elastic force calculated from linear dynamic analyses using the Kocaeli and El Centro ground motions, that is a strength reduction factor of R_μ = 4. It is noted that the yield strengths of the SDOF systems for the two ground motions are of different

magnitude. The EPP and EPSH hysteretic models, Figure 3.9, defined in Chapter 3 have been used in these analyses.

4.2.2 Nonlinear Dynamic Analyses

Nonlinear dynamic analyses were performed for the two ground motions for both the EPP and EPSH material models in order to give results with which to compare the nonlinear static analyses.

The analyses utilised Hilber's *et al.* (1977) implicit integration method. The accelerations were applied horizontally at node 2 of the joint element so as to induce ground motion response, Figure 4.1(b).

Typical displacement - time histories for the SDOF 0.5 system can be observed in Figure 4.2 for the Kocaeli ground motion and the two material models, and in Figure 4.3 for the El Centro ground motion. In the case of the Kocaeli ground motion, the SDOF 0.5 system undergoes considerable deformations in the inelastic regime especially with the EPP model. The EPSH model leads to smaller permanent deformations than the EPP model.

The displacement time histories of the EPP and EPSH models for the El Centro ground motion show similar trends as for the Kocaeli ground motion. However, the effect of including strain hardening in the analysis is not as considerable in this case. These conclusions are reflected in the force-displacement responses of the system, Figure 4.4 for the Kocaeli ground motion, and Figure 4.5 for the El Centro ground motion. The displacement - time histories and force- displacement responses of the remaining SDOF systems studied herein are shown in Appendix B. Additionally, the results for all systems and ground motions are tabulated in Tables 4.1 to 4.24. The quantities presented are the target displacement, reaction force, ductility, and hysteretic energy dissipation.

Figures 4.6 to 4.9 show the energy time histories for the two ground motions and material models for the SDOF 0.5 system. The energy time-histories for the remaining SDOF systems are presented in Appendix B. These results show that the earthquake input energy to a structure is consumed mostly partly by damping and partly by yielding. Other contributions to the input energy arise from the elastic strain energy and

the kinetic energy of the structure. In most of the cases the hysteretic energy, the energy that accounts for yielding, is larger than the damping energy. However for ground motions with considerable ground velocities the damping energy can be larger than the hysteretic energy. For example, the application of the El Centro ground motion to the SDOF 0.5 system, EPP model, resulted in larger energy dissipation due to damping than due to hysteresis which can be attributed to the long duration of the ground motion and also to the increasing magnitude of the ground velocity time-history towards the end of the motion. The same observation holds true for SDOF 0.1, EPSH model, SDOF 0.3, EPSH model, and SDOF 1, EPP and EPSH models.

The energy time-histories however did not aid in understanding how much influence ground motion duration has on the response of SDOF systems. However statistical studies, Iervolino *et al.* (2006), suggested that regardless of the period of the system and the material relationship used the displacement and ductility demands are not affected by the duration of the ground motion. Additionally the duration is correlated with hysteretic energy dissipation.

Furthermore, for both ground motions no clear relationship between the hysteretic energy dissipation and the period of the SDOF system was observed. This means that increasing the period of vibration of a system does not ensure that it will dissipate the hysteretic energy with increasing magnitude.

4.2.3 Nonlinear Static Pushover Analyses

The main step in pushover analysis, as discussed in Chapter 2, is to perform a nonlinear static analysis of the system in order to establish the equivalent SDOF system, ESDOF. Typical nonlinear load - displacement curves for the SDOF 0.5 system are shown in Figures 4.10 and 4.11 for the Kocaeli and El Centro ground motions, respectively.

Because the model is a SDOF system it will only have one mode of vibration. This means that the equations used by the N2, CSM, DCM and MPA methods to transform a MDOF system to its equivalent SDOF need not be used. Additionally the MPA method reduces to either the N2 or the CSM methods.

4.2.3.1 Performance Points

Once the pushover curves are established they need to be transformed to force-displacement relationships for the ESDOF system. In the case of the SDOF system no transformation is necessary. The force-displacement curves need then further be transformed to capacity curves, which have the format of acceleration versus displacement. From these capacity curves it is possible to obtain the yield acceleration, a_y, the acceleration at which yielding of the systems occurs. When performing this task the N2 and CSM methods coincided numerically. For this reason only the N2 and DCM methods will be used to estimate demands for the SDOF system.

The resulting capacity curves and the response spectra need then be superimposed on the same graph. The superposition is shown in Figures 4.12 to 4.17 for the SDOF 0.5 system. The elastic response of the ESDOF system has a gradient equal to the elastic period T_e. The intersection of this line and the elastic response spectrum S_{ae} provides the acceleration and displacement demands required for elastic behaviour to be maintained.

For the N2 method, the performance point or target displacement can be estimated using the graphical procedure or by using the relevant equations, Chapter 2, which should give same results. It has been proposed that utilizing both methods will provide confidence and better visualization of the results, Fajfar (2000). It will be shown here that even though the two methods provide similar performance points the graphical solution can lead to difficulties when inelastic response spectra are used instead of smoothed design spectra. Additionally for short period systems it is not clear how the performance point could be achieved when using the graphical procedure. To explain this, two cases are discussed for the SDOF 0.5 system for the Kocaeli and El Centro ground motions.

The estimates of the target displacements need be based on some form of empirical rule so as to correlate the elastic displacement with the inelastic displacement. Previous studies by Veletsos *et al.* (1960), Veletsos *et al.* (1965), Newmark *et al.* (1973), Clough *et al.* (1993) and Chopra (1995) showed that in the medium- and long period range the inelastic displacement is almost equal to the elastic displacement. In the short-period

range it has been observed that the inelastic displacement is generally larger than the elastic displacement; however in this region the principle of conservation of energy can be used by which the monotonic force-displacement diagram of the elastic system up to the maximum deformation is the same as that of an elastic-perfectly-plastic system, Miranda *et al.* (1994). However it should be noted that as the period gets smaller and the strength reduction factor increases this ceases to apply. In view of the above, for SDOF 0.5, 0.8, 1, and 2 systems, for both material models and ground motions, the equal displacement rule was deemed appropriate. For the short-period systems studied, SDOF 0.1 and SDOF 0.3, the target displacement was estimated using equation 2.36.

In the case of the SDOF 0.5 system, EPP model, subjected to the Kocaeli ground motion for the graphical solution, Figures 4.12, 4.13, the first estimate of the performance point lies outside the bounds of the inelastic response spectra with the value of 0.052 m. This would imply failure of the system; however the fact that the capacity curve extends through the envelope of the ductility demand curves does not justify this conclusion. Furthermore this extension leads to unrealistic values of ductilities since the capacity spectrum does not intersect even a demand curve of $\mu = 10$, as seen in Figure 4.13.

Another interesting point, most obvious from Figure 4.13, is that when the capacity curve is superimposed on the constant-ductility spectra it intersects each of the constant-ductility curves at several points. It can also be seen that as the displacement increases the capacity curve intersects ductility curves of successively smaller magnitude. This probably suggests that the inelastic response spectra might not be appropriate for conducting pushover analyses. Regarding the performance point of the SDOF 0.5 system, EPSH model, Figures 4.14 and 4.15, the same conclusions can be made. A numerical example using the equation-based procedure is given for the SDOF 0.5 system in Appendix C.

Comparisons of the target displacements of the six SDOF systems from the N2 and DCM pushover methods with the maximum displacements from the nonlinear dynamic analyses are shown on Tables 4.1 to 4.24 for both ground motions and both material models. Additionally the ratios of displacement between pushover and dynamic analyses results are presented in Figure 4.18 for the Kocaeli ground motion and Figure 4.19 for the El Centro ground motion.

In the case of the Kocaeli ground motion, for the N2 method, the displacement demands were underestimated for SDOF systems 0.1, 0.3, 0.5 and 0.8 and overestimated for SDOF systems 1 and 2, Tables 4.1-4.12 and Figure 4.18. The N2 method for the short-period systems SDOF 0.1 and SDOF 0.3 provided unsatisfactory results with diminishing accuracy as the period decreased. For the SDOF 01 system, EPP model, the displacement demand was underestimated by as much as 90%. For SDOF 0.5 and 0.8 the displacement demands were underestimated by 40% and 75% respectively for the EPP model, and 30% and 70% for the EPSH model. For SDOF 1 and 2 the displacement demands were overestimated by approximately 50% for the EPP and EPSH models.

Regarding the El Centro case, Tables 4.13-4.24, and Figure 4.19, for the N2 method, the displacement demands of SDOF 0.1, 0.3, and 0.8 were underestimated by about 90%, 50%, and 40% respectively for both material models. For the SDOF 0.5 system the demands were conservative by almost 40%. For systems SDOF 1 and 2 the demands were calculated quite satisfactorily with 10% error.

Thus in general, the N2 method, for the Kocaeli ground motion - a near-fault ground motion-, underestimated the displacement demands for short-period systems, Figure 4.18. The maximum underestimation occurred for the SDOF 0.1 system, which was near the dominant period T_p of the ground motion. For the intermediate-period systems SDOF 0.8, SDOF 1, and SDOF 2 the N2 method mostly overestimated the displacement demands. It is interesting to note that for the near-fault ground motion the results of the pushover analysis change from underestimation to overestimation in the vicinity of T = 1 sec. This is close to half the pulse period of the ground motion, which is approximately T = 1.1 seconds as can be seen from the ground velocity-time series, Figure 3.5. The reader can refer to Sasani *et al.* (2000), Alavi *et al.* (2001), and Akkar *et al.* (2005) for the derivation of the pulse period of a near-fault ground motion. Therefore it seems that for near-fault ground motions the effectiveness of pushover analysis will depend on how the period of the system under study is related to the dominant pulse period of the ground motion.

The N2 method, for the El Centro ground motion - a far-field ground motion-, provided unconservative displacement demands for most of the short-period systems with reducing accuracy as the period decreased, Figure 4.19. In the intermediate-period

region the method yielded good estimates of target displacements. Near the mean period of the ground motion T_m, the N2 method overestimated the displacement demands.

The DCM method provided in general increased estimates of the target displacements for the Kocaeli ground motion for both material models compared to the N2 method, Figure 4.18. However, while it improved the displacement demands for systems SDOF 0.1, 0.3, 0.5, and 0.8, it resulted in a larger overestimation of the demands for SDOF 1 and 2 systems than the N2 method. This can be attributed to the fact that the DCM method has been created for code design purposes and is therefore generally more conservative since conservative target displacements, will lead to conservative design forces. This is preferred in practice. However the results show that the DCM method is not consistently conservative. Additionally, the performance of the DCM depends strongly on the values of the coefficients implying that it is very difficult to bound their numerical values so that they are descriptive of the relationship between elastic and inelastic displacements for all ground motions. It also seems that for near-fault ground motions these factors need to be increased.

For the El Centro case, the DCM method calculated larger displacement demands for each system when compared to the N2 method, Figure 4.19. Displacement demands were largely underestimated for the SDOF 0.1 system by 90% and considerably overestimated by 70% for the SDOF 0.5 system, EPP and EPSH models. For the other systems the DCM method provided fairly reasonable estimates.

4.2.3.2 Ductility

The estimation of ductility is based on the reduction factor R_μ which is defined as the ratio between the elastic and inelastic accelerations. This factor is necessary to obtain the ductility demand of the system according to the R- μ -T relationship defined in Chapter 2. The corresponding equation is given by Eq. 2.34. Other R- μ –T relationships exist but they have not been considered in this study because they generally lead to similar results (Chopra *et al.* 2000).

Tables 4.1 to 4.24, present the actual and normalized results for the Kocaeli and El Centro ground motions. Figures 4.20 and 4.21 show the ratio of ductility derived by

pushover and nonlinear dynamic methods for each of the SDOF systems, for the Kocaeli and El Centro ground motions respectively.

The N2 method predicted ductility demands which follow a similar pattern to the results for the target displacements for the two ground motions and material models. For the short-period systems subjected to the Kocaeli ground motion, Figure 4.20, the ductility was generally underestimated except for the SDOF I system, EPP model, where the ductility was calculated correctly, and the SDOF I system, EPSH model, where the ductility demand was three times larger. The reason for this large overestimation for a short - period system is that the strain-hardening effect becomes considerable with decreasing period, something that is not taken into account in the N2 method. For the intermediate-period systems in which the period is equal to or higher than the dominant period of the ground motion the ductility demands were overestimated by as much as 50%.

The N2 method for the El Centro ground motion, showed some variation in the ductility demands across the period range, Figure 4.21. For the SDOF 0.1 system, the ductility demands were underestimated for the EPP model by approximately 40%, and overestimated for the EPSH model by 16%. For the SDOF 0.3 and 0.5 systems the ductility demands were largely overestimated by more than 50% for both material models. For the intermediate – period systems the ductility demands were neither consistently conservative nor unconservative. This was expected because in this region the predicted inelastic displacements were approximately equal to the elastic ones.

The DCM method, for the Kocaeli ground motion, provided improved ductility estimates in the short-period range compared to the N2 method, Figure 4.20. However for the SDOF 0.1 system, EPP model, the ductility demands were underestimated by 84%. For SDOF 0.5 system, the ductility demands were underestimated by 27% for the EPP system and 16% for the EPSH system respectively. In the intermediate-period range the ductility demands were overestimated by more than 60%.

The DCM method, for the El Centro ground motion, generally overestimated the results except for the short-period systems SDOF 0.1 and SDOF 0.3, Figure 4.22. For SDOF 0.5 system, the DCM overestimated the demands by 78% for the EPP system and 85% for the EPSH system respectively.

In general, the differences between the pushover and nonlinear dynamic ductility demands follow a similar trend to the maximum displacements for both types of analysis. This is consistent with the fact that the displacement and ductility are linked.

4.2.3.3 Reaction Force

Tables 4.1 to 4.24, present the actual and normalized results of the reaction force for the Kocaeli and El Centro ground motions. Figures 4.22 and 4.23 show the ratio of reaction force derived by pushover and nonlinear dynamic methods for each of the SDOF systems for the Kocaeli and El Centro ground motions respectively.

The N2 method provided mostly satisfactory estimates of the restoring force demands for all systems, ground motions and material models, when compared with the nonlinear dynamic analyses results. For the Kocaeli ground motion, EPP model, the demands were estimated almost exactly for all systems, Figure 4.22. For the EPSH model the reaction force was underestimated, especially in the short-period range with the largest error being 43% for SDOF 0.1system. The best estimate for the EPSH model was obtained in the case of the SDOF 2 system with a slight underestimation of 3%.

The N2 method performed similarly for the El Centro ground motion, Figure 4.23, except for the case of SDOF 0.1 for which the reaction force was the same to that obtained from the nonlinear dynamic analysis.

The DCM method provided similar results for both ground motions when the EPP model was used. The use of the DCM method with the EPSH model resulted in a general improvement of the restoring force demands when compared to those calculated with the N2 method. Additionally, the magnitude of this improvement increased for decreasing periods. The results for this model were satisfactory.

It is worth noting that even though the restoring force demands have been approximated satisfactorily the methods show a tendency to consistently underestimate their magnitude. This could lead to an unconservative design, something that would not be appropriate.

4.2.3.4 Hysteretic Energy Dissipation

Tracking of the energy dissipation of a system can provide important information on its damage state. It would be expected that the hysteretic energy dissipation of a nonlinear dynamic system would be underestimated by the nonlinear static system. This is because the nonlinear static analyses produce results that apply to a part of the time-history while the nonlinear dynamic analyses provide results for all the time-history of response.

Tables 4.1 to 4.24, present the actual and normalized results of the hysteretic energy dissipation for the Kocaeli and El Centro ground motions. Figures 4.24 and 4.25 show the ratio of hysteretic energy derived by the pushover analysis and nonlinear dynamic analysis for each of the SDOF systems for the Kocaeli and El Centro ground motions respectively.

The N2 method showed that for short-period systems, for the Kocaeli ground motion, the hysteretic energy was significantly underestimated. It provided increased estimates of hysteretic energy with increasing period. For systems with a period lower than the pulse period of the Kocaeli ground motion the hysteretic energy was underestimated while for higher-period systems the hysteretic energy was overestimated.

For the El Centro ground motion, the hysteretic energy dissipation does not show any clear trend along the period range. For the short-period systems the hysteretic energy was underestimated. Near the predominant period of the ground motion it yielded satisfactory results. In the intermediate-period range the results were on either side of conservatism.

To show the effectiveness of the N2 method the force-displacement relationships of SDOF 0.5, obtained from nonlinear static and nonlinear dynamic analyses for both ground motions and material models, are shown in Figures 4.26 and 4.27. In the case of the Kocaeli ground motion, Figure 4.26, the first deformation cycle shows that the dissipated energy is underestimated by the pushover curves. On the contrary when the SDOF 0.5 system is subjected to the El Centro motion, Figure 4.27, the dissipated energy seems quite satisfactory. These graphs help achieve, qualitatively at least, the same conclusions as the ones drawn from Figures 4.21 and 4.25.

4.3 CONCLUSIONS FOR SDOF SYSTEMS

The study on the SDOF systems resulted in the following general observations when using pushover analysis. These are the following:

- The use of response spectra for the graphical solution of the N2 method can lead to difficulties for deriving a target displacement because for constant yield acceleration and increasing ductility the corresponding displacement decreases. Therefore, it appears that the constant-ductility spectra are not sufficient to capture the displacement demands. This is because these spectra do not contain all the possible yield strengths of a range of SDOF systems for a given ductility factor. Therefore in some cases it will be possible to find the 'correct' SDOF system corresponding to a specified yield strength and ductility factor but in some others not. Chopra (1995) has explained this in much detail.

- The N2 method underestimated the displacement demands in the short-period range for both types of ground motions studied, near-fault and far-field ground motions. Additionally, for decreasing period the underestimation of the displacement demands grew larger.

- The N2 method provided good estimates of target displacement in the intermediate-period range – 0.8 seconds to 2 seconds - for a far-field ground motion.

- The N2 method may underestimate displacement demands for systems with period lower than half the predominant pulse period of the near-fault ground motion and may overestimate the displacement demands for systems with period equal and larger to half the dominant pulse period of the near-fault ground motion.

- The ductility demands followed the same pattern as for the displacement demands for both types of ground motions.

- The reaction force was slightly underestimated for both ground motions when the EPP models were used. For the EPSH model the reaction force was generally underestimated, especially with decreasing period.

- The DCM method proved to be a rapid technique for conducting pushover analysis. The estimates of displacement demands for both types of ground were larger than those calculated from the N2 method. While this resulted in better estimates for the short-period systems it overestimated displacement and ductility demands in the intermediate-period range, something that is basically satisfactory.

- In general, the ductility and displacement demands can be significantly underestimated from a pushover analysis when near-fault ground motions are studied. For far-field ground motions pushover analysis seemed to overestimate the demands.

- The pushover curves manage to 'catch' the onset or first cycle of deformation of the system with no significant deviations in their post-yield branch when compared with the force-displacement relationships derived from the nonlinear dynamic analyses.

- The pushover curves show that there is an amount of dissipated energy that is not included effectively meaning that damage quantification assessment could be misleading.

- It would be interesting to check how the pushover analysis performs when systems are subjected to simpler loading time histories in which the distribution of frequencies is simpler and more distinct. For example loading histories that could be used are sine waves and pulses.

- Finally even if the method is used as a tool to simplify the design or assessment process it depends on available computational tools; such as computer programs for deriving inelastic response spectra, and programs for performing Fourier Analyses. Additionally the applicability of the method can be checked only by considering a reasonable number of ground motions of different intensity,

frequency content, and duration. Also the coupling of the method with some empirical rules such as the equal displacement rule and the decision whether these rules are appropriate for a specific pushover analysis require some engineering experience.

4.4 PUSHOVER ANALYSIS OF A 2-DOF SYSTEM

4.4.1 Introduction

Having described the behaviour of the SDOF system, this section will investigate the seismic response of a two-degree-of-freedom system, 2-DOF, to the two ground motions previously used, through the use of the conventional pushover analysis methods described in Chapter 2. These are the N2 method, the Displacement Coefficient Method, DCM, and the Modal Pushover Analysis, MPA. The study will attempt to appraise the efficiency of each method in terms of calculating important seismic demands such as target displacement, ductility, restoring force.

4.4.2 Modelling

The 2-DOF system was created by connecting in series two SDOF 0.5 systems used in the SDOF study. The theoretical model is presented in Figure 4.28. The same modeling assumptions were considered as in the case of the SDOF systems.

4.4.3 Modes of Vibration

A natural frequency analysis was performed in order to obtain the two natural translational modes of vibration for this model. These are shown in Table 4.25. The natural mode shapes of the system are presented normalised, so that the right-end node mode shape is unity.

4.4.4 Nonlinear Dynamic Analyses

The model was subjected to nonlinear dynamic analyses in order to provide a benchmark for the pushover analysis results. The displacement-time histories of the system are shown in Figures 4.29 and 4.30 for the Kocaeli ground motion and the El Centro ground motion respectively. Figures 4.31 and 4.32 show the total applied force-displacement responses for the Kocaeli ground motion and for the El Centro ground motion respectively.

The results show that the nodes of the system displace in a manner that verifies the first-mode assumption of pushover analysis. From the displacement time-histories for both ground motions it can be seen that the system yielded at approximately the same time instants. Furthermore the system displaced permanently under both ground motions but with not the same amount of permanent deformation. Additionally, observing the two force-displacement responses produced from the two individual excitations both nodes of the system sustain about the same amount of loading for the same ground motion. This occurs at different time instants.

4.4.5 Load Patterns

Seven load patterns have been used for this system. They are:

1. Mode Shape distribution
2. Inverted Triangular distribution
3. The FEMA(1) distribution with $k \approx 1.155$
4. The FEMA(2) distribution with $k = 2$
5. Uniform distribution
6. Kunnath (+) distribution
7. Kunnath (-) distribution

The FEMA(1) load distribution means that the factor k has been derived through linear interpolation between the two extreme values, corresponding to the period of the system. The FEMA(2) distribution considers the extreme value of the factor k. For ease of understanding they are presented in Figures 4.33 & 4.34. Kunnath (+) distribution means the sum of the two mode shape distributions and Kunnath (-) distribution means their difference.

4.4.6 Nonlinear Static Analyses

Nonlinear static analyses on the 2-DOF system were performed by applying the load patterns described in the preceding section. The static solutions for the different load patterns were obtained using the Newton-Raphson nonlinear solution technique.

The results of the nonlinear static analyses, the capacity curves, provided similar values of yield load and yield displacement for the seven different load patterns and the two material models. These are presented in Figures 4.35 & 4.36 for the Kocaeli and El Centro ground motions respectively.

The capacity curves, that means the force-displacement responses, were then transformed to their corresponding capacity spectra that represent the acceleration displacement demands for the equivalent SDOF systems. These are presented in Figures 4.37 & 4.38 for the Kocaeli and El Centro ground motions respectively.

The differences that exist between yield displacements and yield forces and consequently between the yield displacements and yield accelerations for the seven used load patterns can be attributed to the different ratios of loading applied at the nodes of the system causing to yield at different deformation levels, and also due to probable numerical errors in the solution process. However these are not significant, especially for the El Centro ground motion. This insignificant difference implied that at least for the two-degree-of-freedom system utilisation of seven load patterns might not have been needed since each load pattern will provide the same or very similar results.

The capacity curves of the equivalent SDOF systems can be used to obtain the target displacement estimates for the N2 and DCM methods. The MPA method however, required the derivation of force-displacement curves for the two modes of vibration. These are presented in Figures 4.39 and 4.40 for the Kocaeli and El Centro ground motions respectively. Their subsequent transformation to equivalent SDOF systems resulted in Figures 4.41 and 4.42 for the Kocaeli and El Centro ground motions respectively.

When the system is subjected to the second mode load pattern it yields at a lower value of load. However, with increasing load factor the displacements ‘grow’ in the negative

direction. This is because the top node of the system is displacing in the opposite direction of the acceleration and also in the opposite direction of movement relatively to the middle node of the system.

By transforming the bilinear force-deformation relationships of the different modes of vibration and material models to the force-deformation relationships of their equivalent SDOF systems it is seen that the second mode 'equivalent' load pattern attains higher loads than the first mode pattern, Figures 4.41 and 4.42 for the Kocaeli and El Centro ground motions respectively. This suggests that the equivalent SDOF system of the second mode has higher strength than the SDOF system of the first mode and therefore it will displace by a smaller amount.

The maximum displacement of the equivalent SDOF systems can be found by either performing a nonlinear time history analysis or from the inelastic response spectrum. In this study nonlinear time-history analyses were performed for the four equivalent SDOF systems.

4.4.7 Results

4.4.7.1 N2 method

The displacement demands, restoring force and ductility demands of the 2-DOF system for the EPP and EPSH models and the Kocaeli and El Centro ground motions for the N2 method are shown in Tables 4.26, and 4.27, and Figures 4.43-4.44 for the Kocaeli, and in Tables 4.28 & 4.29 and Figures 4.45-4.46 for the El Centro. These have been derived by employing the equal displacement rule since the natural period of the system is larger than the characteristic periods of the ground motions.

Tables 4.26, and 4.27, and Figures 4.43-4.44, show that the N2 method generally underestimates the displacements at both nodes for the EPP and EPSH models and the Kocaeli ground motion. The least effective load distributions were the Uniform load distribution and Kunnath (+) load distribution which underestimated the displacement demands by 32% and 33% respectively for the EPP model. Kunnath(-) load pattern was almost exact for both nodes in the case of the EPP model resulting in a minimal overestimation of 1%. The FEMA(2) load distribution resulted in a slight

overestimation of the displacements by 1% for the EPSH model but was the most effective.

In the case of the El Centro ground motion, Tables 4.28 & 4.29 and Figures 4.45-4.46, the Mode Shape, Inverted Triangular and FEMA(1) distributions were the most accurate for the EPP model. The Mode Shape distribution resulted in a small underestimation by 3% while the Inverted Triangular and FEMA(1) distributions overestimated the displacement demands by 4% and 11%. The least effective load distribution was the uniform distribution for the EPP model resulting in underestimation of 22%. The results for the EPSH model show that all load patterns except for the Uniform overestimate the displacements at both nodes. The mode shape distribution was the most effective for this model with an overestimation of 7%. The Uniform distribution resulted in an underestimation of 14%.

The restoring force demands were generally calculated efficiently using the N2 method for both ground motions especially for the EPP model from all load distributions. For the Kocaeli ground motion, the N2 method resulted mostly in unconservative estimates while for the El Centro ground motion it mostly overestimated the restoring force demands. The Mode Shape distribution performed well for the estimation of this quantity for the two hysteretic models.

The ductility demands calculated using the different load distributions were all underestimated in the case of the Kocaeli ground motion with an error range of 19%-38%. The most effective load distributions in capturing the ductility demand was the FEMA(2) and Kunnath(-) distributions for the EPP model, and the Mode Shape, FEMA(1), FEMA(2) and Kunnath(-) distributions for the EPSH model. In the case of the El Centro ground motion the ductilities were mostly overestimated. However, the Mode Shape distribution provided exact agreement with the nonlinear dynamic analysis result for the EPP model.

4.4.7.2 Displacement Coefficient Method, DCM

Tables 4.30, 4.31, and Figures 4.47 and 4.48, show the displacement demands, restoring force and ductility demands of the system obtained through the DCM method for the

Kocaeli ground motion. Tables 4.32, 4.33, and Figures 4.49 and 4.50, show the displacement demands for the El Centro ground motion.

For the Kocaeli ground motion the FEMA(1) and Kunnath(-) load distributions are the most accurate for the EPP model overestimating the maximum displacement by 2% and 3% respectively. The Inverted Triangular distribution was the most accurate for the EPSH model resulting in a minimal underestimation of 1%. The FEMA(2) distribution produced an upper-bound in the response of the EPP and EPSH models.

For the El Centro ground motion and the EPP model, Kunnath(+) pattern is the most accurate, overestimating the maximum displacement by only 1%. The Inverted Triangular distribution resulted in large overestimation of displacements at both nodes of the system by 83% for the EPP and 46% for the EPSH models. For the EPSH model all load patterns overestimated the demands except for the Uniform distribution which was the most accurate for both EPP and EPSH models.

The DCM method calculated accurately restoring force demands with all load distributions for both ground motions and especially for the EPP model. In general, the method slightly underestimated the restoring force demands for the Kocaeli and the El Centro ground motions with an error from of 0% to 8%.

The results of the ductility demands for this method show similar trends to the N2 method. This means that the DCM method underestimated the ductility demands for the Kocaeli, near-fault ground motion, and overestimated them for the El Centro, far-field ground motion. However the estimates for the Kocaeli ground motion were closer to the 'exact' values derived from nonlinear dynamic analyses than for the El Centro ground motion but they were still unconservative.

4.4.7.3 Modal Pushover Analysis, MPA

The results obtained using the MPA procedure are presented in Tables 4.34 and 4.35 and Figures 4.51 and 4.52 for the Kocaeli ground motion and in Tables 4.36 and 4.37 and Figures 4.53 and 4.54 for the El Centro ground motion.

The MPA procedure resulted in conservative estimates of displacement demands for both ground motions and material models, especially for the EPP model for which the maximum displacement was overestimated by 38%. Additionally, the method did not yield satisfactory estimates for the node 2 of the 2-DOF system. The MPA method provided a conservative estimate of base shear for the EPP model but the error was the same as for the other methods. The ductility demands were estimated more accurately than the N2 and the DCM methods but they were still conservative.

4.4.8 Conclusions on the 2-DOF System

The pushover curves of the system, using the load distributions described, were very similar, especially for the El Centro ground motion, a far-field ground motion. This implied that for systems with a few degrees of freedom subjected to far-field ground motions the utilization of all the available load distributions would not be very efficient. However, the yield displacement can cause considerable variations in the elastic acceleration demands and in the ductility demands when response spectra are used, because it controls the period of vibration of the ESDOF system. This was quite evident for the Kocaeli ground motion, a near-fault ground motion.

The incorporation of different material models produces different results. Therefore pushover analyses can be sensitive to the material model used. When EPP behaviour is considered the demand quantities can ‘grow’ very large especially for near-fault ground motions.

Generally, the FEMA load distributions, and Kunnath load distributions produced the most satisfactory results in most of the cases in terms of accuracy, but the results were mostly unconservative. The mode shape load distribution was not very effective. The Uniform load distribution yielded in general satisfactory estimates

In general the effectiveness of the load distributions differs for different methods and hysteretic models.

The N2 method is not very good in estimating maximum displacements and ductilities especially for the EPP model. They are satisfactory though for base shear estimation. In

general, the N2 method produces the least magnitude of maximum displacements for the system with regard to the other methods.

The estimates of base shear are quite good for all methods. The least precise estimation of base shear was provided by the DCM method for an EPP model but it yielded the most accurate estimate for the EPSH model.

The DCM procedure appeared to be the most convenient in terms of time for calculating the demands of interest and surprisingly in terms of accuracy for the near-fault ground motion.

The MPA method proved to be time-consuming but if more than one loading patterns need to be considered in the other methods, it requires similar effort. The results obtained from this method seem to be conservative for maximum displacement and base shear quantities especially in the case of the EPP model.

The ductility calculated from all the methods for both material models was found to be unsatisfactory. The N2 method did not provide satisfactory estimates of ductility especially for the EPP model. The best estimate of ductility was provided by the MPA method for the elastoplastic with strain hardening material model.

Finally the 2-DOF system study showed that the N2 method underestimated the displacement demand for a near-fault ground motion something that was expected from the conclusions on the SDOF systems as it has a lower period of vibration than half the dominant pulse period of the ground motion.

SDOF 0.1	Kocaeli					
	N2		DCM		Nonlinear Dynamic Analysis	
	α=0	*α=0.03*	*α=0*	*α=0.03*	*α=0*	*α=0.03*
Displacement (m)	0.0014	0.0014	0.0075	0.0075	0.0256	0.0085
Ductility	28	28	8.4	8.4	27.6	9.2
Reaction (kN)	178.02	180.95	178.02	217.37	185.32	317.15
Hysteretic Energy (kNm)	0.35	0.34	4.73	4.59	21.70	11.14

Table 4-1 Comparison of results between pushover analysis and nonlinear dynamic analysis for SDOF 0.1, Kocaeli

SDOF 0.1	Kocaeli					
	N2		DCM		Nonlinear Dynamic Analysis	
	α=0	*α=0.03*	*α=0*	*α=0.03*	*α=0*	*α=0.03*
Displacement (m)	0.05	0.16	0.29	0.89	1.00	1.00
Ductility	1.01	3.04	0.30	0.91	1.00	1.00
Reaction (kN)	0.96	0.57	0.96	0.69	1.00	1.00
Hysteretic Energy (kNm)	0.02	0.03	0.22	0.41	1.00	1.00

Table 4-2 Comparison of normalised results between pushover analysis and nonlinear dynamic analysis for SDOF 0.1, Kocaeli

SDOF 0.3	Kocaeli					
	N2		DCM		Nonlinear Dynamic Analysis	
	α=0	*α=0.03*	*α=0*	*α=0.03*	*α=0*	*α=0.03*
Displacement (m)	0.0256	0.0256	0.0549	0.0549	0.0474	0.0474
Ductility	7.3	7.3	6	6	5	5
Reaction (kN)	200.12	210.97	200.12	230.24	206.77	261.34
Hysteretic Energy (kNm)	13.20	12.81	36.64	35.54	34.93	35.34

Table 4-3 Comparison of results between pushover analysis and nonlinear dynamic analysis for SDOF 0.3, Kocaeli

SDOF 0.3	Kocaeli					
	N2		DCM		Nonlinear Dynamic Analysis	
	α=0	*α=0.03*	*α=0*	*α=0.03*	*α=0*	*α=0.03*
Displacement (m)	0.54	0.54	1.16	1.16	1.00	1.00
Ductility	1.46	1.46	1.20	1.20	1.00	1.00
Reaction (kN)	0.97	0.81	0.97	0.88	1.00	1.00
Hysteretic Energy (kNm)	0.38	0.36	1.05	1.01	1.00	1.00

Table 4-4 Comparison of normalised results between pushover analysis and nonlinear dynamic analysis for SDOF 0.3, Kocaeli

SDOF 0.5	Kocaeli					
	N2		DCM		Nonlinear Dynamic Analysis	
	α=0	*α=0.03*	*α=0*	*α=0.03*	*α=0*	*α=0.03*
Displacement (m)	0.0520	0.0520	0.0620	0.0620	0.0860	0.0740
Ductility	4	4	4.8	4.8	6.6	5.7
Reaction (kN)	102.50	111.74	102.50	115.60	107.12	143.10
Hysteretic Energy (kNm)	16.00	15.52	20.10	19.42	35.76	37.04

Table 4-5 Comparison of results between pushover analysis and nonlinear dynamic analysis for SDOF 0.5, Kocaeli

SDOF 0.5	Kocaeli					
	N2		DCM		Nonlinear Dynamic Analysis	
	α=0	*α=0.03*	*α=0*	*α=0.03*	*α=0*	*α=0.03*
Displacement (m)	0.60	0.70	0.72	0.84	1.00	1.00
Ductility	0.61	0.70	0.73	0.84	1.00	1.00
Reaction (kN)	0.96	0.78	0.96	0.81	1.00	1.00
Hysteretic Energy (kNm)	0.45	0.42	0.56	0.52	1.00	1.00

Table 4-6 Comparison of normalised results between pushover analysis and nonlinear dynamic analysis for SDOF 0.5, Kocaeli

SDOF 0.8	Kocaeli					
	N2		DCM		Nonlinear Dynamic Analysis	
	α=0	*α=0.03*	*α=0*	*α=0.03*	*α=0*	*α=0.03*
Displacement (m)	0.1051	0.1051	0.1262	0.1262	0.2066	0.1798
Ductility	4	4	4.8	4.8	7.7	6.7
Reaction (kN)	81.25	88.54	81.25	90.49	86.68	112.72
Hysteretic Energy (kNm)	25.61	24.84	32.44	31.47	45.81	46.77

Table 4-7 Comparison of results between pushover analysis and nonlinear dynamic analysis for SDOF 0.8, Kocaeli

SDOF 0.8	Kocaeli					
	N2		DCM		Nonlinear Dynamic Analysis	
	α=0	*α=0.03*	*α=0*	*α=0.03*	*α=0*	*α=0.03*
Displacement (m)	0.25	0.29	0.61	0.70	1.00	1.00
Ductility	0.52	0.60	0.62	0.72	1.00	1.00
Reaction (kN)	0.94	0.79	0.94	0.80	1.00	1.00
Hysteretic Energy (kNm)	0.56	0.53	0.71	0.67	1.00	1.00

Table 4-8 Comparison of normalised results between pushover analysis and nonlinear dynamic analysis for SDOF 0.8, Kocaeli

SDOF 1	Kocaeli					
	N2		DCM		Nonlinear Dynamic Analysis	
	α=0	α=0.03	α=0	α=0.03	α=0	α=0.03
Displacement (m)	0.1878	0.1878	0.2253	0.2253	0.1328	0.1318
Ductility	4	4	4.8	4.8	2.8	2.7
Reaction (kN)	93.24	101.56	93.24	103.78	96.68	109.70
Hysteretic Energy (kNm)	52.42	50.85	66.42	64.43	42.26	43.31

Table 4-9 Comparison of results between pushover analysis and nonlinear dynamic analysis for SDOF 1, Kocaeli

SDOF 1	Kocaeli					
	N2		DCM		Nonlinear Dynamic Analysis	
	α=0	α=0.03	α=0	α=0.03	α=0	α=0.03
Displacement (m)	1.41	1.43	1.70	1.71	1.00	1.00
Ductility	1.43	1.48	1.71	1.78	1.00	1.00
Reaction (kN)	0.96	0.93	0.96	0.95	1.00	1.00
Hysteretic Energy (kNm)	1.24	1.17	1.57	1.49	1.00	1.00

Table 4-10 Comparison of normalized results between pushover analysis and nonlinear dynamic analysis for SDOF 1, Kocaeli

SDOF 2	Kocaeli					
	N2		DCM		Nonlinear Dynamic Analysis	
	α=0	α=0.03	α=0	α=0.03	α=0	α=0.03
Displacement (m)	0.4454	0.4454	0.5345	0.5345	0.3318	0.3369
Ductility	4	4	4.8	4.8	2.9	3
Reaction (kN)	55.41	60.34	55.41	61.66	60.33	61.94
Hysteretic Energy (kNm)	73.84	71.63	93.57	90.77	37.86	38.56

Table 4-11 Comparison of results between pushover analysis and nonlinear dynamic analysis for SDOF 2, Kocaeli

SDOF 2	Kocaeli					
	N2		DCM		Nonlinear Dynamic Analysis	
	α=0	α=0.03	α=0	α=0.03	α=0	α=0.03
Displacement (m)	1.34	1.32	1.61	1.59	1.00	1.00
Ductility	1.38	1.33	1.66	1.60	1.00	1.00
Reaction (kN)	0.92	0.97	0.92	1.00	1.00	1.00
Hysteretic Energy (kNm)	1.95	1.86	2.47	2.35	1.00	1.00

Table 4-12 Comparison of normalized results between pushover analysis and nonlinear dynamic analysis for SDOF 2, Kocaeli

SDOF 0.1	El Centro					
	N2		DCM		Nonlinear Dynamic Analysis	
	α=0	*α=0.03*	*α=0*	*α=0.03*	*α=0*	*α=0.03*
Displacement (m)	0.0006	0.0006	0.0036	0.0036	0.0211	0.0104
Ductility	23.75	23.75	9	9	41.3	20.4
Reaction (kN)	79.57	81.00	79.57	98.68	79.79	145.40
Hysteretic Energy (kNm)	0.08	0.07	1.03	1.00	6.83	2.27

Table 4-13 Comparison of results between pushover analysis and nonlinear dynamic analysis for SDOF 0.1, El Centro

SDOF 0.1	El Centro					
	N2		DCM		Nonlinear Dynamic Analysis	
	α=0	*α=0.03*	*α=0*	*α=0.03*	*α=0*	*α=0.03*
Displacement (m)	0.03	0.06	0.17	0.35	1.00	1.00
Ductility	0.58	1.16	0.22	0.44	1.00	1.00
Reaction (kN)	1.00	0.56	1.00	0.68	1.00	1.00
Hysteretic Energy (kNm)	0.01	0.03	0.15	0.44	1.00	1.00

Table 4-14 Comparison of normalized results between pushover analysis and nonlinear dynamic analysis for SDOF 0.1, El Centro

SDOF 0.3	El Centro					
	N2		DCM		Nonlinear Dynamic Analysis	
	α=0	*α=0.03*	*α=0*	*α=0.03*	*α=0*	*α=0.03*
Displacement (m)	0.0119	0.0119	0.0255	0.0255	0.0279	0.0244
Ductility	7.3	7.3	6.1	6.1	4.6	4.1
Reaction (kN)	92.41	97.46	92.41	106.41	93.38	127.16
Hysteretic Energy (kNm)	2.84	2.75	7.87	7.63	12.14	9.74

Table 4-15 Comparison of results between pushover analysis and nonlinear dynamic analysis for SDOF 0.3, El Centro

SDOF 0.3	El Centro					
	N2		DCM		Nonlinear Dynamic Analysis	
	α=0	*α=0.03*	*α=0*	*α=0.03*	*α=0*	*α=0.03*
Displacement (m)	0.43	0.49	0.91	1.05	1.00	1.00
Ductility	1.59	1.78	1.33	1.49	1.00	1.00
Reaction (kN)	0.99	0.77	0.99	0.84	1.00	1.00
Hysteretic Energy (kNm)	0.23	0.28	0.65	0.78	1.00	1.00

Table 4-16 Comparison of normalized results between pushover analysis and nonlinear dynamic analysis for SDOF 0.3, El Centro

SDOF 0.5	El Centro					
	N2		DCM		Nonlinear Dynamic Analysis	
	α=0	*α=0.03*	*α=0*	*α=0.03*	*α=0*	*α=0.03*
Displacement (m)	0.0570	0.0570	0.0680	0.0680	0.0405	0.0399
Ductility	4	4	4.8	4.8	2.7	2.6
Reaction (kN)	111.4	121.6	111.4	124.2	111.4	132.2
Hysteretic Energy (kNm)	19.12	18.54	24.02	23.30	19.35	18.92

Table 4-17 Comparison of results between pushover analysis and nonlinear dynamic analysis for SDOF 0.5, El Centro

SDOF 0.5	El Centro					
	N2		DCM		Nonlinear Dynamic Analysis	
	α=0	*α=0.03*	*α=0*	*α=0.03*	*α=0*	*α=0.03*
Displacement (m)	1.41	1.43	1.68	1.70	1.00	1.00
Ductility	1.48	1.54	1.78	1.85	1.00	1.00
Reaction (kN)	1.00	0.92	1.00	0.94	1.00	1.00
Hysteretic Energy (kNm)	0.99	0.98	1.24	1.23	1.00	1.00

Table 4-18 Comparison of normalized results between pushover analysis and nonlinear dynamic analysis for SDOF 0.5, El Centro

SDOF 0.8	El Centro					
	N2		DCM		Nonlinear Dynamic Analysis	
	α=0	*α=0.03*	*α=0*	*α=0.03*	*α=0*	*α=0.03*
Displacement (m)	0.0790	0.0790	0.0948	0.0948	0.1079	0.0960
Ductility	4	4	4.8	4.8	5.1	4.5
Reaction (kN)	61.47	66.94	61.47	68.40	67.87	75.70
Hysteretic Energy (kNm)	14.53	14.09	18.41	17.86	17.86	18.27

Table 4-19 Comparison of results between pushover analysis and nonlinear dynamic analysis for SDOF 0.8, El Centro

SDOF 0.8	El Centro					
	N2		DCM		Nonlinear Dynamic Analysis	
	α=0	*α=0.03*	*α=0*	*α=0.03*	*α=0*	*α=0.03*
Displacement (m)	0.73	0.82	0.88	0.99	1.00	1.00
Ductility	0.78	0.89	0.94	1.07	1.00	1.00
Reaction (kN)	0.91	0.88	0.91	0.90	1.00	1.00
Hysteretic Energy (kNm)	0.81	0.77	1.03	0.98	1.00	1.00

Table 4-20 Comparison of normalized results between pushover analysis and nonlinear dynamic analysis for SDOF 0.8, El Centro

SDOF 1	El Centro					
	N2		DCM		Nonlinear Dynamic Analysis	
	α=0	*α=0.03*	*α=0*	*α=0.03*	*α=0*	*α=0.03*
Displacement (m)	0.1123	0.1123	0.1348	0.1348	0.1044	0.1022
Ductility	4	4	4.8	4.8	3.1	3
Reaction (kN)	55.88	60.85	55.88	62.80	58.81	61.90
Hysteretic Energy (kNm)	18.77	18.21	23.79	23.01	11.19	11.21

Table 4-21 Comparison of results between pushover analysis and nonlinear dynamic analysis for SDOF 1, El Centro

SDOF 1	El Centro					
	N2		DCM		Nonlinear Dynamic Analysis	
	α=0	*α=0.03*	*α=0*	*α=0.03*	*α=0*	*α=0.03*
Displacement (m)	1.08	1.10	1.29	1.32	1.00	1.00
Ductility	1.29	1.33	1.55	1.60	1.00	1.00
Reaction (kN)	0.95	0.98	0.95	1.01	1.00	1.00
Hysteretic Energy (kNm)	1.68	1.62	2.13	2.05	1.00	1.00

Table 4-22 Comparison of normalized results between pushover analysis and nonlinear dynamic analysis for SDOF 1, El Centro

SDOF 2	El Centro					
	N2		DCM		Nonlinear Dynamic Analysis	
	α=0	*α=0.03*	*α=0*	*α=0.03*	*α=0*	*α=0.03*
Displacement (m)	0.1365	0.1365	0.1638	0.1638	0.1511	0.1515
Ductility	4	4	4.8	4.8	4.3	4.4
Reaction (kN)	16.94	18.45	16.94	18.86	18.32	21.15
Hysteretic Energy (kNm)	6.92	6.72	8.77	8.51	8.58	8.77

Table 4-23 Comparison of results between pushover analysis and nonlinear dynamic analysis for SDOF 2, El Centro

SDOF 2	El Centro					
	N2		DCM		Nonlinear Dynamic Analysis	
	α=0	*α=0.03*	*α=0*	*α=0.03*	*α=0*	*α=0.03*
Displacement (m)	0.90	0.90	1.08	1.08	1.00	1.00
Ductility	0.93	0.91	1.12	1.09	1.00	1.00
Reaction (kN)	0.92	0.87	0.92	0.89	1.00	1.00
Hysteretic Energy (kNm)	0.81	0.77	1.02	0.97	1.00	1.00

Table 4-24 Comparison of normalized results between pushover analysis and nonlinear dynamic analysis for SDOF 2, El Centro

MODE	EIGENVALUE	FREQUENCY (Hz)	PERIOD (s)
1	60.3525	1.23643	0.81
2	413.662	3.23700	0.31

$\Phi_1 = \{0.619\ 1.0\}^T$ and $\Phi_2 = \{-1.615\ 1.0\}^T$

Table 4-25 Modes of vibration of 2-DOF system

KOCAELI	N2														*N-RHA*	
	Mode Shape		Inverted Triangular		FEMA(1)		FEMA(2)		Uniform		Kunnath (+)		Kunnath (-)			
	α=0	α=0.03	α=0	α=0.03	α=0	α=0.03	α=0	α=0.03	α=0	α=0.03	α=0	α=0.03	α=0	α=0.03	α=0	α=0.03
Displacement (m) (node 3)	0.1274	0.1575	0.1437	0.1437	0.1575	0.1575	0.1768	0.1768	0.1269	0.1269	0.1250	0.1250	0.1871	0.1871	0.1857	0.1743
Displacement (m) (node 2)	0.1131	0.1410	0.1283	0.1262	0.1415	0.1390	0.1558	0.1551	0.1153	0.1140	0.1190	0.1156	0.1651	0.1154	0.1698	0.1484
Base Shear (kN)	182.65	210.93	183	202.6	183	210.5	183	214.27	183	204.07	183	200.5	183	204.87	186.7	239
Ductility	3.4	4	3.7	3.7	4	4	4.2	4.2	3.6	3.6	4	4	4.1	4.1	5.5	5.2

Table 4-26 Comparison of results between pushover analysis and nonlinear dynamic analysis for a 2-DOF system

KOCAELI	N2													
	Mode Shape		Inverted Triangular		FEMA(1)		FEMA(2)		Uniform		Kunnath (+)		Kunnath (-)	
	α=0	α=0.03	α=0	α=0.03	α=0	α=0.03	α=0	α=0.03	α=0	α=0.03	α=0	α=0.03	α=0	α=0.03
Displacement (m) (node 3)	0.68	0.90	0.77	0.82	0.85	0.90	0.95	1.01	0.68	0.73	0.67	0.72	1.01	1.07
Displacement (m) (node 2)	0.67	0.95	0.76	0.85	0.83	0.94	0.92	1.05	0.68	0.77	0.70	0.78	0.97	0.78
Base Shear	0.98	0.88	0.98	0.85	0.98	0.88	0.98	0.90	0.98	0.85	0.98	0.84	0.98	0.86
Ductility	0.62	0.77	0.67	0.71	0.73	0.77	0.76	0.81	0.65	0.69	0.73	0.77	0.75	0.79

Table 4-27 Comparison of normalised results between pushover analysis and nonlinear dynamic analysis for a 2-DOF system

EL CENTRO	N2														N-RHA	
	Mode Shape		Inverted Triangular		FEMA(1)		FEMA(2)		Uniform		Kunnath (+)		Kunnath (-)			
	α=0	α=0.03	α=0	α=0.03	α=0	α=0.03	α=0	α=0.03	α=0	α=0.03	α=0	α=0.03	α=0	α=0.03	α=0	α=0.03
Displacement (m) (node 3)	0.0990	0.0990	0.1063	0.1127	0.1127	0.1127	0.1227	0.1261	0.0799	0.0799	0.0860	0.1065	0.1261	0.1261	0.1019	0.0927
Displacement (m) (node 2)	0.0881	0.0870	0.0945	0.0993	0.1005	0.0988	0.1125	0.1097	0.0710	0.0703	0.0763	0.0954	0.0812	0.1147	0.0989	0.0867
Base Shear (kN)	139.85	156.33	139.9	159.23	139.9	159.12	138.05	161.71	139.9	151.02	139.9	158.32	139.9	161.62	139.9	169.5
Ductility	3.5	3.4	3.6	3.7	3.8	3.7	3.9	3.9	3	3	3.1	3.6	3.9	3.9	3.5	3.2

Table 4-28 Comparison of results between pushover analysis and nonlinear dynamic analysis for a 2-DOF system (El Centro ground motion)

EL CENTRO	N2													
	Mode Shape		Inverted Triangular		FEMA(1)		FEMA(2)		Uniform		Kunnath (+)		Kunnath (-)	
	α=0	α=0.03	α=0	α=0.03	α=0	α=0.03	α=0	α=0.03	α=0	α=0.03	α=0	α=0.03	α=0	α=0.03
Displacement (m) (node 3)	0.97	1.07	1.04	1.22	1.11	1.22	1.20	1.36	0.78	0.86	0.84	1.15	1.24	1.36
Displacement (m) (node 2)	0.89	1.00	0.96	1.15	1.02	1.14	1.14	1.27	0.72	0.81	0.77	1.10	0.82	1.32
Base Shear	1.00	0.92	1.00	0.94	1.00	0.94	0.99	0.95	1.00	0.89	1.00	0.93	1.00	0.95
Ductility	1.00	1.06	1.03	1.16	1.09	1.16	1.11	1.22	0.86	0.94	0.89	1.13	1.11	1.22

Table 4-29 Comparison of normalised results between pushover analysis and nonlinear dynamic analysis for a 2-DOF system (El Centro ground motion)

KOCAELI	DCM														*N-RHA*	
	Mode Shape		Inverted Triangular		FEMA(1)		FEMA(2)		Uniform		Kunnath (+)		Kunnath (-)			
	α=0	α=0.03	α=0	α=0.03	α=0	α=0.03	α=0	α=0.03	α=0	α=0.03	α=0	α=0.03	α=0	α=0.03	α=0	α=0.03
Displacement (m) (node 3)	0.1530	0.1891	0.1724	0.1724	0.1891	0.1891	0.2122	0.2122	0.1524	0.1524	0.1500	0.1500	0.1905	0.1905	0.1857	0.1743
Displacement (m) (node 2)	0.1387	0.1720	0.1570	0.1543	0.1731	0.1701	0.1870	0.1886	0.1408	0.1391	0.1429	0.1404	0.1685	0.1172	0.1698	0.1484
Base Shear (kN)	182.65	218.3	183	214.1	183	217.8	183	222.3	183	210.47	183	210.71	183	205.3	186.7	239
Ductility	4.1	4.7	4.5	4.5	4.8	4.8	5.1	5.1	4.3	4.4	4.7	4.7	4.2	4.2	5.5	5.2

Table 4-30 Comparison of results between pushover analysis and nonlinear dynamic analysis for a 2-DOF system

KOCAELI	DCM													
	Mode Shape		Inverted Triangular		FEMA(1)		FEMA(2)		Uniform		Kunnath (+)		Kunnath (-)	
	α=0	α=0.03	α=0	α=0.03	α=0	α=0.03	α=0	α=0.03	α=0	α=0.03	α=0	α=0.03	α=0	α=0.03
Displacement (m) (node 3)	0.82	1.08	0.93	0.99	1.02	1.08	1.14	1.22	0.82	0.87	0.81	0.86	1.03	1.09
Displacement (m) (node 2)	0.82	1.16	0.92	1.04	1.02	1.15	1.10	1.27	0.83	0.94	0.84	0.95	0.99	0.79
Base Shear (kN)	0.98	0.91	0.98	0.90	0.98	0.91	0.98	0.93	0.98	0.88	0.98	0.88	0.98	0.86
Ductility	0.75	0.90	0.82	0.87	0.87	0.92	0.93	0.98	0.78	0.85	0.85	0.90	0.76	0.81

Table 4-31 Comparison of normalised results between pushover analysis and nonlinear dynamic analysis for a 2-DOF system

EL CENTRO	DCM														N-RHA	
	Mode Shape		Inverted Triangular		FEMA(1)		FEMA(2)		Uniform		Kunnath (+)		Kunnath (-)			
	α=0	α=0.03	α=0	α=0.03	α=0	α=0.03	α=0	α=0.03	α=0	α=0.03	α=0	α=0.03	α=0	α=0.03	α=0	α=0.03
Displacement (m) (node 3)	0.1195	0.1195	0.1868	0.1352	0.1352	0.1352	0.1473	0.1514	0.0971	0.0971	0.1029	0.1276	0.1514	0.1514	0.1019	0.0927
Displacement (m) (node 2)	0.1086	0.1069	0.1740	0.1213	0.1230	0.1208	0.1333	0.1344	0.0882	0.0872	0.0932	0.1162	0.0975	0.1396	0.0989	0.0867
Base Shear (kN)	139.85	156.33	139.9	159.23	139.9	159.12	138.05	161.71	139.9	155	139.9	163.23	139.9	167.43	139.9	169.5
Ductility	4.2	4.1	6.3	4.5	4.5	4.4	4.7	4.7	3.6	3.6	3.8	4.3	4.7	4.6	3.5	3.2

Table 4-32 Comparison of results between pushover analysis and nonlinear dynamic analysis for a 2-DOF system (El Centro ground motion)

EL CENTRO	DCM													
	Mode Shape		Inverted Triangular		FEMA(1)		FEMA(2)		Uniform		Kunnath (+)		Kunnath (-)	
	α=0	α=0.03	α=0	α=0.03	α=0	α=0.03	α=0	α=0.03	α=0	α=0.03	α=0	α=0.03	α=0	α=0.03
Displacement (m) (node 3)	1.17	1.29	1.83	1.46	1.33	1.46	1.45	1.63	0.95	1.05	1.01	1.38	1.49	1.63
Displacement (m) (node 2)	1.10	1.23	1.76	1.40	1.24	1.39	1.35	1.55	0.89	1.01	0.94	1.34	0.99	1.61
Base Shear (kN)	1.00	0.92	1.00	0.94	1.00	0.94	0.99	0.95	1.00	0.91	1.00	0.96	1.00	0.99
Ductility	1.20	1.28	1.80	1.41	1.29	1.38	1.34	1.47	1.03	1.13	1.09	1.34	1.34	1.44

Table 4-33 Comparison of normalised results between pushover analysis and nonlinear dynamic analysis for a 2-DOF system (El Centro ground motion)

KOCAELI	MPA		*N-RHA*	
	α=0	α=0.03	α=0	α=0.03
Displacement (m) (node 3)	0.2565	0.2067	0.1857	0.1743
Displacement (m) (node 2)	0.2422	0.1889	0.1698	0.1484
Base Shear (kN)	190	237	186.7	239
Ductility	6.9	5.8	5.5	5.2

Table 4-34 Comparison of results between modal pushover analysis and nonlinear dynamic analysis for a 2-DOF system

KOCAELI	MPA	
	α=0	α=0.03
Displacement (m) (node 3)	1.38	1.19
Displacement (m) (node 2)	1.43	1.27
Base Shear (kN)	1.02	0.99
Ductility	1.25	1.12

Table 4-35 Comparison of normalised results between modal pushover analysis and nonlinear dynamic analysis for a 2-DOF system

EL CENTRO	MPA		N-RHA	
	α=0	α=0.03	α=0	α=0.03
Displacement (m) (node 3)	0.1399	0.1237	0.1019	0.0927
Displacement (m) (node 2)	0.1290	0.1110	0.0989	0.0867
Base Shear (kN)	145.35	167.63	139.9	169.5
Ductility	4.8	4.2	3.5	3.2

Table 4-36 Comparison of results between modal pushover analysis and nonlinear dynamic analysis for a 2-DOF system (El Centro ground motion)

EL CENTRO	MPA	
	α=0	α=0.03
Displacement (m) (node 3)	1.37	1.33
Displacement (m) (node 2)	1.30	1.28
Base Shear (kN)	1.04	0.99
Ductility	1.37	1.31

Table 4-37 normalised results between modal pushover analysis and nonlinear dynamic analysis for a 2-DOF system (El Centro ground motion)

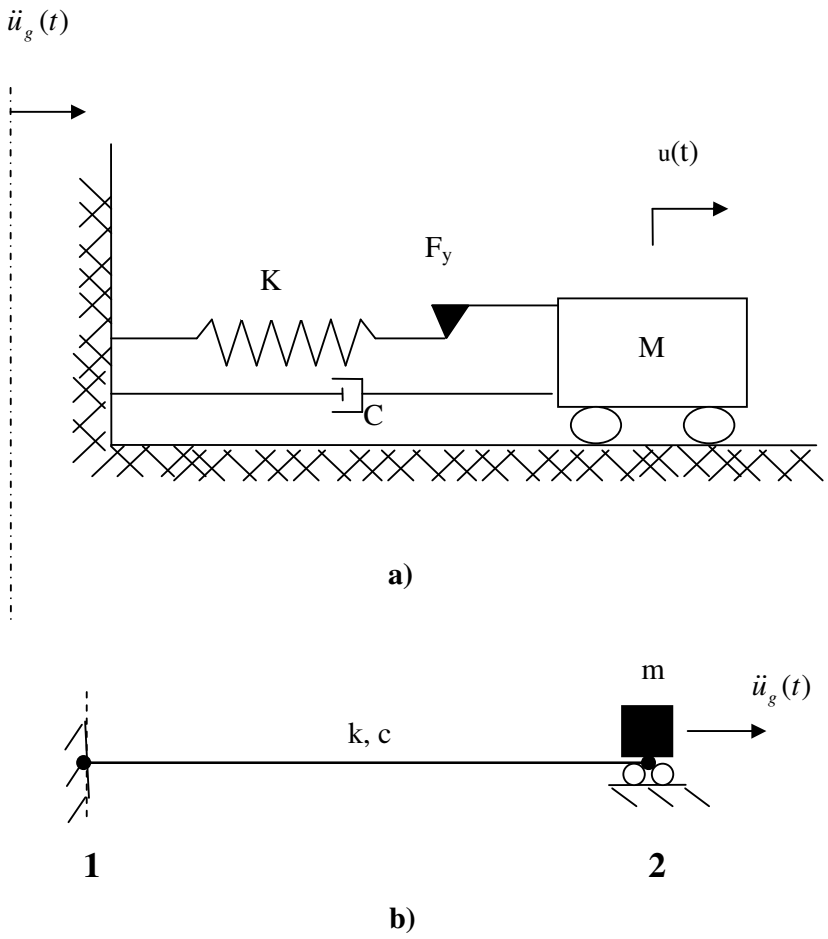

Figure 4-1 SDOF model a) Physical model b) FE model

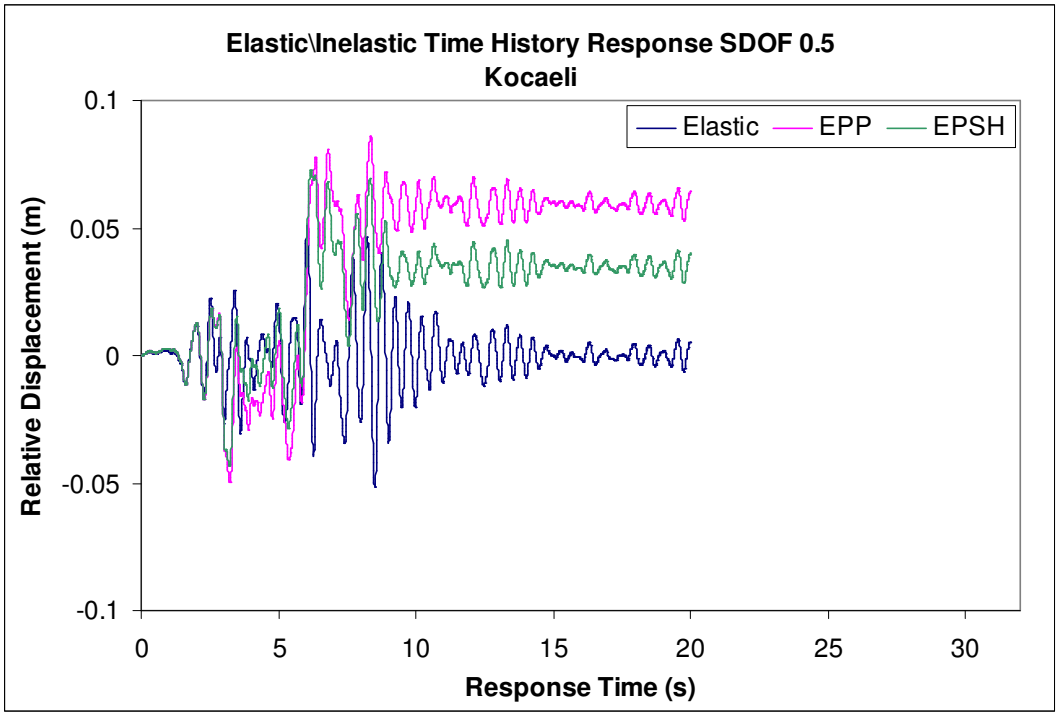

Figure 4-2 Displacement Time-Histories of SDOF 0.5 for the Kocaeli ground motion

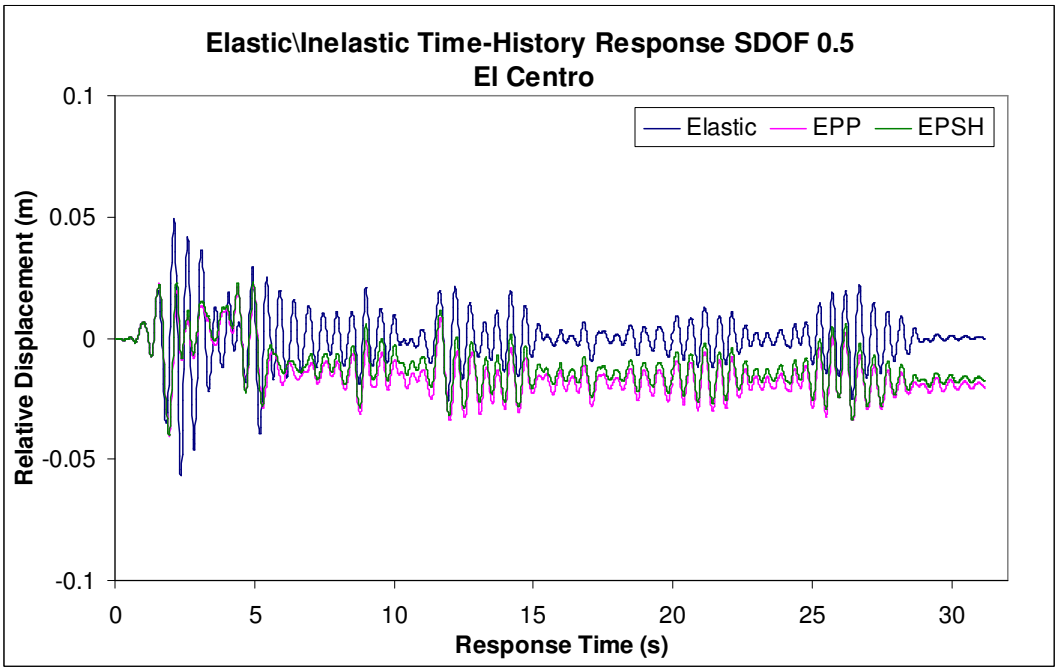

Figure 4-3 Displacement Time-Histories of SDOF 0.5 for the El Centro ground motion

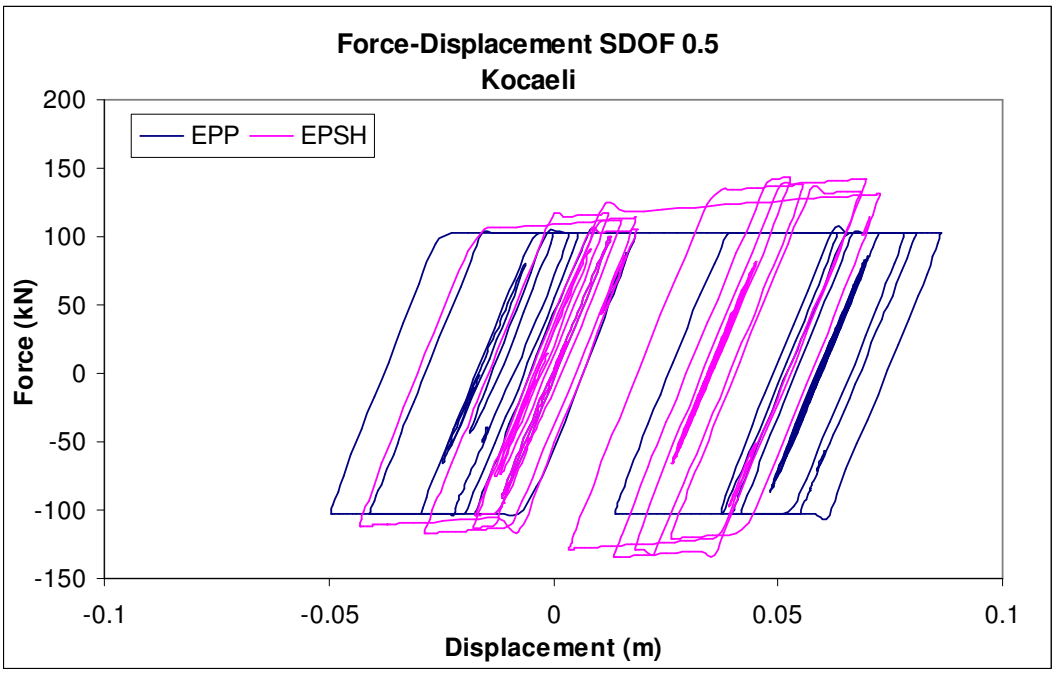

Figure 4-4Force - Displacement Response of SDOF 0.5 system for the Kocaeli ground motion

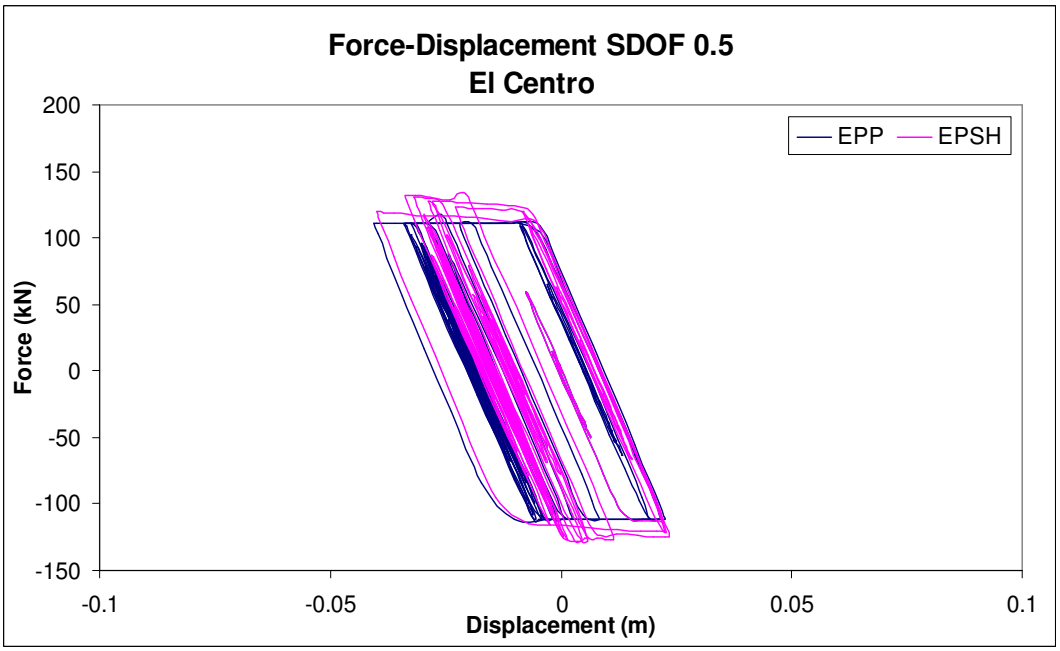

Figure 4-5 Force - Displacement Response of SDOF 0.5 system for the El Centro ground motion

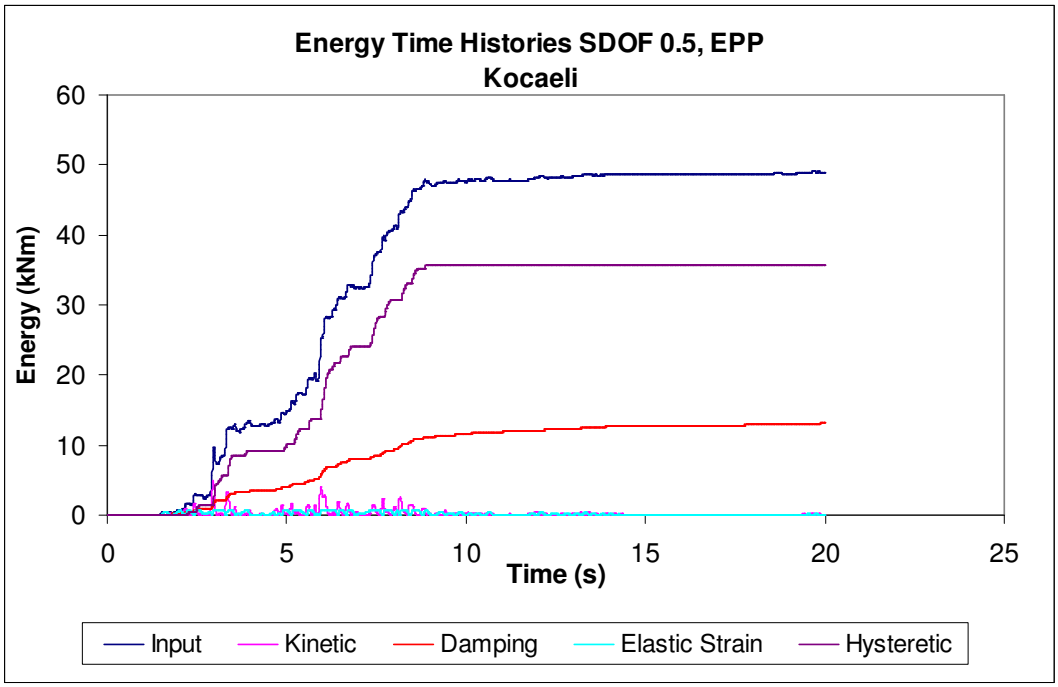

Figure 4-6 Energy Time-Histories SDOF 0.5, EPP, Kocaeli ground motion

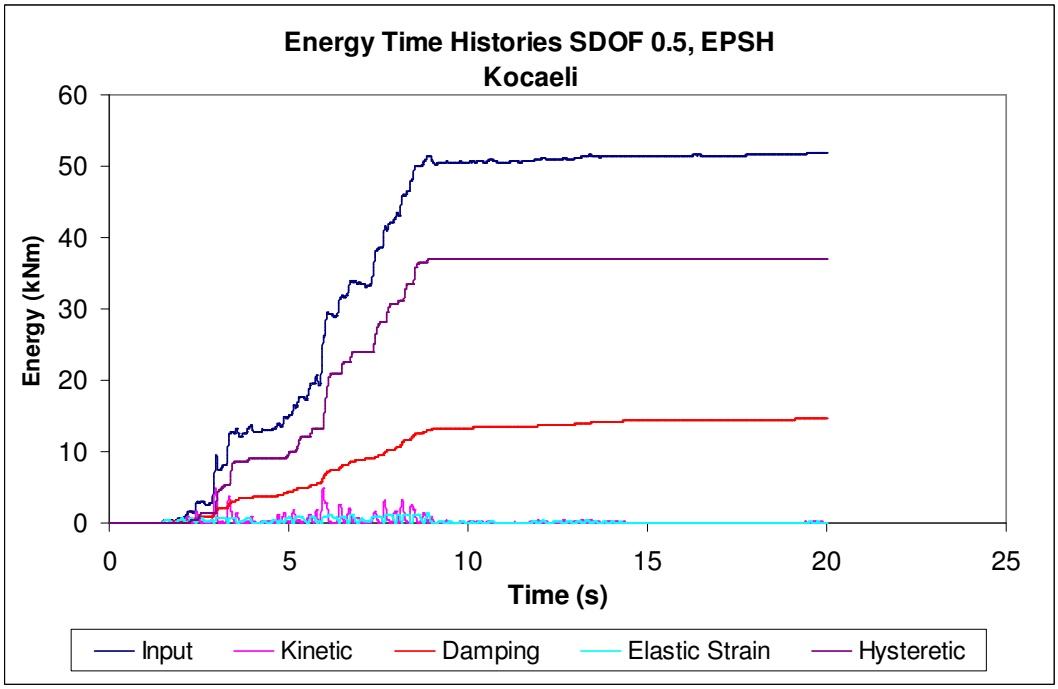

Figure 4-7 Energy Time-Histories SDOF 0.5, EPSH, Kocaeli ground motion

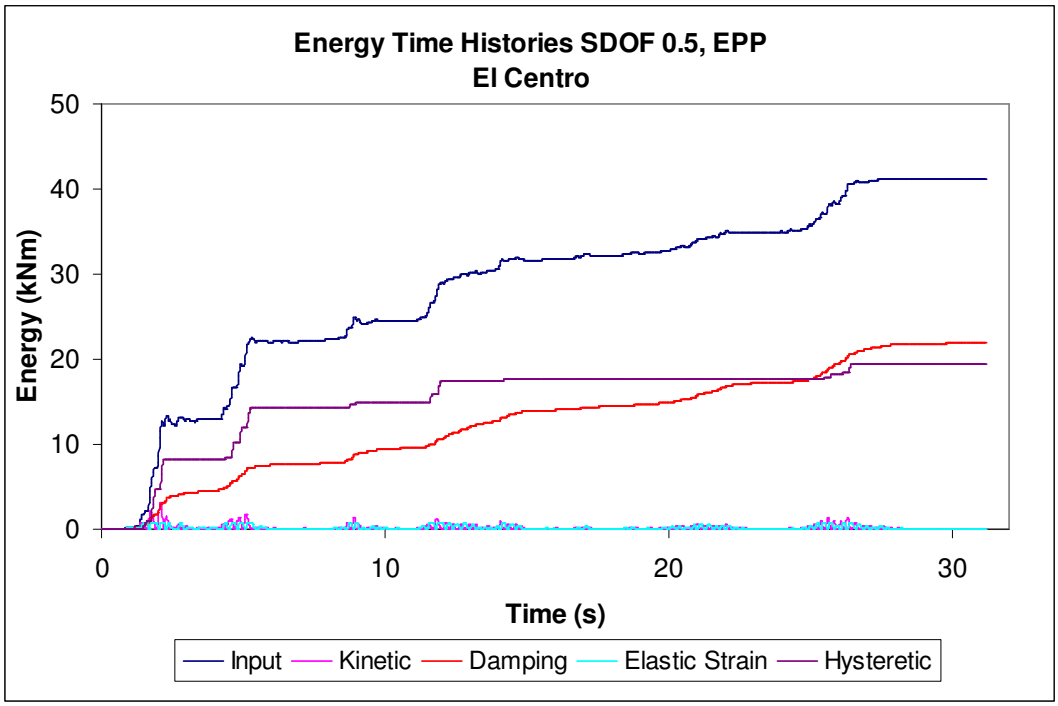

Figure 4-8 Energy Time-Histories SDOF 0.5, EPP, El Centro ground motion

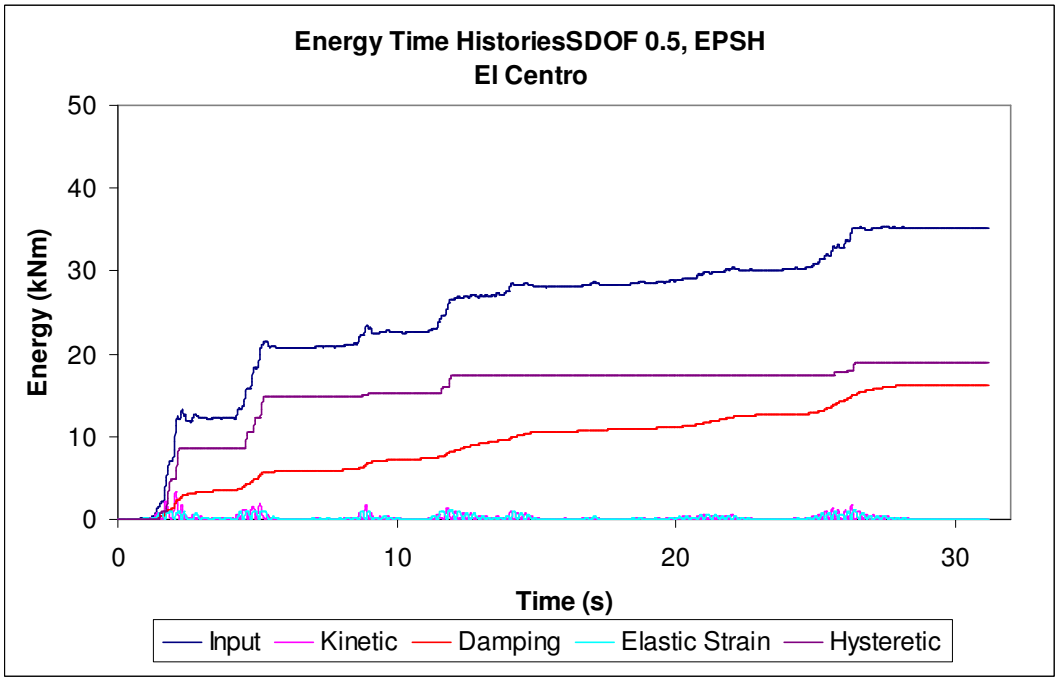

Figure 4-9 Energy Time-Histories SDOF 0.5, EPSH, El Centro ground motion

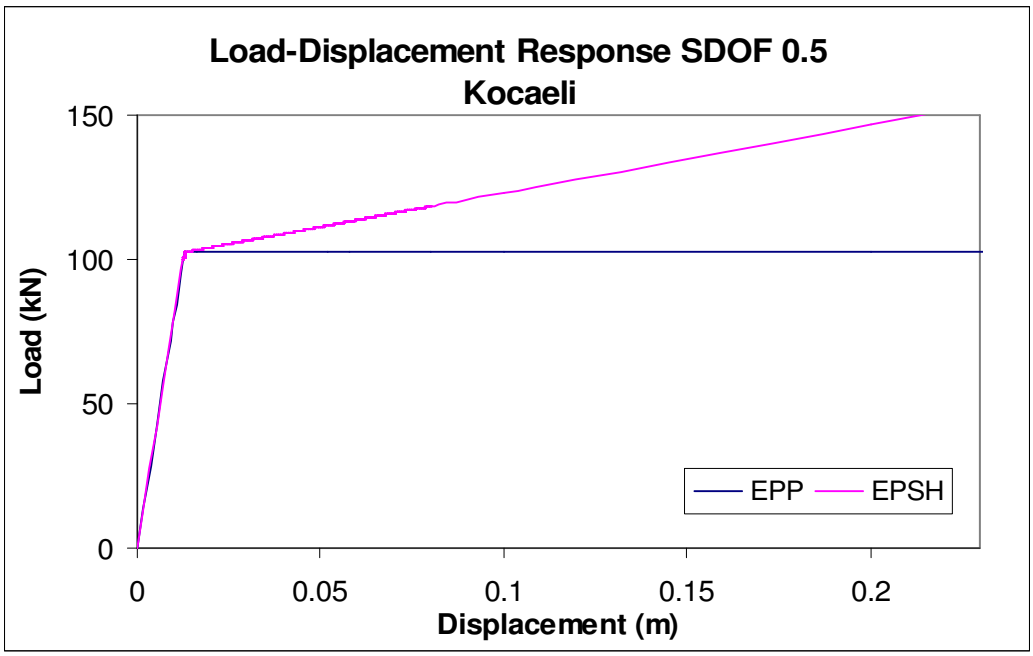

Figure 4-10 Pushover curves SDOF 0.5 for the two material models, Kocaeli ground motion

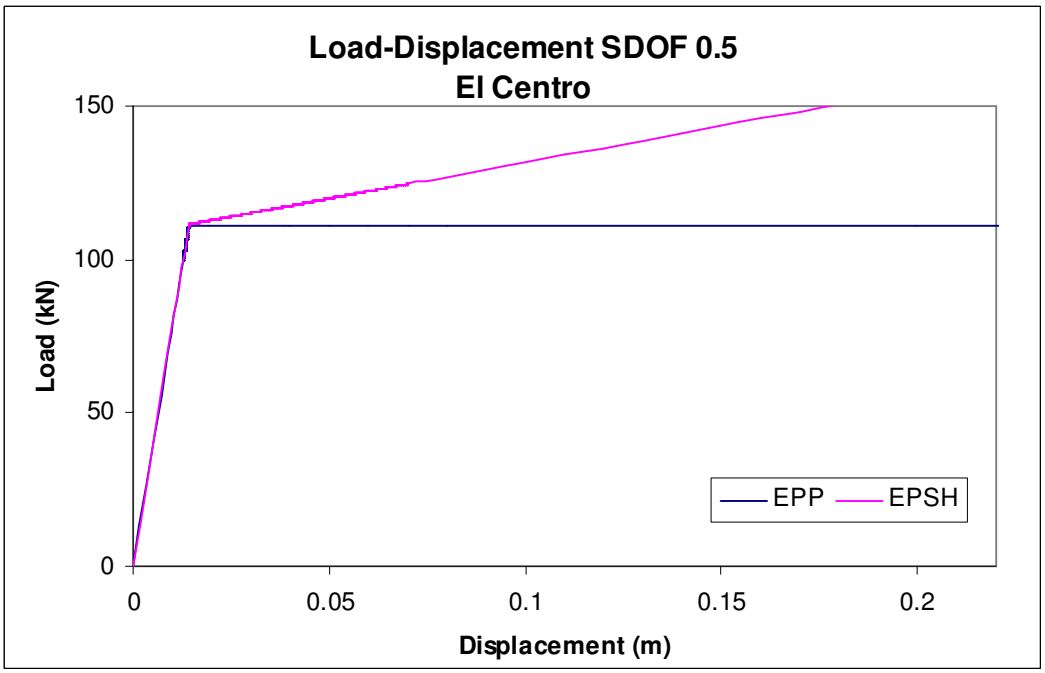

Figure 4-11 Pushover curves SDOF 0.5 for the two material models, El Centro ground motion

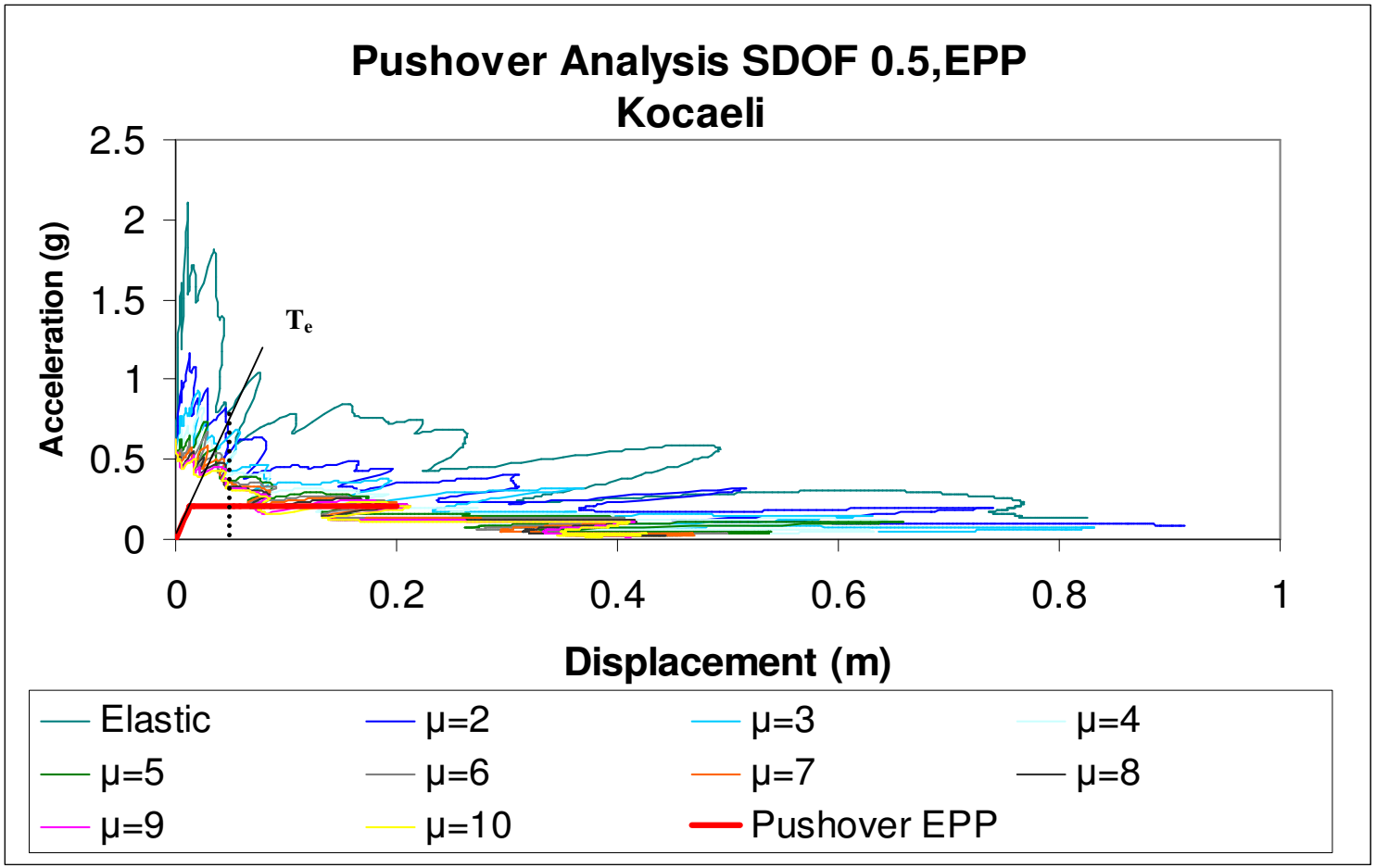

Figure 4-12 Pushover Analysis SDOF 0.5, EPP, Kocaeli ground motion

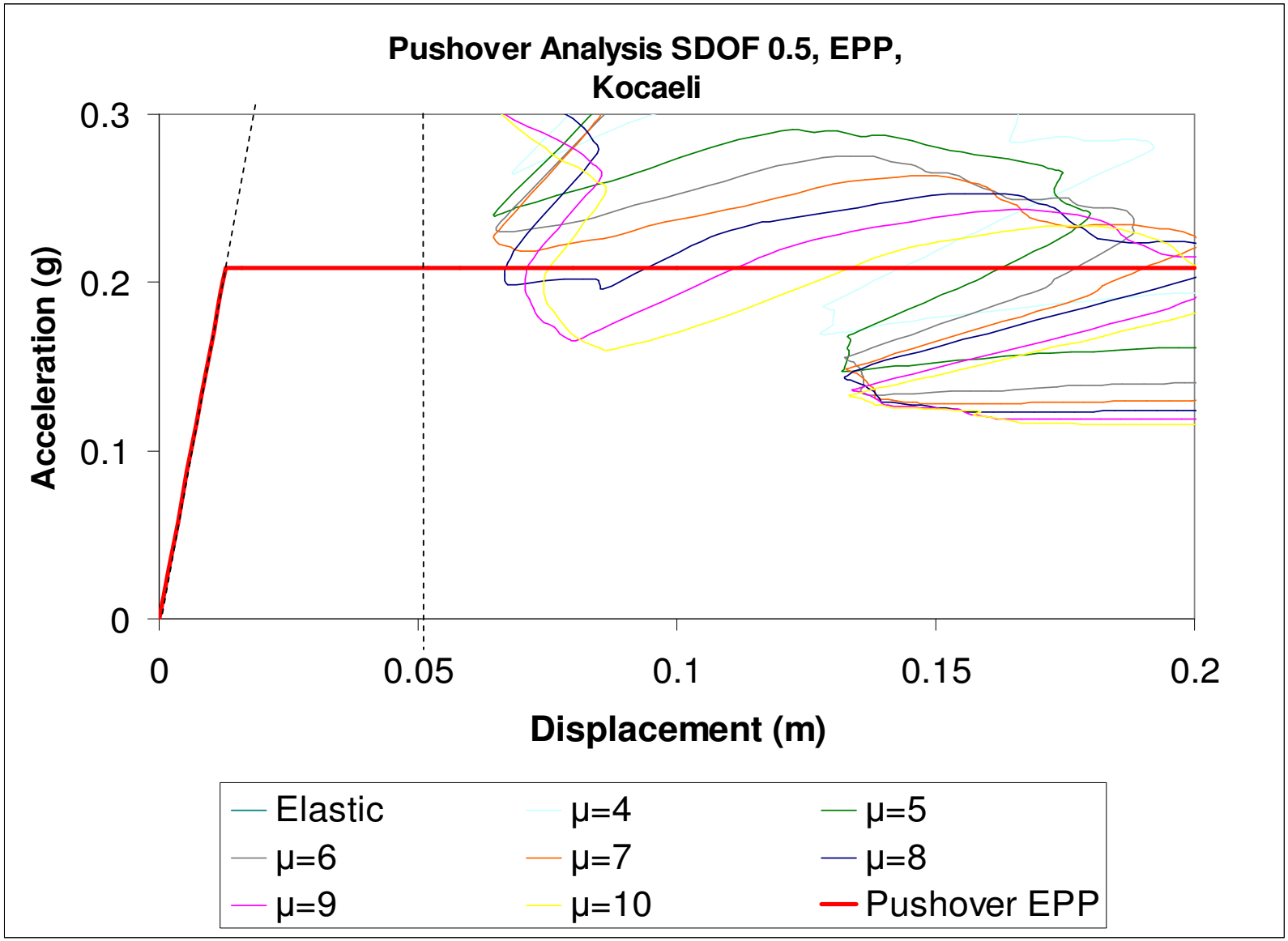

Figure 4-13 Insight into the estimation of target displacement for the EPP SDOF III, Kocaeli ground motion

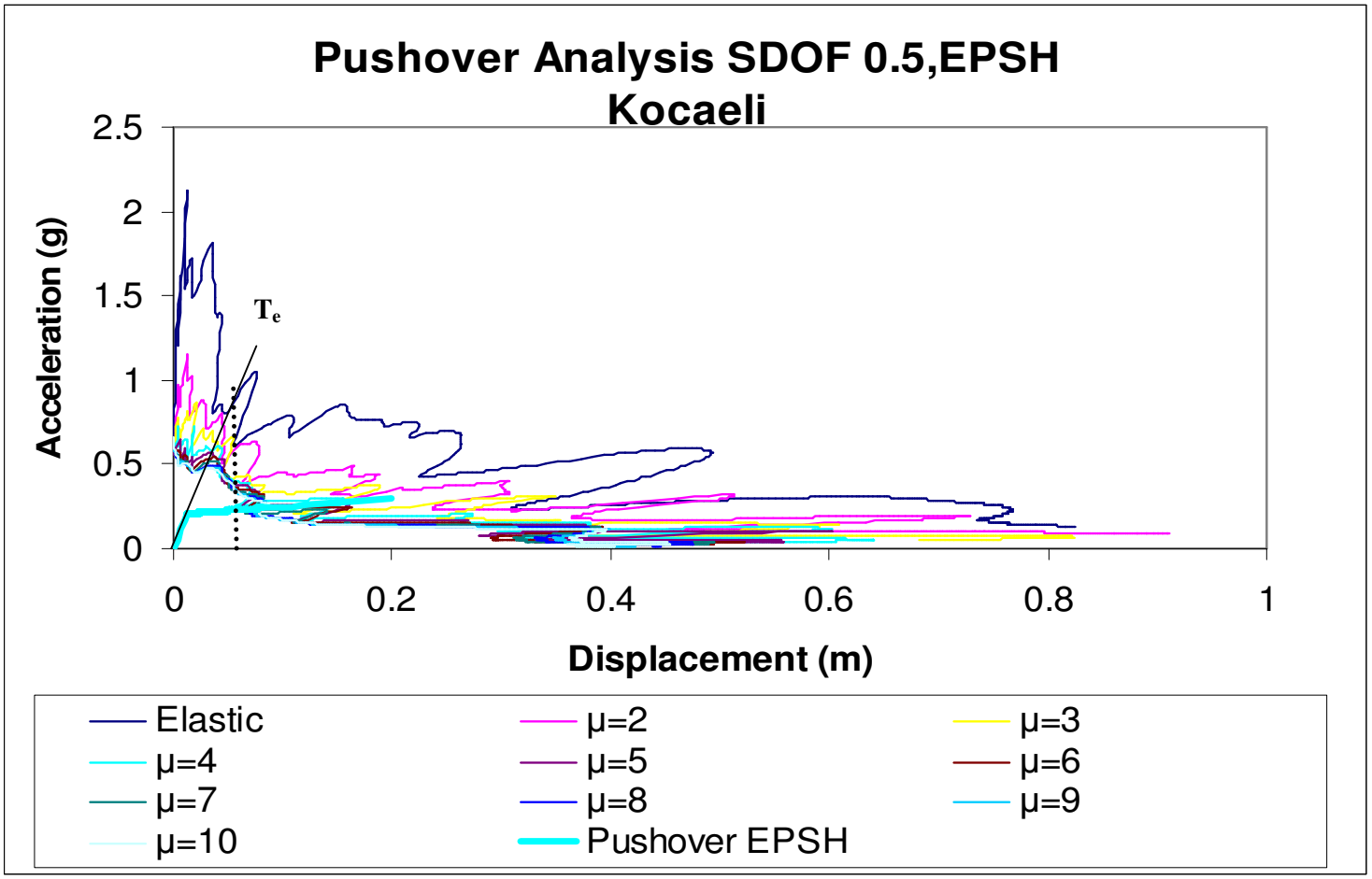

Figure 4-14 Pushover Analysis SDOF 0.5, EPSH, Kocaeli ground motion

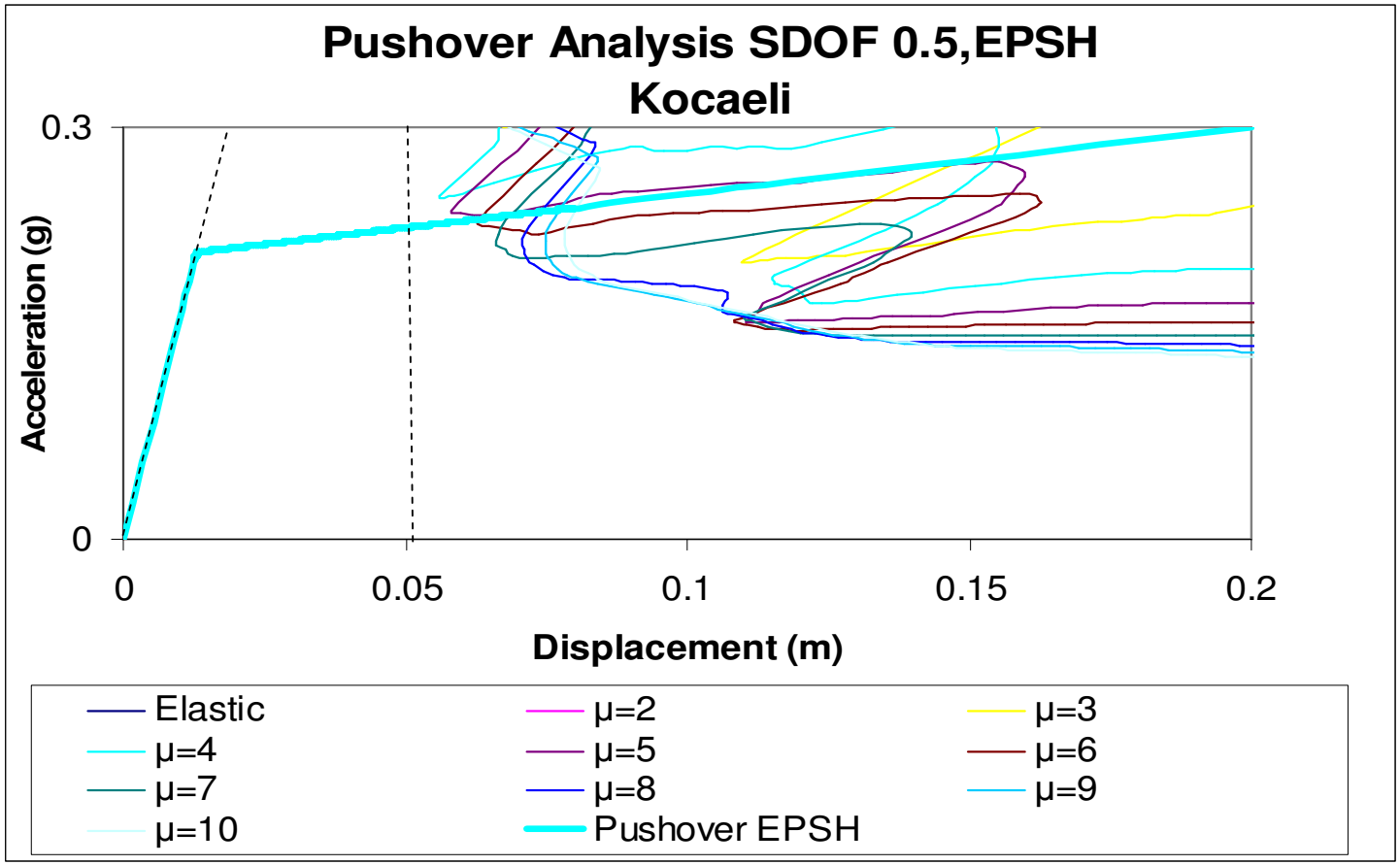

Figure 4-15 Insight into the estimation of target displacement for the EPSH SDOF 0.5, Kocaeli ground motion

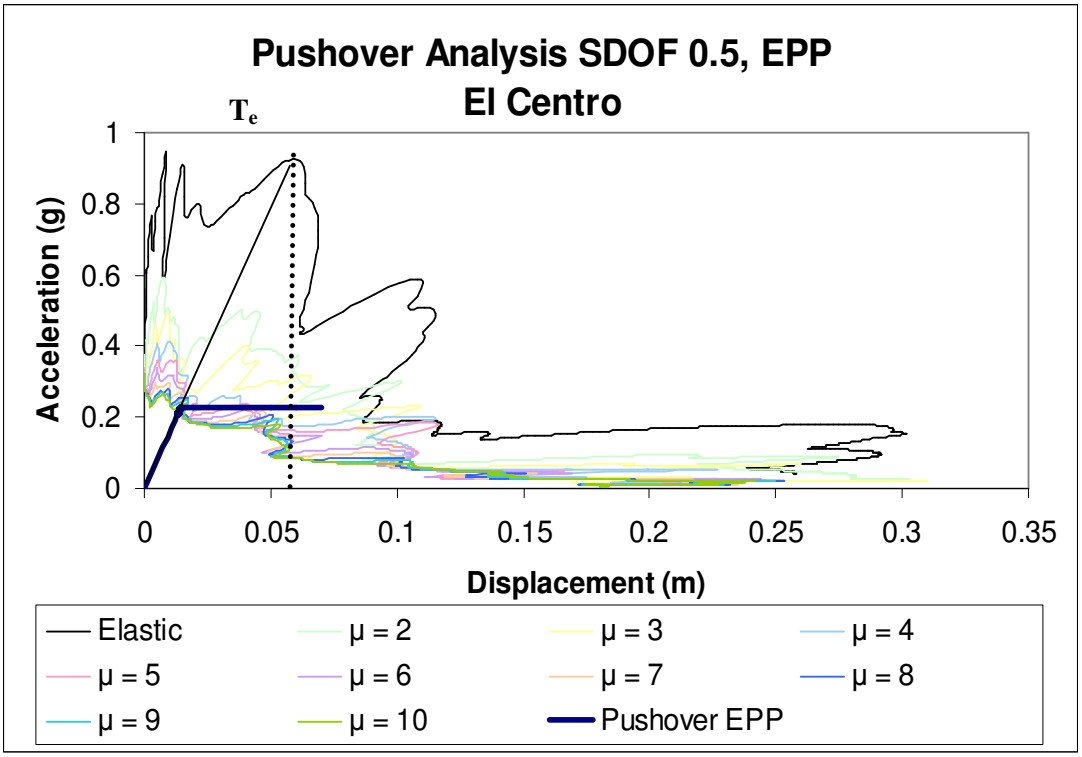

Figure 4-16 Pushover Analysis SDOF 0.5, EPP, El Centro ground motion

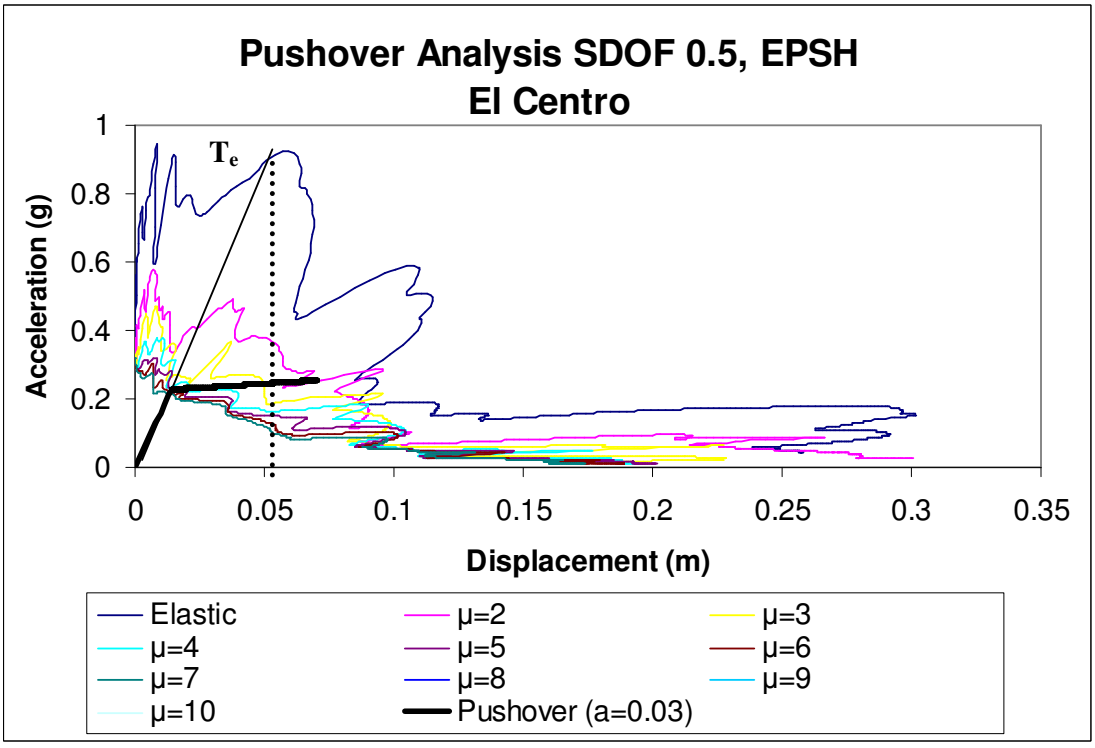

Figure 4-17 Pushover Analysis SDOF 0.5, EPSH, El Centro ground motion

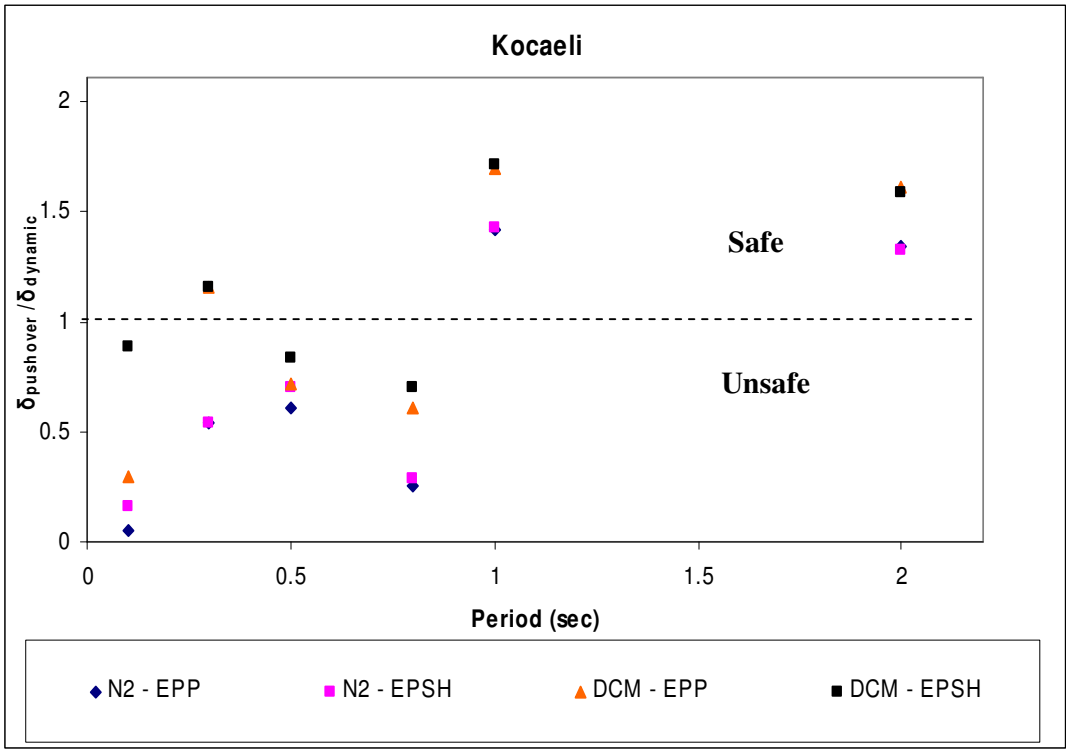

Figure 4-18 $\delta_{pushover}/\delta_{dynamic}$ estimates for N2 and DCM methods, Kocaeli

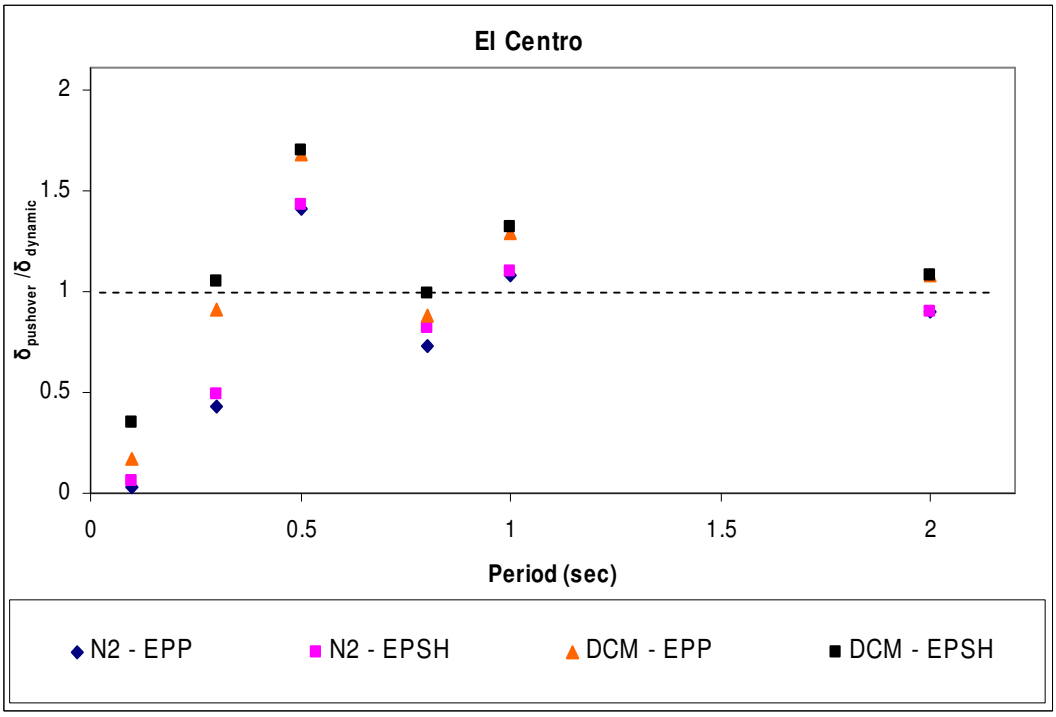

Figure 4-19 $\delta_{pushover}/\delta_{dynamic}$ estimates for N2 and DCM methods, El Centro

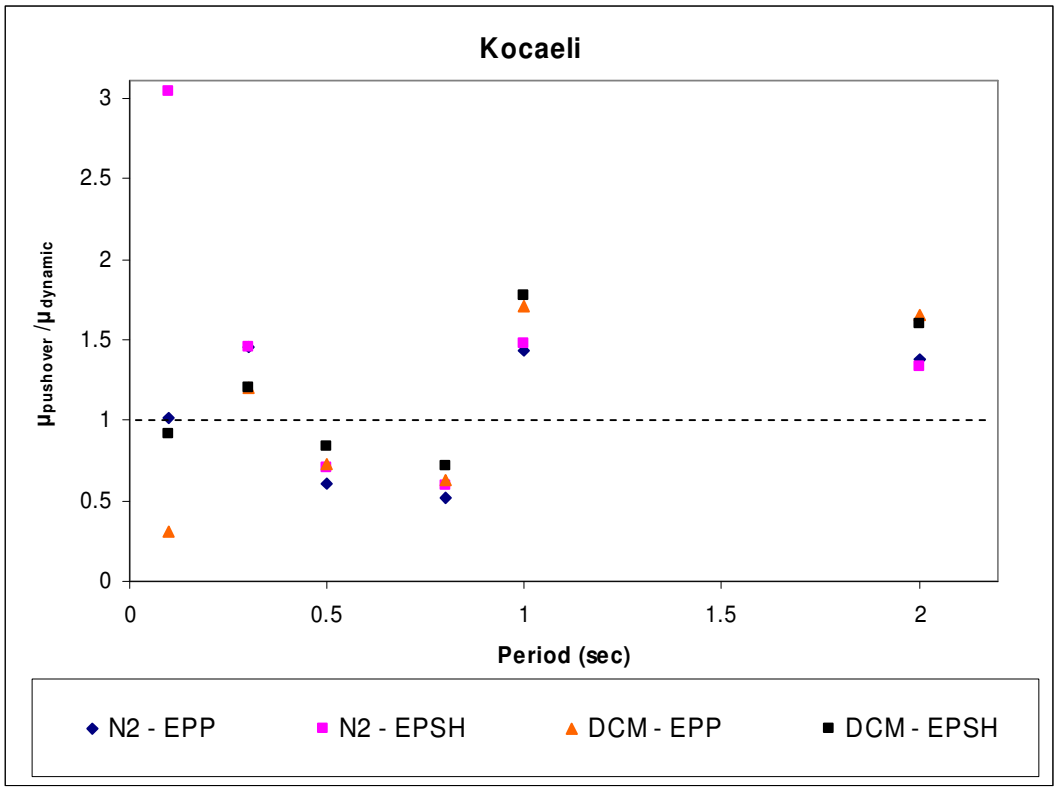

Figure 4-20 $\mu_{pushover}/\ \mu_{dynamic}$ estimates for N2 and DCM methods, Kocaeli

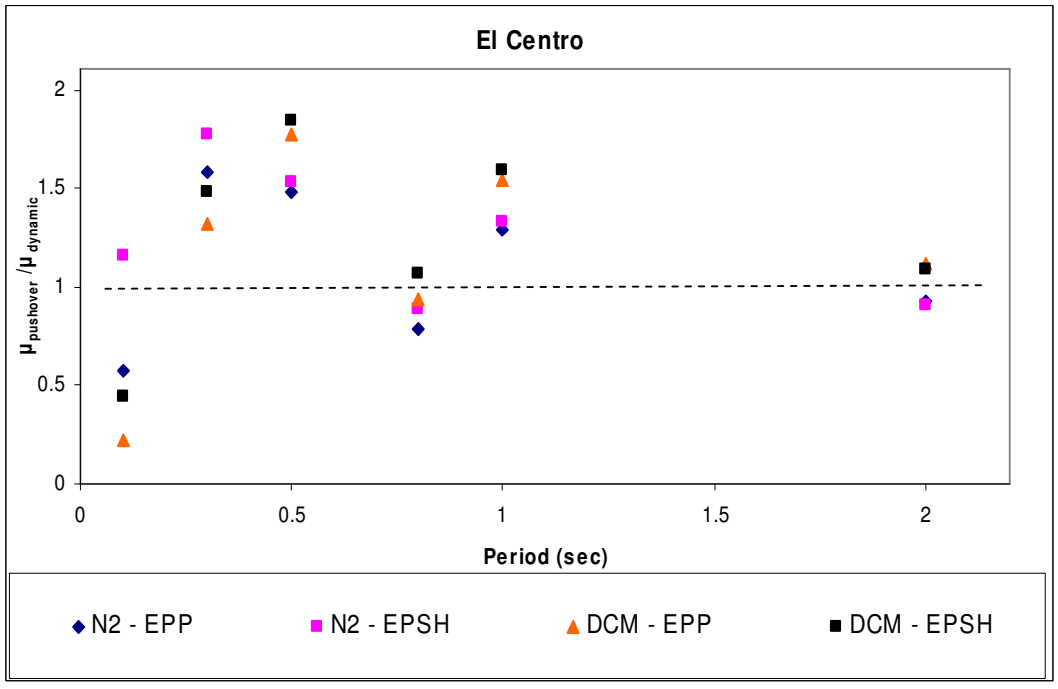

Figure 4-21 $\mu_{pushover}/\ \mu_{dynamic}$ estimates for N2 and DCM methods, El Centro

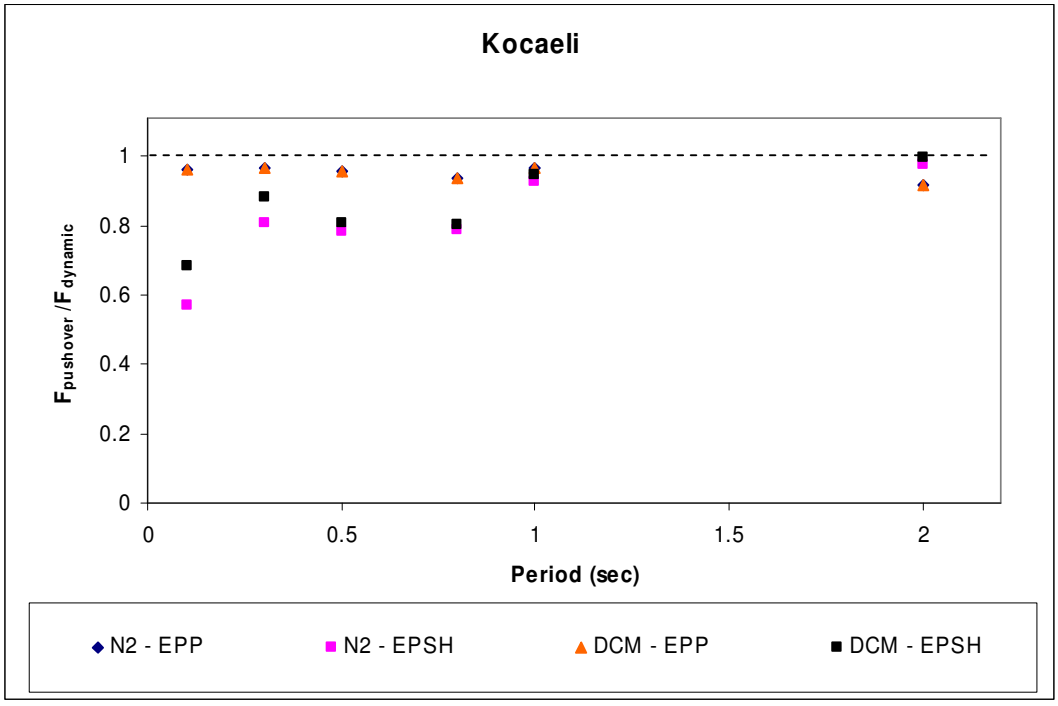

Figure 4-22 $F_{pushover}$/ $F_{dynamic}$ estimates for N2 and DCM methods, Kocaeli

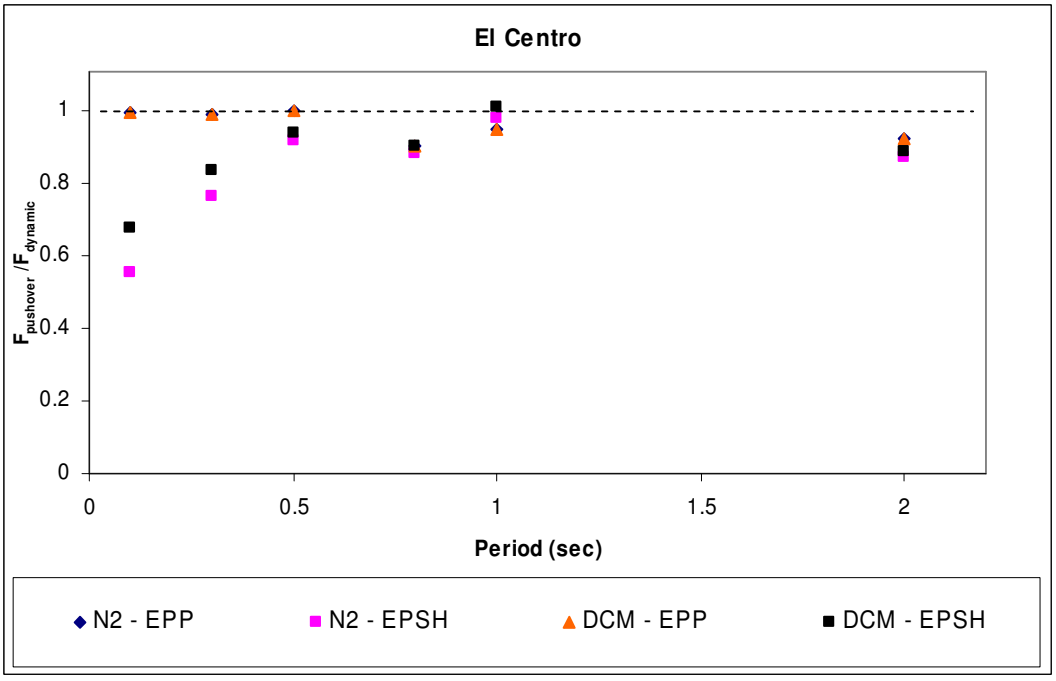

Figure 4-23 $F_{pushover}$/ $F_{dynamic}$ estimates for N2 and DCM methods, El Centro

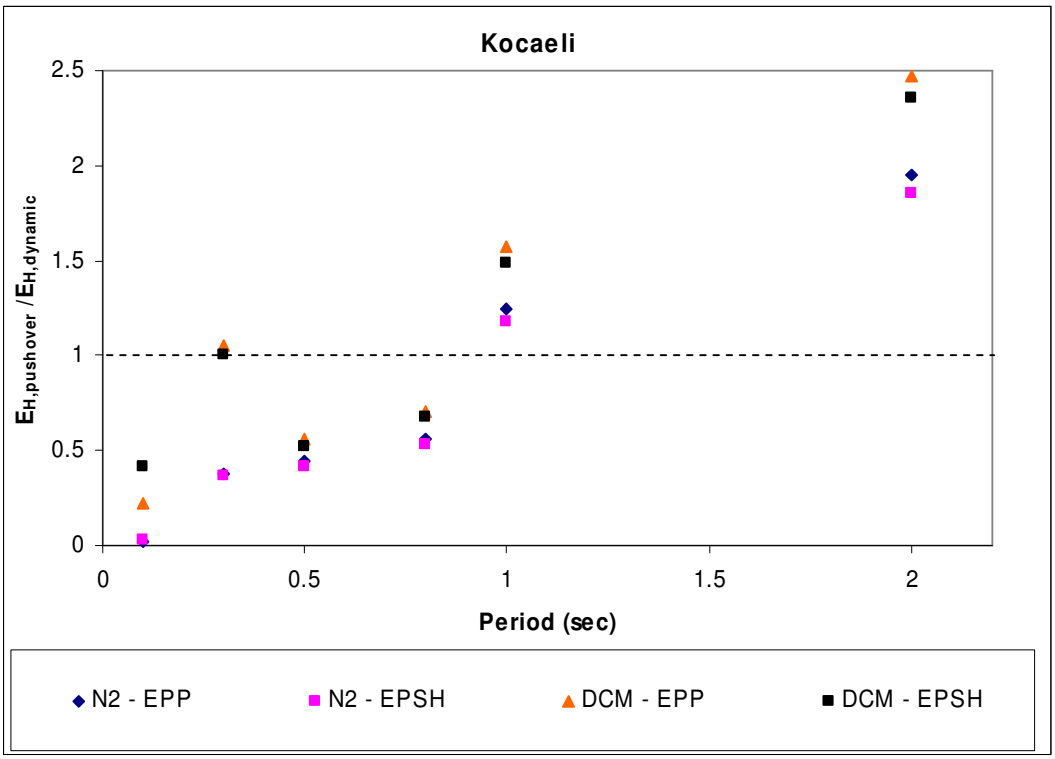

Figure 4-24 $E_{H,pushover}$/ $E_{H,\ dynamic}$ estimates for N2 and DCM methods, Kocaeli

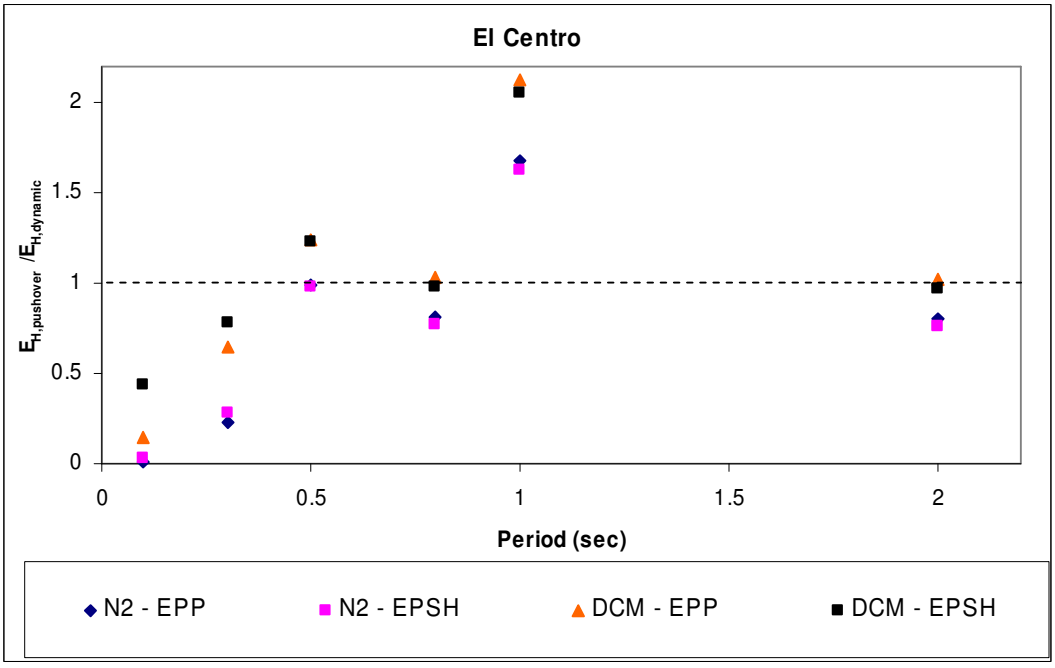

Figure 4-25 $E_{H,pushover}$/ $E_{H,\ dynamic}$ estimates for N2 and DCM methods, El Centro

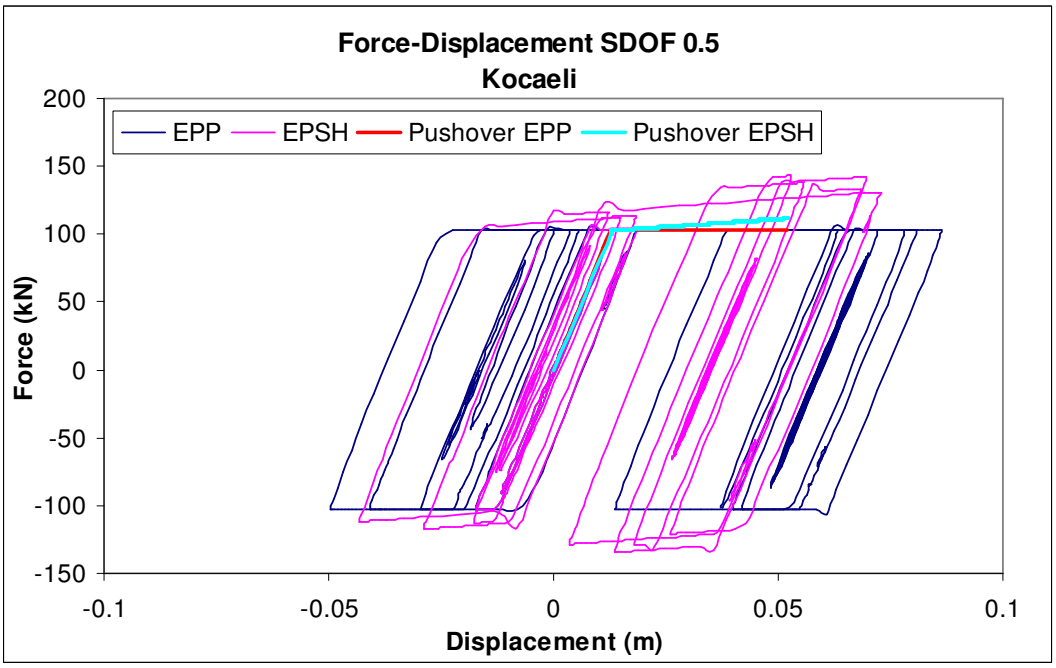

Figure 4-26 Force – Displacement Relationship from Nonlinear Dynamic and Pushover Analyses, Kocaeli ground motion

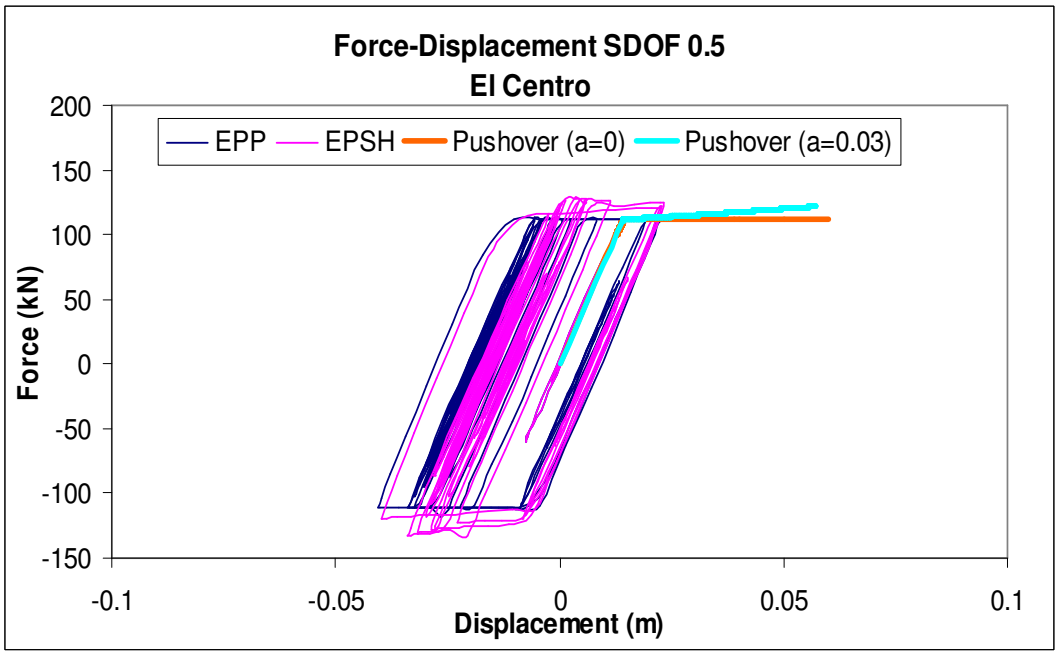

Figure 4-27 Force - Displacement -Relationships from Nonlinear Dynamic and Pushover Analyses, El Centro ground motion

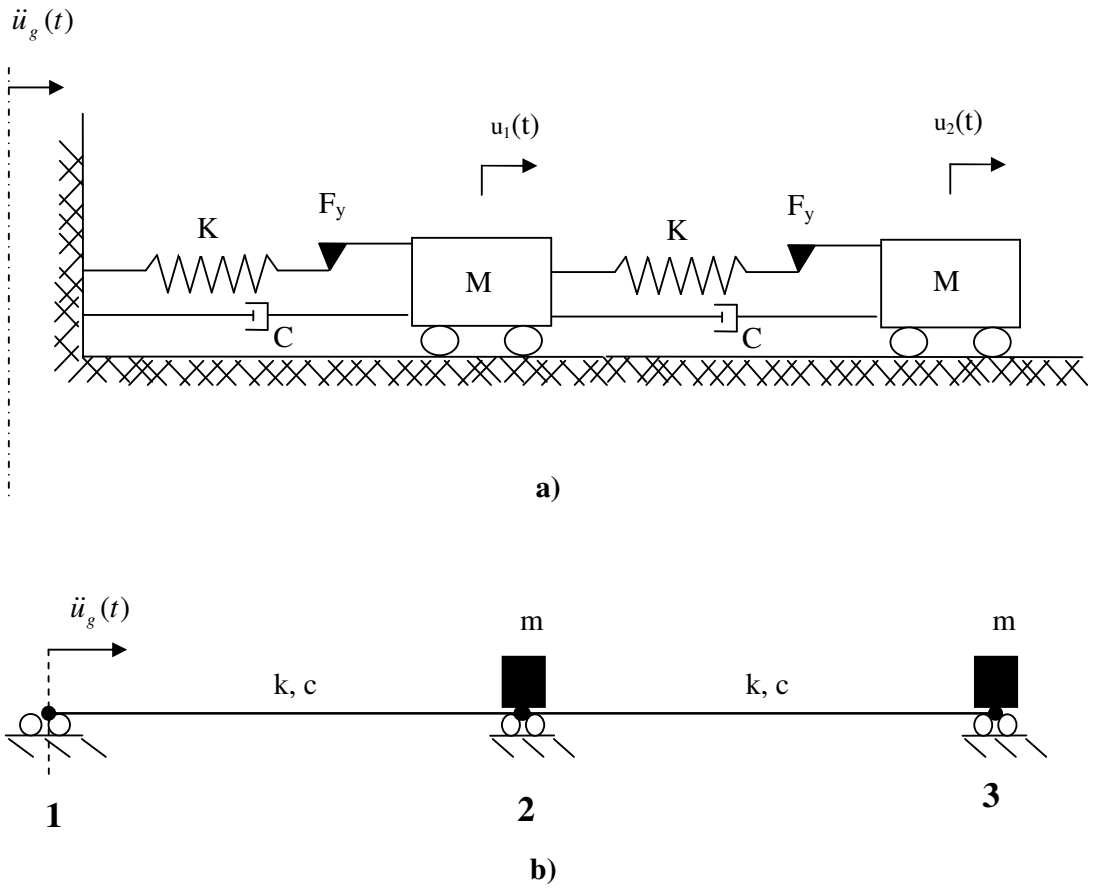

Figure 4-28 a) Physical model of 2-DOF system, b) FE model of 2-DOF system

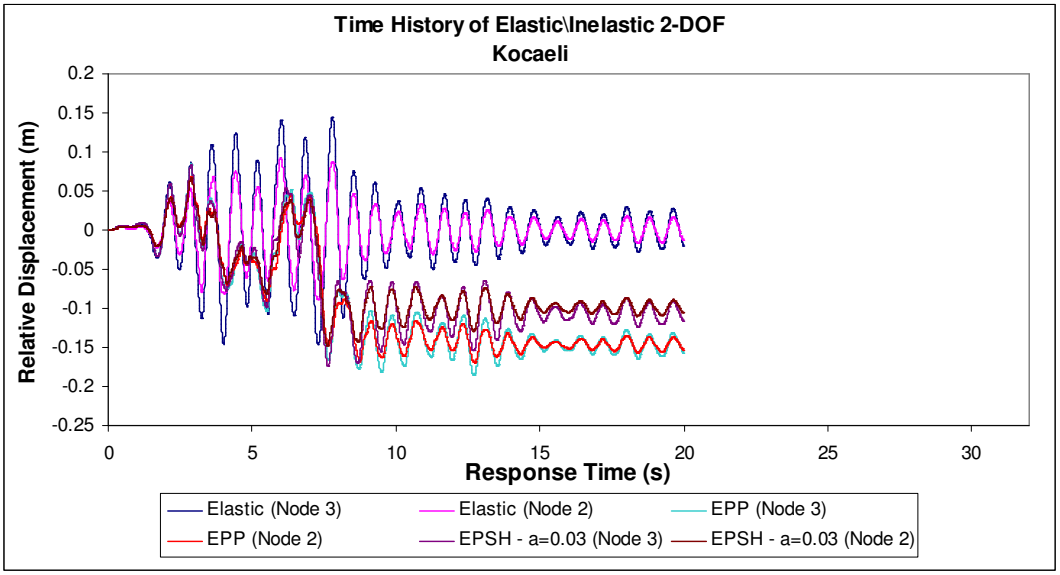

Figure 4-29 Time History of Elastic/Inelastic 2-DOF - Kocaeli ground motion

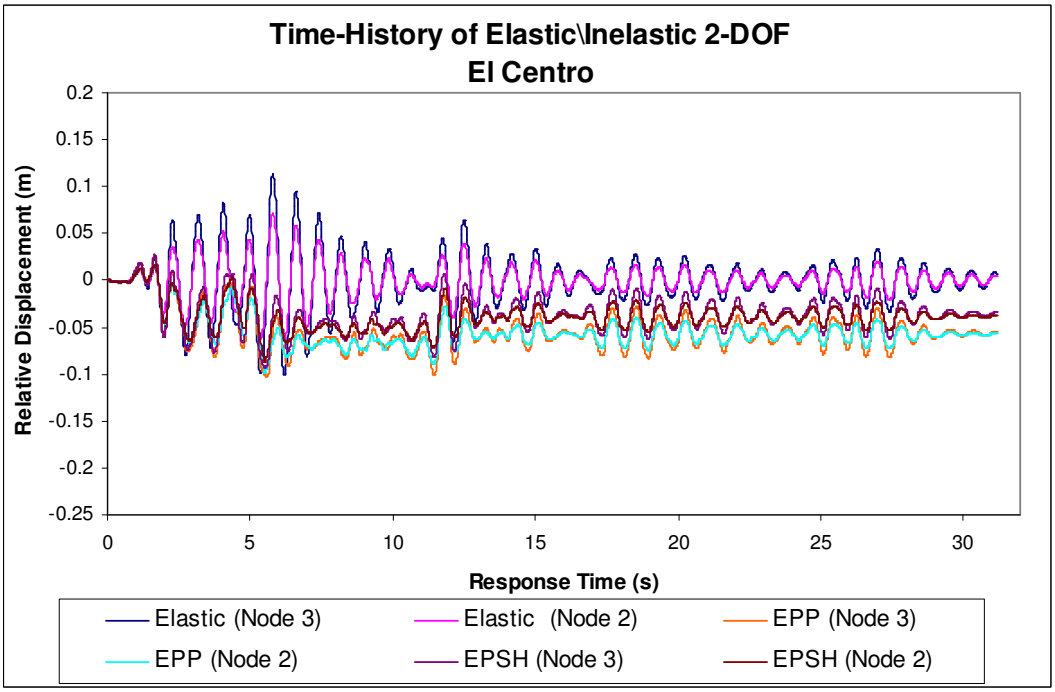

Figure 4-30 Time History of Elastic/Inelastic 2-DOF - El Centro ground motion

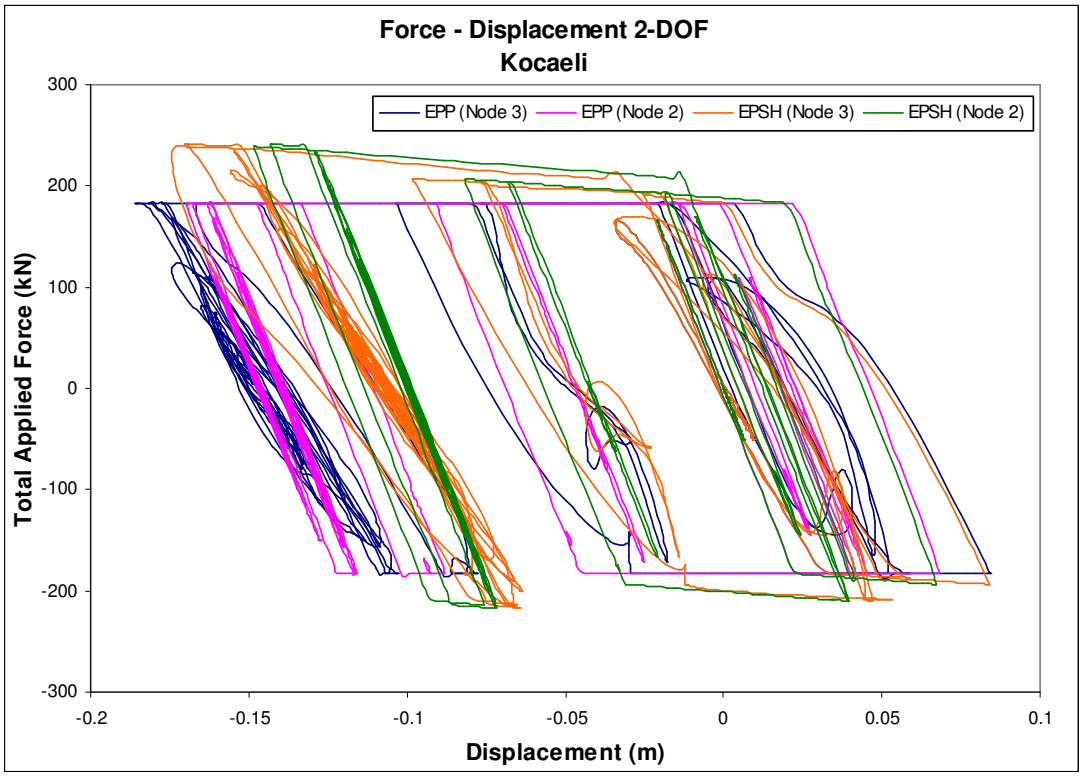

Figure 4-31 Force-displacement behaviour from the Kocaeli Ground Motion

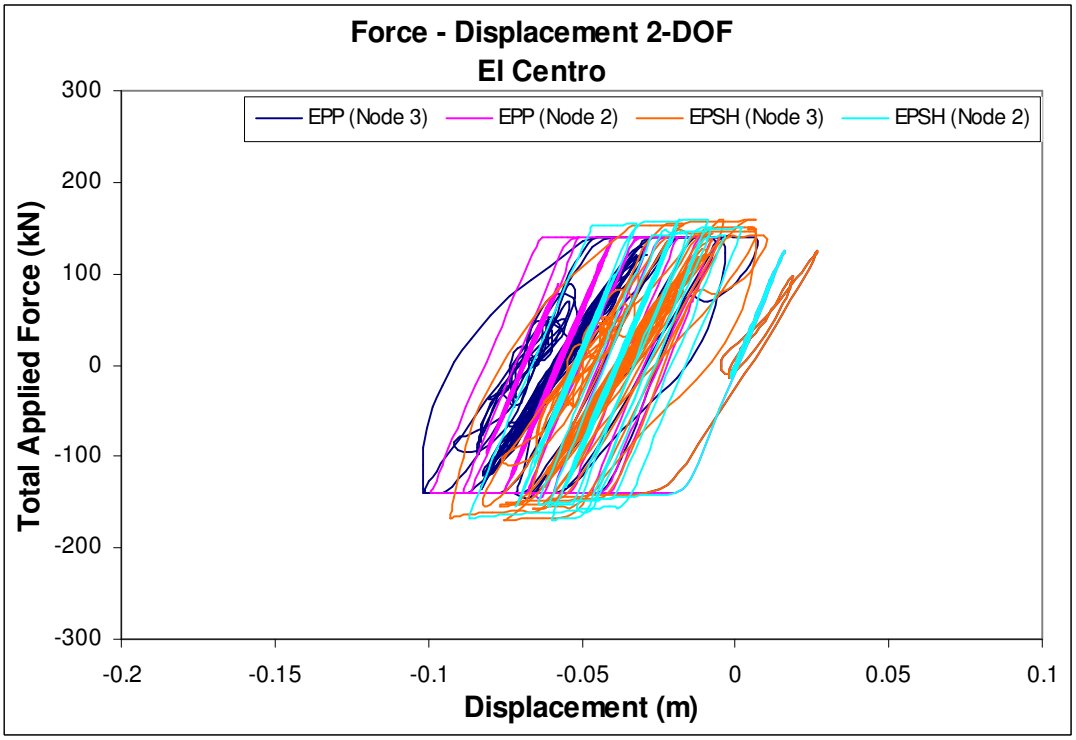

Figure4-32 Force-displacement behaviour from the El Centro ground motion

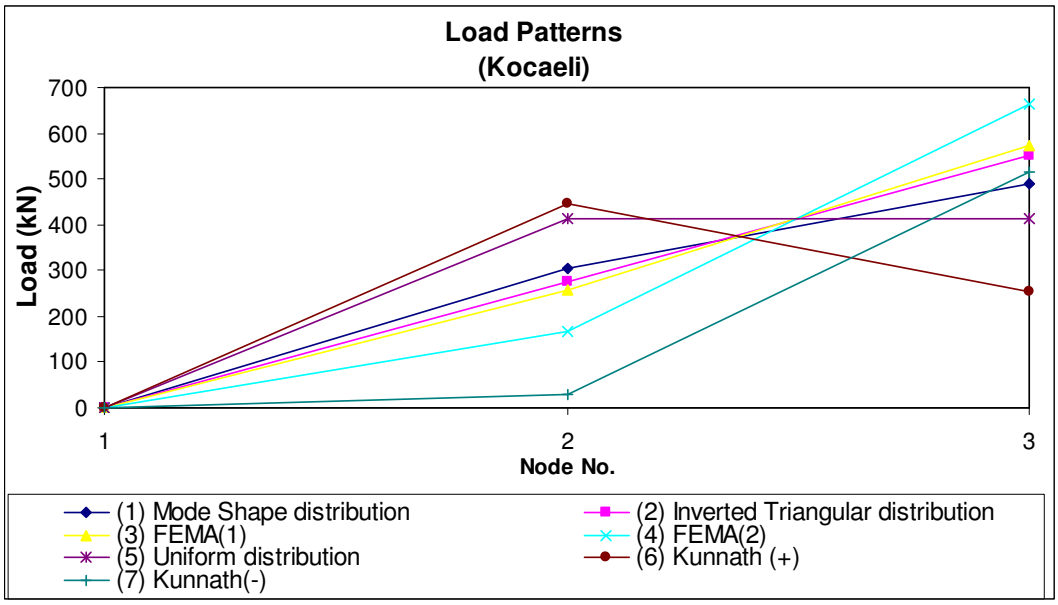

Figure 4-33 Load Patterns for 2-DOF pushover analysis (Kocaeli ground motion)

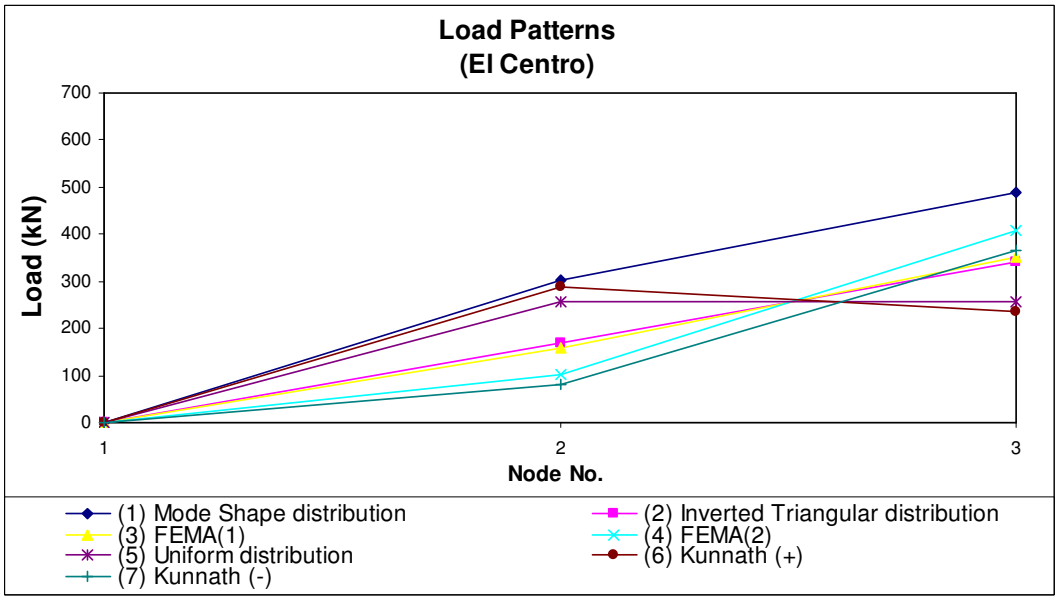

Figure 4-34 Load Patterns for 2-DOF pushover analysis (El Centro ground motion)

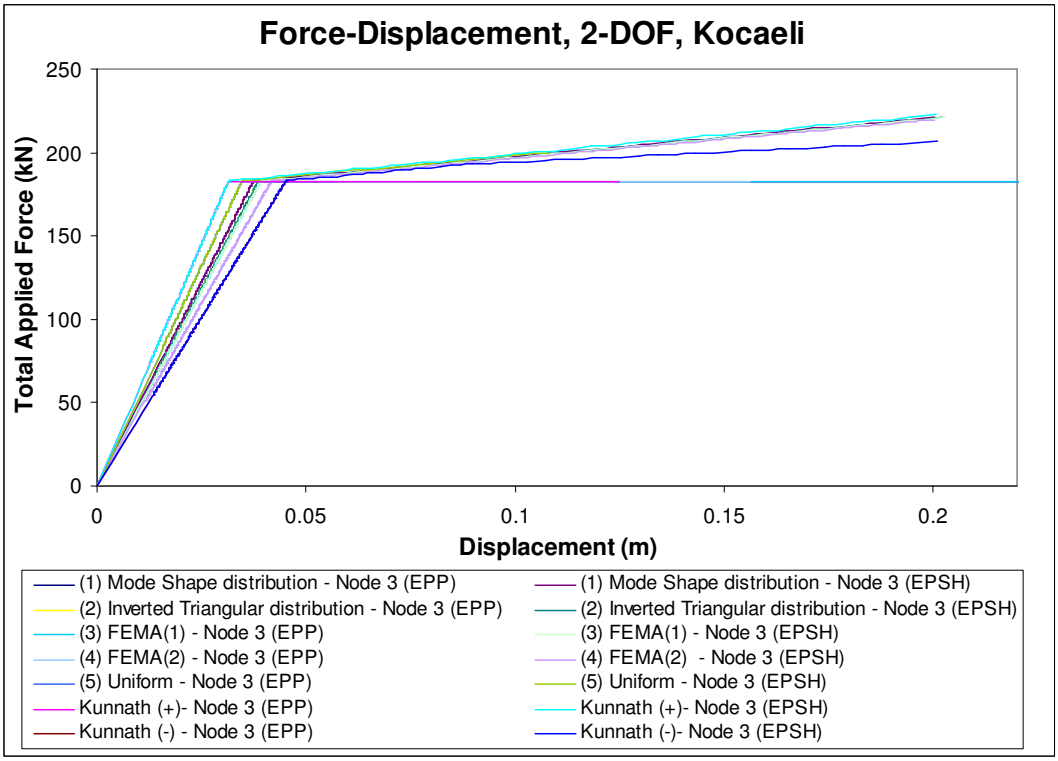

Figure 4-35 Pushover curves for the two material models, Kocaeli ground motion

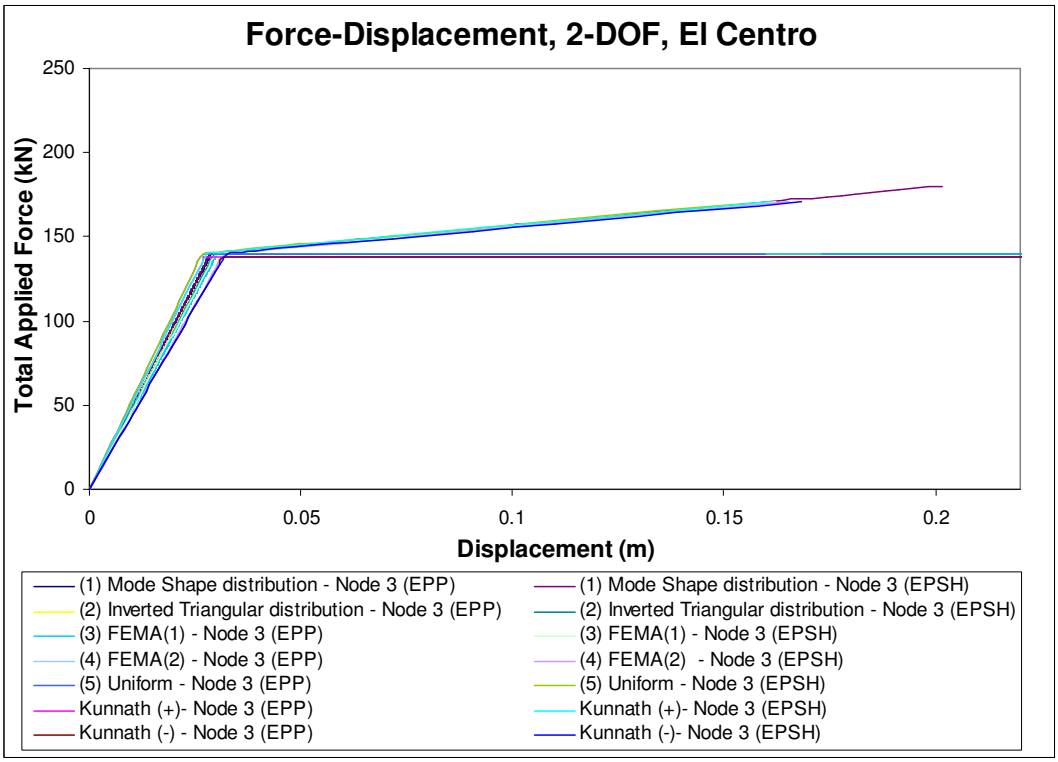

Figure 4-36 Pushover curves for the two material models, El Centro ground motion

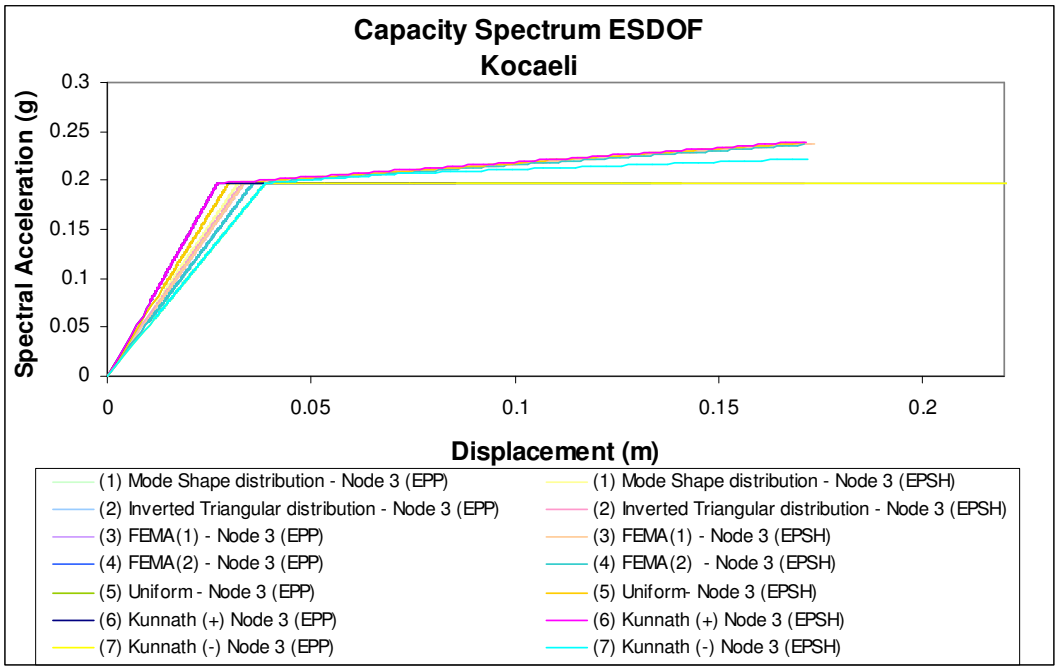

Figure 4-37 Equivalent SDOF system, Kocaeli ground motion

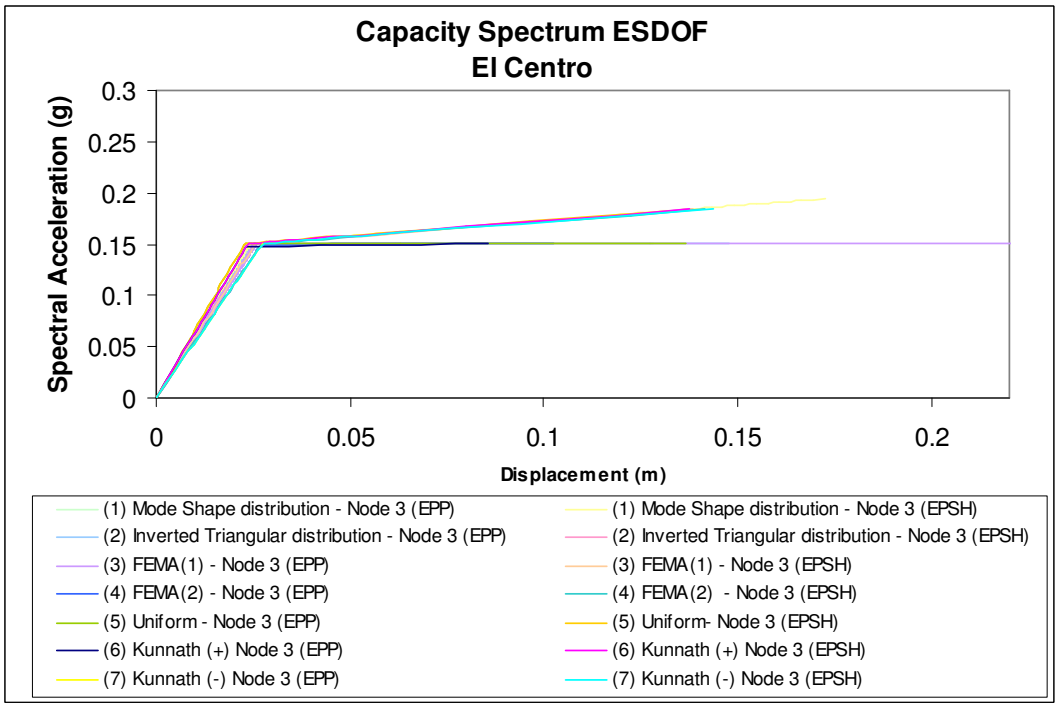

Figure 4-38 Equivalent SDOF system, El Centro ground motion

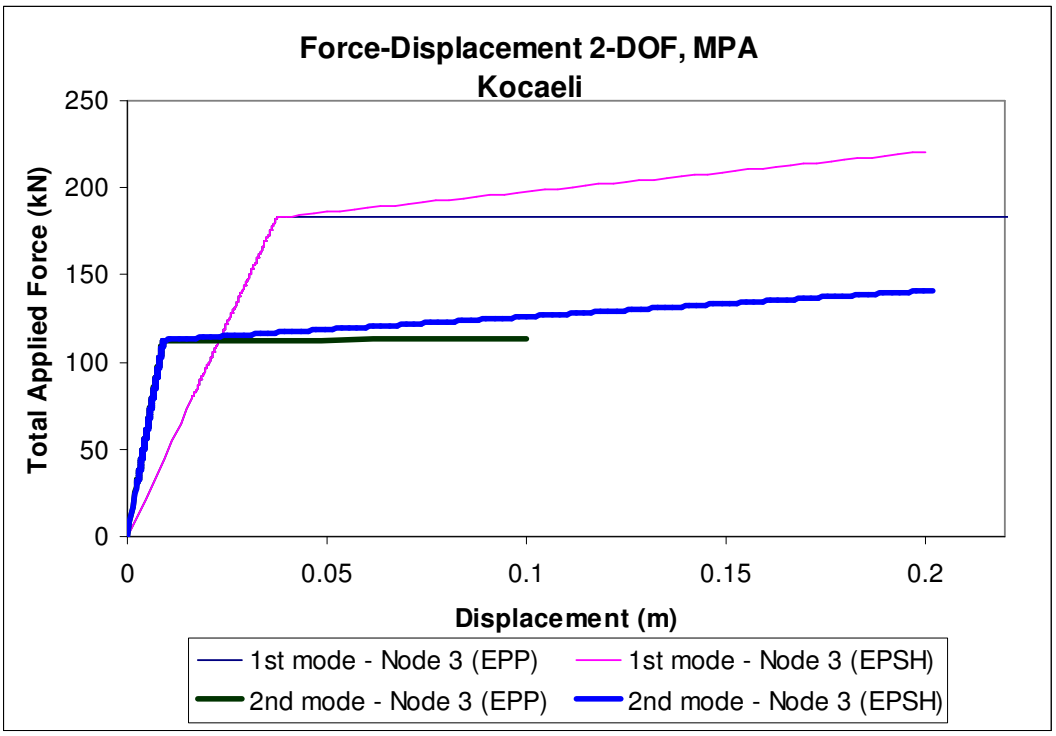

Figure 4-39 Force -Displacement relationships derived considering two modes of vibration and two material models (Kocaeli ground motion)

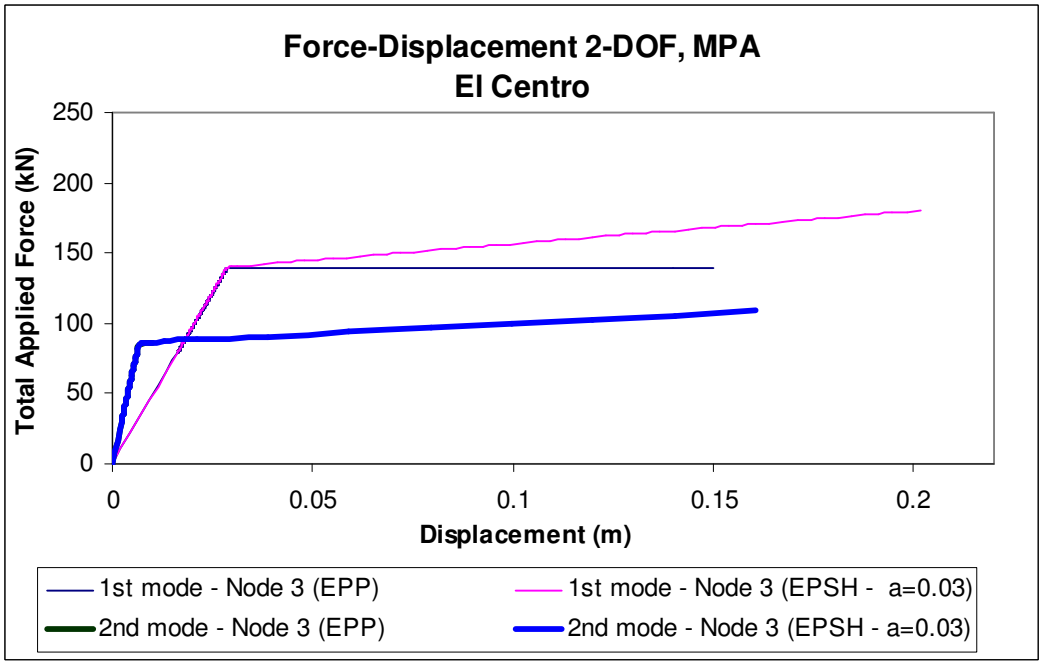

Figure 4-40 Force -Displacement relationships derived considering two modes of vibration and two material models (El Centro ground motion)

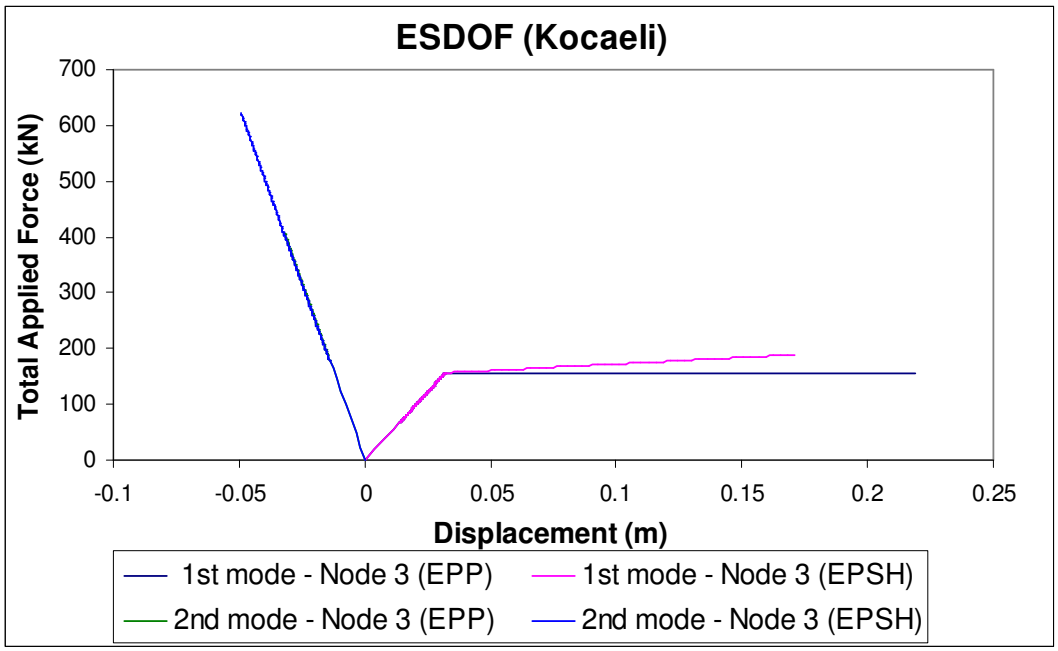

Figure 4-41 Equivalent SDOF Force -Displacement relationships derived considering two modes of vibration and two material models (Kocaeli ground motion)

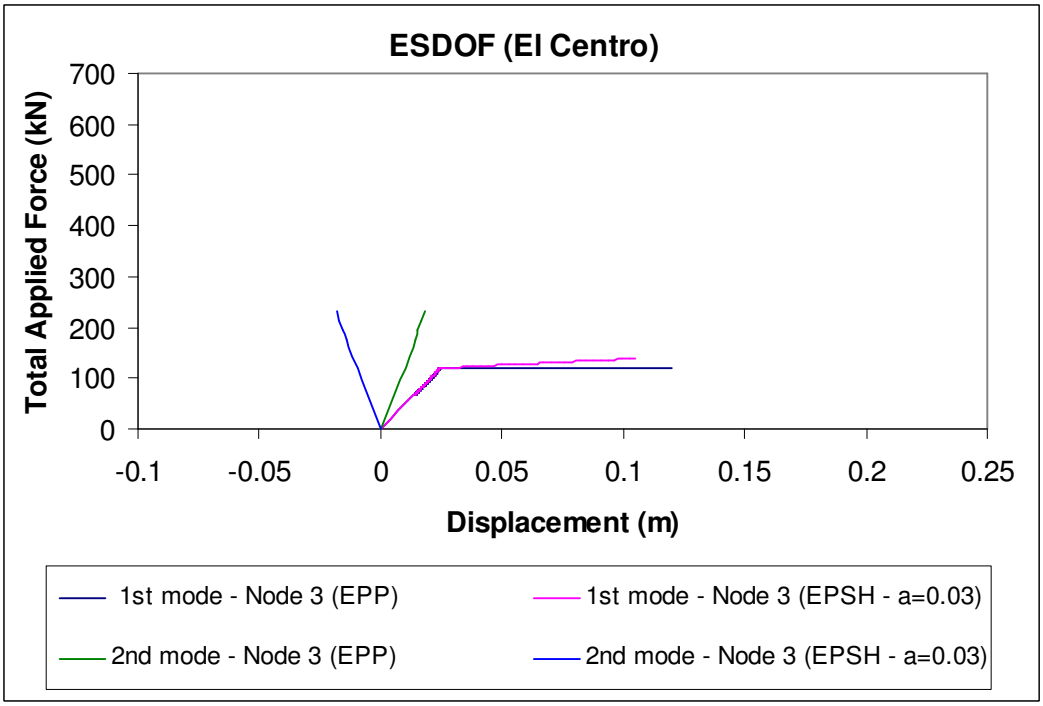

Figure 4-42 Equivalent Force -Displacement relationships derived considering two modes of vibration and two material models (El Centro ground motion)

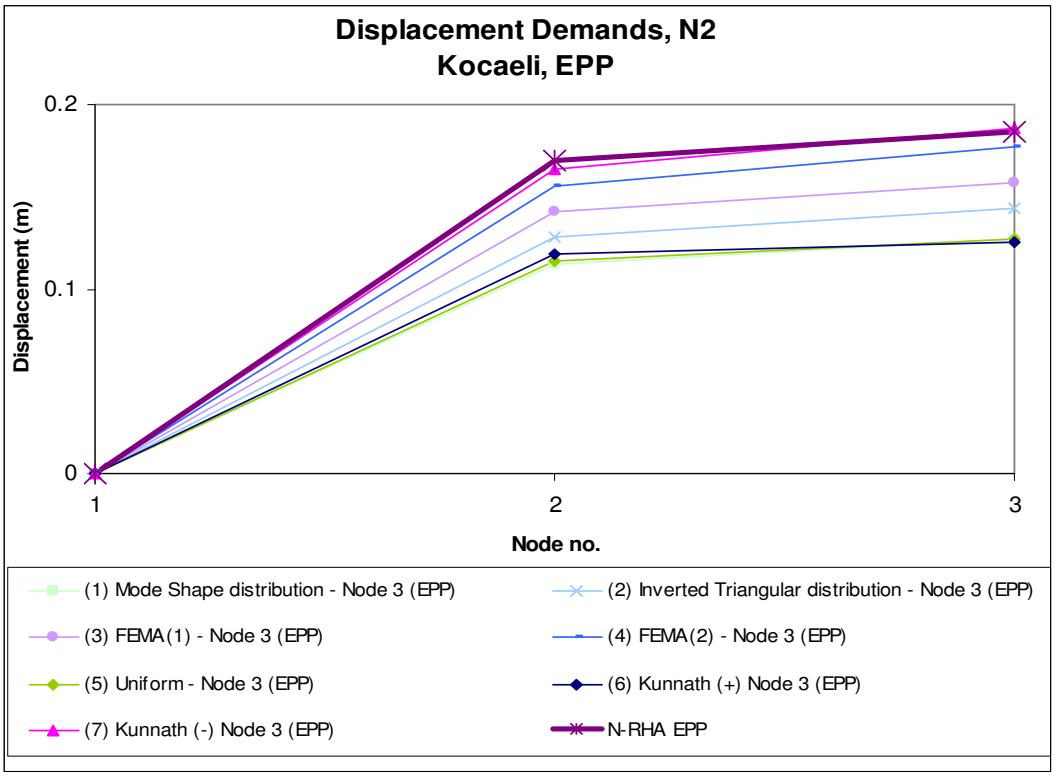

Figure 4-43 Displacement Demands obtained from N2 method (Kocaeli, EPP)

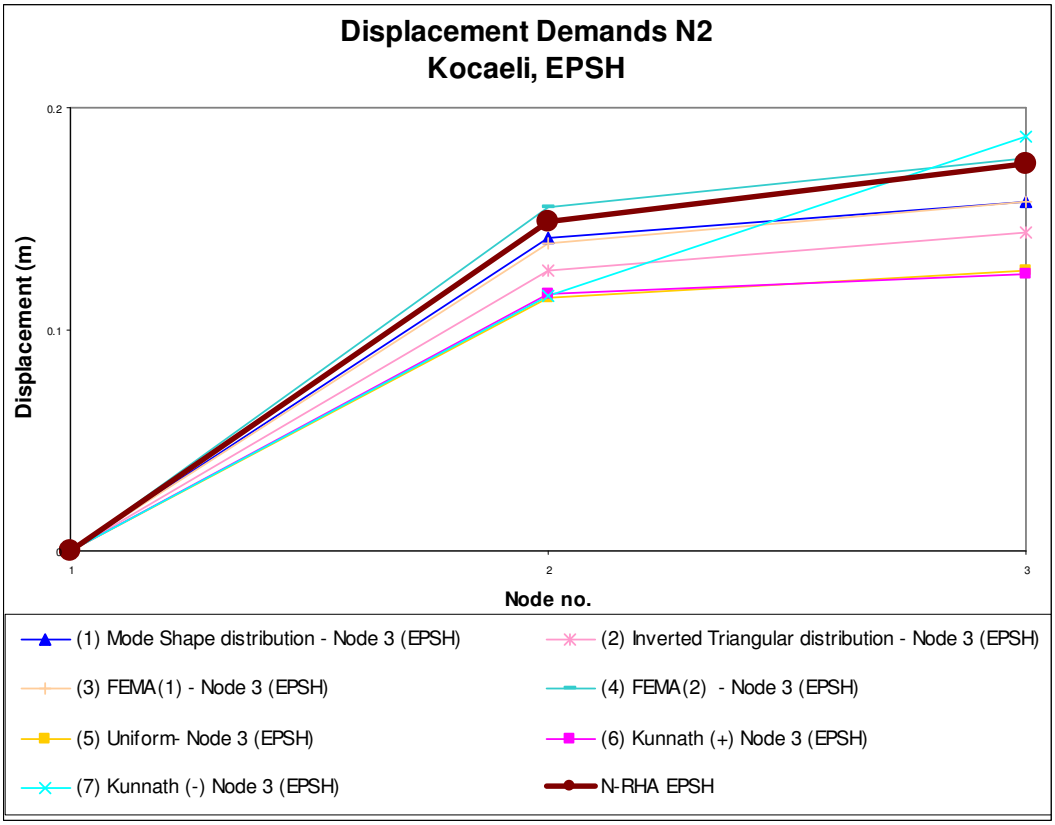

Figure 4-44 Displacement Demands obtained from N2 method (Kocaeli, EPSH)

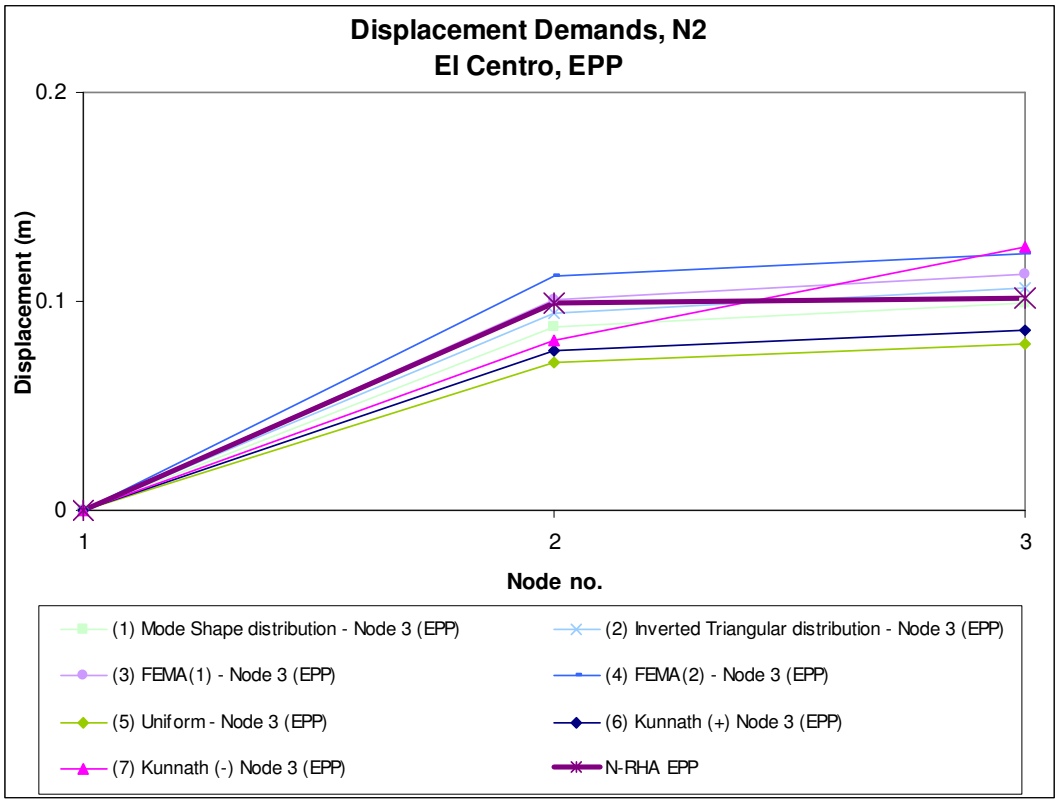

Figure 4-45 Displacement Demands - N2 method (El Centro, EPP)

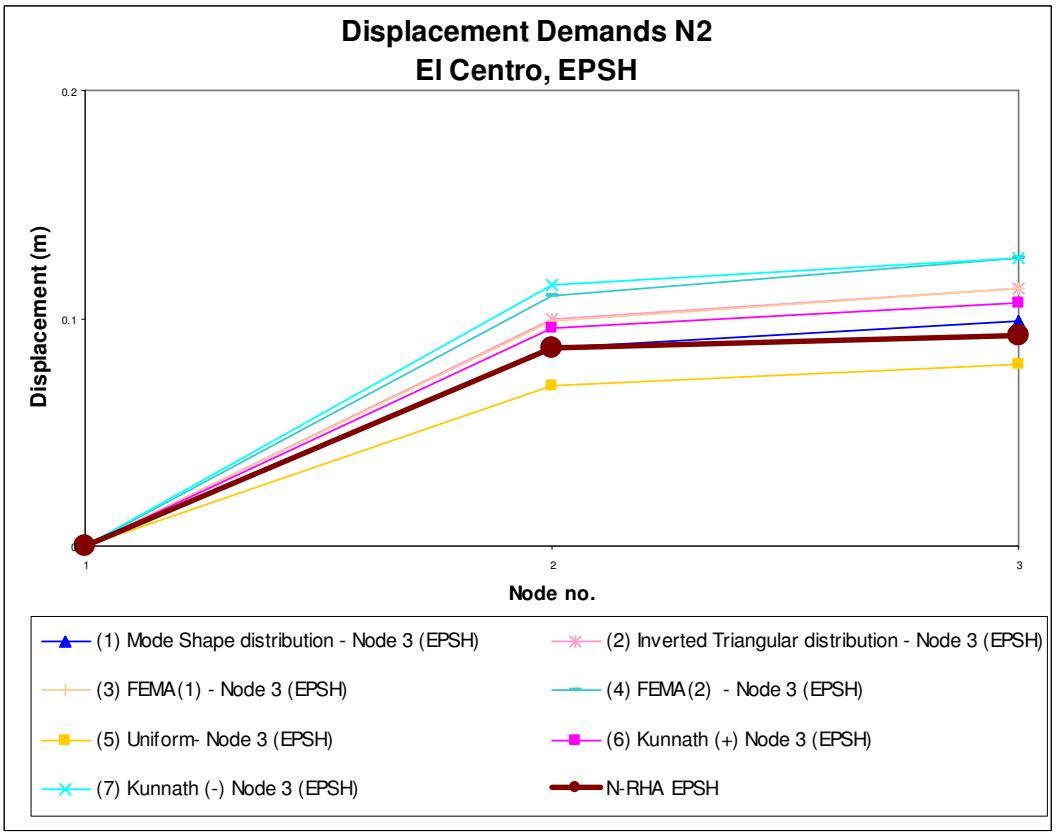

Figure 4-46 Displacement Demands - N2 method (El Centro, EPSH)

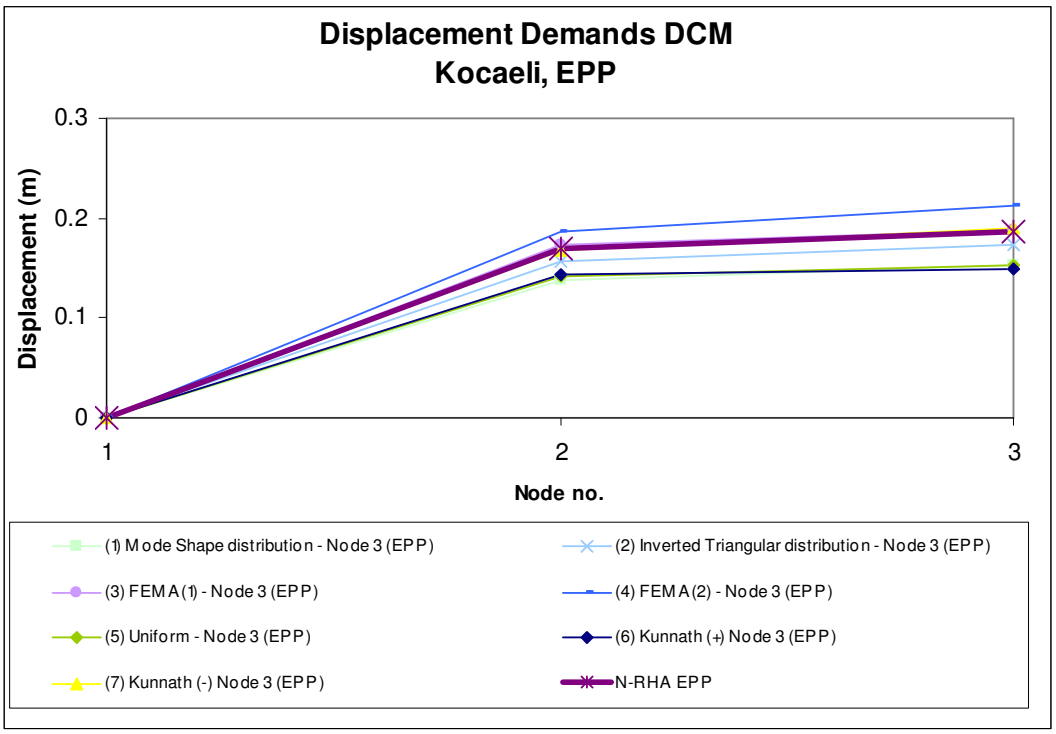

Figure 4-47 Displacement Demands obtained from DCM method (Kocaeli, EPP)

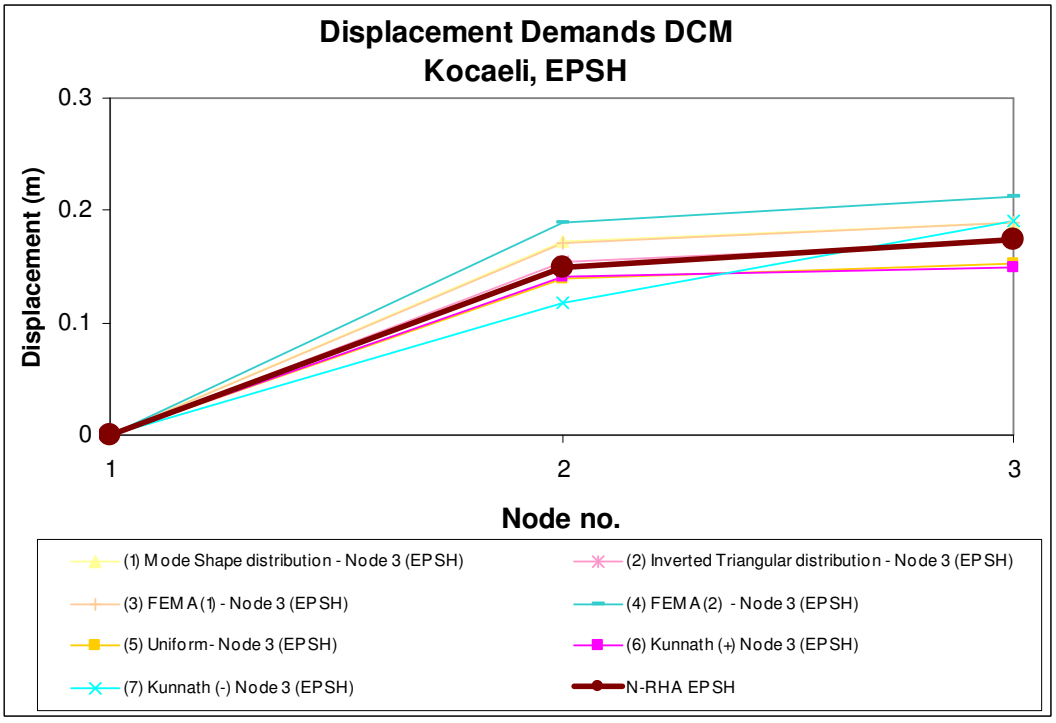

Figure 4-48 Displacement Demands obtained from DCM method (Kocaeli, EPSH)

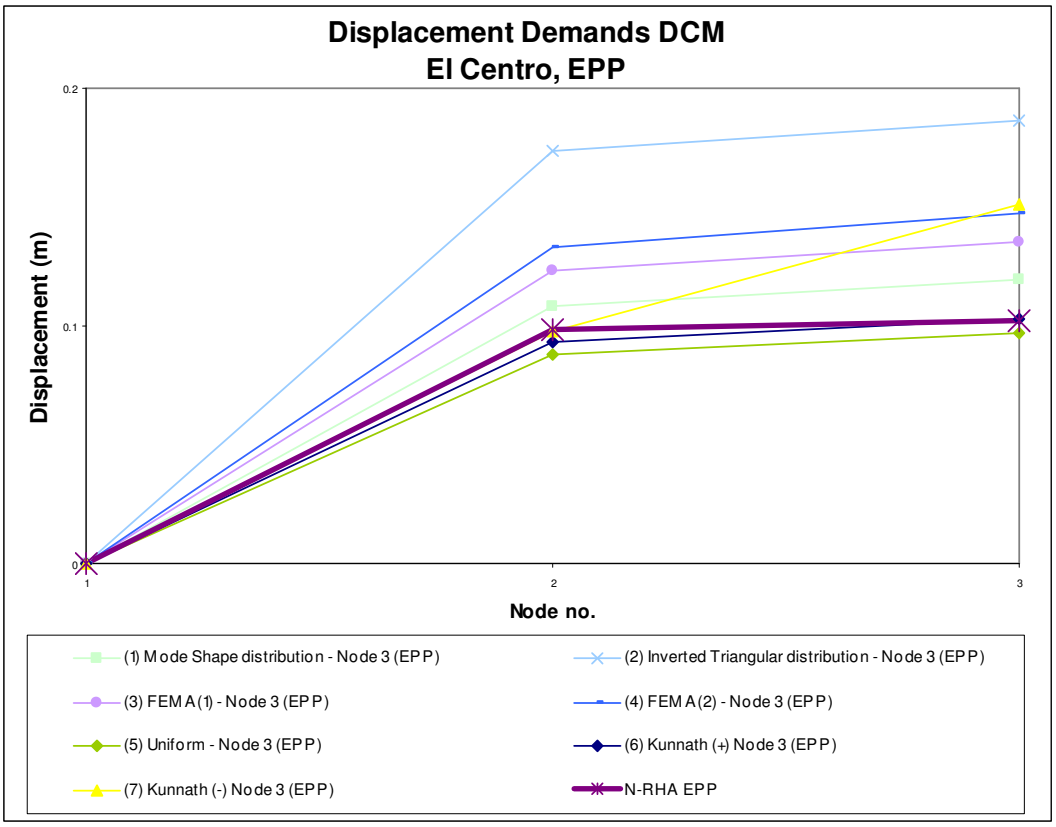

Figure 4-49 Displacement Demands - DCM method (El Centro, EPP)

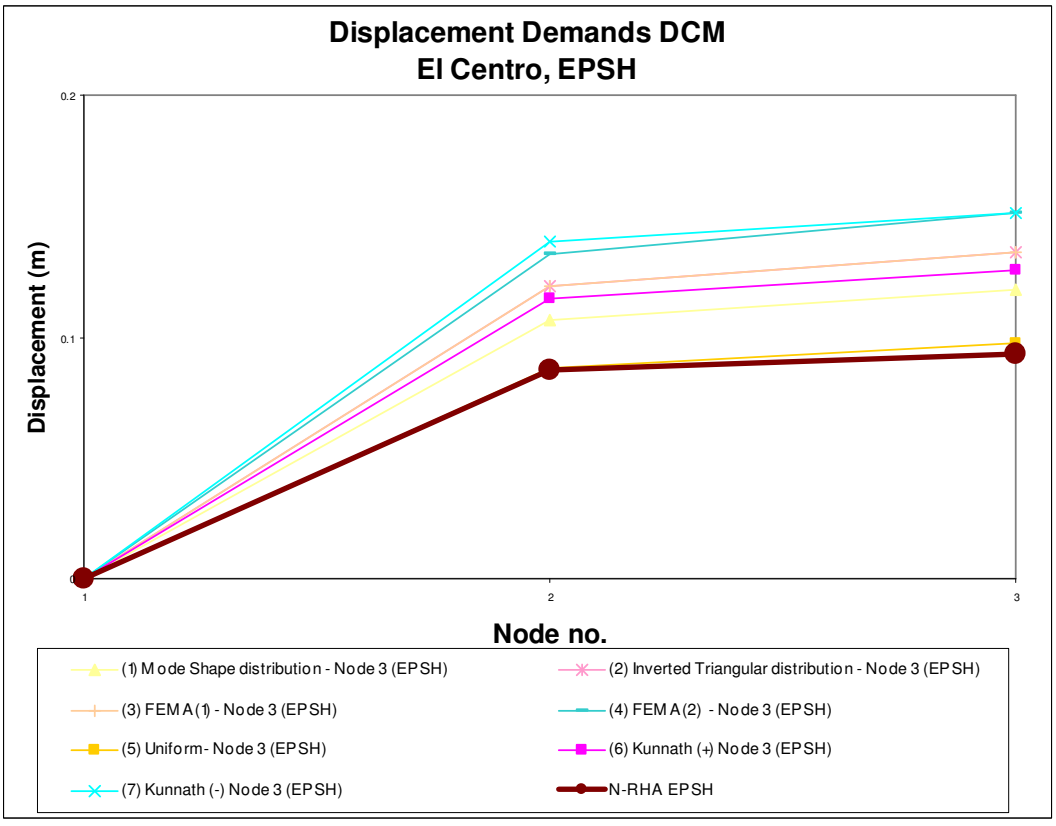

Figure 4-50 Displacement Demands - DCM method (El Centro, EPSH)

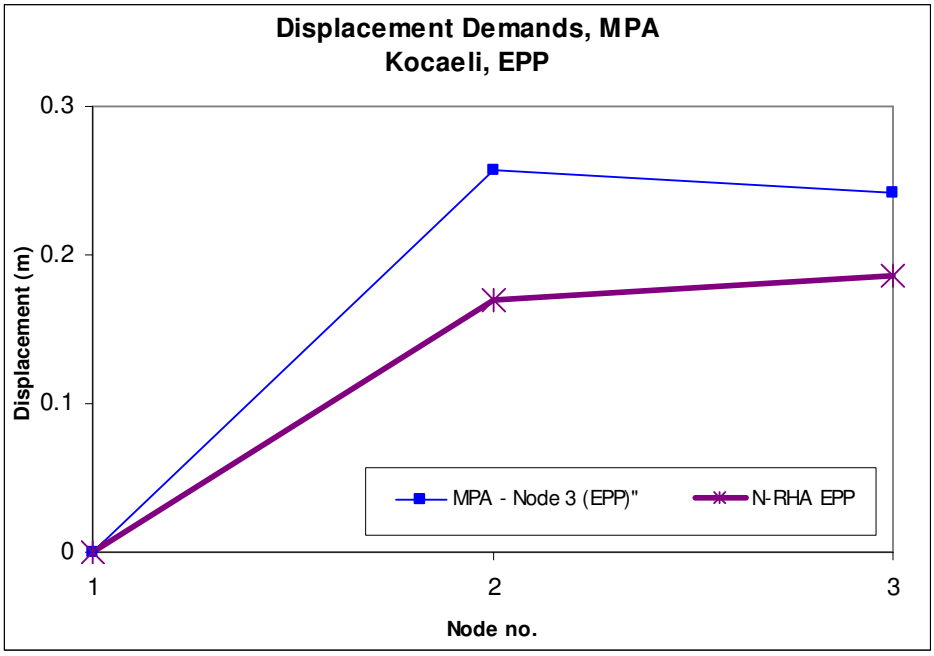

Figure 4-51 Displacement Demands obtained from MPA method (Kocaeli, EPP)

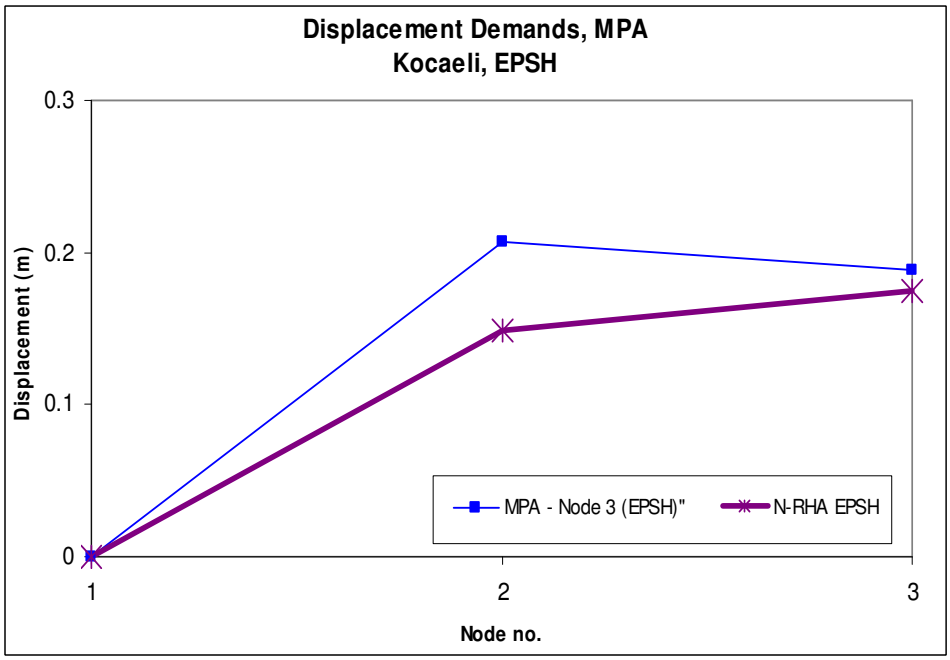

Figure 4-52 Displacement Demands obtained from MPA method (Kocaeli, EPSH)

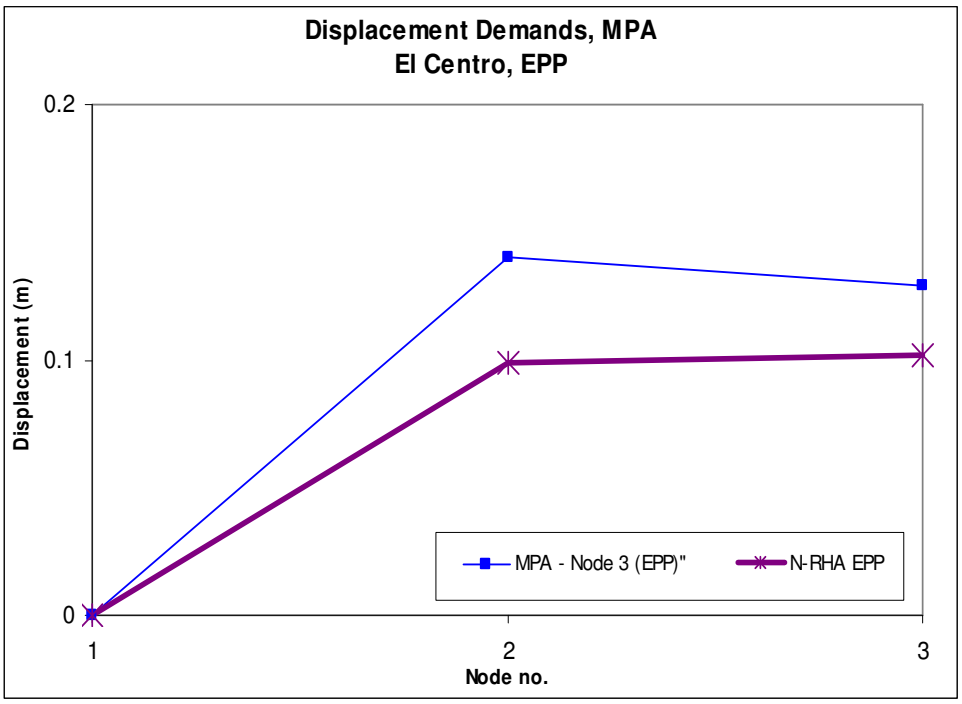

Figure 4-53 Displacement Demands - MPA method (El Centro, EPP)

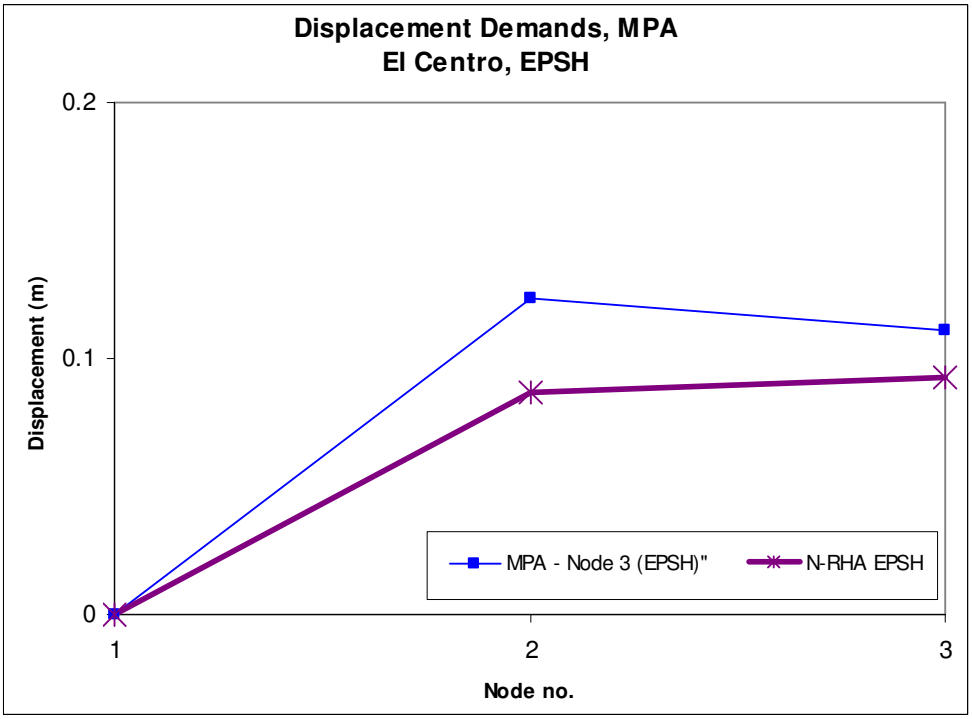

Figure 4-54 Displacement Demands - MPA method (El Centro, EPSH)

CHAPTER 5
PUSHOVER ANALYSIS OF A 4-STOREY RC FRAME STRUCTURE

5.1 INTRODUCTION

In this chapter the accuracy of the N2, DCM and MPA methods compared to nonlinear time-history analysis is assessed through their application to a four-storey single bay reinforced concrete frame. The results of these analyses will be shown in non-dimensionalised form. This low-rise structure has also been studied by Pankaj *et al.* (2005).

5.2 STRUCTURE

The geometric properties of the frame and the cross-sections of the reinforced concrete elements are shown in Figure 5.1. The total mass of the frame is approximately 97000 kg including live loads. A damping ratio of 5% has been assumed as was done by Pankaj *et al.* (2005). The columns were assumed fixed at the base.

5.3 FEA MODELLING

The structural elements were modelled using the 2D Kirchhoff thin beam element with quadrilateral cross-section (BMX3), Figure 5.2. The thin beam element is parabolically curved, non-conforming, and neglects shear deformations. The formulation of the Kirchhoff thin beam is based on the constrained super-parametric approach. The axial force along the beam-column element is linearly varied. The displacement is varied quadratically in the local x-direction and cubically in the local y-direction. The shear force is assumed constant. Each beam-column structural element was divided into 15 finite elements.

The material properties of the reinforced concrete elements were based on equivalent concrete properties assuming uncracked sections. The nonlinear behaviour of the structure was modelled using the elastic - perfectly plastic material model, EPP, and the

elastoplastic with strain hardening material model, EPSH. The Drucker-Prager yield criterion was used for both material models to define the evolution of the yield surface. The Drucker-Prager criterion idealizes concrete as homogeneous. For the EPP model the Drucker-Prager criterion does not cause changes to the shape of the yield surface with increasing plastic strains. For the EPSH model the Drucker-Prager criterion assumes an isotropic expansion of the yield surface. The material properties used are given in Table 5.1.

In general, the Drucker-Prager criterion approximates the Mohr-Coulomb criterion, Figure 5.3. It belongs to the family of classical continuum formulation models where the plastic strains are integrated according to a strict interpretation of the flow rules that govern their evolution. This model provides a smooth conical yield surface that avoids numerical instabilities in the solution unlike the Mohr-Coulomb criterion whose yield surface is hexagonal (Pankaj *et al.* 2005). It has been concluded (Lowes, 1999) that the Drucker-Prager criterion can represent reasonably well the behaviour of plain concrete when subjected to multi-axial compression but for compression-tension and tension-tension type loadings it will generally over-estimate the capacity of concrete. Nevertheless the Drucker-Prager model has been the basis for more sophisticated concrete models such as the micro-plane model (Bazant *et al.* 1985) or the concrete damage plasticity model (Lubliner *et al.* 1989) which are more efficient in capturing concrete behaviour under cyclic loading histories.

The Drucker-Prager model was the most appropriate yield criterion for conducting nonlinear static and nonlinear dynamic analyses due to element compatibility restrictions. For the EPSH model a hardening modulus of 5% of the elastic modulus was used.

5.4 DESIGN SPECTRUM & EARTHQUAKE LOADING

The frame has been designed to Eurocode 8, EC8 (2003), using an elastic design spectrum that corresponds to a peak ground acceleration of 0.3g, subsoil Class B with 5% critical damping and an amplification factor of 2.5. For the nonlinear time-history analyses the Kocaeli and the El Centro ground motions were used, scaled to a peak ground acceleration of 0.3g. For pushover analyses the use of the elastic design spectrum was found to be inappropriate because it did not match very well the

individual response spectra of the Kocaeli and El Centro ground motions. Therefore the individual response spectra should be used instead. A comparison of the pseudo-acceleration and displacement design and response spectra is provided in Figures 5.4 and 5.5.

5.5 NONLINEAR TIME-HISTORY ANALYSES

Nonlinear time-history analyses of the structure subject to the Kocaeli and El Centro ground motions were carried out for the two material models, EPP and EPSH. The analyses were performed without gravity loads and geometric nonlinearity, as in Ramirez et al. (2001).

The results of the analyses for the two ground motions are displayed in Tables 5.2 and 5.3. The roof displacement time-histories of the 4-storey frame subjected to the Kocaeli and El Centro ground motions are shown in Figures 5.6 and 5.7 respectively. The base shear time-histories are shown in Figures 5.8 and 5.9 and the base moment time-histories in Figures 5.10 and 5.11.

The inclusion of strain hardening in the analysis seemed to have insignificant effect on the displacement response of the structure for the El Centro ground motion, giving similar results with the EPP model. However, in the case of the Kocaeli ground motion the strain hardening effect was more pronounced as shown by the displacement time-histories. Typical base shear-roof displacement responses for both ground motions are shown in Figures 5.12 and 5.13 for the Kocaeli and El Centro ground motions respectively from which can be seen the complexity of the structure's response.

The formation of the plastic hinges was captured in these analyses for both ground motions. Figure 5.14 shows the 1st hinge formation from El Centro and Kocaeli ground motions. Figure 5.15 shows the hinge locations at the collapse stage of the structure for the El Centro and Kocaeli ground motions.

5.6 LOAD PATTERNS

Nine load patterns were used in the pushover analyses of the structure, for the N2 and DCM methods, Figure 5.16 and 5.17. These are:

1. Mode Shape distribution
2. Inverted Triangular distribution
3. The FEMA(1) distribution with $k \approx 1.315$
4. The FEMA(2) distribution with $k = 2$
5. Uniform distribution
6. Kunnath (1) distribution
7. Kunnath (2) distribution
8. Kunnath (3) distribution
9. Kunnath (4) distribution

The last four variations of the Kunnath load pattern take into account the first four modes of vibration, even though studies (Kunnath 2004) have shown that the first two modes could have sufficed. The variations had the following form:

- Kunnath (1) = Mode 1 + Mode 2 + Mode 3 + Mode 4
- Kunnath (2) = Mode 1 - Mode 2 + Mode 3 - Mode 4
- Kunnath (3) = Mode 1 - Mode 2 - Mode 3 - Mode 4
- Kunnath (4) = Mode 1 + Mode 2 - Mode 3 - Mode 4

More variations of Kunnath's load patterns could easily be assumed. However, based on the Kunnath study it was unclear whether using more of these patterns could provide better estimates of seismic demands.

It should be recognised that load patterns 1-5 will provide the same pushover curves for both ground motions even though the base shear magnitude for each ground motion is not the same. This is because the base shear for each case is distributed across the floors through the same ratios. However Kunnath's load variations will differ for each ground motion, Figures 5.16 and 5.17. For the El Centro case Kunnath (2) and Kunnath (3) load patterns resulted in a very small base shear and therefore will not be considered.

The load distribution for the 4-storey frame for the MPA method accounted for 4 modes of vibration. The load patterns used for the MPA method, Figure 5.18, will be the same for both ground motions and therefore the same pushover curves will apply to both cases.

The aforementioned load patterns, except for the Uniform use as a basic quantity the base shear and distribute it across the floor levels according to the weight of the structure and the normalised mode shape. These load patterns therefore use dynamic information based on the elastic acceleration ordinate of the response spectrum and the weight of the structure.

It becomes apparent then that the load patterns are dependent on the geometric and material properties of the structural elements. The fact that the elastic acceleration ordinate is used instead of the inelastic acceleration ordinate of the spectrum does not have any effect on the accuracy of the nonlinear static analysis since it is the relative difference in magnitude of the loads across the floors that control the response of the structure rather than their individual magnitudes.

The Uniform load pattern assumes that during the response of the structure the entire mass of each floor is participating in the response. While this assumption may not be realistic if the first mode does not dominate the response, it should provide an upper bound to the response. Kunnath's load patterns use as information the –pseudo-acceleration ordinates of the response spectra corresponding to the modes of interest, the participation factor, and mode shape for each mode, and the weight of the floor. These load patterns therefore use the base shear developed during each mode of vibration, distributed across the floor levels according to the shape of the mode of interest and amplify or reduce its magnitude according to the participation factor of each mode. These load patterns can be thought to be a conceptual improvement over the other load patterns.

5.7 PUSHOVER ANALYSES

The pushover analyses utilised the same material models as the nonlinear dynamic analyses. The pushover curves were stopped at the point where convergence of the

solution failed. This could physically imply the onset of the collapse or failure mechanism of the structure, Figure 5.19.

Figures 5.20 and 5.21 show the pushover curves for all load patterns, for the Kocaeli ground motion, for the EPP and EPSH material models, respectively. It can be seen that the responses produced by the two material behaviours do not differ significantly. Figures 5.22 and 5.23 show the pushover curves for all load patterns, for the El Centro ground motion, for the EPP and EPSH material models, respectively. In general it should be noted that the EPP model has the tendency to cause the structure to displace at larger displacement levels than the EPSH model.

Inspecting the pushover curves for both ground motions it can be seen that they are separated into three distinct groups of different base shear magnitude. For the Kocaeli ground motion, Kunnath (1), Kunnath (4) and the Uniform load distributions provided an upper bound to the global base-shear roof displacement response. This can be attributed to the fact that in Kunnath (1) and (4) distributions a summation of the first two modes was considered thus leading to a high magnitude of base shear. Kunnath (2) and Kunnath (3) load patterns provided a lower bound to the global base shear-roof displacement response. This can be attributed to the fact that the influence of the second mode was substracted from the first mode thus leading to a reduced base shear. Additionally the alternating direction of the loads across the floors resulted in collapse of the frame at a lower magnitude of base shear. The remaining load distributions, Inverted Triangular, Mode Shape, FEMA (1) and FEMA (2) performed in between the aforementioned load distributions.

For the El Centro ground motion the load patterns provided the same upper and lower bounds as in the Kocaeli ground motion. However the total magnitude of the base shear for the El Centro ground motion was slightly larger than the base shear for the Kocaeli ground motion when Kunnath (1) and Kunnath (4) load patterns were used. This can be attributed to the larger difference in the relative ratios of the forces acting on the floors to the total force at the base of the structure as can be seen in Figures 5.16 and 5.17.

The pushover curves for the MPA method are given in Figure 5.24. For this method the first four modes of vibration were considered. It can be seen that except for the first mode all the remaining modes resulted in almost elastic pushover curves.

5.8 DISPLACEMENT DEMANDS

Once the pushover curves are established, they need to be transformed into capacity curves for each ground motion in order to perform the pushover analyses. The N2, DCM and MPA methods were used to estimate the seismic demands for the 4-storey structure.

In case of the displacement demands' estimation, the N2 method tended to underestimate the displacement response of the structure at all floor levels for both ground motions and material models. For the Kocaeli ground motion and the EPP material model, Tables 5.2 to 5.5 and Figure 5.25, the best estimate was provided by FEMA (2) load distribution which underestimated the response by 8%. The FEMA (1), Mode Shape, and Inverted Triangular load patterns also provided reasonable estimates with underestimations of 13%, 14% and 16% respectively. The worst estimate was provided by Kunnath (1) load pattern with an underestimation of 48% respectively. Finally, The Uniform and Kunnath (4) load distributions resulted in underestimations of 28% and 23% respectively while Kunnath (2) and Kunnath (3) load distributions in overestimations of 19% and 22% respectively.

For the Kocaeli ground motion and the EPSH material model, Tables 5.2 to 5.5 and Figure 5.26, the accuracy of pushover analysis was improved when compared to its performance with the EPP model. For the EPSH model the closest estimate was achieved by the FEMA (2) load distribution with an underestimation of 2%. Satisfactory estimates were also provided by the FEMA (1), Inverted Triangular, and Mode Shape load patterns with errors of 5%, 8% and 10% respectively. For this case the worst approximation was provided by the Kunnath (1) and Kunnath (4) load distributions with error of 38%. The Uniform load pattern resulted in an underestimation of 28%. Finally Kunnath (2) and Kunnath (3) load distributions overestimated the displacement demands by 27% and 26% respectively.

In the case of the El Centro ground motion and the EPP material model, Tables 5.6 to 5.9 and Figure 5.27, the N2 method underestimated the displacement demands for all load patterns with estimates greater than 50%. The closest estimate was provided by the FEMA (2) load distribution with an underestimation of 52 %, followed by the Mode Shape, and the Inverted Triangular load distributions with an error 58%. The worst

estimate was provided by Kunnath (1) and Kunnath (4) with an error of 73%. For the El Centro ground motion and the EPSH model, Tables 5.6 to 5.9 and Figure 5.28, the results follow the same pattern as for the EPP model.

The DCM method gave generally similar displacement estimates to the N2 method, especially at roof level, for both ground motions and material models. The displacement demands are shown in Tables 5.10 to 5.13 and Figures 5.29 to 5.30 for the Kocaeli ground motion, and Tables 5.14 to 5.17 and Figures 5.31 to 5.32 for the El Centro ground motion. These estimates where calculated using a C_2 factor of 1.0 which accounted for a structural performance level of immediate occupancy.

The MPA method resulted in very small underestimations of the deflections at the floor levels especially for the third and fourth floors for the Kocaeli ground motion. However the displacement demands for the El Centro ground motion were largely underestimated by more than 50%. This is shown in Tables 5.18 & 5.19 and Figures 5.33 & 5.34 for the Kocaeli ground motion and Tables 5.20 to 5.21 and Figures 5.35 to 5.36 for the El Centro ground motion. Two variations of the MPA method were considered – the first took account of the first four modes and the second only the first two modes. The variation using the first two modes resulted in similar displacements for the first and second floor levels and smaller displacements for the third and fourth floor levels compared to the estimates obtained when four modes were used.

5.9 ROTATION DEMANDS

The maximum rotations at the right-hand ends of each floor were also determined from the nonlinear dynamic and pushover analyses. For the Kocaeli ground motion and the EPP material model, Tables 5.2 to 5.5 and Figure 5.37 and 5.38, the rotations were mostly underestimated. The closest estimates for all the floors were provided by the FEMA (2) load distribution which underestimated the top floor rotation by 17% and the 2^{nd} floor level rotation by 8%. The remaining load patterns provided estimates higher that 30% with the largest errors given by Kunnath (1) and Kunnath (4) load patterns with errors of 71% and 75% respectively. For the EPSH model the rotation estimates were improved with respect to the EPP model. The closest estimate for the first floor level was provided by Kunnath (2) with an error of 5% and for the remaining floors by FEMA (2) load pattern with an error of 4%.

For the El Centro ground motion the N2 method largely underestimated the rotations at all floors by more than 50% for both material models, Figures 5.39 and 5.40. Kunnath(1) and Kunnath(4) load distributions provided the least accurate estimates with errors up to 96% for both the EPP and EPSH models. These inaccuracies are the result of the small displacement estimates obtained.

The DCM method provided, in general, similar estimates of rotations at all floor levels to the N2 method. For the Kocaeli ground motion, satisfactory estimates were given by FEMA (2) load distribution with underestimations of 17% and 4% for the EPP and the EPSH models respectively. For the El Centro ground motion, Figures 5.43 and 5.44, FEMA(1) load distribution provided satisfactory estimates for the EPP model at all floor levels and especially for the two lower floors.

The MPA method underestimated the floor rotations at all floor levels, Tables 5.18, 5.19 and Figures 5.45 and 5.46, for the Kocaeli ground motion. The floor rotations for the El Centro ground motion are presented in Tables 5.20, 5.21 and Figures 5.47 and 5.48. Again for this method the rotation estimates were in closer agreement for the Kocaeli ground motion than for the El Centro ground motion. Additionally, using only the first two modes did not affect the accuracy of the rotation demands for the two lower storeys but reduced their magnitude for the third and four storeys.

5.10 BASE SHEAR

The base shear obtained from the pushover analyses is presented in Tables 5.4 to 5.23. The N2 and DCM methods underestimated the base shear for both ground motions, and material models. Kunnath (4) load variation provided the best estimate of base shear for the Kocaeli ground motion, EPP model, with an error of 9%. Kunnath (2) and Kunnath (3) resulted in large underestimation by 65% and 64% respectively for the Kocaeli ground motion, EPP model. The use of the strain-hardening model resulted in larger errors for both ground motions than for the EPP model but still at a reasonable accuracy. The MPA method provided improved estimates of base shear for both ground motions when compared to the N2 and DCM methods. The use of the first two modes gave a better estimate than including the first four modes.

5.11 BASE MOMENT

The N2 and DCM methods provided similar estimates of the base moment at the right-hand end of the structure for all load patterns and both the EPP and EPSH models. For the Kocaeli ground motion, when the EPP model was considered, most of the estimates were within 10% error with the Kunnath (4) load pattern providing an almost exact estimate. However, the base shear estimates were less accurate for the EPSH model.

For the El Centro ground motion the N2 and DCM methods underestimated the base moment in all cases by more than 40%. The best estimate in this case was provided by Kunnath (4) for both the EPP and EPSH models, with an overestimation of 42% and 41% respectively.

The MPA method provided similar estimates of base moment for the Kocaeli ground motion and improved estimates of base moment for the El Centro ground motion. Generally the MPA method overestimated the base moment when the EPP model was considered and underestimated it with the EPSH model. Additionally it is worth noting that the inclusion of the four modes of vibration resulted in larger overestimation of the base moment for the Kocaeli ground motion, when the EPP model was used.

5.12 GLOBAL DUCTILITY

The global ductility of the structure is compared in Tables 5.4 to 5.23 for the N2, DCM and MPA methods. In general the three methods resulted in an underestimation of the global ductility. However the estimates can be considered to be reasonable in the case of the MPA method, Kocaeli ground motion, EPP model. For the El Centro ground motion all the methods estimated the ductility to be less than half of the value from the nonlinear dynamic analysis. Also for the El Centro ground motion the ductility was calculated to be less than unity. This signified collapse of the structure. Therefore if pushover analysis was used without complementing it with nonlinear dynamic analyses it would be able to predict the collapse but not at the same magnitude of displacement.

5.13 PLASTIC HINGES

The plastic hinge formation predicted by the various pushover methods was the same as that predicted by the nonlinear dynamic analyses. The first plastic hinge predicted by all the nonlinear dynamic analyses and pushover analyses was at the second floor level, Figure 5.14. Identification of plastic hinge formation is an important feature of pushover analysis as it can give the designer an insight into which parts of the structure need special considerations in the design process. However it has been shown that this ability of pushover methods in capturing local quantities such as the formation of plastic hinges diminishes as the structure grows taller (Krawinkler *et al.* 1994).

The inclusion in the analyses of the strain hardening effect did not delay the occurrence of the first hinge with respect to the EPP model but it did delay the occurrence of the mechanism's formation. The development of the plastic hinges predicted by both nonlinear dynamic analyses and pushover analyses are shown in Figure 5.15.

5.14 CONCLUSIONS

The seismic response of a four storey RC frame has been calculated using nine different load patterns, and three different nonlinear static pushover methods – N2, DCM, and MPA. The results of these analyses have been compared with the results of the nonlinear dynamic analyses for a near-fault ground motion, Kocaeli ground motion, and a far-field ground motion, El Centro ground motion. Estimates of displacements and rotations at all floor levels; base shear, base moment, and global ductility were obtained.

The nine load patterns resulted in small variability in the displacement demands when either the N2 or DCM methods were utilized. The Uniform and the Kunnath (1) load distributions provided the worst estimates for all quantities of interest for both ground motions. This implies that the Uniform load distribution might not be adequate to use in the estimation of the displacement demands. However the same cannot be said for Kunnath (1) variation, because it seems that Kunnath's load patterns do not apply to all cases of pushover analysis. Also not all Kunnath's variations are effective in all cases for providing the displacement demands. There needs to be further consideration on which combinations need to be used for each case. These should be consistent with the

influence of the ground motions on the response of the structure implying that at least a linear dynamic analysis or a modal analysis would be necessary. Additionally some load patterns could produce very small base shears and therefore need not be considered. The performance of the load patterns show that some amplification factors should be considered when calculating the load vectors for nonlinear static analysis. Further research is needed on this aspect of pushover analysis.

In general the pushover methods underestimated the deflections at all floor levels with increasing error from the lower storeys to the upper storeys, for both ground motions. This implies that the accuracy of pushover analysis in estimating deflection profiles is a function of the height of the structure, as suggested by Krawinkler *et al.* (1996). Therefore pushover analysis can be thought to be more able to estimate seismic demands for low-rise structures than for high-rise structures. This conclusion is consistent with findings of previous studies, Faella (1996), Gupta *et al.* (2000), Jan *et al.* (2004), Papanikolaou *et al.* (2005), Tjhin *et al.* (2006).

The N2 and DCM methods provided very similar results for all the load patterns, material models and ground motions. In the case of the Kocaeli ground motion the displacement demands were in good agreement with the results from nonlinear dynamic analyses. This can be attributed to the high magnitude of spectral accelerations and displacements of the Kocaeli ground motion. However in the case of the El Centro ground motion the displacement demands were not estimated satisfactorily mainly due to the small magnitude of the spectral accelerations and displacements at the considered modal periods of the structure. It therefore appears that the accuracy of pushover analysis is also a function of the severity of the ground motions studied.

The accuracy of pushover analysis for the near-fault ground motion might imply that it is governed by the relative position in the period spectrum of the fundamental period of the structure with respect to the pulse period of the ground motion. This means that for structures with fundamental period close to the pulse period of the ground motion pushover analysis will perform well. This conclusion is quite consistent with the findings of the effectiveness of pushover analysis on SDOF systems.

The rotation demands at each floor level showed similar trends to the deflection profiles. The biggest deviations from the nonlinear dynamic analysis response occurred at roof level.

For the Kocaeli ground motion, the estimates of base shear, base moment and global ductility were in closer agreement to the nonlinear dynamic response than the deflection and rotational profiles. However the estimates of these quantities for the El Centro ground motion were rather worrying, mainly because it was expected that for this structure and ground motion the method would yield good estimates.

The MPA method performed similarly to the N2 and DCM methods in terms of accuracy of the displacement demands. However the amount of effort required for this analysis is considerably less than using the N2 or DCM methods with more load patterns. Additionally, the results show that Kunnath (1) and Kunnath (4) load distributions could be used with the N2 or DCM method instead of the MPA method and provide satisfactorily accurate results, with approximately the same effort.

The comparison of the nonlinear dynamic and pushover analysis displacement results from the N2 and DCM methods are generally in reasonable agreement with the results presented in Pankaj *et al.* (2004) study. The discrepancies between the two studies can be mainly attributed to the difference in the number of load patterns used and the fact that Pankaj utilised ground motions whose response spectra matched the design spectrum while in this study the results were based on the individual response spectra of two distinctly different ground motions.

Young's Modulus, E	28.6E6 kN/m^2
Poisson's ratio, ν	0.15
Friction angle, β	15º
Compressive yield strength, $f_c^{'}$	20.86E3 kN/m^2

Table 5-1 Drucker-Prager material model properties

Kocaeli	EPP	EPSH
Rel Disp (1st) (m)	0.0221	0.0198
Rel Disp (2nd) (m)	0.0586	0.0542
Rel Disp (3rd) (m)	0.0943	0.0882
Rel Disp (4th) (m)	0.1302	0.1234
Rotation (1st)	-0.0106	-0.0098
Rotation (2nd)	-0.0128	-0.0123
Rotation (3rd)	-0.0135	-0.0123
Rotation (4th)	-0.0120	-0.0105
Base Shear (kN)	214.20	218.75
Base Moment node (kNm)	315.13	318.08
Ductility	4.6	4.4

Table 5-2 Nonlinear Time-History Results, Kocaeli ground motion

El Centro	EPP	EPSH
Rel Disp (1st) (m)	0.0160	0.0160
Rel Disp (2nd) (m)	0.0442	0.0446
Rel Disp (3rd) (m)	0.0737	0.0741
Rel Disp (4th) (m)	0.0997	0.0998
Rotation (1st)	-0.0080	-0.0081
Rotation (2nd)	-0.0102	-0.0102
Rotation (3rd)	-0.0099	-0.0098
Rotation (4th)	-0.0084	-0.0082
Base Shear (kN)	198.92	199.29
Base Moment node (kNm)	316.41	322.08
Ductility	3.7	3.7

Table 5-3 Nonlinear Time-History Results, El Centro ground motion

N2					Nonlinear Dynamic	
Kocaeli	Mode Shape Distribution _ EPP	Mode Shape Distribution _ EPSH	Inverted Triangular Distribution _ EPP	Inverted Triangular Distribution _ EPSH	EPP	EPSH
Rel Disp (1st) (m)	0.0160	0.0160	0.0163	0.0176	0.0221	0.0198
Rel Disp (2nd) (m)	0.0481	0.0481	0.0481	0.0513	0.0586	0.0542
Rel Disp (3rd) (m)	0.0825	0.0826	0.0815	0.0870	0.0943	0.0882
Rel Disp (4th) (m)	0.1115	0.1115	0.1093	0.1172	0.1302	0.1234
Rotation (1st)	-0.0086	-0.0085	-0.0086	-0.0090	-0.0106	-0.0098
Rotation (2nd)	-0.0114	-0.0113	-0.0111	-0.0116	-0.0128	-0.0123
Rotation (3rd)	-0.0104	-0.0103	-0.0100	-0.0106	-0.0135	-0.0123
Rotation (4th)	-0.0082	-0.0082	-0.0079	-0.0085	-0.0120	-0.0105
Base Shear (kN)	143.36	139.21	148.78	145.51	214.20	218.75
Base Moment node (kNm)	288.54	284.57	290.72	292.55	315.13	318.08
Ductility	2	2.1	1.9	1.8	4.6	4.4

Table 5-4 Comparison of results between N2 method and Nonlinear Dynamic Analyses, Kocaeli

N2															Nonlinear Dynamic	
Kocaeli	FEMA (1) _ EPP	FEMA (1) _ EPSH	FEMA (2) _ EPP	FEMA (2) _ EPSH	Uniform _ EPP	Uniform _ EPSH	Kunnath (1) _ EPP	Kunnath (1)_ EPSH	Kunnath (2) _ EPP	Kunnath (2) _ EPSH	Kunnath (3) _ EPP	Kunnath (3) _ EPSH	Kunnath (4) _ EPP	Kunnath (4) _ EPSH	EPP	EPSH
Rel Disp (1st) (m)	0.0162	0.0157	0.0158	0.0157	0.0175	0.0175	0.0131	0.0150	0.0163	0.0158	0.0153	0.0153	0.0271	0.0168	0.0221	0.0198
Rel Disp (2nd) (m)	0.0487	0.0475	0.0490	0.0487	0.0470	0.0470	0.0354	0.0400	0.0565	0.0555	0.0541	0.0539	0.0628	0.0443	0.0586	0.0542
Rel Disp (3rd) (m)	0.0837	0.0820	0.0866	0.0863	0.0742	0.0742	0.0545	0.0615	0.1083	0.1067	0.1047	0.1045	0.0874	0.0652	0.0943	0.0882
Rel Disp (4th) (m)	0.1137	0.1137	0.1203	0.1203	0.0943	0.0943	0.0678	0.0765	0.1589	0.1571	0.1549	0.1549	0.1001	0.0765	0.1302	0.1234
Rotation (1st)	-0.0087	-0.0085	-0.0087	-0.0086	-0.0086	-0.0086	-0.0066	-0.0074	-0.0096	-0.0094	-0.0091	-0.0091	-0.0117	-0.0083	-0.0106	-0.0098
Rotation (2nd)	-0.0115	-0.0113	-0.0121	-0.0121	-0.0096	-0.0096	-0.0070	-0.0078	-0.0158	-0.0156	-0.0153	-0.0153	-0.0102	-0.0083	-0.0128	-0.0123
Rotation (3rd)	-0.0107	-0.0106	-0.0118	-0.0119	-0.0076	-0.0076	-0.0051	-0.0057	-0.0172	-0.0171	-0.0170	-0.0170	-0.0056	-0.0049	-0.0135	-0.0123
Rotation (4th)	-0.0086	-0.0085	-0.0099	-0.0101	-0.0054	-0.0054	-0.0035	-0.0039	-0.0157	-0.0155	-0.0156	-0.0157	-0.0030	-0.0027	-0.0120	-0.0105
Base Shear (kN)	142.51	138.46	133.24	129.65	180.26	175.77	178.33	180.48	80.48	79.31	78.02	75.71	195.86	173.61	214.20	218.75
Base Moment node (kNm)	288.57	282.86	283.94	280.53	302.82	297.96	280.40	290.07	262.36	261.81	256.49	254.27	313.54	296.64	315.13	318.08
Ductility	1.9	2.1	2	2	1.7	1.7	1.1	1.3	2.3	2.4	2.4	2.5	1.3	1.4	4.6	4.4

Table 5-5 Comparison of results between N2 method and Nonlinear Dynamic Analyses, Kocaeli (continued)

N2				
Kocaeli	Mode Shape Distribution _ EPP	Mode Shape Distribution _ EPSH	Inverted Triangular Distribution _ EPP	Inverted Triangular Distribution _ EPSH
Rel Disp (1st) (m)	0.72	0.81	0.74	0.89
Rel Disp (2nd) (m)	0.82	0.89	0.82	0.95
Rel Disp (3rd) (m)	0.87	0.94	0.86	0.99
Rel Disp (4th) (m)	0.86	0.90	0.84	0.95
Rotation (1st)	0.81	0.87	0.81	0.91
Rotation (2nd)	0.89	0.91	0.87	0.94
Rotation (3rd)	0.77	0.84	0.74	0.86
Rotation (4th)	0.69	0.78	0.66	0.80
Base Shear (kN)	0.67	0.64	0.69	0.67
Base Moment node (kNm)	0.92	0.89	0.92	0.92
Ductility	0.43	0.47	0.41	0.41

Table 5-6 Comparison of normalised results between N2 method and Nonlinear Dynamic Analyses, Kocaeli

N2														
Kocaeli	FEMA (1) _ EPP	FEMA (1) _ EPSH	FEMA (2) _ EPP	FEMA (2) _ EPSH	Uniform _ EPP	Uniform _ EPSH	Kunnath (1) _ EPP	Kunnath (1)_ EPSH	Kunnath (2) _ EPP	Kunnath (2) _ EPSH	Kunnath (3) _ EPP	Kunnath (3) _ EPSH	Kunnath (4) _ EPP	Kunnath (4) _ EPSH
Rel Disp (1st) (m)	0.73	0.79	0.71	0.79	0.79	0.88	0.59	0.76	0.74	0.80	0.69	0.77	1.23	0.85
Rel Disp (2nd) (m)	0.83	0.88	0.84	0.90	0.80	0.87	0.60	0.74	0.96	1.02	0.92	0.99	1.07	0.82
Rel Disp (3rd) (m)	0.89	0.93	0.92	0.98	0.79	0.84	0.58	0.70	1.15	1.21	1.11	1.18	0.93	0.74
Rel Disp (4th) (m)	0.87	0.92	0.92	0.98	0.72	0.76	0.52	0.62	1.22	1.27	1.19	1.26	0.77	0.62
Rotation (1st)	0.82	0.86	0.81	0.87	0.81	0.87	0.62	0.76	0.90	0.95	0.86	0.92	1.10	0.84
Rotation (2nd)	0.90	0.92	0.94	0.98	0.75	0.78	0.54	0.63	1.23	1.27	1.19	1.24	0.80	0.67
Rotation (3rd)	0.79	0.86	0.87	0.96	0.56	0.62	0.37	0.46	1.27	1.39	1.26	1.38	0.41	0.39
Rotation (4th)	0.72	0.81	0.83	0.96	0.45	0.51	0.29	0.37	1.31	1.48	1.30	1.50	0.25	0.26
Base Shear (kN)	0.67	0.63	0.62	0.59	0.84	0.80	0.83	0.83	0.38	0.36	0.36	0.35	0.91	0.79
Base Moment node (kNm)	0.92	0.89	0.90	0.88	0.96	0.94	0.89	0.91	0.83	0.82	0.81	0.80	0.99	0.93
Ductility	0.41	0.47	0.43	0.45	0.37	0.39	0.24	0.30	0.50	0.55	0.52	0.57	0.28	0.32

Table 5-7 Comparison of normalised results between N2 method and Nonlinear Dynamic Analyses, Kocaeli (continued)

N2					Nonlinear Dynamic	
El Centro	Mode Shape Distribution _ EPP	Mode Shape Distribution _ EPSH	Inverted Triangular Distribution _ EPP	Inverted Triangular Distribution _ EPSH	EPP	EPSH
Rel Disp (1st) (m)	0.0064	0.0063	0.0066	0.0065	0.0160	0.0160
Rel Disp (2nd) (m)	0.0189	0.0189	0.0193	0.0193	0.0442	0.0446
Rel Disp (3rd) (m)	0.0315	0.0315	0.0320	0.0321	0.0737	0.0741
Rel Disp (4th) (m)	0.0414	0.0414	0.0419	0.0421	0.0997	0.0998
Rotation (1st)	-0.0034	-0.0034	-0.0035	-0.0033	-0.0080	-0.0081
Rotation (2nd)	-0.0042	-0.0042	-0.0042	-0.0040	-0.0102	-0.0102
Rotation (3rd)	-0.0036	-0.0036	-0.0036	-0.0034	-0.0099	-0.0098
Rotation (4th)	-0.0027	-0.0027	-0.0027	-0.0025	-0.0084	-0.0082
Base Shear (kN)	85.26	82.94	90.09	86.01	198.92	199.29
Base Moment node (kNm)	144.18	142.04	149.81	146.25	316.41	322.08
Ductility	0.7	0.8	0.7	0.7	3.7	3.7

Table 5-8 Comparison of results between N2 method and Nonlinear Dynamic Analyses, El Centro

N2											Nonlinear Dynamic	
El Centro	FEMA (1) _ EPP	FEMA (1) _ EPSH	FEMA (2) _ EPP	FEMA (2) _ EPSH	Uniform _ EPP	Uniform _ EPSH	Kunnath (1) _ EPP	Kunnath (1)_ EPSH	Kunnath (4) _ EPP	Kunnath (4) _ EPSH	EPP	EPSH
Rel Disp (1st) (m)	0.0063	0.0063	0.0069	0.0069	0.0064	0.0064	0.0060	0.0064	0.0077	0.0077	0.0160	0.0160
Rel Disp (2nd) (m)	0.0186	0.0188	0.0209	0.0209	0.0178	0.0178	0.0154	0.0164	0.0201	0.0202	0.0442	0.0446
Rel Disp (3rd) (m)	0.0311	0.0314	0.0357	0.0356	0.0281	0.0281	0.0226	0.0241	0.0267	0.0268	0.0737	0.0741
Rel Disp (4th) (m)	0.0410	0.0414	0.0477	0.0477	0.0358	0.0358	0.0274	0.0292	0.0267	0.0268	0.0997	0.0998
Rotation (1st)	-0.0084	-0.0027	-0.0037	-0.0037	-0.0032	-0.0032	-0.0029	-0.0031	-0.0038	-0.0039	-0.0080	-0.0081
Rotation (2nd)	-0.0105	-0.0036	-0.0048	-0.0048	-0.0036	-0.0036	-0.0027	-0.0029	-0.0033	-0.0033	-0.0102	-0.0102
Rotation (3rd)	-0.0091	-0.0041	-0.0043	-0.0043	-0.0028	-0.0028	-0.0018	-0.0019	-0.0008	-0.0008	-0.0099	-0.0098
Rotation (4th)	-0.0067	-0.0033	-0.0033	-0.0033	-0.0020	-0.0020	-0.0012	-0.0013	0.0004	0.0004	-0.0084	-0.0082
Base Shear (kN)	83.67	84.49	88.00	87.92	98.51	98.48	107.42	114.31	120.54	120.67	198.92	199.29
Base Moment node (kNm)	141.41	142.88	153.86	153.78	151.00	150.97	150.01	159.70	182.43	182.86	316.41	322.08
Ductility	0.7	0.8	0.8	0.8	0.65	0.65	0.5	0.6	0.6	0.7	3.7	3.7

Table 5-9 Comparison of results between N2 method and Nonlinear Dynamic Analyses, El Centro (continued)

N2				
El Centro	Mode Shape Distribution _ EPP	Mode Shape Distribution _ EPSH	Inverted Triangular Distribution _ EPP	Inverted Triangular Distribution _ EPSH
Rel Disp (1st) (m)	0.40	0.40	0.41	0.41
Rel Disp (2nd) (m)	0.43	0.42	0.44	0.43
Rel Disp (3rd) (m)	0.43	0.43	0.43	0.43
Rel Disp (4th) (m)	0.42	0.42	0.42	0.42
Rotation (1st)	0.42	0.42	0.43	0.40
Rotation (2nd)	0.41	0.41	0.41	0.39
Rotation (3rd)	0.36	0.37	0.36	0.35
Rotation (4th)	0.31	0.32	0.32	0.31
Base Shear (kN)	0.43	0.42	0.45	0.43
Base Moment node (kNm)	0.46	0.44	0.47	0.45
Ductility	0.19	0.22	0.19	0.19

Table 5-10 Comparison of normalised results between N2 method and Nonlinear Dynamic Analyses, El Centro

N2										
El Centro	FEMA (1) _ EPP	FEMA (1) _ EPSH	FEMA (2) _ EPP	FEMA (2) _ EPSH	Uniform _ EPP	Uniform _ EPSH	Kunnath (1) _ EPP	Kunnath (1)_ EPSH	Kunnath (4) _ EPP	Kunnath (4) _ EPSH
Rel Disp (1st) (m)	0.39	0.39	0.43	0.43	0.40	0.40	0.38	0.40	0.48	0.50
Rel Disp (2nd) (m)	0.42	0.42	0.47	0.47	0.40	0.40	0.35	0.37	0.45	0.47
Rel Disp (3rd) (m)	0.42	0.42	0.48	0.48	0.38	0.38	0.31	0.33	0.36	0.37
Rel Disp (4th) (m)	0.41	0.42	0.48	0.48	0.36	0.36	0.27	0.29	0.27	0.27
Rotation (1st)	1.05	0.33	0.46	0.46	0.40	0.40	0.36	0.38	0.48	0.50
Rotation (2nd)	1.04	0.35	0.47	0.47	0.35	0.35	0.27	0.28	0.32	0.33
Rotation (3rd)	0.93	0.42	0.44	0.44	0.29	0.29	0.19	0.20	0.09	0.09
Rotation (4th)	0.80	0.41	0.39	0.40	0.24	0.25	0.15	0.16	-0.04	-0.04
Base Shear (kN)	0.42	0.42	0.44	0.44	0.50	0.49	0.54	0.57	0.61	0.63
Base Moment node (kNm)	0.45	0.44	0.49	0.48	0.48	0.47	0.47	0.50	0.58	0.59
Ductility	0.19	0.22	0.22	0.22	0.18	0.18	0.14	0.16	0.16	0.19

Table 5-11 Comparison of normalised results between N2 method and Nonlinear Dynamic Analyses, El Centro (continued)

DCM					Nonlinear Dynamic	
Kocaeli	Mode Shape Distribution _ EPP	Mode Shape Distribution _ EPSH	Inverted Triangular Distribution _ EPP	Inverted Triangular Distribution _ EPSH	EPP	EPSH
Rel Disp (1st) (m)	0.0162	0.0160	0.0163	0.0160	0.0221	0.0198
Rel Disp (2nd) (m)	0.0484	0.0481	0.0481	0.0473	0.0586	0.0542
Rel Disp (3rd) (m)	0.0827	0.0824	0.0815	0.0804	0.0943	0.0882
Rel Disp (4th) (m)	0.1115	0.1115	0.1093	0.1080	0.1302	0.1234
Rotation (1st)	-0.0086	-0.0085	-0.0086	-0.0083	-0.0106	-0.0098
Rotation (2nd)	-0.0114	-0.0113	-0.0111	-0.0108	-0.0128	-0.0123
Rotation (3rd)	-0.0104	-0.0103	-0.0100	-0.0098	-0.0135	-0.0123
Rotation (4th)	-0.0082	-0.0082	-0.0079	-0.0077	-0.0120	-0.0105
Base Shear (kN)	143.35	139.21	148.78	144.59	214.20	218.75
Base Moment node (kNm)	288.54	284.52	290.72	285.57	315.13	318.08
Ductility	2	2.1	1.9	1.8	4.6	4.4

Table 5-12 Comparison of results between DCM method and Nonlinear Dynamic Analyses, Kocaeli

DCM															Nonlinear Dynamic	
Kocaeli	FEMA (1) _ EPP	FEMA (1) _ EPSH	FEMA (2) _ EPP	FEMA (2) _ EPSH	Uniform _ EPP	Uniform _ EPSH	Kunnath (1) _ EPP	Kunnath (1)_ EPSH	Kunnath (2) _ EPP	Kunnath (2) _ EPSH	Kunnath (3) _ EPP	Kunnath (3) _ EPSH	Kunnath (4) _ EPP	Kunnath (4) _ EPSH	EPP	EPSH
Rel Disp (1st) (m)	0.0162	0.0154	0.0158	0.0157	0.0175	0.0175	0.0131	0.0150	0.0165	0.0158	0.0153	0.0153	0.0271	0.0168	0.0221	0.0198
Rel Disp (2nd) (m)	0.0487	0.0467	0.0490	0.0487	0.0470	0.0470	0.0354	0.0400	0.0571	0.0555	0.0541	0.0539	0.0628	0.0443	0.0586	0.0542
Rel Disp (3rd) (m)	0.0837	0.0805	0.0866	0.0863	0.0742	0.0742	0.0545	0.0615	0.1094	0.1067	0.1047	0.1045	0.0874	0.0652	0.0943	0.0882
Rel Disp (4th) (m)	0.1137	0.1093	0.1203	0.1203	0.0943	0.0943	0.0678	0.0765	0.1605	0.1571	0.1549	0.1549	0.1001	0.0765	0.1302	0.1234
Rotation (1st)	-0.0087	-0.0083	-0.0087	-0.0086	-0.0086	-0.0086	-0.0066	-0.0074	-0.0097	-0.0094	-0.0091	-0.0091	-0.0117	-0.0083	-0.0106	-0.0098
Rotation (2nd)	-0.0115	-0.0111	-0.0121	-0.0121	-0.0096	-0.0096	-0.0070	-0.0078	-0.0159	-0.0156	-0.0153	-0.0153	-0.0102	-0.0083	-0.0128	-0.0123
Rotation (3rd)	-0.0107	-0.0103	-0.0118	-0.0119	-0.0076	-0.0076	-0.0051	-0.0057	-0.0174	-0.0171	-0.0170	-0.0170	-0.0056	-0.0049	-0.0135	-0.0123
Rotation (4th)	-0.0086	-0.0083	-0.0099	-0.0101	-0.0054	-0.0054	-0.0035	-0.0039	-0.0158	-0.0156	-0.0156	-0.0157	-0.0030	-0.0027	-0.0120	-0.0105
Base Shear (kN)	142.51	138.96	133.24	129.67	180.26	175.77	178.33	180.48	80.47	79.31	78.02	75.71	195.86	173.61	214.20	218.75
Base Moment node (kNm)	288.57	281.49	283.94	280.57	302.82	297.96	280.40	290.07	263.49	261.81	256.49	254.27	313.54	296.64	315.13	318.08
Ductility	1.9	2.1	2	2	1.7	1.7	1.1	1.3	2.4	2.4	2.4	2.5	1.3	1.4	4.6	4.4

Table 5-13 Comparison of results between DCM method and Nonlinear Dynamic Analyses, Kocaeli (continued)

DCM				
Kocaeli	Mode Shape Distribution _ EPP	Mode Shape Distribution _ EPSH	Inverted Triangular Distribution _ EPP	Inverted Triangular Distribution _ EPSH
Rel Disp (1st) (m)	0.73	0.81	0.74	0.81
Rel Disp (2nd) (m)	0.83	0.89	0.82	0.87
Rel Disp (3rd) (m)	0.88	0.93	0.86	0.91
Rel Disp (4th) (m)	0.86	0.90	0.84	0.88
Rotation (1st)	0.81	0.87	0.81	0.85
Rotation (2nd)	0.89	0.91	0.87	0.88
Rotation (3rd)	0.77	0.84	0.74	0.79
Rotation (4th)	0.69	0.78	0.66	0.73
Base Shear (kN)	0.67	0.64	0.69	0.66
Base Moment node (kNm)	0.92	0.89	0.92	0.90
Ductility	0.43	0.47	0.41	0.41

Table 5-14 Comparison of normalised results between DCM method and Nonlinear Dynamic Analyses, Kocaeli

DCM														
Kocaeli	FEMA (1) _ EPP	FEMA (1) _ EPSH	FEMA (2) _ EPP	FEMA (2) _ EPSH	Uniform _ EPP	Uniform _ EPSH	Kunnath (1) _ EPP	Kunnath (1)_ EPSH	Kunnath (2) _ EPP	Kunnath (2) _ EPSH	Kunnath (3) _ EPP	Kunnath (3) _ EPSH	Kunnath (4) _ EPP	Kunnath (4) _ EPSH
Rel Disp (1st) (m)	0.73	0.78	0.71	0.79	0.79	0.88	0.59	0.76	0.75	0.80	0.69	0.77	1.23	0.85
Rel Disp (2nd) (m)	0.83	0.86	0.84	0.90	0.80	0.87	0.60	0.74	0.98	1.02	0.92	0.99	1.07	0.82
Rel Disp (3rd) (m)	0.89	0.91	0.92	0.98	0.79	0.84	0.58	0.70	1.16	1.21	1.11	1.18	0.93	0.74
Rel Disp (4th) (m)	0.87	0.89	0.92	0.98	0.72	0.76	0.52	0.62	1.23	1.27	1.19	1.26	0.77	0.62
Rotation (1st)	0.82	0.85	0.81	0.87	0.81	0.87	0.62	0.76	0.91	0.95	0.86	0.92	1.10	0.84
Rotation (2nd)	0.90	0.90	0.94	0.98	0.75	0.78	0.54	0.63	1.24	1.26	1.19	1.24	0.80	0.67
Rotation (3rd)	0.79	0.84	0.87	0.96	0.56	0.62	0.37	0.46	1.29	1.39	1.26	1.38	0.41	0.39
Rotation (4th)	0.72	0.79	0.83	0.96	0.45	0.51	0.29	0.37	1.32	1.49	1.30	1.50	0.25	0.26
Base Shear (kN)	0.67	0.64	0.62	0.59	0.84	0.80	0.83	0.83	0.38	0.36	0.36	0.35	0.91	0.79
Base Moment node (kNm)	0.92	0.88	0.90	0.88	0.96	0.94	0.89	0.91	0.84	0.82	0.81	0.80	0.99	0.93
Ductility	0.41	0.47	0.43	0.45	0.37	0.39	0.24	0.30	0.52	0.55	0.52	0.57	0.28	0.32

Table 5-15 Comparison of normalised results between N2 method and Nonlinear Dynamic Analyses, Kocaeli (continued)

DCM					Nonlinear Dynamic	
El Centro	Mode Shape Distribution _ EPP	Mode Shape Distribution _ EPSH	Inverted Triangular Distribution _ EPP	Inverted Triangular Distribution _ EPSH	EPP	EPSH
Rel Disp (1st) (m)	0.0064	0.0063	0.0066	0.0065	0.0160	0.0160
Rel Disp (2nd) (m)	0.0189	0.0189	0.0193	0.0193	0.0442	0.0446
Rel Disp (3rd) (m)	0.0315	0.0315	0.0320	0.0321	0.0737	0.0741
Rel Disp (4th) (m)	0.0414	0.0414	0.0419	0.0421	0.0997	0.0998
Rotation (1st)	-0.0034	-0.0034	-0.0035	-0.0033	-0.0080	-0.0081
Rotation (2nd)	-0.0042	-0.0042	-0.0042	-0.0040	-0.0102	-0.0102
Rotation (3rd)	-0.0036	-0.0036	-0.0036	-0.0034	-0.0099	-0.0098
Rotation (4th)	-0.0027	-0.0027	-0.0027	-0.0025	-0.0084	-0.0082
Base Shear (kN)	85.26	82.94	90.09	86.01	198.92	199.29
Base Moment node (kNm)	144.18	142.04	149.81	146.25	316.41	322.08
Ductility	0.7	0.8	0.7	0.7	3.7	3.7

Table 5-16 Comparison of results between DCM method and Nonlinear Dynamic Analyses, El Centro

DCM											Nonlinear Dynamic	
El Centro	FEMA (1) _ EPP	FEMA (1) _ EPSH	FEMA (2) _ EPP	FEMA (2) _ EPSH	Uniform _ EPP	Uniform _ EPSH	Kunnath (1) _ EPP	Kunnath (1)_ EPSH	Kunnath (4) _ EPP	Kunnath (4) _ EPSH	EPP	EPSH
Rel Disp (1st) (m)	0.0063	0.0064	0.0069	0.0069	0.0064	0.0064	0.0062	0.0066	0.0077	0.0080	0.0160	0.0160
Rel Disp (2nd) (m)	0.0186	0.0190	0.0209	0.0209	0.0178	0.0178	0.0159	0.0171	0.0202	0.0209	0.0442	0.0446
Rel Disp (3rd) (m)	0.0311	0.0318	0.0357	0.0356	0.0281	0.0281	0.0233	0.0250	0.0268	0.0277	0.0737	0.0741
Rel Disp (4th) (m)	0.0410	0.0419	0.0477	0.0477	0.0358	0.0358	0.0282	0.0303	0.0268	0.0268	0.0997	0.0998
Rotation (1st)	-0.0084	-0.0034	-0.0037	-0.0037	-0.0032	-0.0032	-0.0030	-0.0032	-0.0039	-0.0040	-0.0080	-0.0081
Rotation (2nd)	-0.0105	-0.0042	-0.0048	-0.0048	-0.0036	-0.0036	-0.0028	-0.0030	-0.0033	-0.0034	-0.0102	-0.0102
Rotation (3rd)	-0.0091	-0.0037	-0.0043	-0.0043	-0.0028	-0.0028	-0.0019	-0.0020	-0.0008	-0.0009	-0.0099	-0.0098
Rotation (4th)	-0.0067	-0.0027	-0.0033	-0.0033	-0.0020	-0.0020	-0.0013	-0.0014	0.0004	0.0004	-0.0084	-0.0082
Base Shear (kN)	83.67	85.44	88.00	87.92	98.51	98.48	110.38	118.45	120.97	124.66	198.92	199.29
Base Moment node (kNm)	141.41	144.56	153.86	153.78	151.00	150.97	154.15	165.57	183.09	189.01	316.41	322.08
Ductility	0.7	0.8	0.8	0.8	0.65	0.65	0.5	0.6	0.6	0.7	3.7	3.7

Table 5-17 Comparison of results between DCM method and Nonlinear Dynamic Analyses, El Centro (continued)

DCM				
El Centro	Mode Shape Distribution _ EPP	Mode Shape Distribution _ EPSH	Inverted Triangular Distribution _ EPP	Inverted Triangular Distribution _ EPSH
Rel Disp (1st) (m)	0.40	0.40	0.41	0.41
Rel Disp (2nd) (m)	0.43	0.42	0.44	0.43
Rel Disp (3rd) (m)	0.43	0.43	0.43	0.43
Rel Disp (4th) (m)	0.42	0.42	0.42	0.42
Rotation (1st)	0.42	0.42	0.43	0.40
Rotation (2nd)	0.41	0.41	0.41	0.39
Rotation (3rd)	0.36	0.37	0.36	0.35
Rotation (4th)	0.31	0.32	0.32	0.31
Base Shear (kN)	0.43	0.42	0.45	0.43
Base Moment node (kNm)	0.46	0.44	0.47	0.45
Ductility	0.19	0.22	0.19	0.19

Table 5-18 Comparison of normalised results between DCM method and Nonlinear Dynamic Analyses, El Centro

DCM										
El Centro	FEMA (1) _ EPP	FEMA (1) _ EPSH	FEMA (2) _ EPP	FEMA (2) _ EPSH	Uniform _ EPP	Uniform _ EPSH	Kunnath (1) _ EPP	Kunnath (1)_ EPSH	Kunnath (4) _ EPP	Kunnath (4) _ EPSH
Rel Disp (1st) (m)	0.39	0.40	0.43	0.43	0.40	0.40	0.39	0.41	0.48	0.50
Rel Disp (2nd) (m)	0.42	0.43	0.47	0.47	0.40	0.40	0.36	0.38	0.46	0.47
Rel Disp (3rd) (m)	0.42	0.43	0.48	0.48	0.38	0.38	0.32	0.34	0.36	0.37
Rel Disp (4th) (m)	0.41	0.42	0.48	0.48	0.36	0.36	0.28	0.30	0.27	0.27
Rotation (1st)	1.05	0.42	0.46	0.46	0.40	0.40	0.37	0.40	0.48	0.50
Rotation (2nd)	1.04	0.41	0.47	0.47	0.35	0.35	0.27	0.29	0.32	0.33
Rotation (3rd)	0.93	0.37	0.44	0.44	0.29	0.29	0.19	0.21	0.09	0.09
Rotation (4th)	0.80	0.33	0.39	0.40	0.24	0.25	0.15	0.17	-0.04	-0.04
Base Shear (kN)	0.42	0.43	0.44	0.44	0.50	0.49	0.55	0.59	0.61	0.63
Base Moment node (kNm)	0.45	0.45	0.49	0.48	0.48	0.47	0.49	0.51	0.58	0.59
Ductility	0.19	0.22	0.22	0.22	0.18	0.18	0.14	0.16	0.16	0.19

Table 5-19 Comparison of normalised results between N2 method and Nonlinear Dynamic Analyses, El Centro (continued)

MPA					Nonlinear Dynamic	
Kocaeli	4-modes_ EPP	4-modes _ EPSH	2-modes_ EPP	2-modes _ EPSH	EPP	EPSH
Rel Disp (1st) (m)	0.0178	0.0168	0.0168	0.0167	0.0221	0.0198
Rel Disp (2nd) (m)	0.0512	0.0489	0.0490	0.0487	0.0586	0.0542
Rel Disp (3rd) (m)	0.0892	0.0830	0.0827	0.0825	0.0943	0.0882
Rel Disp (4th) (m)	0.1288	0.1134	0.1118	0.1119	0.1302	0.1234
Rotation (1st)	0.0092	0.0088	0.0088	0.0087	-0.0106	-0.0098
Rotation (2nd)	0.0120	0.0113	0.0114	0.0113	-0.0128	-0.0123
Rotation (3rd)	0.0136	0.0111	0.0108	0.0107	-0.0135	-0.0123
Rotation (4th)	0.0134	0.0095	0.0088	0.0089	-0.0120	-0.0105
Base Shear (kN)	234.63	190.37	187.24	182.22	214.20	218.75
Base Moment node (kNm)	427.93	319.16	394.30	313.32	315.13	318.08
Ductility	2.4	2.1	2.0	2.1	4.6	4.4

Table 5-20 Comparison of results between MPA method and Nonlinear Dynamic Analyses, Kocaeli

MPA				
Kocaeli	4-modes_ EPP	4-modes _ EPSH	2-modes_ EPP	2-modes _ EPSH
Rel Disp (1st) (m)	0.80	0.85	0.76	0.84
Rel Disp (2nd) (m)	0.87	0.90	0.84	0.90
Rel Disp (3rd) (m)	0.95	0.94	0.88	0.93
Rel Disp (4th) (m)	0.99	0.92	0.86	0.91
Rotation (1st)	-0.86	-0.89	-0.83	-0.88
Rotation (2nd)	-0.94	-0.92	-0.89	-0.91
Rotation (3rd)	-1.01	-0.90	-0.80	-0.87
Rotation (4th)	-1.12	-0.91	-0.73	-0.85
Base Shear (kN)	1.10	0.87	0.87	0.83
Base Moment node (kNm)	1.36	1.00	1.25	0.99
Ductility	0.51	0.49	0.44	0.48

Table 5-21 Comparison of normalised results between MPA method and Nonlinear Dynamic Analyses, Kocaeli

MPA					Nonlinear Dynamic	
El Centro	4-modes_ EPP	4-modes _ EPSH	2-modes_ EPP	2-modes _ EPSH	EPP	EPSH
Rel Disp (1st) (m)	0.0091	0.0084	0.0088	0.0083	0.0160	0.0160
Rel Disp (2nd) (m)	0.0221	0.0210	0.0215	0.0209	0.0442	0.0446
Rel Disp (3rd) (m)	0.0332	0.0319	0.0317	0.0316	0.0737	0.0741
Rel Disp (4th) (m)	0.0468	0.0435	0.0428	0.0428	0.0997	0.0998
Rotation (1st)	0.0042	0.0040	0.0042	0.0040	-0.0080	-0.0081
Rotation (2nd)	0.0043	0.0042	0.0042	0.0042	-0.0102	-0.0102
Rotation (3rd)	0.0057	0.0051	0.0052	0.0050	-0.0099	-0.0098
Rotation (4th)	0.0057	0.0050	0.0050	0.0048	-0.0084	-0.0082
Base Shear (kN)	188.91	163.90	179.72	162.17	198.92	199.29
Base Moment node (kNm)	386.01	216.86	380.60	215.28	316.41	322.08
Ductility	0.9	0.9	0.8	0.9	3.7	3.7

Table 5-22 Comparison of results between MPA method and Nonlinear Dynamic Analyses, El Centro

MPA				
El Centro	4-modes_ EPP	4-modes _ EPSH	2-modes_ EPP	2-modes _ EPSH
Rel Disp (1st) (m)	0.57	0.52	0.55	0.52
Rel Disp (2nd) (m)	0.50	0.47	0.49	0.47
Rel Disp (3rd) (m)	0.45	0.43	0.43	0.43
Rel Disp (4th) (m)	0.47	0.44	0.43	0.43
Rotation (1st)	-0.53	-0.49	-0.52	-0.49
Rotation (2nd)	-0.42	-0.41	-0.41	-0.41
Rotation (3rd)	-0.58	-0.52	-0.53	-0.51
Rotation (4th)	-0.67	-0.60	-0.59	-0.59
Base Shear (kN)	0.95	0.82	0.90	0.81
Base Moment node (kNm)	1.22	0.67	1.20	0.67
Ductility	0.23	0.25	0.22	0.24

Table 5-23 Comparison of normalised results between MPA method and Nonlinear Dynamic Analyses, El Centro

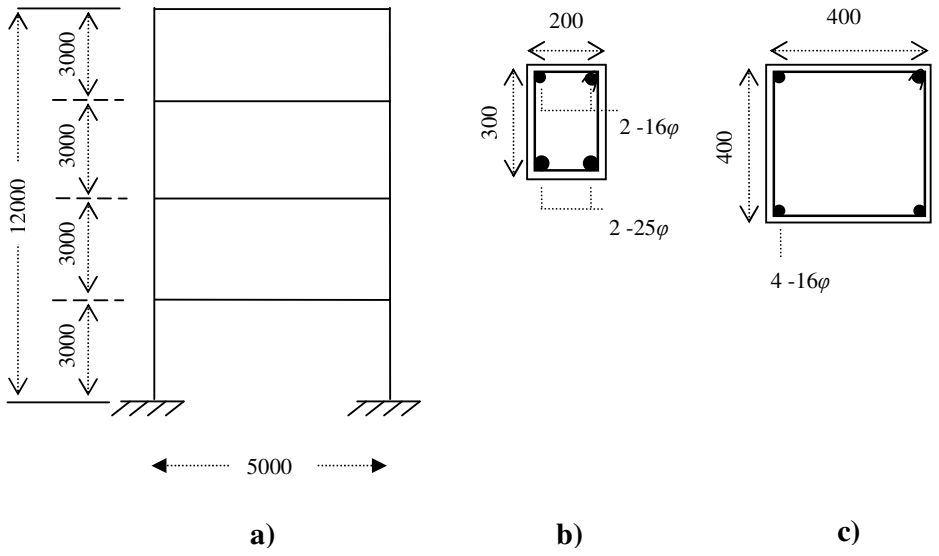

Figure 5-1 4-storey RC frame: a) elevation; b) beam cross-section; c) column cross-section. All dimensions in mm.

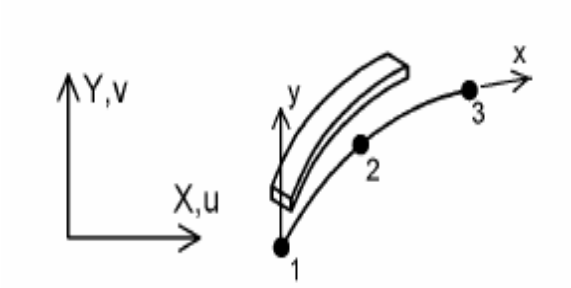

Figure 5-2 - 2D Kirchhoff thin beam element with quadrilateral cross-section

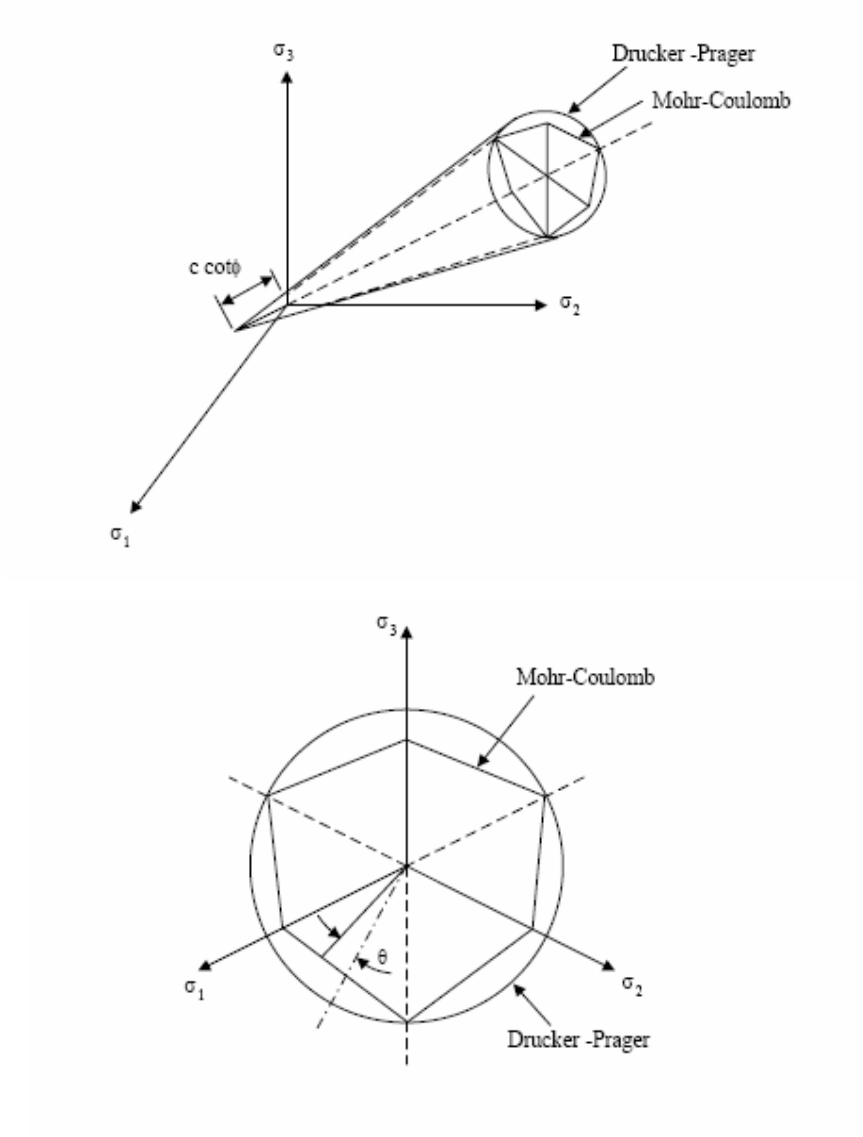

Figure 5-3 Drucker-Prager criterion

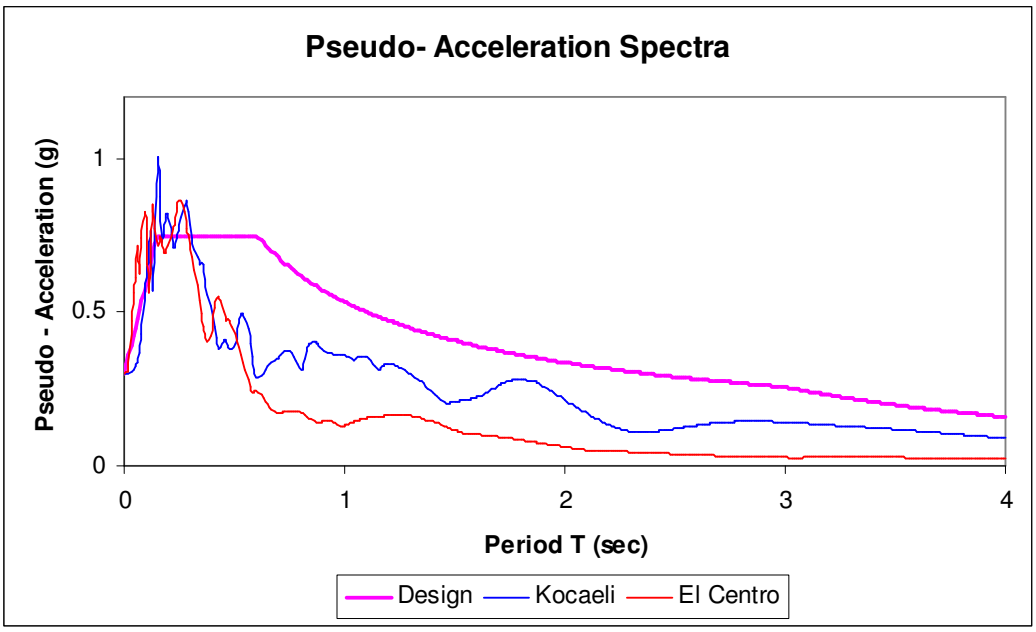

Figure 5-4 Comparison of the Elastic Design Acceleration spectrum with the Kocaeli and El Centro Acceleration spectra

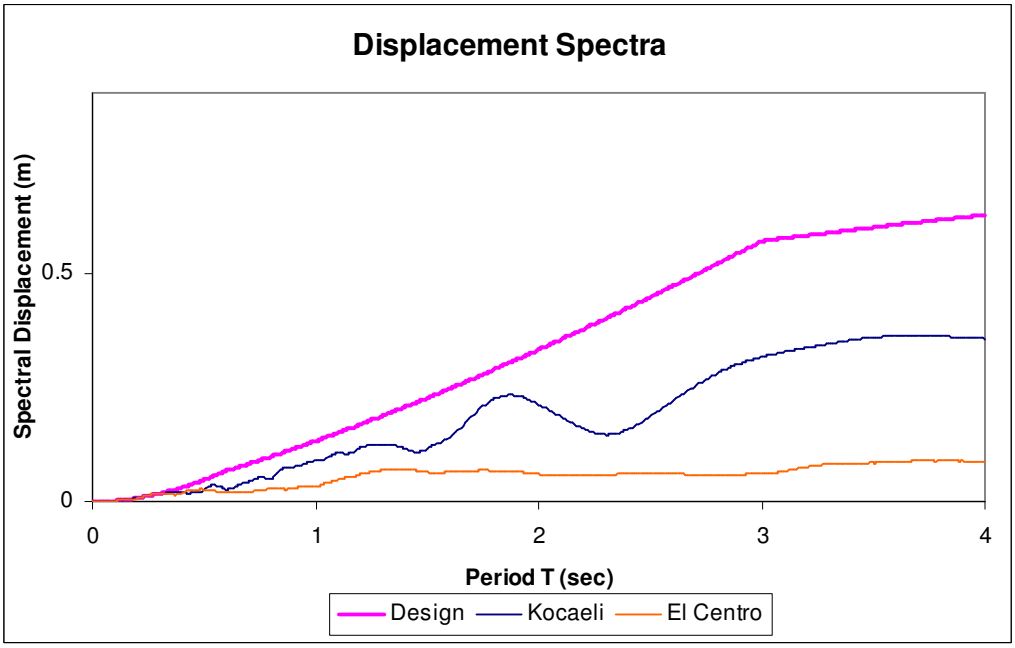

Figure 5-5 Comparison of the Elastic Design Displacement spectrum with the Kocaeli and El Centro Displacement spectra

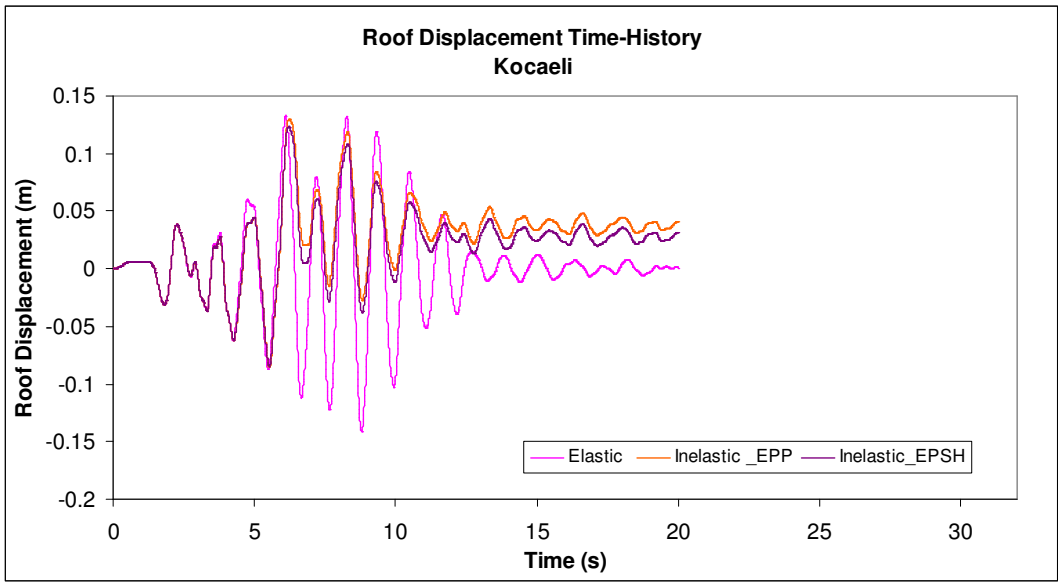

Figure 5-6 Elastic/Inelastic Displacement Time histories of the roof for EPP and EPSH models, Kocaeli ground motion

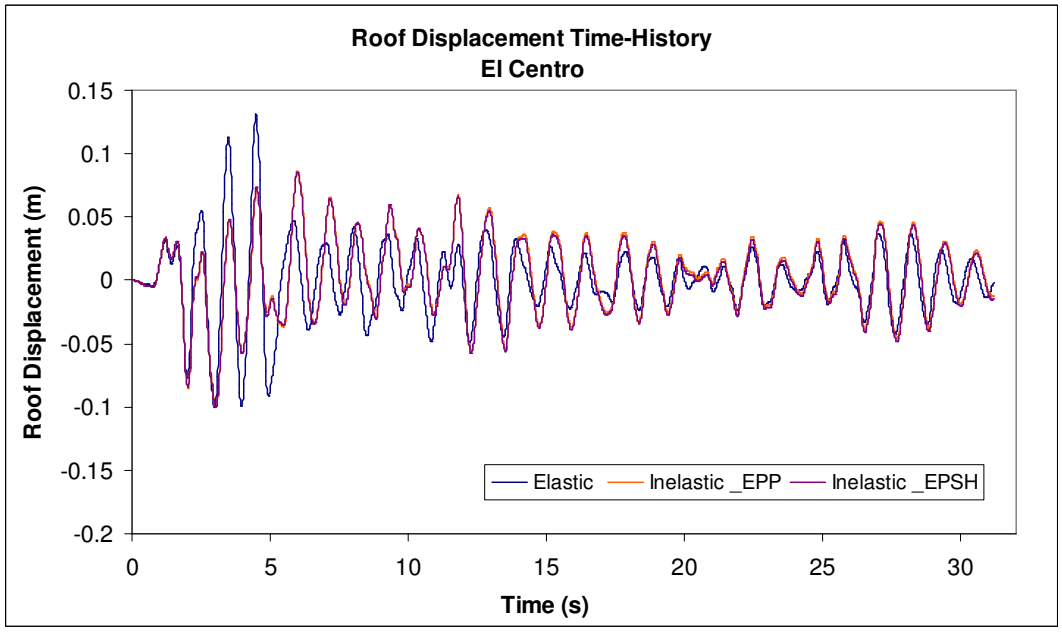

Figure 5-7 Elastic/Inelastic Displacement Time histories of the roof for EPP and EPSH models with and without P- delta effects (El Centro ground motion)

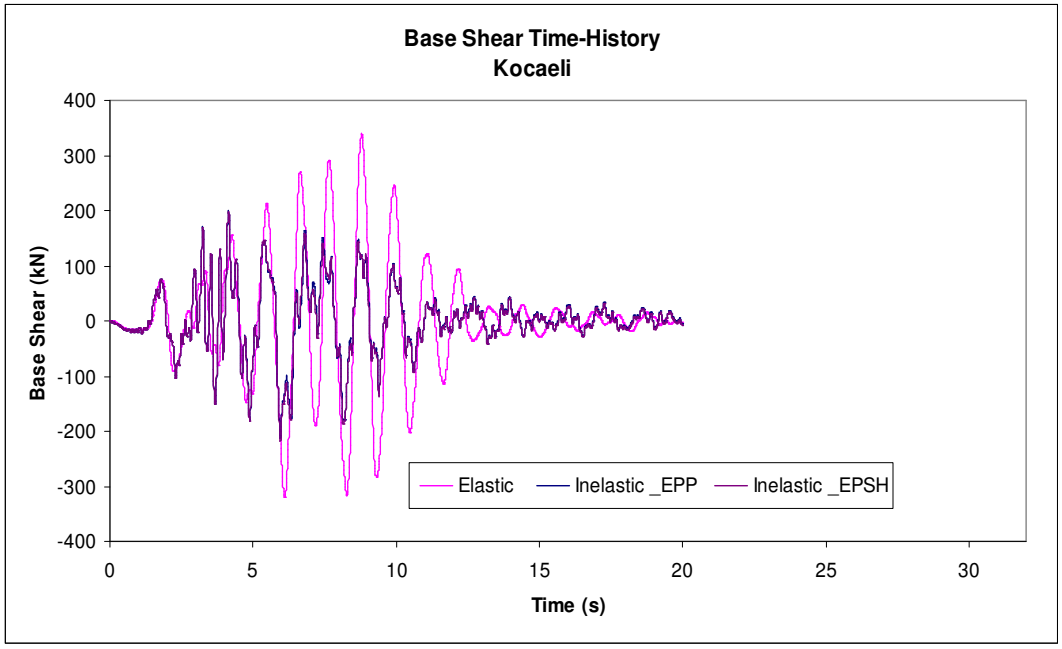

Figure 5-8 Elastic/Inelastic Base Shear Time histories for EPP and EPSH models Kocaeli ground motion)

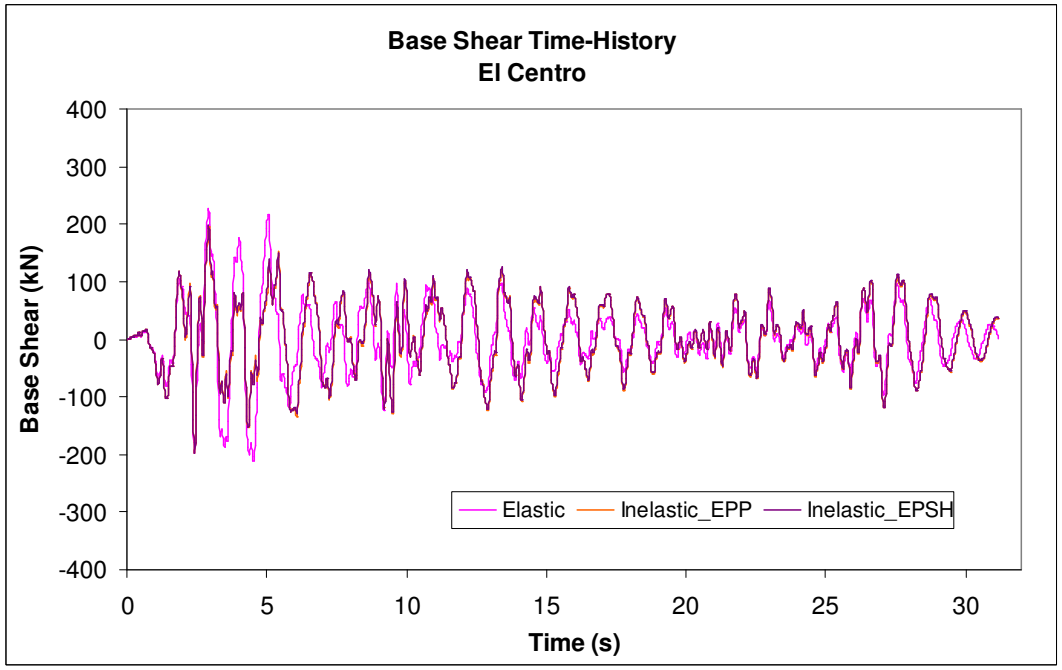

Figure 5-9 Elastic/Inelastic Base Shear Time histories for EPP and EPSH models with and without P- delta effects (El Centro ground motion)

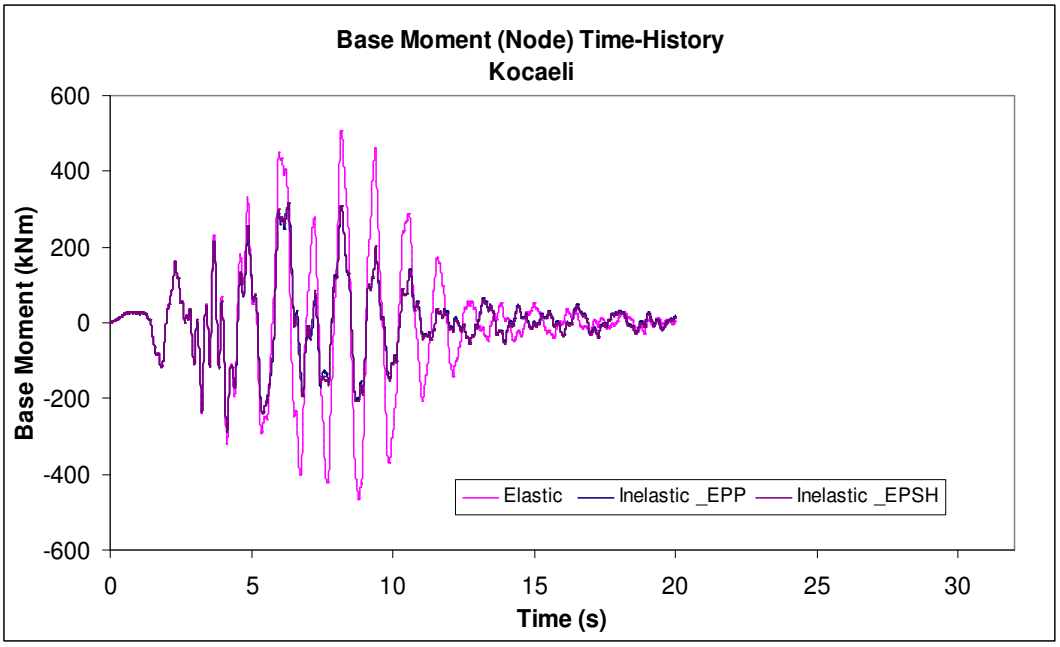

Figure 5-10 Elastic/Inelastic Base Moment (right-end node) Time histories for EPP and EPSH models with and without P- delta effects (Kocaeli ground motion)

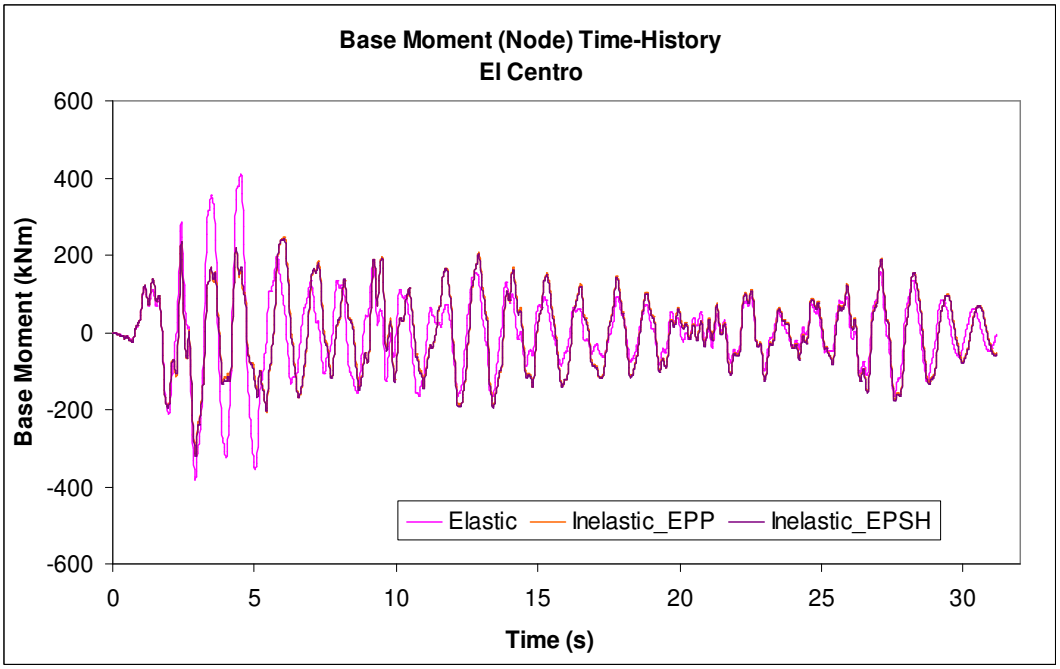

Figure 5-11 Elastic/Inelastic Base Moment (right-end node) Time histories for EPP and EPSH models, El Centro ground motion

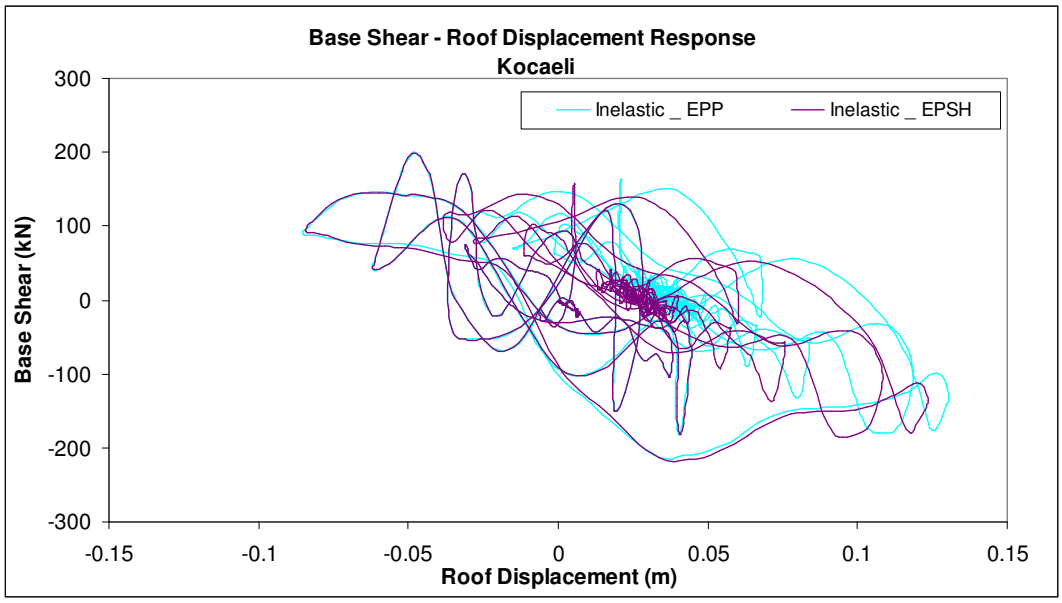

Figure 5-12 Typical inelastic base shear-roof displacement response of 4-storey frame for EPP and EPSH models with and without P- delta effects (Kocaeli ground motion)

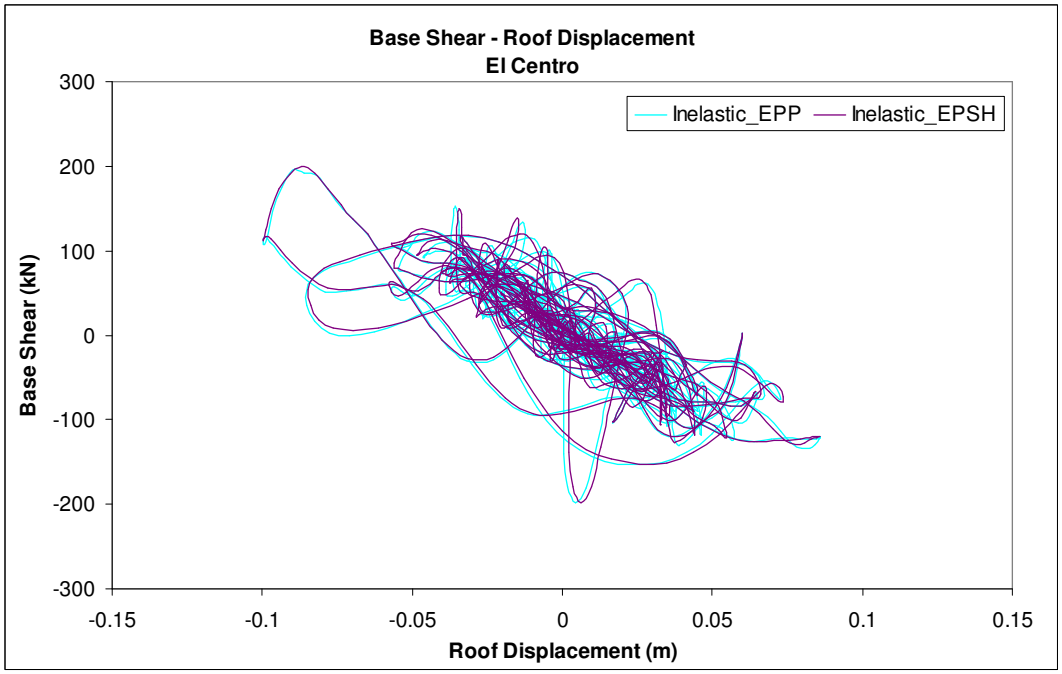

Figure 5-13 Typical inelastic base shear-roof displacement response of 4-storey frame for EPP and EPSH models with and without P- delta effects (El Centro ground motion)

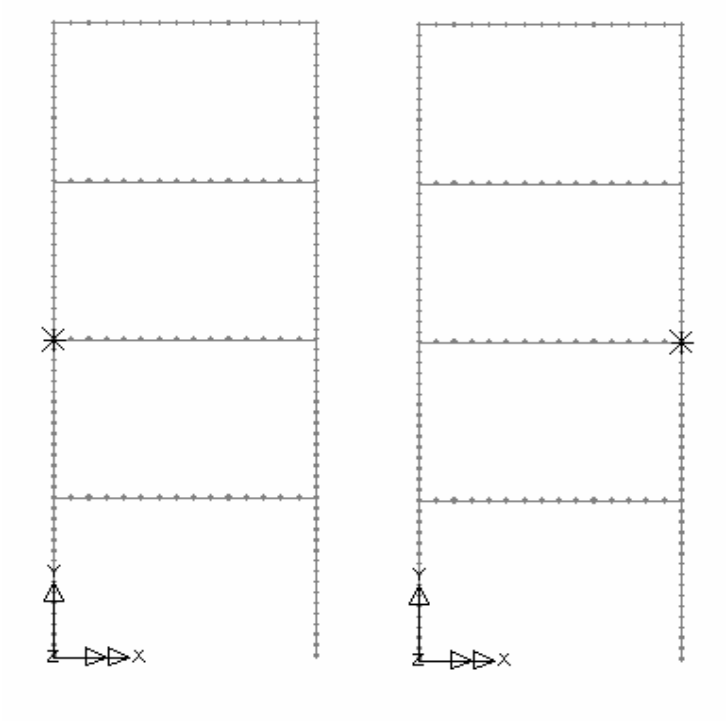

(a) **(b)**

Figure 5-14 1st hinge formation for (a) El Centro & (b) Kocaeli ground motions

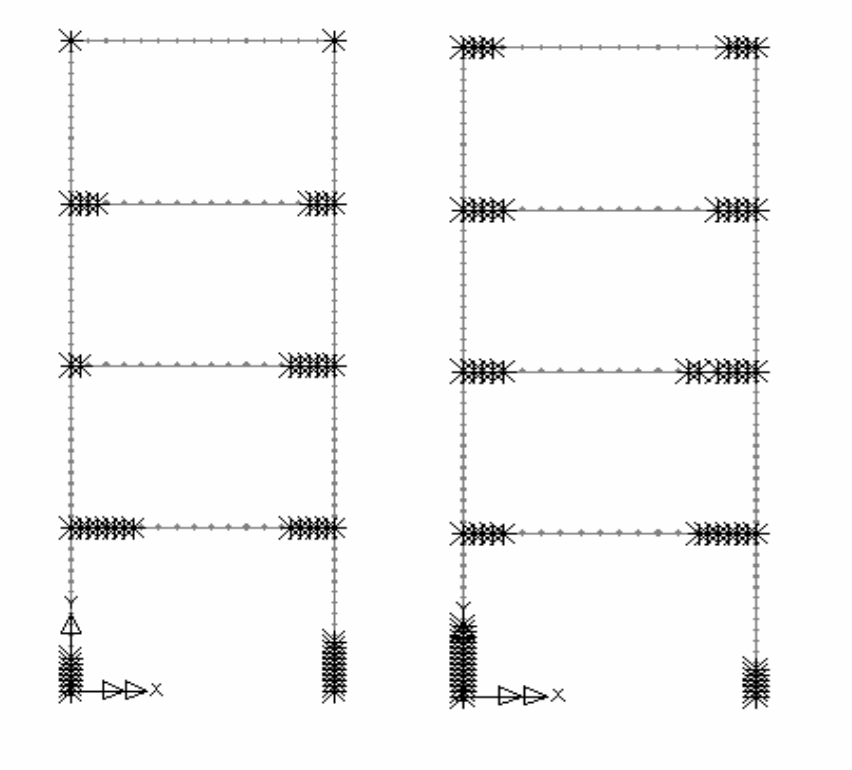

(a) **(b)**

Figure 5-15 Plastic hinges at collapse for (a) El Centro and (b) Kocaeli ground motions

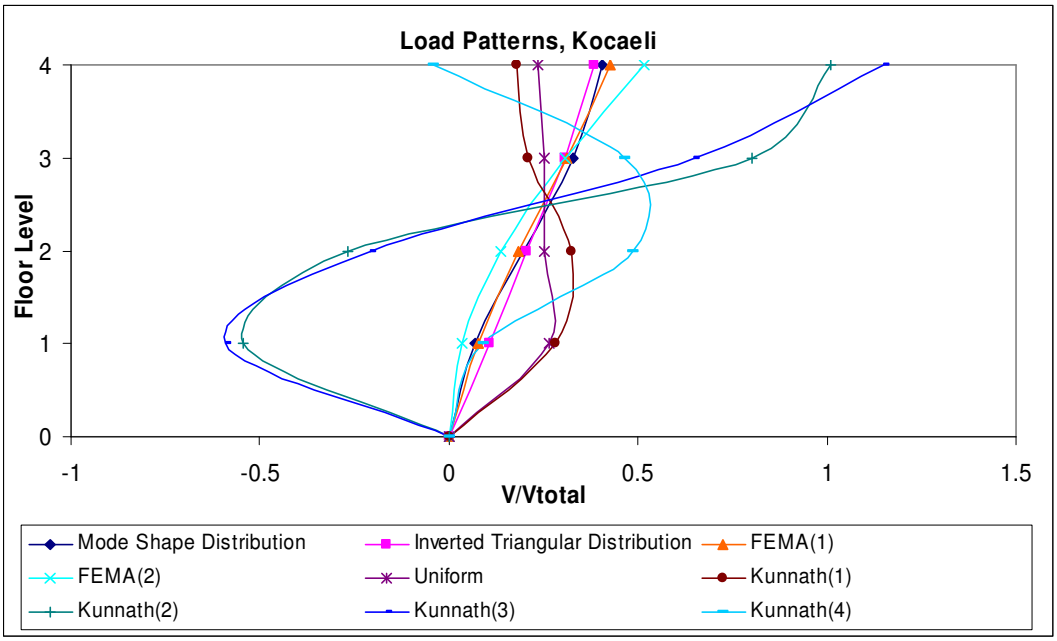

Figure 5-16 Load Patterns used for pushover analyses, Kocaeli ground motion

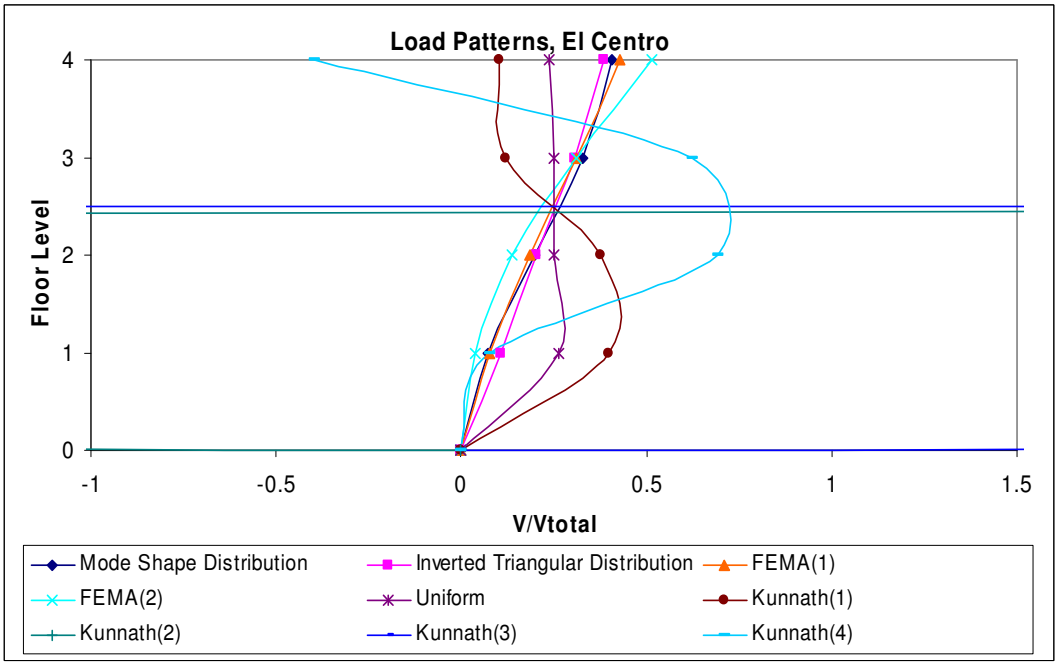

Figure 5-17 Load Patterns used for pushover analyses, El Centro ground motion

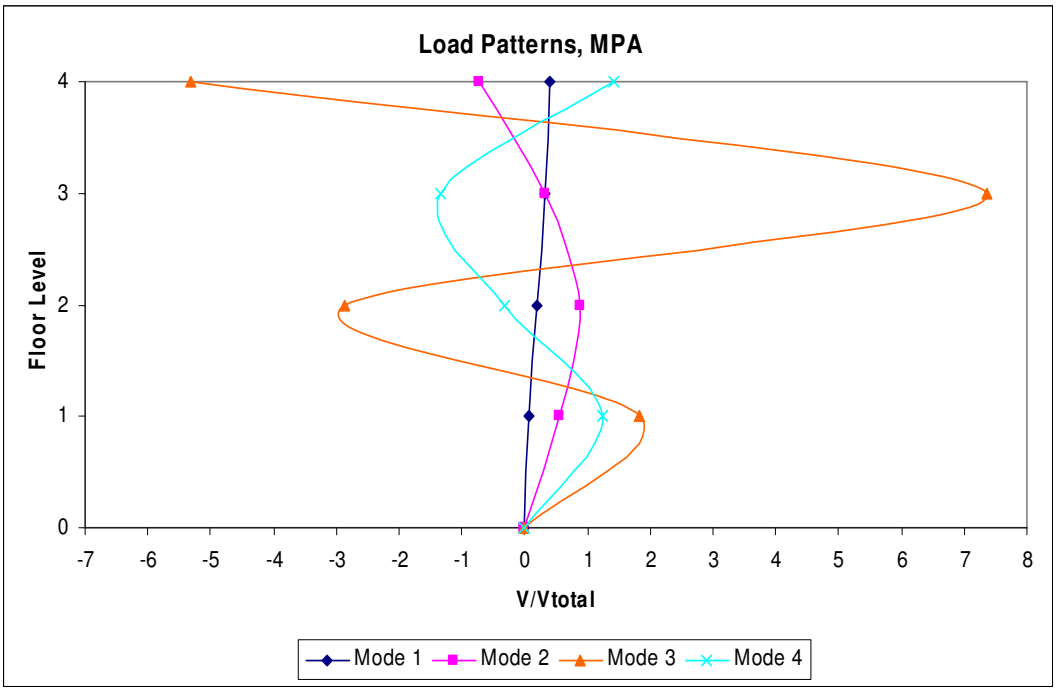

Figure 5-18 MPA load patterns

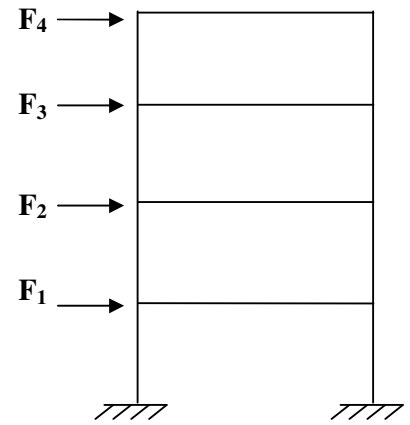

a) Structure Loading

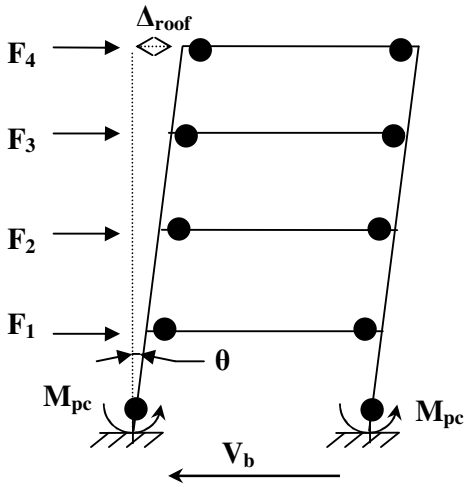

b) Assumed Collapse Mechanism

Figure 5-19 a) Loading, b) Assumed Collapse Mechanism

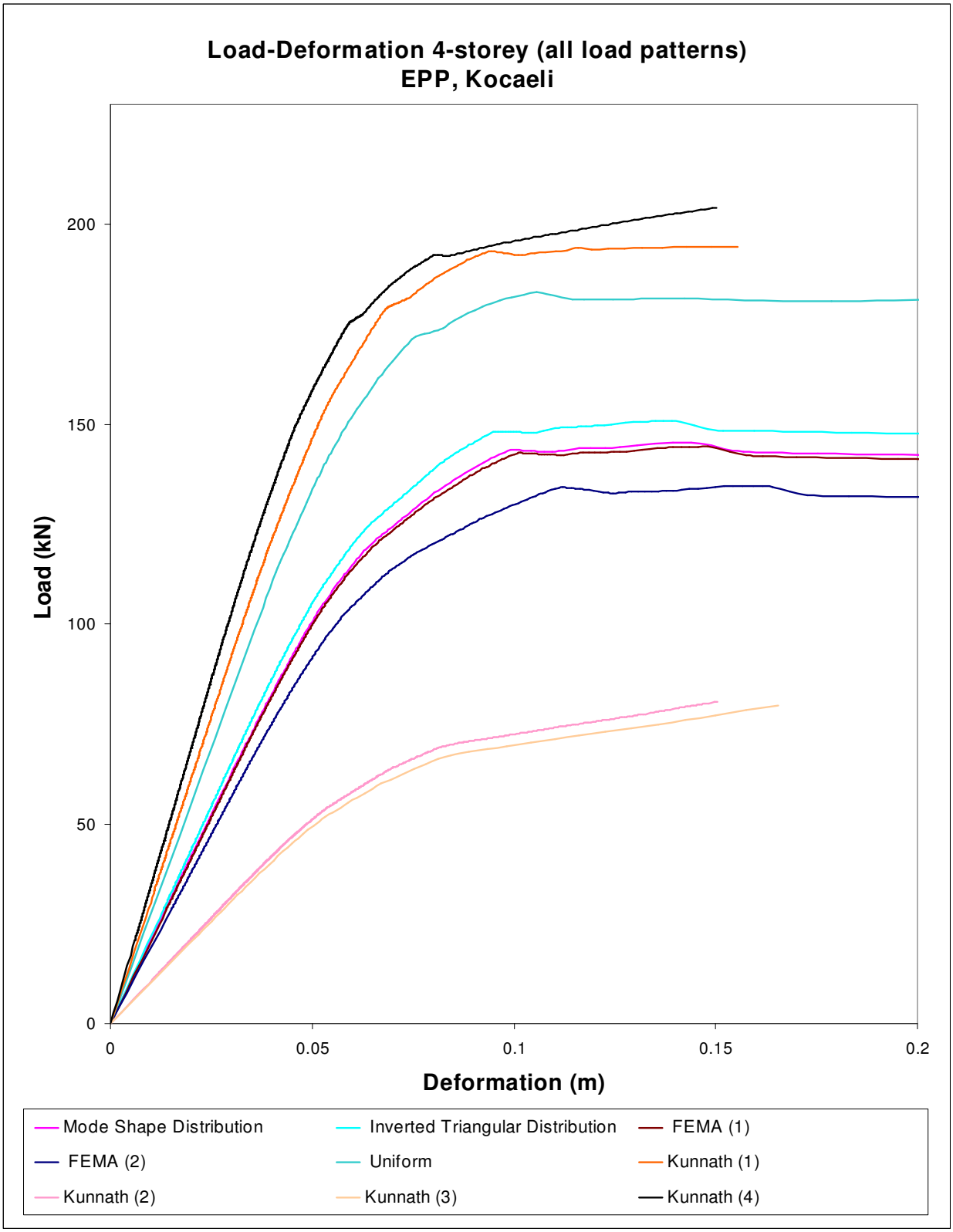

Figure 5-20 Base Shear – Roof Displacement of 4-storey frame subjected to nine different load patterns – EPP model with and without P-delta effects, Kocaeli ground motion

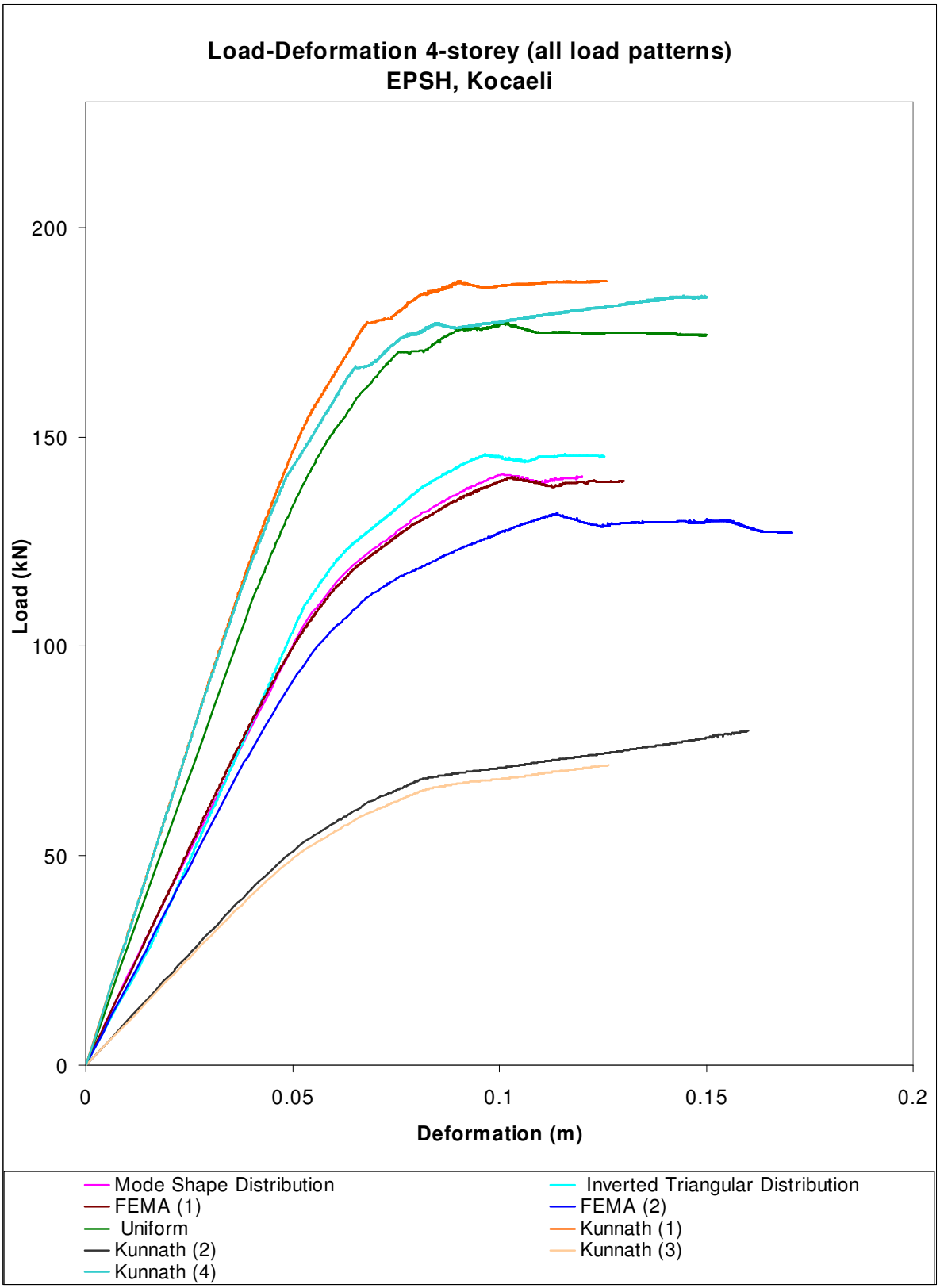

Figure 5-21 Base Shear – Roof Displacement of 4-storey frame subjected to nine different load patterns – EPSH model with and without P-delta effects

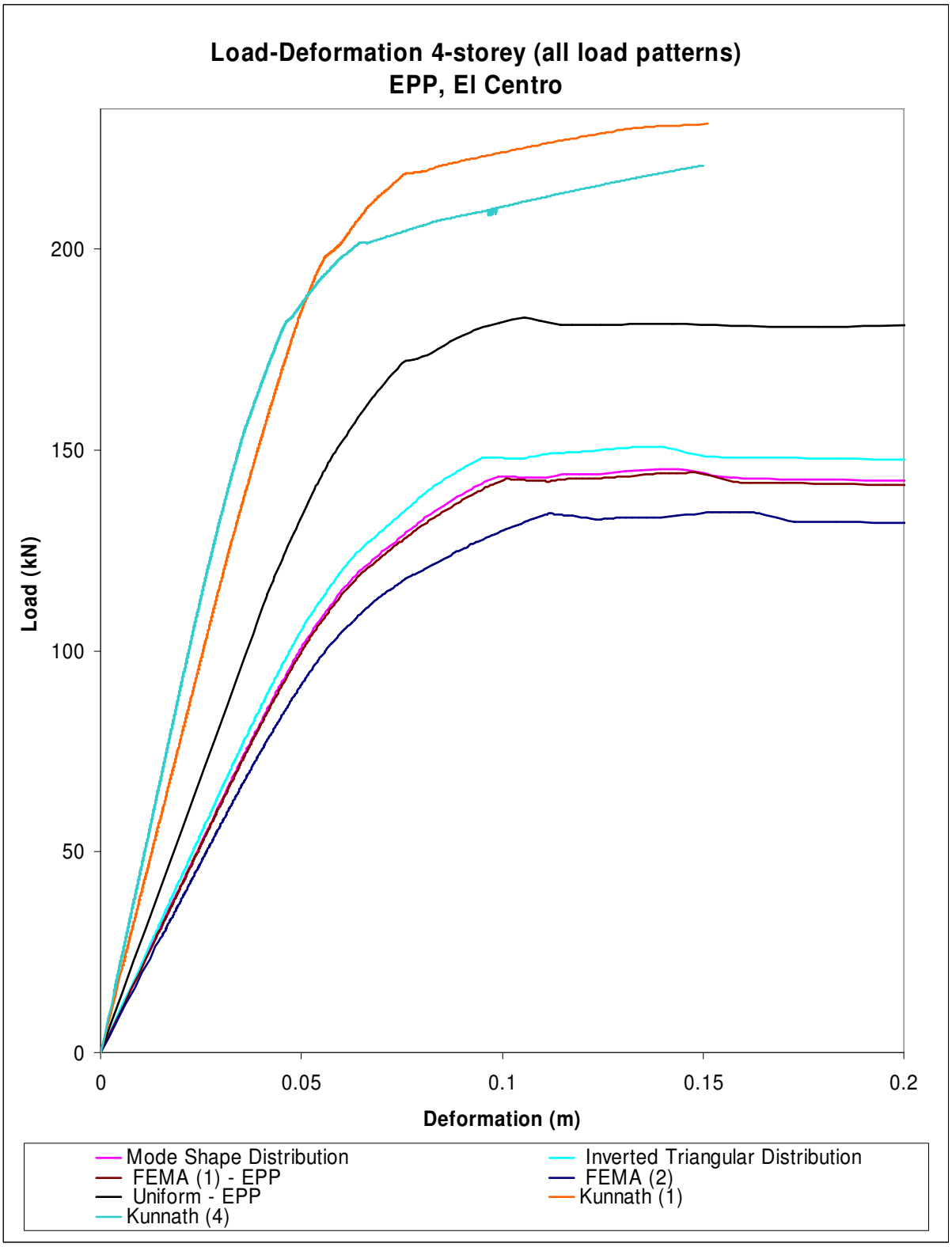

Figure 5-22 Base Shear – Roof Displacement of 4-storey frame subjected to nine different load patterns – EPP and EPSH model with P-delta effects, Kocaeli ground motion

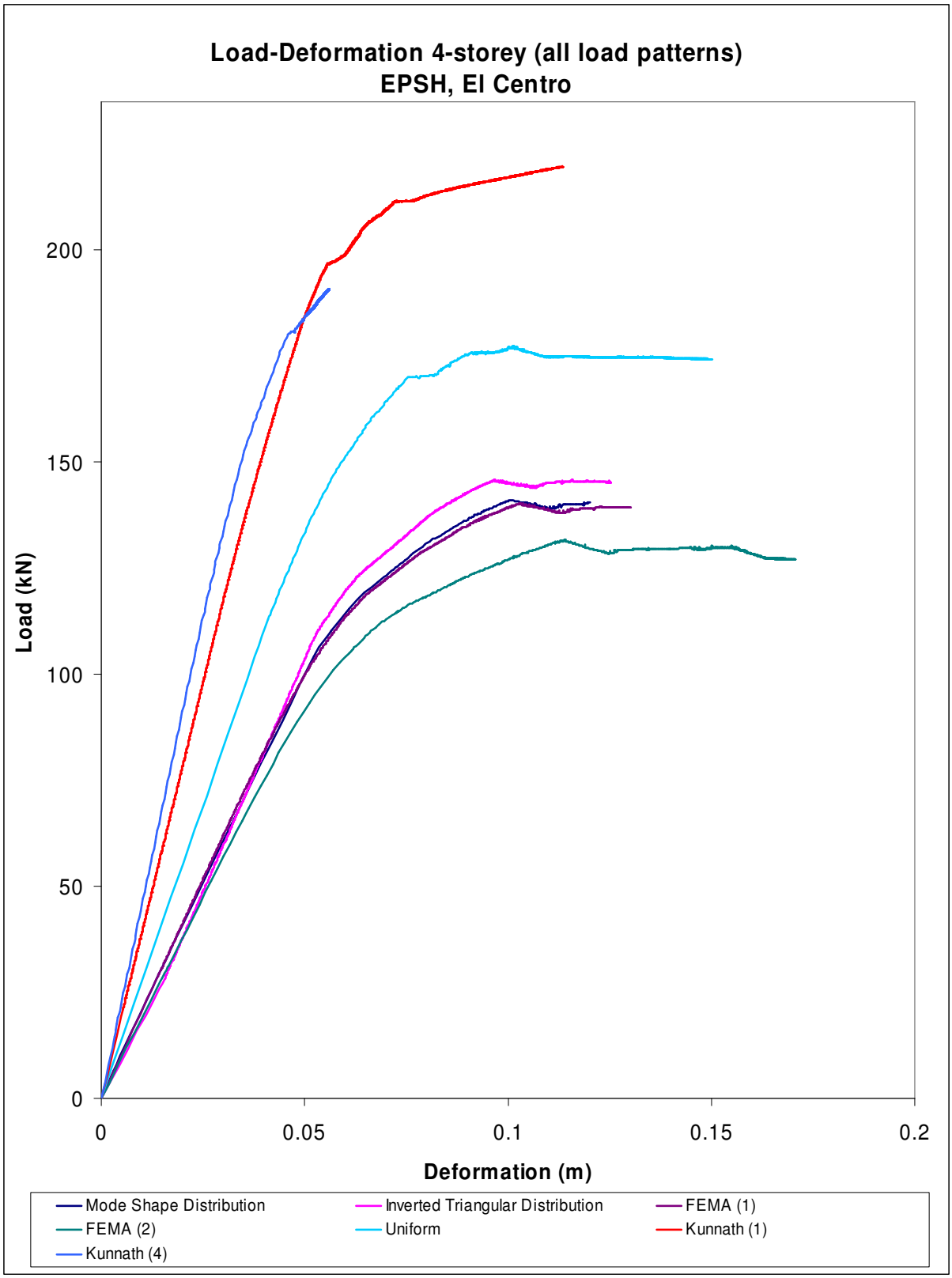

Figure 5-23 Base Shear – Roof Displacement of 4-storey frame subjected to nine different load patterns – EPP and EPSH model with P-delta effects, El Centro ground motion

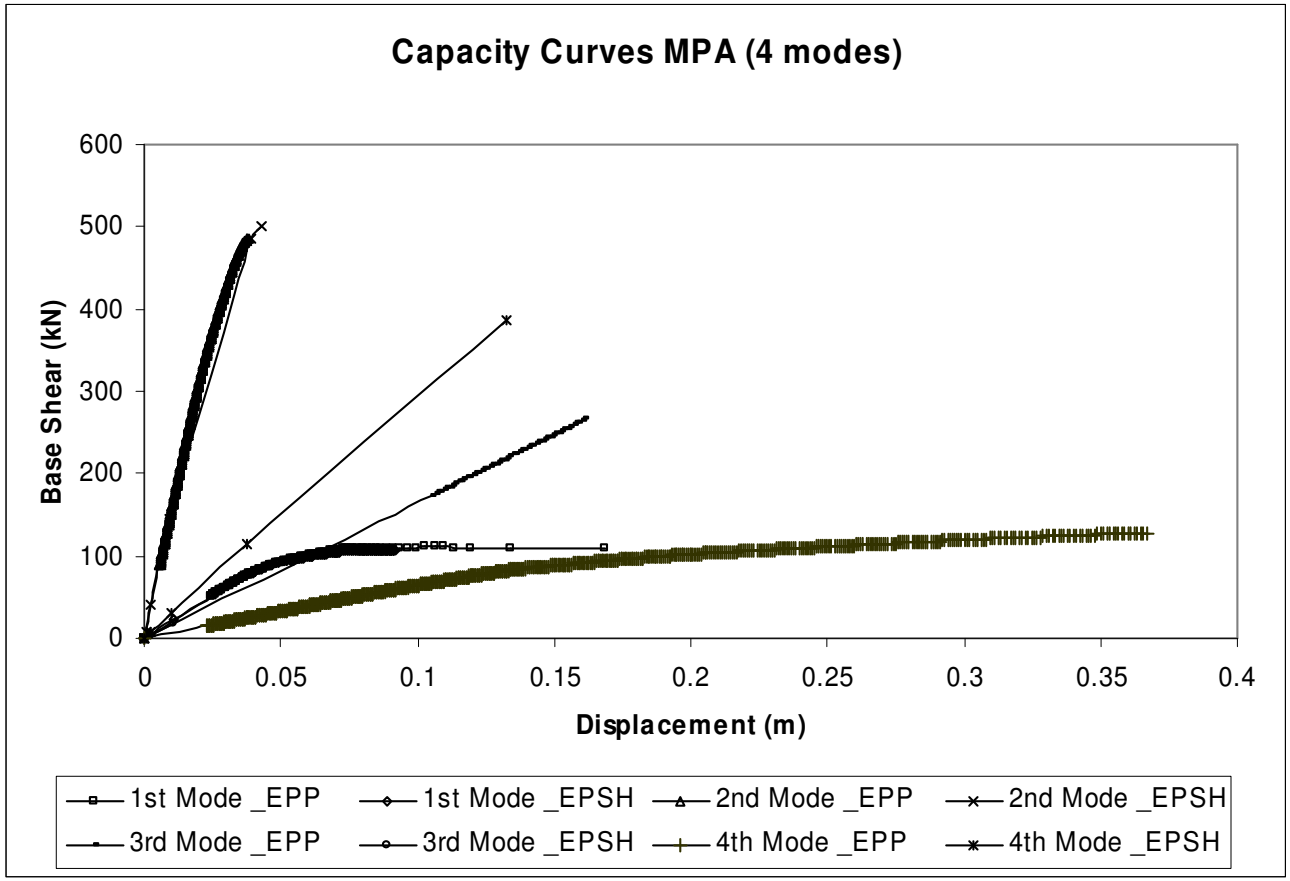

Figure 5-24 Capacity Curves for 4 modes of vibration utilizing MPA method

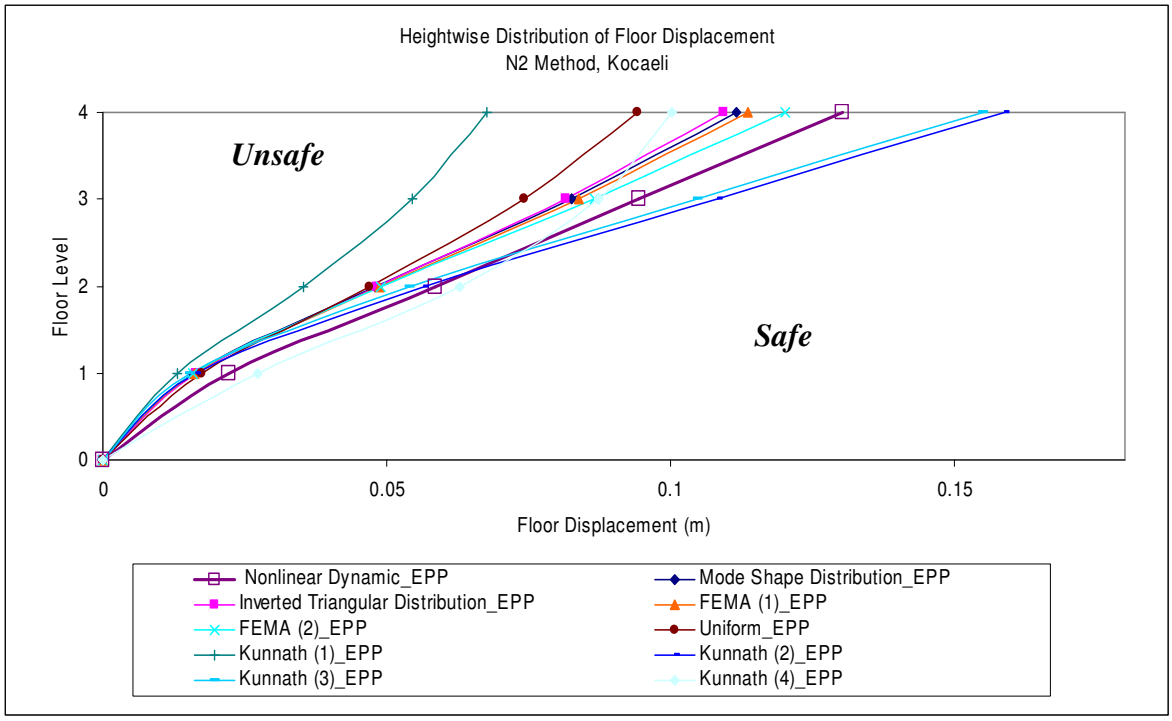

Figure 5-25 Comparison of Deflection Profiles between nonlinear dynamic and N2 methods for all load patterns –EPP model, Kocaeli

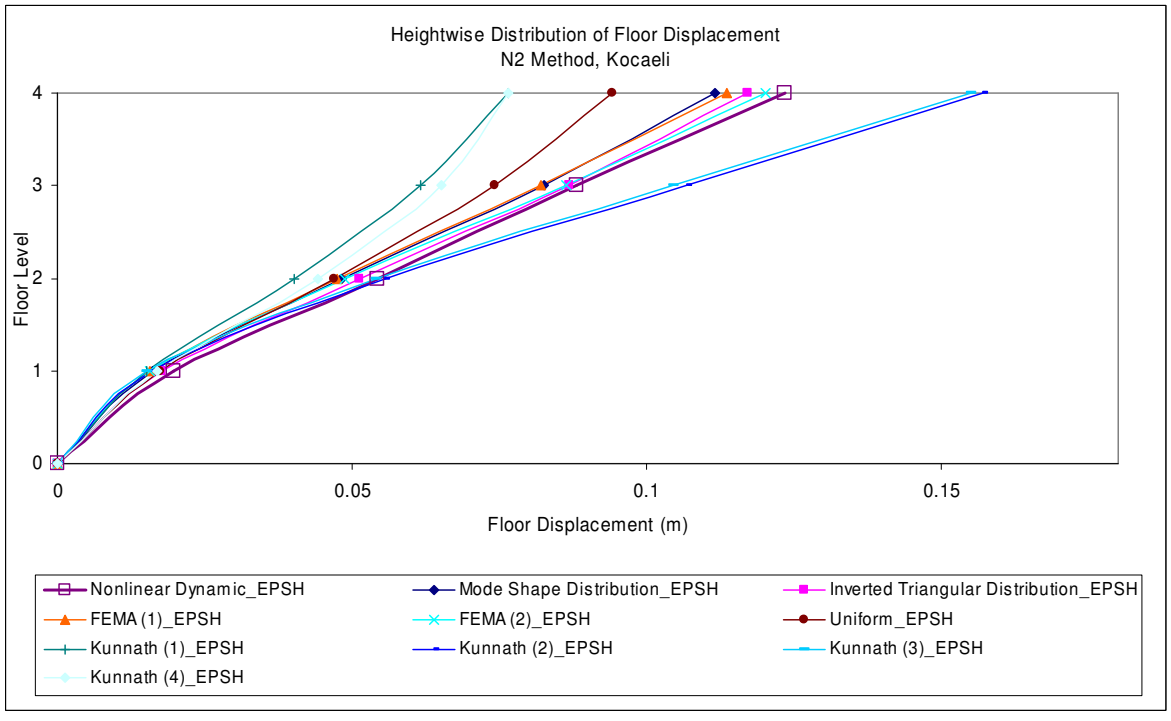

Figure 5-26 Comparison of Deflection Profiles between nonlinear dynamic and N2 methods for all load patterns –EPSH model, Kocaeli

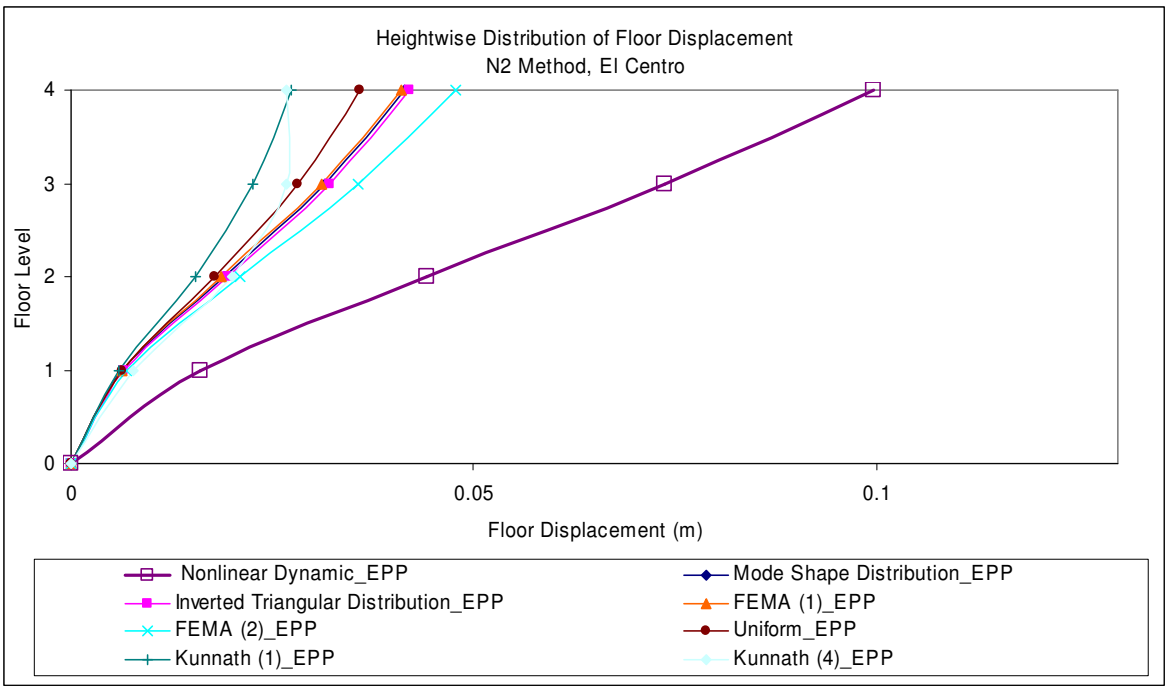

Figure 5-27 Comparison of Deflection Profiles between nonlinear dynamic and N2 methods for all load patterns –EPP model, El Centro

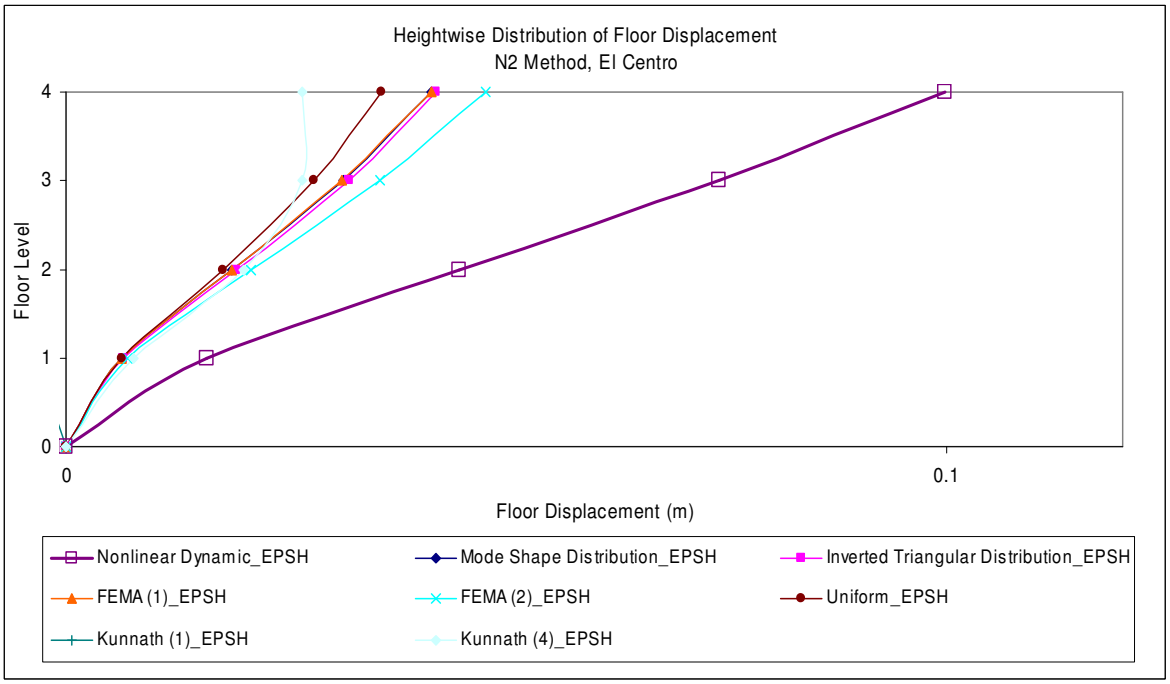

Figure 5-28 Comparison of Deflection Profiles between nonlinear dynamic and N2 methods for all load patterns –EPSH model, El Centro

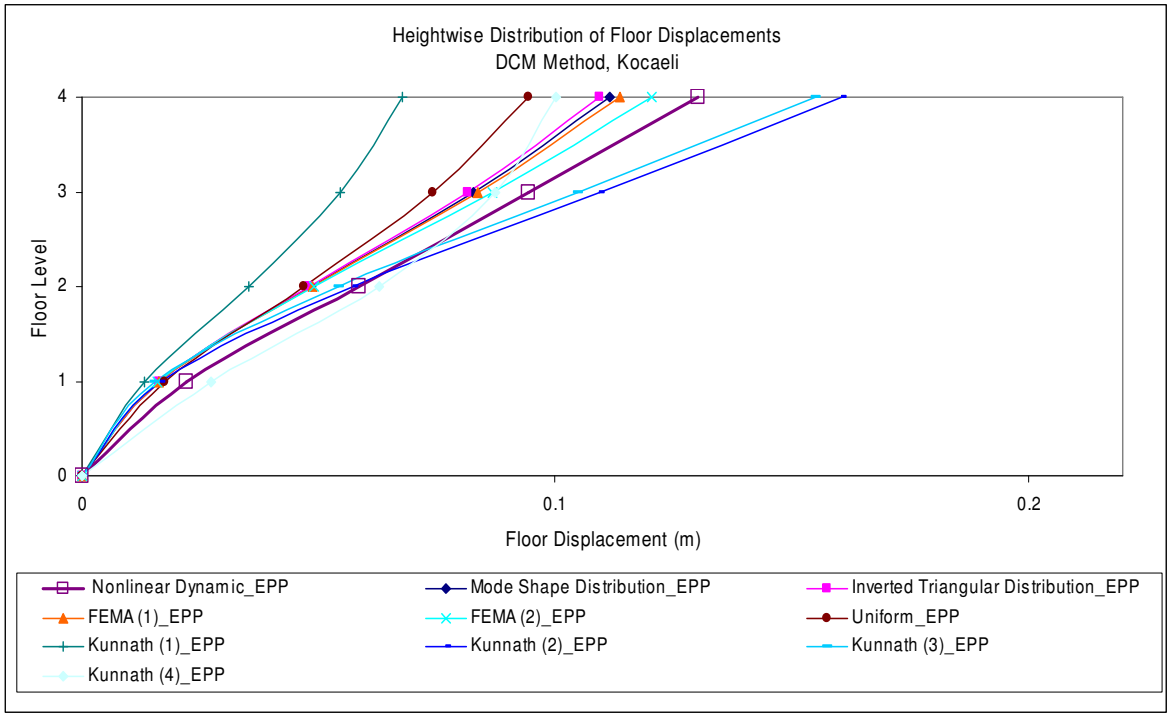

Figure 5-29 Comparison of Deflection Profiles between nonlinear dynamic and DCM methods for all load patterns –EPP model, Kocaeli

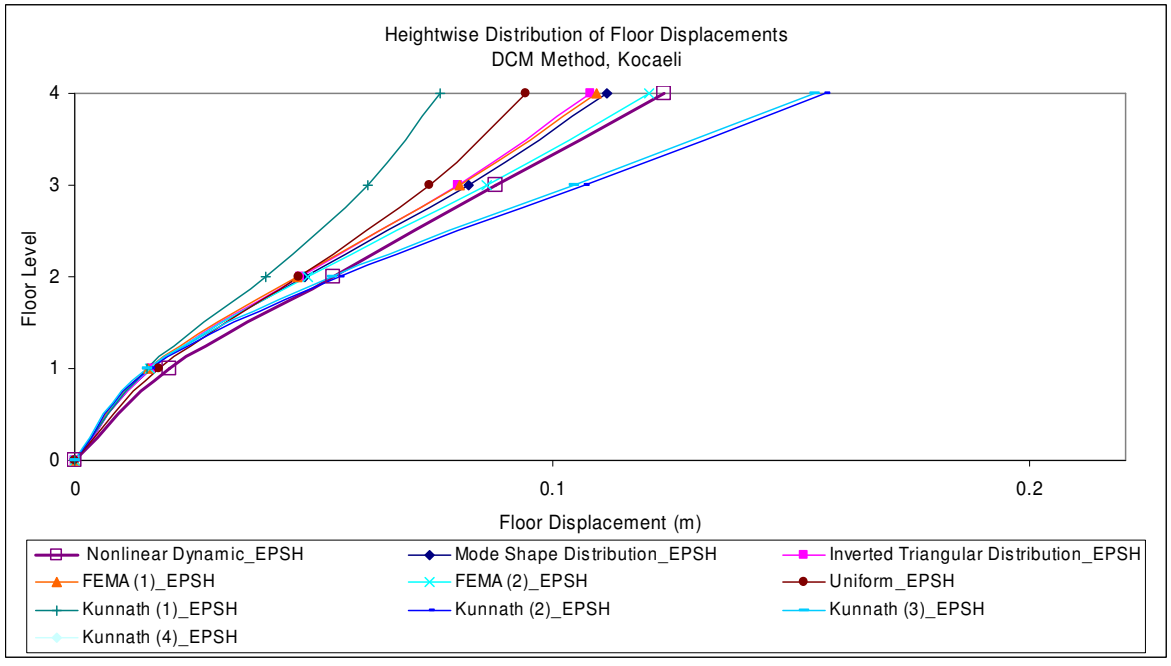

Figure 5-30 Comparison of Deflection Profiles between nonlinear dynamic and DCM methods for all load patterns –EPSH model, Kocaeli

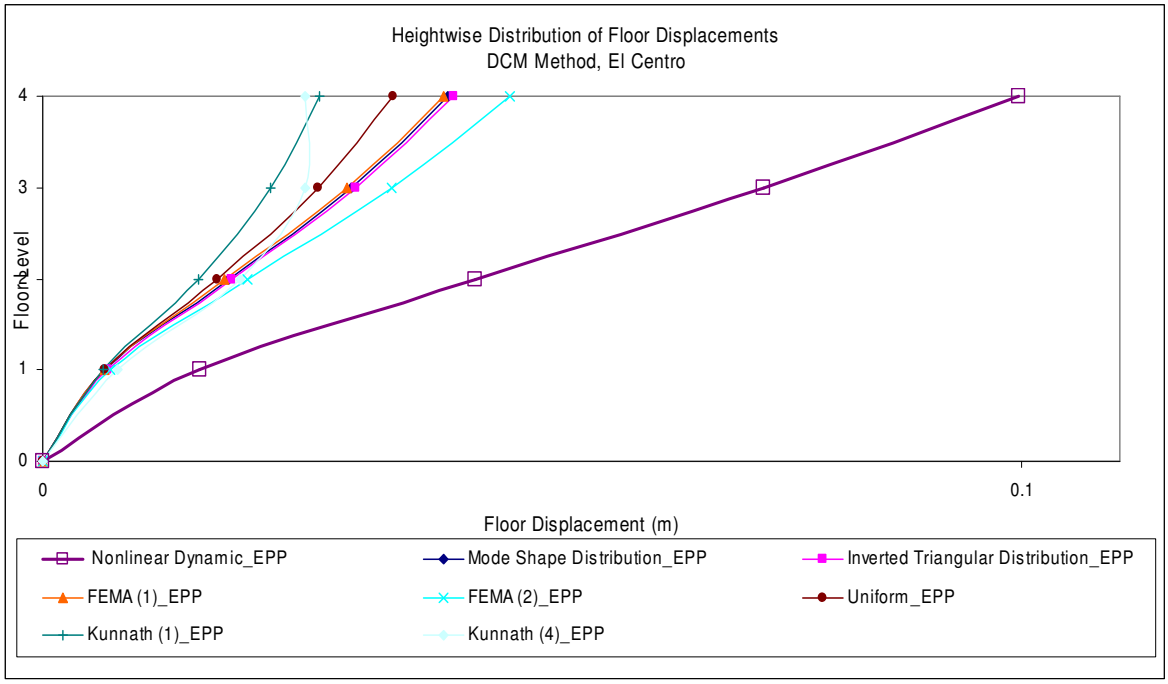

Figure 5-31 Comparison of Deflection Profiles between nonlinear dynamic and DCM methods for all load patterns –EPP model, El Centro

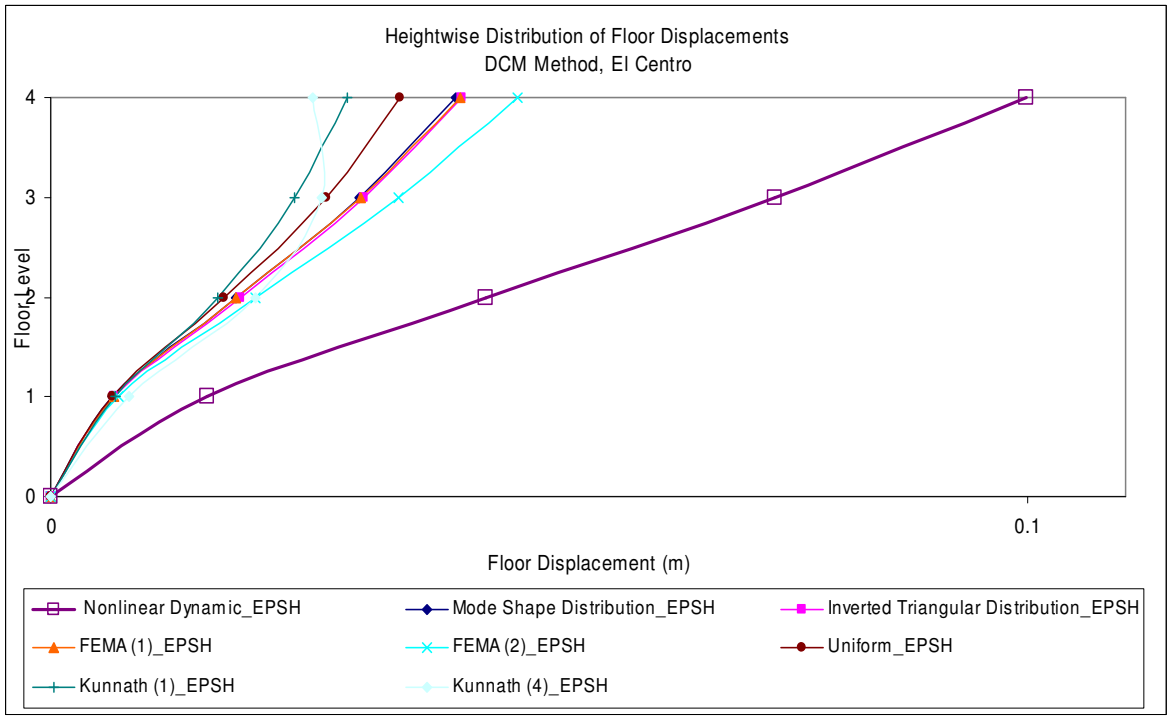

Figure 5-32 Comparison of Deflection Profiles between nonlinear dynamic and DCM methods for all load patterns –EPSH model, El Centro

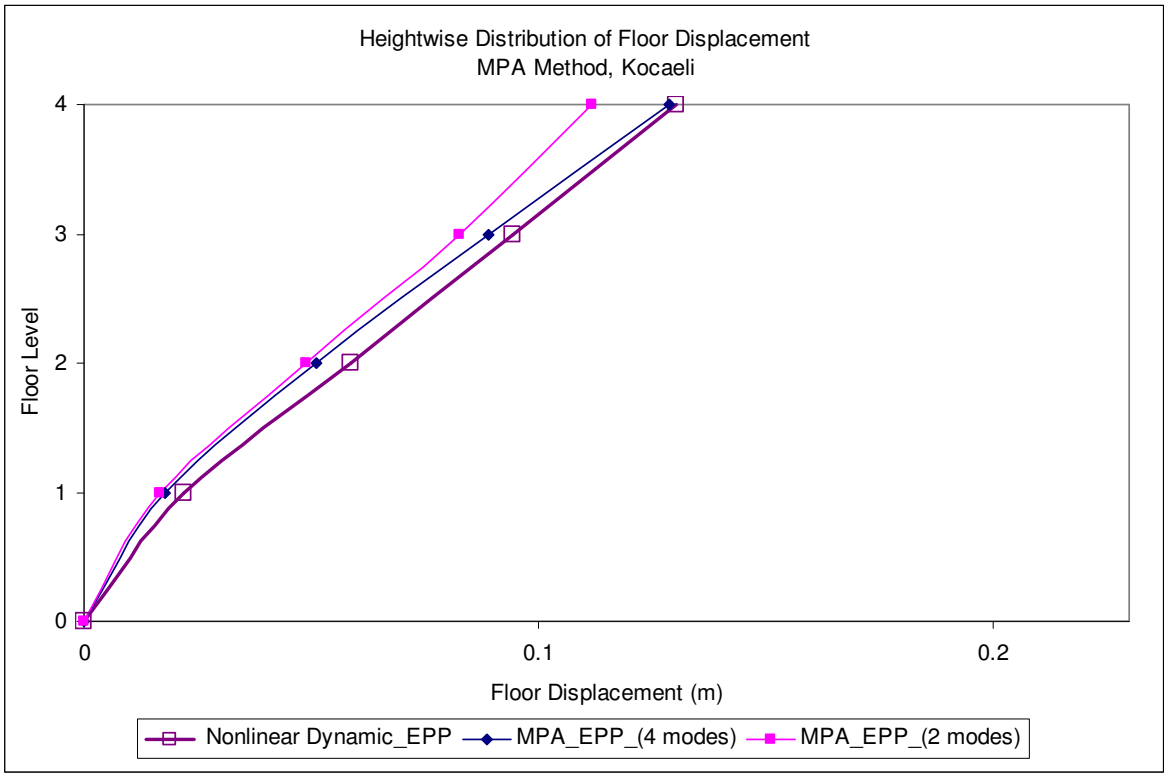

Figure 5-33 Comparison of Deflection Profiles between nonlinear dynamic and MPA methods (two variations) – EPP model, Kocaeli

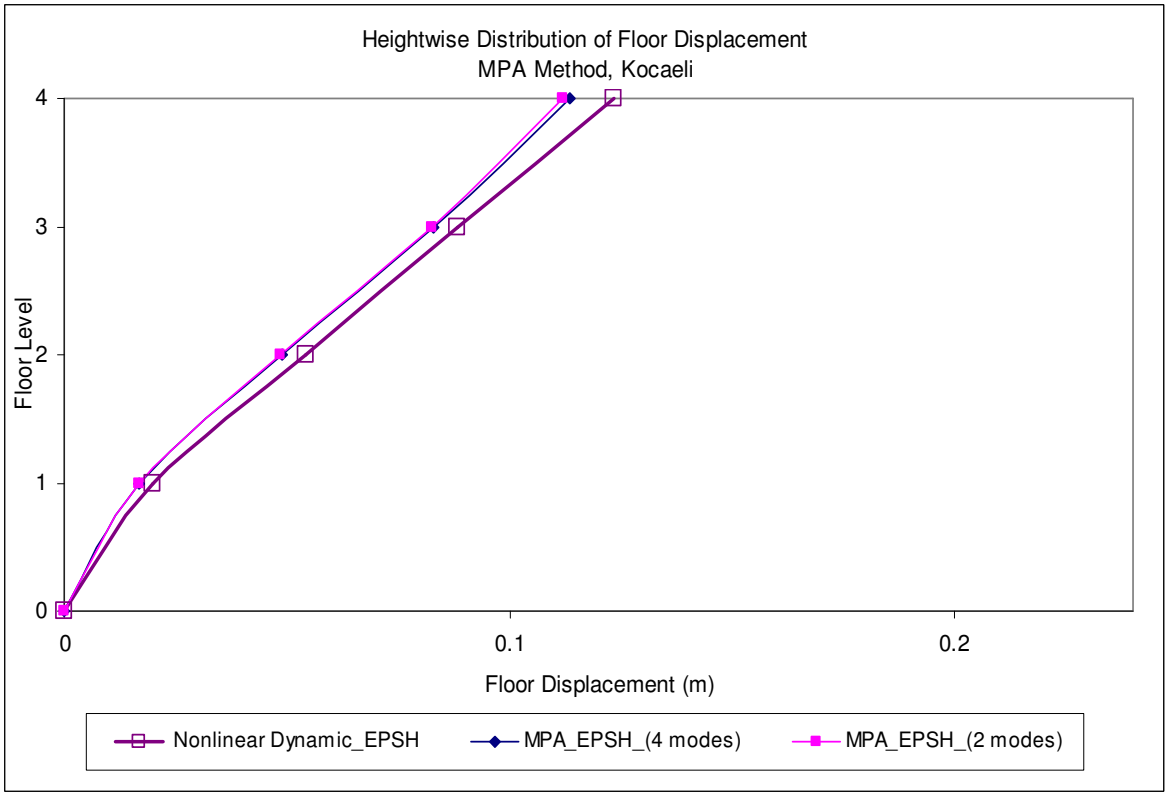

Figure 5-34 Comparison of Deflection Profiles between nonlinear dynamic and MPA methods (two variations) – EPSH model, Kocaeli

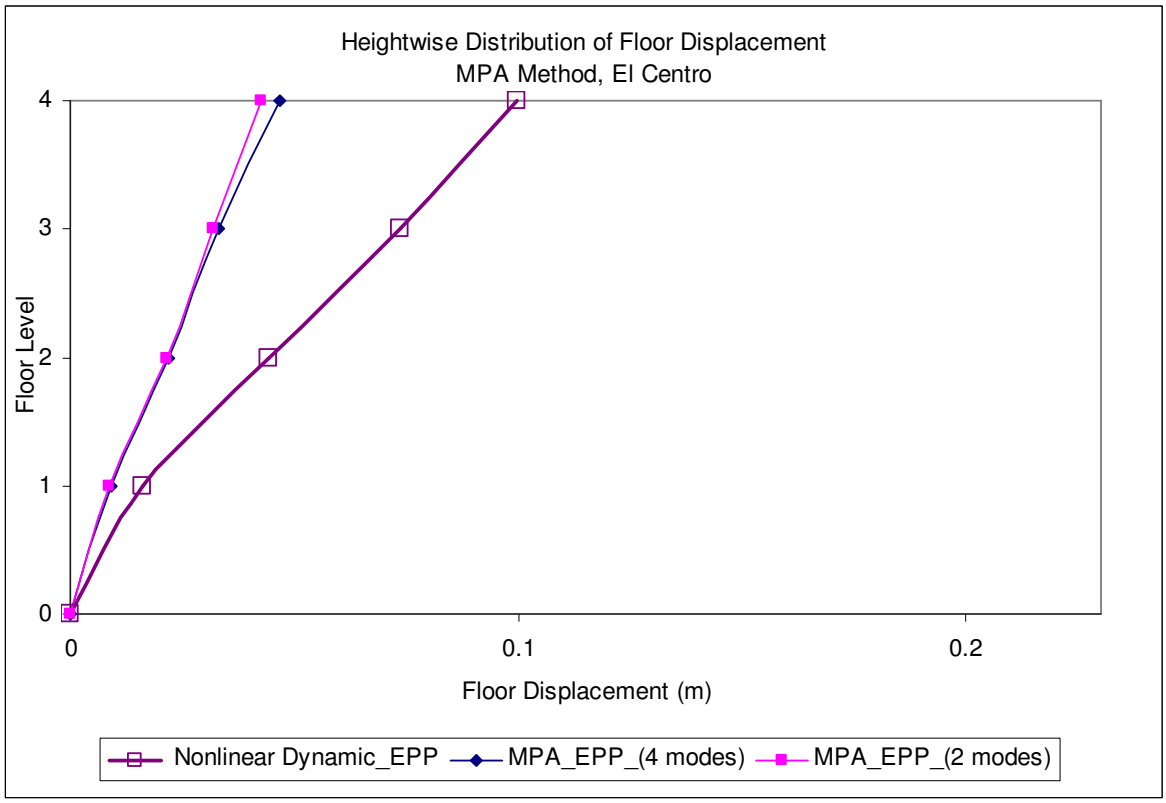

Figure 5-35 Comparison of Deflection Profiles between nonlinear dynamic and MPA methods (two variations) – EPP model, El Centro

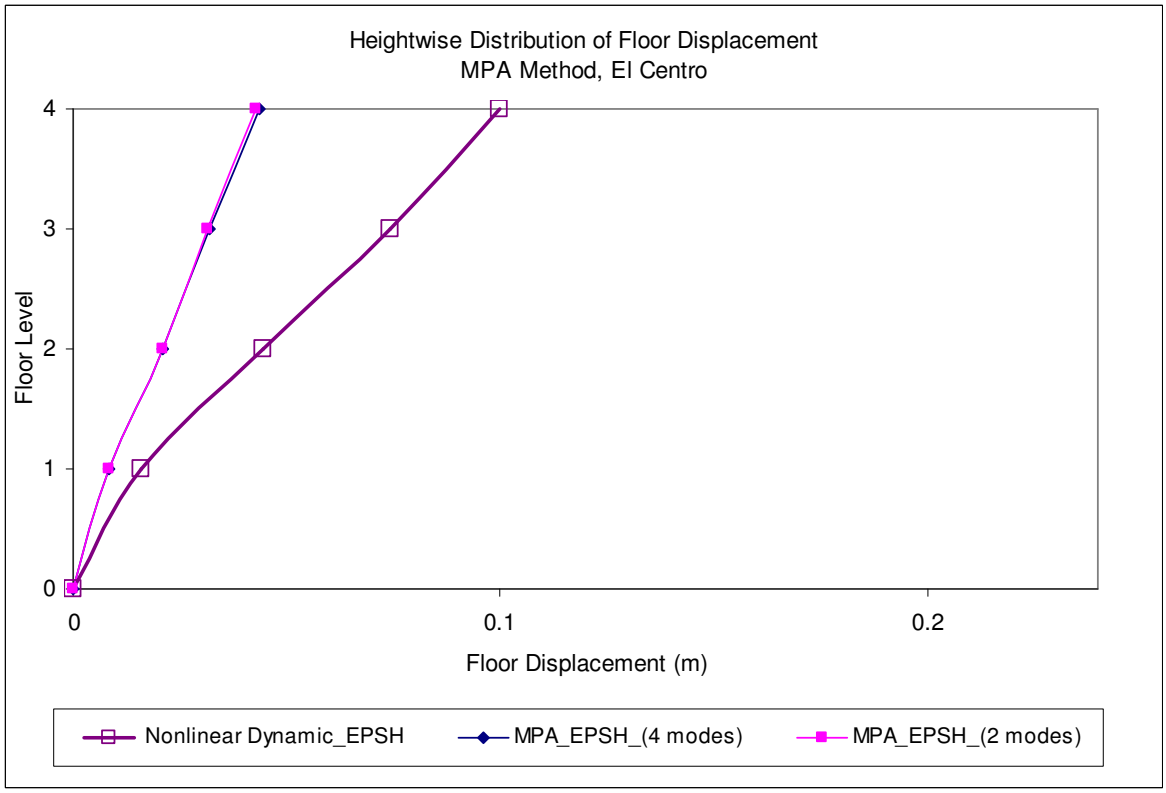

Figure 5-36 Comparison of Deflection Profiles between nonlinear dynamic and MPA methods (two variations) – EPSH model, El Centro

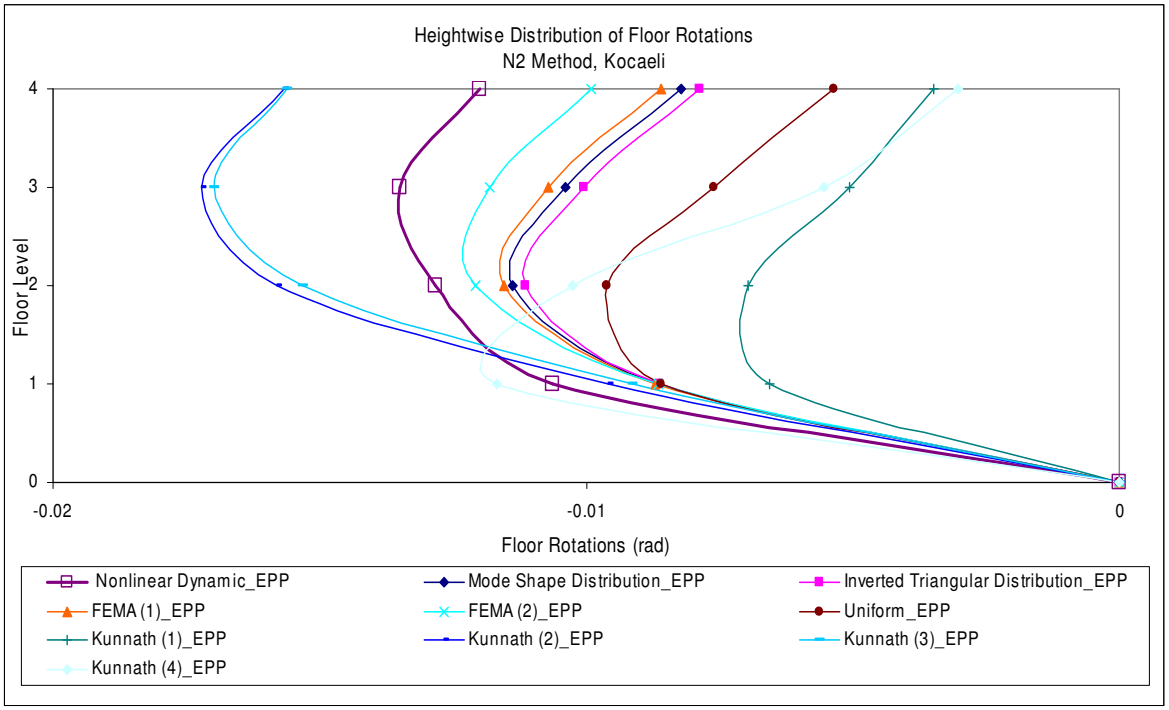

Figure 5-37 Comparison of Rotation Profiles across floor levels between nonlinear dynamic and N2 methods for all load patterns –EPP model, Kocaeli

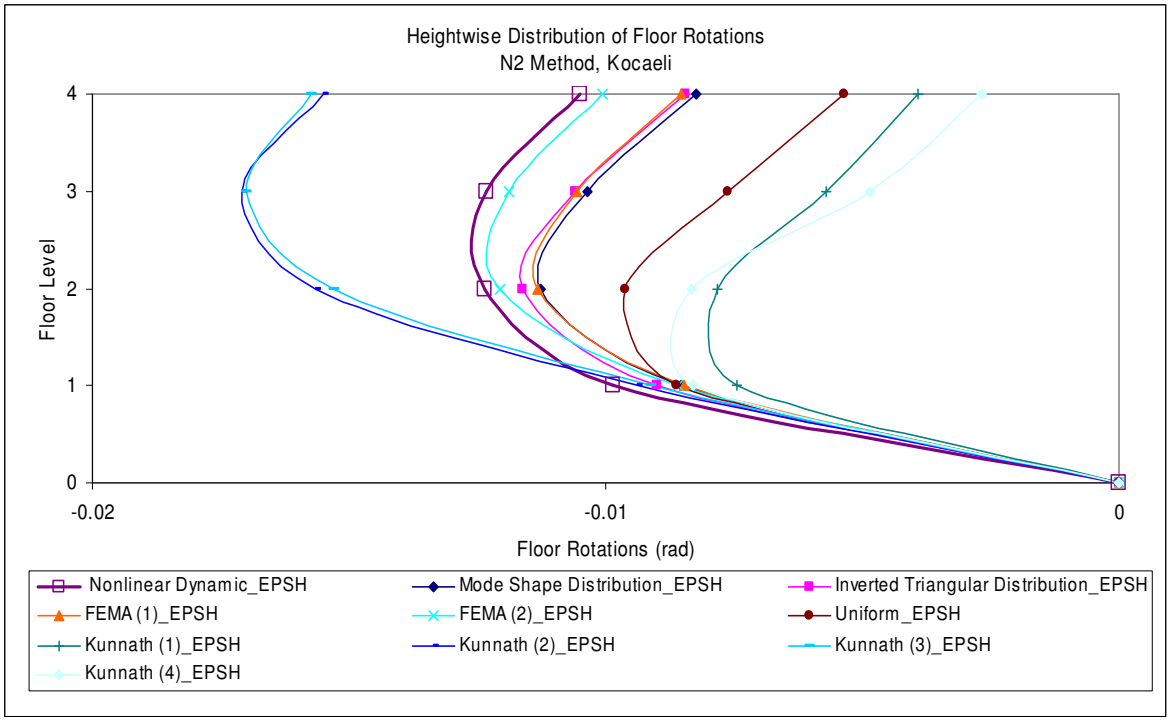

Figure 5-38 Comparison of Rotation Profiles across floor levels between nonlinear dynamic and N2 methods for all load patterns –EPSH model, Kocaeli

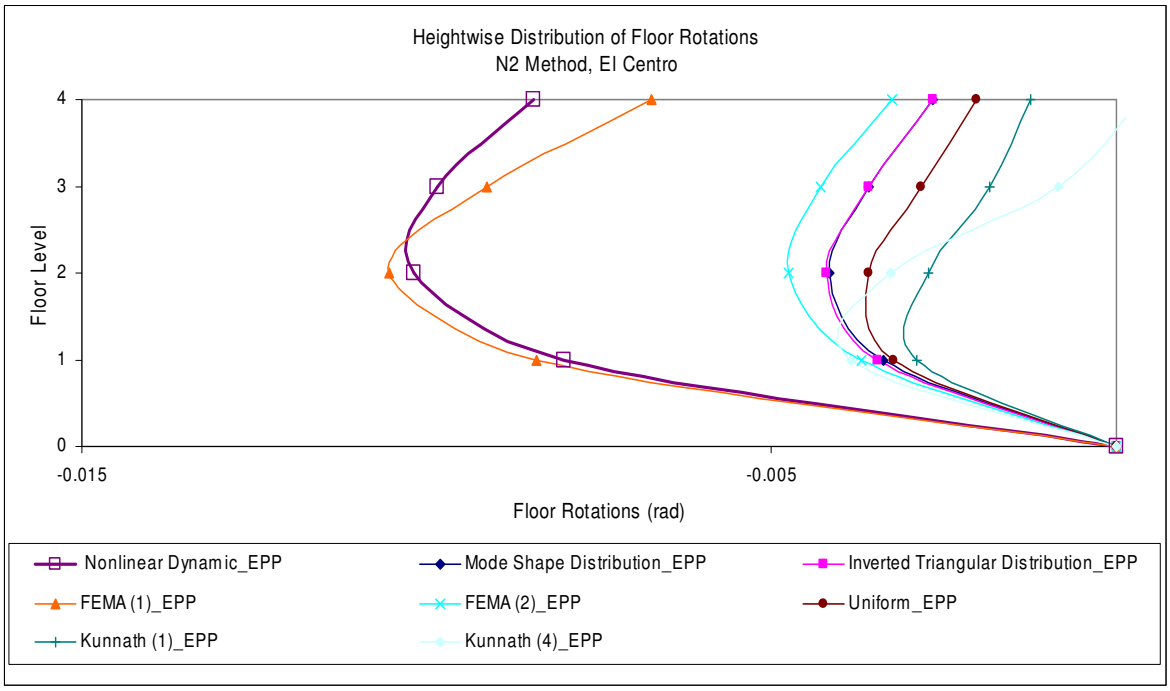

Figure 5-39 Comparison of Rotation Profiles across floor levels between nonlinear dynamic and N2 methods for all load patterns –EPP model, El Centro

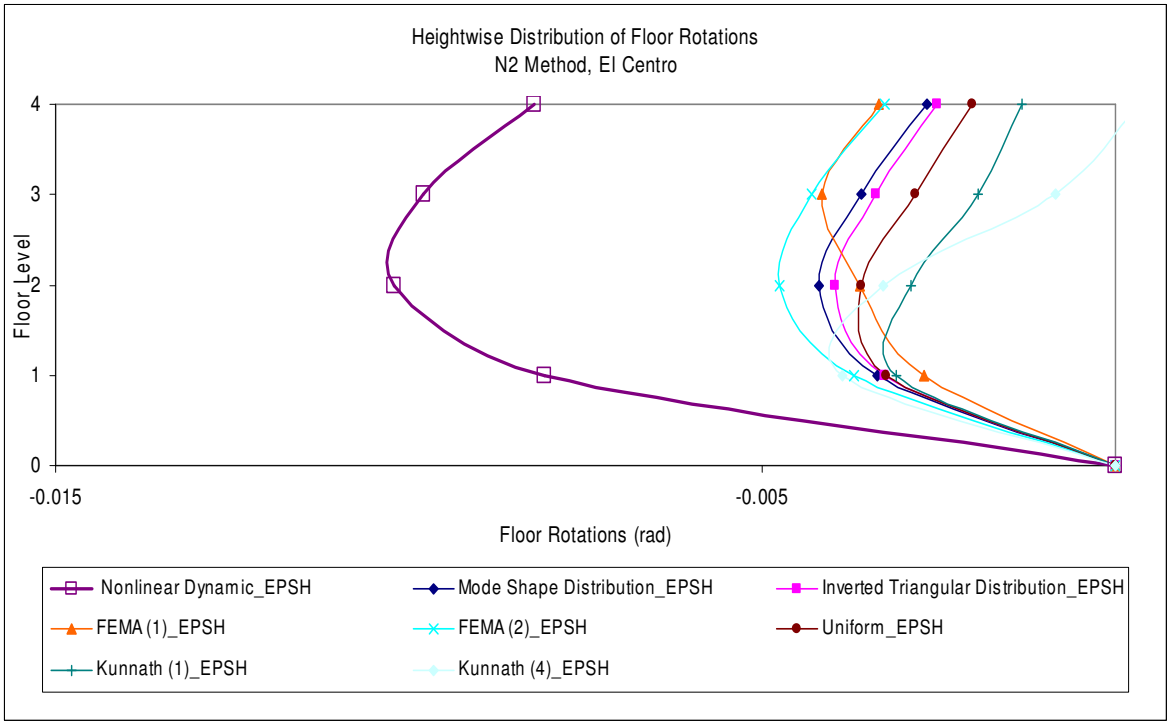

Figure 5-40 Comparison of Rotation Profiles across floor levels between nonlinear dynamic and N2 methods for all load patterns –EPSH model, El Centro

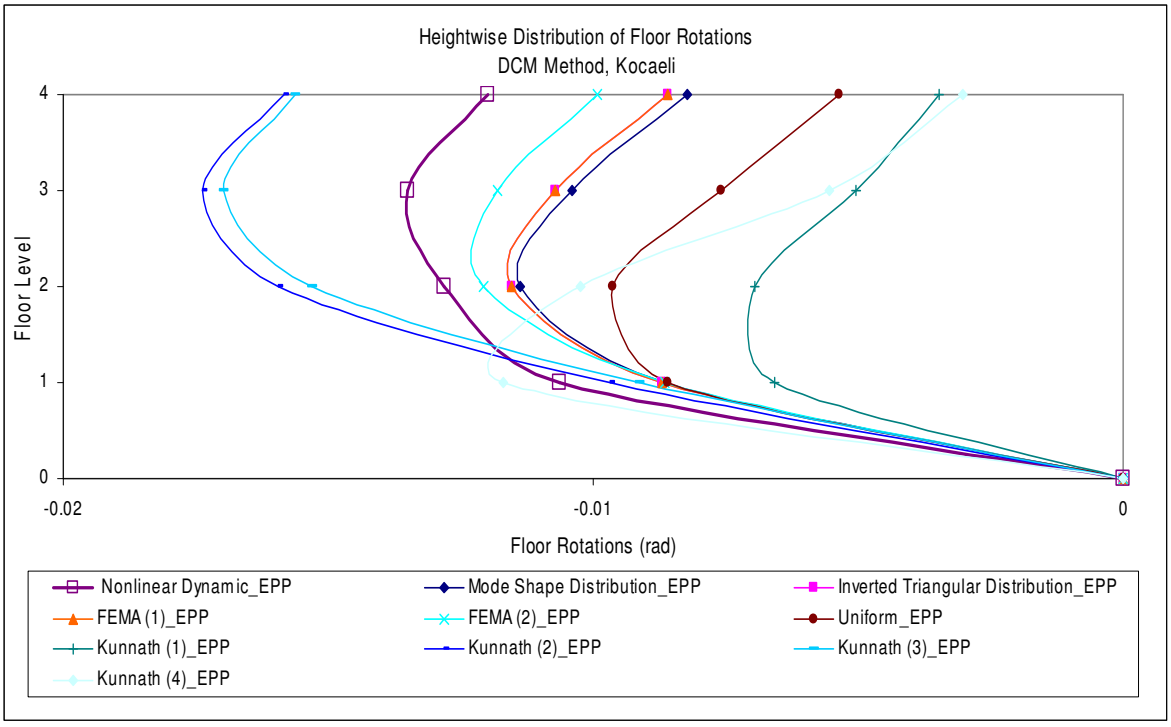

Figure 5-41 Comparison of Rotation Profiles across floor levels between nonlinear dynamic and DCM methods for all load patterns –EPP model, Kocaeli

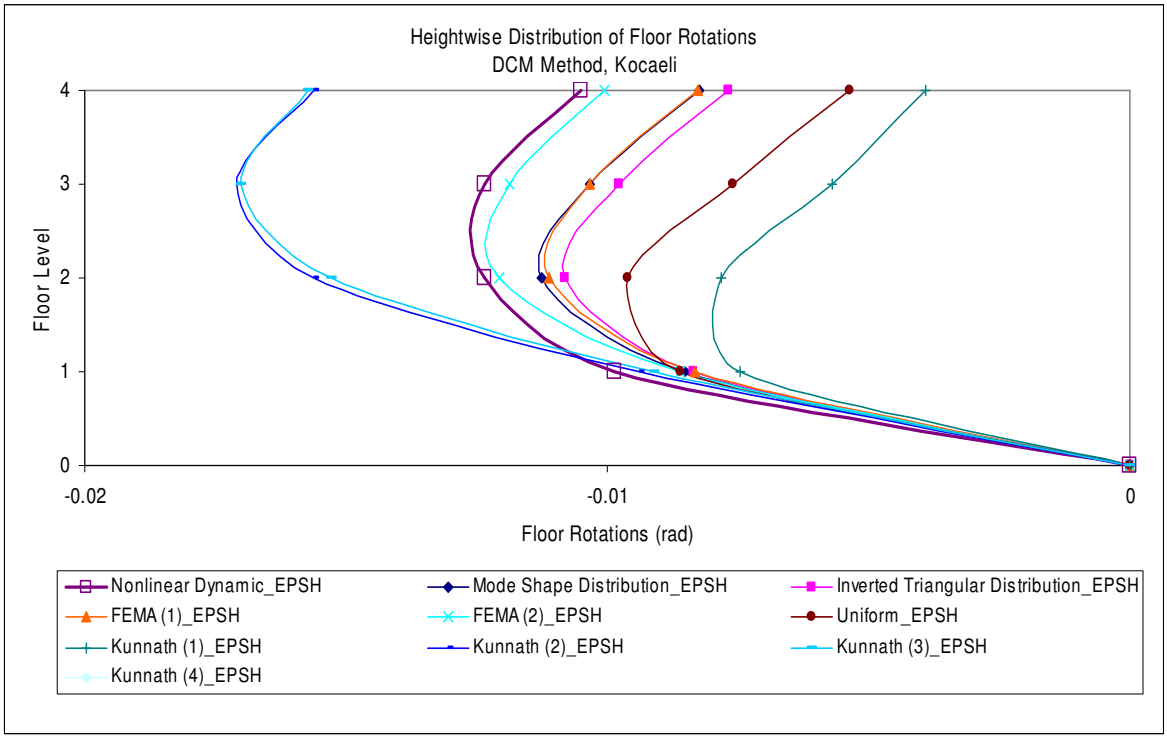

Figure 5-42 Comparison of Rotation Profiles across floor levels between nonlinear dynamic and DCM methods for all load patterns –EPSH model, Kocaeli

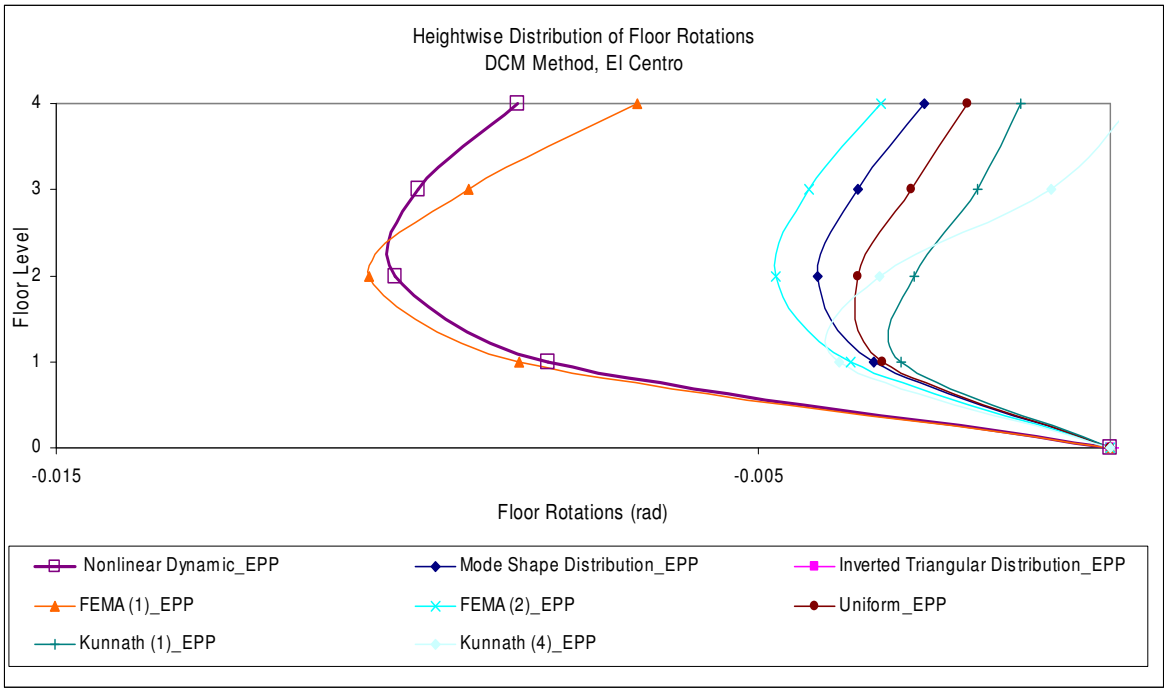

Figure 5-43 Comparison of Rotation Profiles across floor levels between nonlinear dynamic and DCM methods for all load patterns –EPP model, El Centro

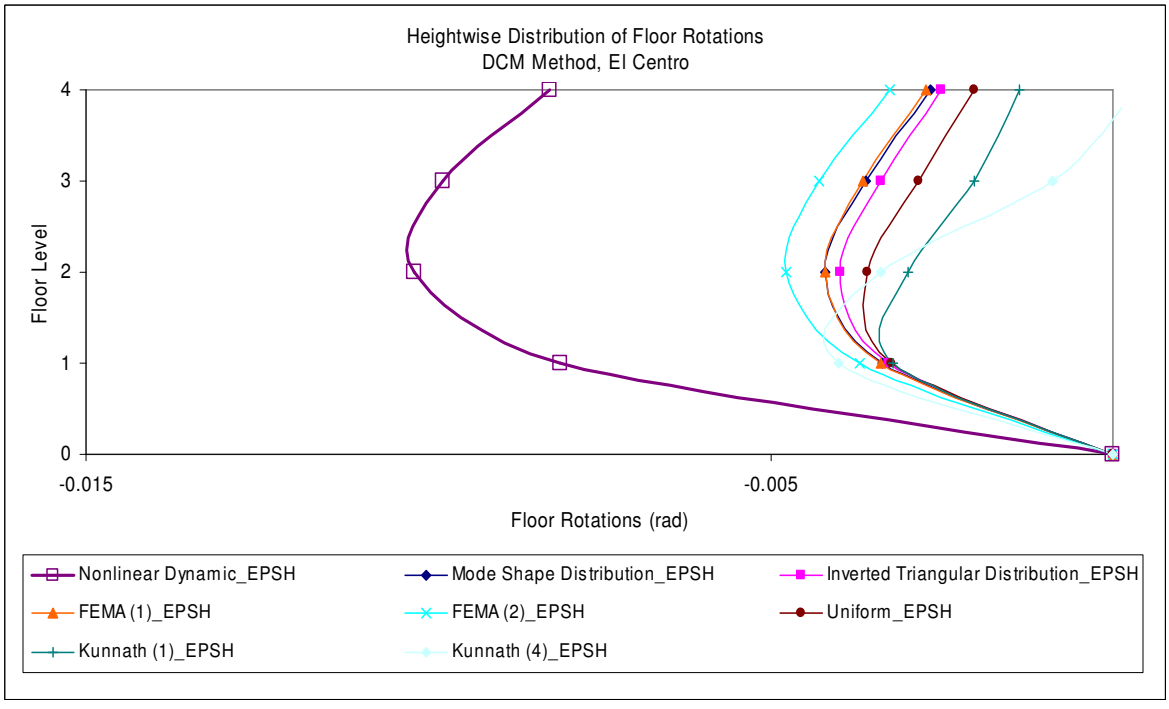

Figure 5-44 Comparison of Rotation Profiles across floor levels between nonlinear dynamic and DCM methods for all load patterns –EPSH model, El Centro

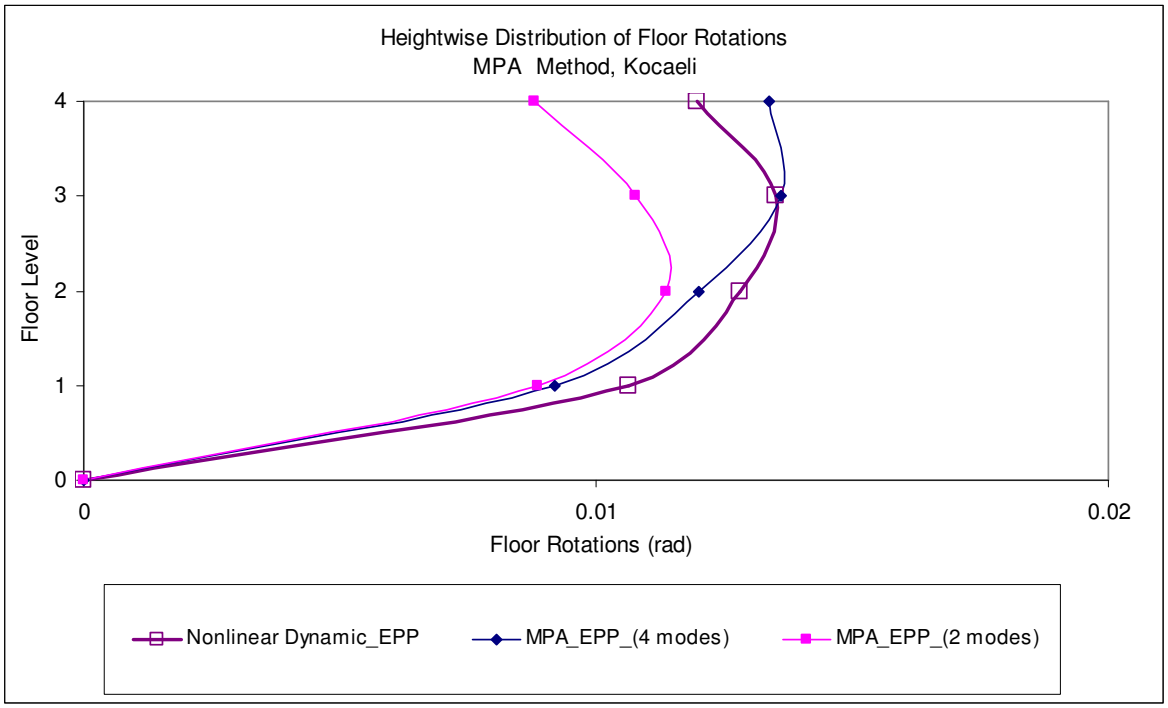

Figure 5-45 Comparison of Rotation Profiles across floor levels between nonlinear dynamic and MPA methods (two variations) – EPP model, Kocaeli

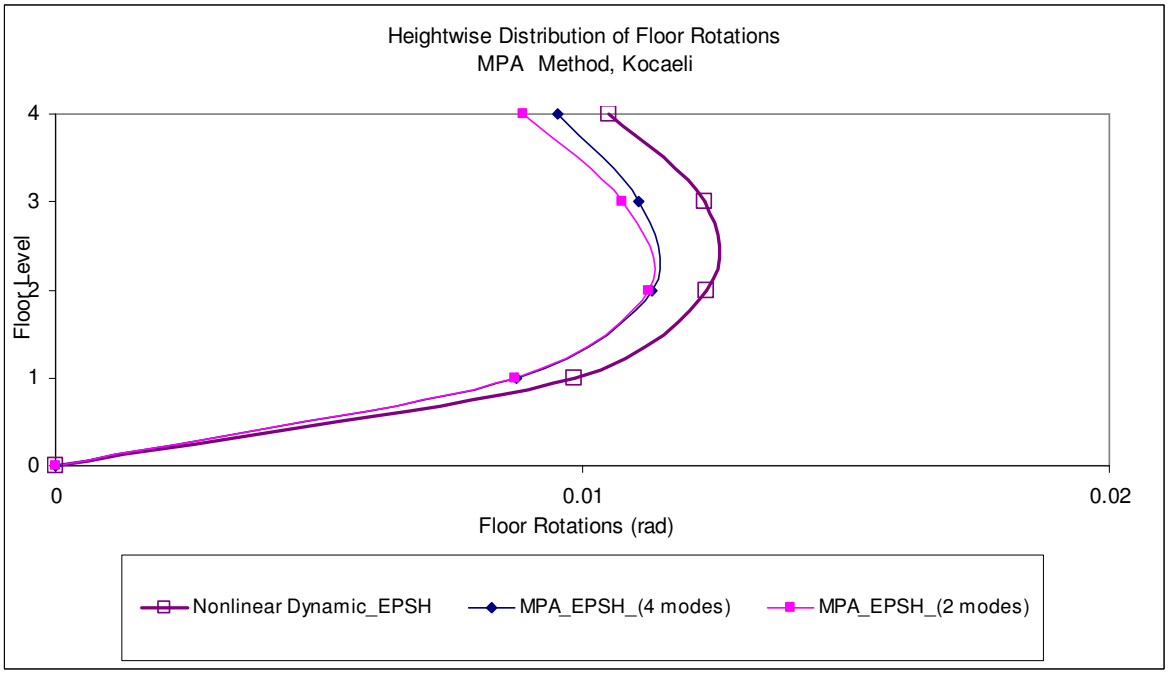

Figure 5-46 Comparison of Deflection Rotation Profiles across floor levels between nonlinear dynamic and MPA methods (two variations) – EPSH model, Kocaeli

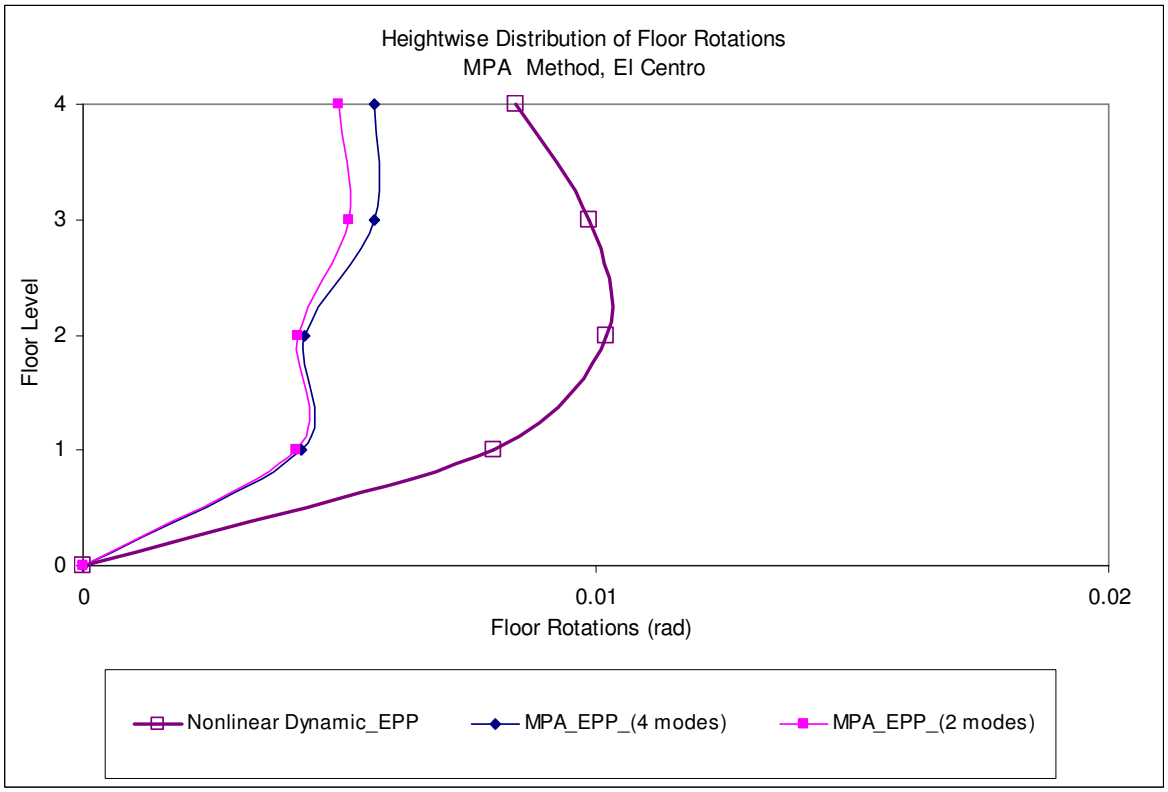

Figure 5-47 Comparison of Rotation Profiles across floor levels between nonlinear dynamic and MPA methods (two variations) – EPP model, El Centro

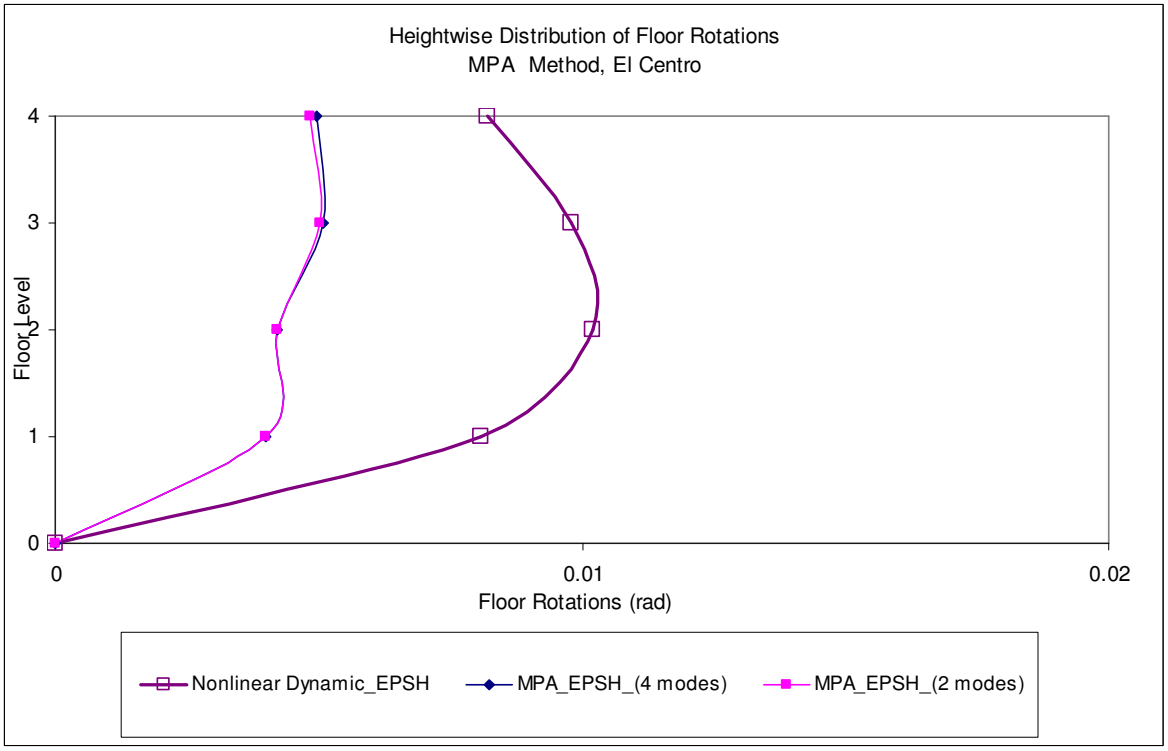

Figure 5-48 Comparison of Deflection Rotation Profiles across floor levels between nonlinear dynamic and MPA methods (two variations) – EPSH model, El Centro

CHAPTER 6
CONCLUSIONS AND RECOMMENDATIONS

6.1 CONCLUSIONS

This research provided some basic information on the use, and accuracy of the various pushover analysis methods in the seismic assessment and design of structures. The research comprised the following aspects:

The basic concept of pushover analysis was explained, and the various pushover analysis methods were described. A comprehensive review of previous findings on pushover analysis was provided.

Pushover analyses were conducted on six SDOF systems and a 2-DOF system for two ground motions of different nature. The effectiveness of the N2, DCM and MPA methods in predicting important seismic demands such as maximum displacements, reaction force and ductility and hysteretic energy was studied.

Pushover analyses were subsequently performed on a four-storey reinforced concrete frame designed to EC8. The effectiveness of the N2, DCM and MPA methods in predicting maximum displacements across the floor levels, the base shear and the ductility was assessed.

The most important conclusions drawn from the study on the SDOF systems are the following:

- The use of inelastic response spectra can lead to difficulties in the interpretation of results when conducting pushover analysis because, for increasing ductility factor, the demand displacement sometimes decreases.

- The accuracy of the N2 and DCM methods is diminishing for SDOF systems in the short-period range. In the intermediate period range the methods provide in general satisfactory estimates of seismic demands.

- The base shear was calculated satisfactorily in most of the cases except for the short-period systems. However the estimates were unconservative implying that the N2 and DCM method may lead to unsafe design or assessment.

- The pushover curves tend to underestimate the actual dissipated energy implying that assessment of damage in structures could be erroneous.

The most important conclusions drawn from the study on the MDOF systems are the following:

- The load distributions available to the engineers will generally provide different results for different material models and pushover methods. The results were shown to be dependent on the severity of the ground motion and the frequency content and distribution of frequencies in the ground motion.

- The N2 method needs to be used cautiously when estimating maximum displacements and ductilities.

- The FEMA(1) load pattern, and Kunnath(1) load pattern can be considered as two load patterns that should be used for pushover analyses at least in the case of low-rise structures.

- All pushover methods will generally provide good estimates of base shear, but care should be taken because the estimate might be unconservative. This implies that it is difficult to justify the use of pushover analysis without complementing it with a nonlinear dynamic analysis.

- The DCM procedure seems the most convenient method for use in practice.

- The MPA method proved to be time-consuming. The results obtained from this method were conservative for maximum displacement and base shear quantities.

Finally the study speculated some findings that need further research to adequately verify. These are:

- The accuracy of pushover analysis is a function of the severity of the used ground motions.

- Pushover analysis might perform well for structures with fundamental period close to the maximum Fourier Amplitude period of the ground motion.

- The N2 method may underestimate displacement demands for systems with period lower than half the predominant pulse period of the near-fault ground motion and may overestimate the displacement demands for systems with period equal or larger to half the dominant pulse period of the near-fault ground motion.

6.2 RECOMMENDATIONS

The following recommendations for future research should be considered:

Further research is needed on the development of appropriate response spectra for use in design and assessment that take into account more variables than period, damping, ductility and yield strength for a SDOF system.

There seems to be a need to develop different $R_\mu - \mu - T$ relationships for all different geological profiles and ranges of SDOF systems so as to have a choice of the most appropriate relationship for use in practice.

Further studies are needed to verify whether pushover analysis has the tendency to underestimate displacement demands for systems with periods lower than half the predominant pulse period of the near-fault ground motion and to overestimate displacement

demands for systems with period equal or larger to half the dominant pulse period of the near-fault ground motion.

Additionally it would be of interest to check if pushover analysis performs satisfactorily for systems with period close to the maximum Fourier Amplitude period of a ground motion.

It would be appropriate to study the method for systems subjected to simpler loading time-histories, such as sine waves or pulses that are characterized by smaller amount of dominant frequencies and in which the distribution of frequencies is clearly defined.

Additionally the applicability of the methods needs to be assessed to more reinforced concrete structural systems with the inclusion in the analyses of infill panels, semi-rigid beam-column connections, semi-rigid floor diaphragms, in order to bound its potential and limitations. Also the effect of soil-structure interaction needs to be adequately addressed.

REFERENCES

Akiyama H. (1988), 'Earthquake Resistant Design Based on the Energy Concept', paper 8-1-2, Vol. V, IX WCEE, Tokyo-Kyoto, August 2-9.

Akkar S.D., Miranda E.M., (2005) ' Statistical Evaluation of Approximate Methods for Estimating Maximum Deformation Demands on Existing Structures', *Journal of Structural Engineering, ASCE, 131(1), 160-172.*

Akkar S.D., Yazgan U., Gulkan P., (2005) 'Drift Estimates in Frame Buildings Subjected to Near-Fault Ground Motions', *Journal of Structural Engineering, ASCE, 131(7), 1014-1024.*

Alavi B., Krawinkler H., (2001), 'Effects of near-fault ground motions on frame structures' *TR 138: The John A. Blume Earthquake Engineering Center, Stanford University, Stanford.*

Albanesi T., Nuti C., Vanzi I., (2000) 'A Simplified Procedure to Assess the Seismic Response of Nonlinear Structures', *Earthquake Spectra, Vol. 16, No. 4, pp. 715-734.*

Albanesi T., Biondi S., Petrangeli. (2002) 'Pushover analysis: An energy based approach.' *Proceedings of the 12th European Conference on Earthquake Engineering, Paper 605. Elsevier Science Ltd.*

Almeida R. F., Barros R. C. (2003) 'A New Multimode Load Pattern for Pushover Analysis: the Effect of Higher Modes of Vibration.' In: *Earthquake Resistant Engineering Structures IV, Ed.: G. Latini and C.A. Brebbia, WIT Press, U.K., p. 3-13.*

Anderson J.G., Sucuoğlu H., Erberik A., Yılmaz T., (2000) 'Strong Motions from the 1999 Kocaeli Earthquake: Implications for Seismic Hazard Analysis', *Earthquake Spectra, Supplement A to Vol. 16, 113-137.*

Antoniou, S. (2002) 'Advanced Inelastic Static Analysis for Seismic Assessment of Structures', *PhD Thesis, Engineering Seismology and Earthquake Engineering Section, Imperial College, London, UK*.

Antoniou S., Pinho R. (2004) 'Development and verification of a displacement-based adaptive pushover procedure'. *Journal of Earthquake Engineering, Vol. 8, No. 5, pp.643-661.*

Archer G.C., (2001) 'A Constant Displacement Iteration Algorithm for Nonlinear Static Push-Over Analyses', *Electronic Journal of Structural Engineering, Vol. 2, 120-134*.

Aschheim M. A., Maffei J., Black E. (1998), 'Nonlinear Static Procedures and Earthquake Displacement Demands." *Proceedings of 6th U.S. National Conference on Earthquake Engineering*, *Earthquake Engineering Research Institute, Seattle, WA.*

Applied Technology Council (ATC). (1996). 'Seismic evaluation and retrofit of concrete buildings.' *Rep. No. ATC-40,* Volumes 1 and 2, Redwood City, Calif.

Applied Technology Council (ATC). (2005). 'Improvement of nonlinear static seismic analysis procedures.' *Rep. No. ATC-55,* Redwood City, California.

Baez J. I., Miranda E., (2000), 'Amplification factors to estimate inelastic displacement demands for the design of structures in the near field', *Proceedings of the 12th World Conference on Earthquake Engineering, CD-ROM, Paper 1561, New Zealand Society for Earthquake Engineering, Auckland*.

Baik S.-W., Lee D.-G., Krawinkler H.(1988) 'A simplified model for seismic response prediction of steel frame structures', *Proc. 9th world conference earthquake engineering., Tokyo, Kyoto, Vol. 5, , pp. 375-380*.

Barros R.C., Almeida R., (2005) 'Pushover Analysis of Asymmetric Three-Dimensional Building Frames', *Journal of Civil Engineering and Management, Vol.XI, No. 1, 3-12.*

Bazant Z.P., Oh B.H., (1985) 'Microplane model for progressive fracture of concrete and rock.', *Journal of Engineering Mechanics, Trans. ASCE 111, 559–582.*

Bertero V.V., Aktan A.E., Charney F.A., Sause R., (1984) 'U.S. - Japan Cooperative Earthquake Research Program: Earthquake Simulation Tests and Associated Studies of a l/5th Scale Model of a 7-Story Reinforced Concrete Test Structure', *Report No. UBC/EERC-84/05, University of California, Berkeley.*

Bertero V.V., Uang C., (1997) 'Issues and Future Directions in the Use of an Energy Approach for Seismic-Resistant Design of Structures' , in *Nonlinear Seismic Analysis and Design of Reinforced Concrete Buildings, P. Fajfar and H. Krawinkler, Eds., Elsevier Applied Science, London and New York, 3-21.*

Bischoff P.H., Perry S.H. (1991) 'Compressive behaviour of concrete at high strain rates.', *Materials and Structures, Vol. 24, 425-450.*

Bracci J. M, Kunnath S. K. Reinhorn A. M. (1997) 'Seismic performance and retrofit evaluation of reinforced concrete structures.'*, ASCE, ST Division 123(1), 3-10.*

Chai Y.H., Fajfar P., Romstad K.M, (1998), 'Formulation of duration-dependent inelastic seismic design spectrum', *Journal of Structural Engineering,* ASCE, *124, 913-921.*

Chintanapakdee C., Chopra A.K. (2003) 'Evaluation of Modal Pushover Analysis Using Generic Frames.' *Earthquake Engineering & Structural* Dynamics, 32, 417-442.

Chintanapakdee C., Chopra A.K. (2004) 'Seismic Response of Vertically Irregular Frames: Response History and Modal Pushover Analyses', *Journal of Structural Engineering, ASCE, 130, 1177-1185.*

Choi W.H, Lee D.G., (2001), 'Evaluation of Seismic Performance for Multistorey Buildings using improved Capacity Spectrum Method', *The Eighth East Asia-Pacific*

Conference on Structural Engineering and Construction, Paper No. 1404, 5-7 December, Nanyang Technological University, Singapore.

Chopra A. (1995). "Dynamics of Structures: Theory and Applications to Earthquake Engineering", Prentice Hall.

Chopra A.K., Goel R.K. (1999). 'Capacity-Demand-Diagram Methods Based on Inelastic Design Spectrum', *Earthquake Spectra, Vol. 15, No. 4, pp. 637-656.*

Chopra A.K., Goel R.K. (2000). 'Evaluation of NSP to estimate seismic deformation: SDF systems.' *Journal of Structural Engineering,* 126(4), 482-490.

Chopra A.K., Goel R.K. (2001). 'A modal pushover analysis procedure for estimating seismic demands for buildings: Theory and preliminary evaluation.' *PEER Report 2001/2003, Pacific Earthquake Engineering Research Center, College of Engineering, University of California, Berkeley.*

Chopra A.K., Goel R.K. (2002). 'A modal pushover analysis procedure for estimating seismic demands for buildings.' *Earthquake Engineering and Structural Dynamics,* 31(3), 561 -582.

Chopra A.K., Goel R.K. (2003) 'A Modal Pushover Analysis Procedure to Estimate Seismic Demands for Buildings: Summary and Evaluation.' *5th National Conference on Earthquake Engineering*, *May, Istanbul, Turkey*.

Chopra A.K., Goel R.K., Chintanapakdee C. (2003), 'Statistics of single-degree-of-freedom estimate of displacement for pushover analysis of buildings.' *ASCE, Journal of Structural Engineering, 119:459-469.*

Chopra A.K., Chintanapakdee C. (2004). 'Inelastic deformation ratios for design and evaluation of structures.' ASCE, *Journal of Structural Engineering*, 130: 1309-1319.

Chopra A.K., Goel R.K, Chintanapakdee C. (2004). 'Evaluation of a Modified MPA Procedure Assuming Higher Modes as Elastic to Estimate Seismic Demands.' *Earthquake Spectra, 20, 757-778.*

Clough R., Penzien J. (1993) 'Dynamics of Structures', McGraw-Hill, New York.

Coleman J., Spacone E., (2001) 'Localization Issues in Nonlinear Force-Based Frame Elements.' *ASCE Journal of Structural Engineering, 127(11), 1257-1265.*

Cosenza E., Manfredi G., (1992), 'Seismic analysis of degrading models by means of damage functions concept', in *Nonlinear Seismic Analysis and Design of Reinforced Concrete Buildings, P. Fajfar and H. Krawinkler, Eds., Elsevier Applied Science, London and New York, 77-93.*

D'Ayala D., Free M., Bilham R., Doyle P., Evans R., Greening P., May R., Stewart A., Teymur B., Vince D., (2003), 'The Kocaeli, Turkey Earthquake of 17 August 1999: *A Field Report By EEFIT', Institution of Structural Engineers, London.*

Deierlein G., Hsieh S.H. (1990), 'Seismic response of steel frames with semi-rigid connections using the capacity spectrum method' *Proceedings 4th US National Conference on Earthquake Engineering, Vol.2, 863-72.*

Dolsek M., Fajfar P. (2004). 'Inelastic spectra for infilled reinforced concrete frames.' *Earthquake Engineering and Structural Dynamics, 33, 1395-1416.*

Dolsek M., Fajfar P. (2005). 'Simplified nonlinear seismic analysis of infilled reinforced concrete frames.' *Earthquake Engineering and Structural Dynamics, 34, 49-66.*

EC8 (2003) *Eurocode 8: Design of Structures for Earthquake Resistance. General Rules, Seismic Actions and Rules for Buildings*. EN1998-1:2003, British Standards Institution, London.

Elnashai A.S. (2000) 'Advanced inelastic static (pushover) analysis for seismic design and assessment,' *G. Penelis International Symposium on Concrete and Masonry Structures, Aristotle University of Thessaloniki, Greece.*

Elnashai A.S. (2002) 'Do we really need inelastic dynamic analysis?' *Journal of Earthquake Engineering* 6 *(Special Issue 1), 123-130.*

Faella G. (1996) 'Evaluation of RC structures seismic response by means of nonlinear static pushover analyses', *11th World Conference on Earthquake Engineering*, *Acapulco, Mexico, Paper no. 1146.*

Fajfar P. (2000). 'A nonlinear analysis method for performance-based seismic design", *Earthquake Spectra*, Vol.16, No. 3, 573-592.

Fajfar P., Fischinger M., (1987) 'Non-linear Seismic Analysis of RC Buildings: Implications of a Case Study', *European Earthquake Engineering, 1, 31-43.*

Fajfar P., Fischinger M. (1988) 'N2 – A Method for Non-linear Seismic Analysis of Regular Structures.' *Proc. 9th World Conf. on Earthquake Engineering*, *Tokyo/Kyoto*, *Vol. 5, 111-116.*

Fajfar P., Fischinger M. (1990), 'Earthquake Design Spectra Considering Duration of Ground Motion', *Proc. 4th U.S. National Conference on Earthquake Engineering., Palm Springs, California, Vol. 2, pp. 15-24.*

Fajfar P., Fischinger M. (1990), 'A Seismic Procedure Including Energy Concept', *Proceedings of IX ECEE, Moscow, September, Vol. 2, 312-321.*

Fajfar P., Gaspersic P. (1996), 'The N2 method for the seismic damage analysis for RC buildings.' *Earthquake Engineering Structural Dynamics*, *25(1), 23–67.*

Fajfar P., Gaspersic P., Drobnic D. (1997), 'A simplified nonlinear method for seismic damage analysis of structures.', *Proceedings Workshop on Seismic Design Methodologies for the Next Generation of Codes, Rotterdam; Balkema*.

Fajfar P., Krawinkler H. (2004), 'Performance-Based Seismic Design Concepts and Implementation - *Proceedings of the International Workshop Bled, Slovenia, June 28 - July 1, 2004. PEER Report 2004/05, College of Engineering, University of California, Berkeley.*

FEMA (2000), 'Prestandard and Commentary for the Seismic Rehabilitation of Buildings.', *Report FEMA 356*, Federal Emergency Management Agency, Washington DC.

Fischinger F., Fajfar P., (1990), 'On the Response Modification Factors for Reinforced Concrete Buildings,' *Proc. 4th U.S. National Conference on Earthquake Engineering, Palm Springs, California, Vol. 2, pp. 249-258.*

Freeman S.A., (1978), 'Prediction of Response of Concrete Buildings to Severe Earthquake Motion,' Douglas McHenry *International Symposium on Concrete and Concrete Structures, SP-55, American Concrete Institute, Detroit, Michigan, pp. 589-605.*

Freeman S.A., (1998). 'Development and Use of Capacity Spectrum Method', *Proceedings of 6th US National Conference on Earthquake Engineering, Seattle, Washington, U.S.A., Paper No. 269.*

Freeman S.A., Nicoletti J.P., Tyrell J.V. (1975). 'Evaluations of Existing Buildings for Seismic Risk - A Case Study of Puget Sound Naval Shipyard, Bremerton, Washington', *Proceedings of U.S. National Conference on Earthquake Engineering, Berkeley, U.S.A., pp. 113-122.*

Fuentes F.S., Sakai Y., Kabeyasawa T., (2001) 'Nonlinear Static Analysis Considering Effects of Higher Mode', *The Eighth East Asia-Pacific Conference on Structural*

Engineering and Construction, Paper No. 1472, 5-7 December, Nanyang Technological University, Singapore.

Fujii K., Nakano Y., Sanada Y., (2004) 'A Simplified Nonlinear Analysis Procedure for Single-Story Asymmetric Buildings', *Journal of Japan Association for Earthquake Engineering, Vol. 4 No.2.*

Gaspersic P., Fajfar P., Fischinger M. (1992), 'An approximate method for seismic damage analysis of buildings', *Proc. I0th world conference in earthquake engineering, Balkema, Rotterdam, Vol. 7, pp. 3921-3926.*

Ghosh K.S., Munshi J.A., (1996) 'Assessment of Seismic Performance of a Code Designed Reinforced Concrete Building', *Proceedings of the 11th World Conference on Earthquake Engineering, No. 756, Acapulco, Mexico.*

Goel R.K., Chopra A.K. (2003) 'Evaluation of Modal and FEMA Pushover Analyses: SAC Buildings.', *Earthquake Spectra, Vol. 20(1), 225-254.*

Goel R.K., Chopra A.K. (2005) 'Role of Higher-'Mode' Pushover Analyses in Seismic Analysis of Buildings.', *Earthquake Spectra, Vol. 21(4), 1027-1041.*

Gulkan P., Sozen M.A. (1974) 'Inelastic response of reinforced concrete structures to earthquake motions.', *ACI Journal 71, 601-610.*

Gupta B., (1998) 'Enhanced pushover procedure and inelastic demand estimation for performance-based seismic evaluation of buildings', Ph.D. Dissertation, Orlando, Florida, University of Central Florida.

Gupta B., Kunnath S.K. (1999) 'Pushover analysis of isolated flexural reinforced concrete walls.' *Structural Engineering in the 21st Century, Proc. Structures Congress, New Orleans.*

Gupta B., Kunnath S.K. (2000) 'Adaptive spectra-based pushover procedure for seismic evaluation of structures.' *Earthquake Spectra*, 16 (2), 367–391.

Hamburger R.O., (1997) 'Defining Performance objectives', Proceedings of the International Workshop *on Seismic design methodologies for the next generation of codes, , P. Fajfar and H. Krawinkler, eds., Bled, Slovenia, 33-42.*

Henmandez-Montes E., Kwon O.-S., Aschheim M. (2004), 'An energy-based formulation for first- and multiple-mode nonlinear static (pushover) analyses.' *Journal of Earthquake Engineering, 8(1), 69-88.*

Hilber H.M., Hughes T.J.R., Taylor R.L. (1977). 'Improved Numerical Dissipation for Time Integration Algorithms in Structural Dynamics.', *Earthquake Engineering and Structural Dynamics, Vol. 5: 283-292.*

Hosseini M., Vayeghan F.Y. (2000) 'Design Verification of an Existing 8-Story Irregular Steel Building by 3-D Dynamic and Pushover Analyses', *Proceedings of the 12th World Conference on Earthquake Engineering, CD-ROM, Paper 0609, New Zealand Society for Earthquake Engineering, Auckland.*

Iervolino I., Manfredi G., Cosenza E., (2006) 'Ground Motion Duration Effects on Nonlinear Seismic Response' *Earthquake Engineering and Structural Dynamics, Vol. 35, pp. 21-38.*

Inel M., Tjhin T., Aschheim A., (2003), 'The significance of lateral load pattern in pushover analysis'. *Fifth National Conference on Earthquake Engineering, May 26-30, Istanbul, Turkey, Paper AE-009.*

Iwan W.D., (1999) 'Implications of Near-Fault Ground Motion for Structural Design' *Proceedings of the US-Japan Workshop on Performance-Based Earthquake Engineering Methodology for R/C Building Structures, PEER Center Report, UC Berkeley - 17-25, Maui, Hawai.*

Jan, T.S., Liu, M.W., Kao, Y.C., (2004), 'An upper-bound pushover analysis procedure for estimating the seismic demands of high-rise buildings.' *Engineering Structures, 26(1), 117-128.*

Jingjiang S., Ono T., Yangang Z., Wei W., (2003), 'Lateral load pattern in pushover analysis.' *Earthquake Engineering and Engineering Vibration, Vol. 2(1), 99-107.*

Jun D.H., Kang P.D., Kim J.U., (2001), 'The Response Characteristics of Pushover Analysis with Variations in the Upper Stories of the Multi-Purpose Building Structures', *The Eighth East Asia-Pacific Conference on Structural Engineering and Construction, Paper No. 1187, 5-7 December, Nanyang Technological University, Singapore.*

Kabeyasawa T., Shiohara H., Otani S., Aoyama H., (1983) 'Analysis of the Full-Scale Seven Story Reinforced Concrete Test Structure', *Journal of the Faculty of Engineering, The University of Tokyo. Vol. XXXVII, 431-478.*

Kalkan E., Kunnath S.K., (2004) ' Method of Modal Combinations for Pushover Analysis of Buildings', *13th World Conference on Earthquake Engineering, August 1-6, Vancouver, Canada, Paper 2713.*

Kalkan E., Kunnath S.K., (2004) 'Lateral load distribution in nonlinear static procedures for seismic design', *Structures ASCE, http://www.ascelibrary.org/.*

Kalkan E, Kunnath S.K. (2006) 'Adaptive modal combination procedure for nonlinear static analysis of building structures.' *ASCE Journal of Structural Engineering, 132(11), 1721-1731.*

Kalkan E, Kunnath S.K. (2007) 'Assessment of current nonlinear static procedures for seismic evaluation of buildings.', *Engineering Structures, 29, 305-316.*

Kappos A.J., Manafpour A., (2001) 'Seismic design of R/C buildings with the aid of advanced analytical techniques' *Engineering Structures*, *23, 319-332.*

Kilar, V., Fajfar, P. (1997) 'Simplified Pushover Analysis of Building Structures.' *Proceedings of the 11th World Conference on Earthquake Engineering, No. 1011, Acapulco, Mexico.*

Kilar V, Fajfar P. (1997) 'Simple Pushover Analysis of Asymmetric Buildings.' *Earthquake Engineering and Structural Dynamics; 26(2): 233-49.*

Kim S., D'Amore E., (1999) 'Pushover Analysis Procedure in Earthquake Engineering', *Earthquake Spectra, Vol. 15, No. 3, pp. 417-434.*

Kim S.D., Jeong S.C., (2001) 'Inelastic Behavior of 2-Story 2-Bay Steel Moment-Resisting Frame Under Pushover and Cyclic Loading Test', *The Eighth East Asia-Pacific Conference on Structural Engineering and Construction, Paper No. 1440, 5-7 December, Nanyang Technological University, Singapore.*

Kim S.D., Kim M.H., Kim S.J., (2001) 'Determination of System Ductility Capacity using Nonlinear Dynamic Analysis', *The Eighth East Asia-Pacific Conference on Structural Engineering and Construction, Paper No. 1442, 5-7 December, Nanyang Technological University, Singapore.*

Kramer S. (1996) Geotechnical earthquake engineering. Prentice Hall, New Jersey.

Krawinkler H. (1995) 'New trends in seismic design methodology.' *Proceedings 10th ECEE, The Netherlands, Rotterdam, pp. 821-830.*

Krawinkler H. (1996) 'Pushover Analysis: Why, How, When and When Not to Use It' *Structural Engineers Association of California, Stanford University, 17-36.*

Krawinkler H., Seneviratna G. (1998) 'Pros and Cons of a Pushover Analysis for Seismic Performance Evaluation.' *Engineering Structures*, *20, 452-464.*

Kunnath S.K. (2004). 'Identification of modal combinations for nonlinear static analysis of building structures.' *Computer-Aided Civil and Infrastructure Engineering, 19, 282-295.*

Kunnath S.K., Valles-Mattox R.E., Reinhorn A.M., (1996) 'Evaluation of Seismic Damageability of a Typical R/C Building in Midwest United States', *11th World Conference on Earthquake Engineering*, *Acapulco, Mexico.*

Kunnath S.K, Gupta B. (1999) 'Spectra-Compatible Pushover Analysis of Structures' *Proceedings of U.S.–Japan Workshop on Performance-Based Earthquake Engineering Methodology for Reinforced Concrete Building Structures, Sapporo, Hokkaido, Japan, 69–78.*

Kunnath S.K, Gupta B. (1999) 'Validity of deformation demand estimates using nonlinear static procedures.' *Proceedings of U.S.–Japan Workshop on Performance-Based Earthquake Engineering Methodology for Reinforced Concrete Building Structures, Sapporo, Hokkaido, Japan, 117–128.*

Kunnath S.K., John A.Jr. (2000), 'Validity of static procedures in performance-based seismic design', in *Proceedings of ASCE Structures Congress, Philadelphia*.

Kuramoto H., Teshigawara M., (1999) 'Prediction of Earthquake Response of Buildings using Equivalent Single-Degree-of-Freedom System', *Proceedings of the US-Japan Workshop on Performance-Based Earthquake Engineering Methodology for R/C Building Structures, PEER Center Report, UC Berkeley - 53-67, Maui, Hawaii.*

Lashkari-Irvani B., Krawinkler H. (1982), 'Damage Parameters for Bilinear Single Degree of Freedom Systems', *Vol. 3, 5-16, ECEE, Athens.*

Lawson R.S., Vance V., Krawinkler H. (1994) 'Nonlinear Static Pushover Analysis – Why, When and How?' *Proc. 5th US Conf. on Earthquake Engineering*, *Chicago IL, Vol. 1, 283-292.*

Lew H.S., Kunnath S.K., (2001) 'Evaluation of Nonlinear Static Procedures for Seismic Design of Buildings', *Presented at the 33rd Joint Meeting of the UJNR Panel on Wind and Seismic Effects, 1-17.*

Lin E., Pankaj P. (2004) 'Nonlinear static and dynamic analysis - the influence of material modelling in reinforced concrete frame structures.', *13th World Conference on Earthquake Engineering, Paper No 430, Vancouver, Canada.*

Long P., Limin S., Lichu F., (2001) 'Evaluation of PC Continuous Girder Bridge with High Piers by Means of Nonlinear Pushover Analyses', *The Eighth East Asia-Pacific Conference on Structural Engineering and Construction, Paper No. 1336, 5-7 December, Nanyang Technological University, Singapore.*

Lowes L., (1999) 'Finite Element Modeling of Reinforced Concrete Beam Column Bridge Connections,' PhD dissertation, University of California, Berkeley, California.

Lubliner J., Oliver J., Oller S., Onate E., (1989) 'A plastic-damage model for concrete' *Int. J. Solids and Struct., 25(3), 299-326.*

LUSAS *Finite Element Program*, Version 14.1, FEA Ltd., Surrey, UK

McCabe S. L., Hall W. J., (1989), 'Assessment of seismic structural damage.', *Journal of Structural Engineering, ASCE, 115, 2166-2183.*

MacRae G.A, Morrow D.V, Roeder C.W., (2001) 'Near-fault ground motion effects on simple structures.', *Journal of Structural Engineering, ASCE, Vol. 127, 996-1004.*

Magenes G. (2000), 'A method for pushover analysis in seismic assessment of masonry buildings'. *12 WCEE, CD-ROM, Paper 1866, New Zealand.*

Mahaney J.A., Paret T.F., Kehoe B.E., Freeman S.A. (1993). 'The Capacity Spectrum Method for Evaluating Structural Response during the Loma Prieta Earthquake' in *'Earthquake Hazard Reduction in the Central and Eastern United States: A Time for*

Examination and Action', Proceedings of 1993 National Earthquake Conference, Earthquake Engineering Research Institute, Oakland, CA, U.S.A., pp. 501-510.

Makarios T.K., (2004) 'Optimum definition of equivalent non-linear SDF system in pushover procedure of multistory r/c frames', *Engineering Structures, Vol. 27, pp 814-825.*

Matsumori T., Otani S., Shiohara H., Kabeyasawa T. (1999) 'Earthquake member deformation demands in reinforced concrete frame structures', *Proceedings of the US-Japan Workshop on Performance-Based Earthquake Engineering Methodology for R/C Building Structures, PEER Center Report, UC Berkeley - 79-94, Maui, Hawaii.*

Medina R.A, Krawinkler H., (2005) 'Evaluation of Drift Demands for the Seismic Performance Assessment of Frames', *Journal of Structural Engineering, ASCE, 131(7), 1003-1013.*

Memari A.M., Rafiee S., Motlagh A.Y., Scanlon A., (2001) 'Comparative Evaluation of Seismic Assessment Methodologies Applied to a 32-Story Reinforced Concrete Office Building', *JSEE, Vol. 3, No. 1, 31-43.*

Meyer I.F., Kratzing W.B., Stangerberg F., Meskouris K. (1988), 'Damage Prediction in Reinforced Concrete Frames Under Seismic Actions', *European Earthquake Engineering, No. 3, 9-15.*

Miranda, E., (1991) 'Seismic Evaluation and Upgrading of Existing Buildings,' *Ph.D. Thesis*, University of California at Berkeley.

Miranda E., (1993a), 'Evaluation of site-dependent inelastic seismic design spectra,' *Journal of Structural Engineering, ASCE, Vol. 119, No. 5, 1319-1338.*

Miranda E., (1993b) 'Site-Dependent Strength Reduction Factors,' J*ournal of Structural Engineering, ASCE, Vol. 119, No. 12, 3503-3519.*

Miranda E., (2000), 'Inelastic displacement ratios for displacement-based earthquake resistant design', *Proceedings of the 12th World Conference on Earthquake Engineering Auckland, CD-ROM, Paper 1096, New Zealand Society for Earthquake Engineering.*

Miranda E., Bertero V.V., (1994), 'Evaluation of Strength Reduction Factors for Earthquake-Resistant Design,' *Earthquake Spectra, Earthquake Engineering Research Institute, Oakland, California, Vol. 10, No. 2.*

Moehle J.P. (1992), 'Displacement based design of RC structures', *Proc. I0th world conference in earthquake engineering, Balkema, Rotterdam, Vol. 8, pp. 4297-4302.*

Moghadam A.S., Tso W.K. (1996) 'Damage Assessment of Eccentric Multistory Buildings using 3D Pushover Analysis'. *11WCEE, Elsevier Science, Paper No. 997.*

Moghadam A.S., Tso W.K. (1998) 'Pushover analysis for asymmetrical multistorey buildings.' 6th US *National Conference on Earthquake Engineering, Seattle, Washington.*

Moghadam A.S, Tso W.K. (2000) '3-D Pushover analysis for Damage Assessment of Buildings.' *JSEE, Vol. 2, No.3.*

Moghaddam H., Hajirasouliha I., (2006) 'An investigation on the accuracy of pushover analysis for estimating the seismic deformation of braced steel frames.', *Journal of Computational Steel Research, 62, 343-351.*

Mostafaei H., Kabeyasawa T. (2001) 'Correlation between Nonlinear Time History Analysis and Capacity-Demand Diagram Method.' *1st International Conference on Concrete and Development*, *Tehran, Iran, Vol. 2, 143-152.*

Mwafy A.M., Elnashai A.S. (2000) 'Static Pushover versus Dynamic Collapse Analysis of RC Buildings', *Journal of Engineering Structures, 23, pp. 407-424, 2001.*

Naeim F., Lobo R.M., (1998) 'Common Pitfalls in Pushover Analysis', *SEAOC Convention, T1-T13.*

NEHRP – National Earthquake Hazard Reduction Program (1997), 'NEHRP Recommended Provisions for Seismic Regulations for New Buildings and Other Structures', Federal Emergency Management Agency, Report No. FEMA 302, Washington, D.C.

Newmark N.M. (1959) 'A method of computation for structural dynamics.', *Journal of Engineering Mechanics Division, Proceedings ASCE, Vol. 85(EM3), 67-94.*

Newmark, N.M., Hall, W.J., (1973) 'Seismic Design Criteria for Nuclear Reactor Facilities,' Report No. 46, Building Practices for Disaster Mitigation, National Bureau of Standards, U.S. Department of Commerce, 209-236.

Okamoto S., Kitagawa Y., Nakata S., Yoshimura M., Kaminosono T., (1984) 'U.S. - Japan Cooperative Research on R/C Full-Scale Building Test, Part *2:* Damage Aspects and Response Properties before Repair Works', *Proceedings 8th WCEE, San Francisco, Prentice Hall, Vol. VI., 593-706.*

Pankaj P., Lin E., (2005) 'Material modeling in the seismic response analysis for the design of RC framed structures.', *Engineering Structures, Vol. 27, pp 1014-1023.*

Papanikolaou V.K., Elnashai A.S., (2005) 'Evaluation of Conventional and Adaptive Pushover Analysis I: Methodology' Journal of *Earthquake Engineering, Vol. 9, No. 6, 923-941.*

Papanikolaou V.K., Elnashai A.S., Pareja J.F., (2005) 'Evaluation of Conventional and Adaptive Pushover Analysis II: Comparative Results' *Journal of Earthquake Engineering, Vol. 10, No. 1, 127-151.*

Parducci A., Comodini F., Lucarelli M., Mezzi M., Tomassoli E. (2006) 'Energy-Based Non Linear Static Analysis.', *1st European Conference on Earthquake Engineering and Seismology Paper 1178*, *Geneva, Switzerland.*

Paret T.F., Sasaki K.K., Eilbeck D.H., Freeman S.A. (1996). 'Approximate Inelastic Procedures to Identify Failure Mechanisms from Higher Mode Effects', *Proceedings of the 11th World Conference on Earthquake Engineering, No. 966, Acapulco, Mexico.*

Park Y.J., Ang A.H. (1985). 'Mechanistic Seismic Damage Model for Reinforced Concrete'*, Journal of Structural Division, Proc. ASCE, Vol. 111, No. ST4, pp. 740-757.*

Park, Y.J., Ang, H.S., Wen, Y.K. (1985) 'Seismic damage analysis of reinforced concrete buildings,' *Journal of Structural Engineering*, *111(4), 740-757.*

Penelis G.G, Kappos A.J. (1997) Earthquake-resistant concrete structures. London: E & FN SPON (Chapman & Hall).

Penelis G.G, Kappos A.J. (2002) '3D Pushover Analysis: The Issue of Torsion', *12th European Conference on Earthquake Engineering, Paper No. 015*.

Peter K., Badoux M., (2000) 'Application of the Capacity Spectrum Method to R.C. Buildings with Bearing Walls' *Proceedings of the 12th World Conference on Earthquake Engineering Auckland, CD-ROM, Paper 0609, New Zealand Society for Earthquake Engineering.*

Phan V., Saiidi M., Anderson J., (2005). 'Near Fault (Near Field). Ground Motion Effects on Reinforced Concrete Bridge Column.*', Center of Civil Engineering Earthquake Research, Department of Civil Engineering, University of Nevada, Reno, Nevada, Report No. CCEER-05-7.*

Pinho, R., Elnashai, A.S. (2000) 'Dynamic collapse testing of a full-scale four story RC frame', *ISET Journal of Earthquake Technology 37(4) (Special Issue), 143-164.*

Priestley M.J.N., Calvi G.M. (1997), 'Concepts and procedures for direct displacement-based design and assessment' *Seismic Design Methodologies for the Next Generation of Codes, Fajfar and Krawinkler (eds), Balkema, Rotterdam, 171-181.*

Ramirez O.M., Constantinou M.C., Kircher C.A., Whittaker A.S., Johnson M.W., Gomez J.D., Chrysostomou C.Z., (2001) 'Development and Evaluation of Simplified Procedures for Analysis and Design of Buildings with Passive Energy Dissipation Systems' *Technical Report MCEER-00-0010:Revision 1, University of Buffalo, State University of New York, New York.*

Rathje E.M., Abrahamson A., Bray J.D., (1998) 'Simplified Frequency Content Estimates of Earthquake Ground Motions', *Journal of Geotechnical and Geoenvironmental Engineering, Vol. 124, No.2, 150-159.*

Reinhorn A.M. (1996), 'Introduction to Dynamic and Static Inelastic Analysis Techniques', *Proceedings of the 1996 Annual Meeting, Los Angeles Tall Buildings Structural Design Council, Los Angeles, CA.*

Reinhorn A. (1997). 'Inelastic analysis techniques in seismic evaluations.' *Seismic design methodologies for the next generation of codes, Proc. of the International Workshop, P. Fajfar and H. Krawinkler, eds., Bled, Slovenia.*

Reinhorn A.M., Mander J.B., Bracci J., Kunnath S.K. (1990), 'A Post-Earthquake Damage Evaluation Strategy for R/C Buildings.', *Proceedings of Fourth U.S. National Conference on Earthquake Engineering, May 20-24, Palm Springs, Vol. 2, 1047-1056.*

Requena M., Ayala A.V. (2000), 'Evaluation of a simplified method for determination of the nonlinear seismic response of RC frames.' *12th World Conference on Earthquake Engineering*, *New Zealand, Paper 2109.*

Saiidi M., Sozen M.A. (1979). 'Simple and Complex Models for Nonlinear Seismic Response of Reinforced Concrete Structures', *Civil Engineering Studies, Report No 465, Univ. of Illinois, Urbana, Illinois.*

Saiidi M., Sozen M.A. (1981). 'Simple Nonlinear Seismic Analysis of R/C Structures', *Journal of the Structural Division, Vol. 107, ST5, ASCE, 937-952.*

Salonikios T., Karakostas C., Lekidis V., Anthoine A. (2003), 'Comparative inelastic pushover analysis of masonry frames' *Engineering Structures, Vol. 25, 1515-1523.*

Sasaki K.K., Freeman S.A., Paret T.F. (1998), 'Multi-Mode Pushover Procedure (MMP) — A Method to Identify the Effects of Higher Modes in a Pushover Analysis', *Proceedings of 6th US National Conference on Earthquake Engineering, Seattle, Washington, U.S.A., Paper No. 271.*

Sasani M., Bertero V.V., (2000) 'Importance of Severe Pulse-Type Ground Motions in Performance-Based Engineering: Historical and Critical Review.', *Proceedings of the 12th World Conference on Earthquake Engineering Auckland, Paper 1302, New Zealand Society for Earthquake Engineering.*

Satyarno I., Carr A.J., Restrepo J. (1998), 'Refined pushover analysis for the assessment of older reinforced concrete buildings.', *NZSEE Technology Conference*, *Wairakei, New Zealand, 75-82.*

SEAOC, (1995), 'Performance based seismic engineering of Buildings' *Vision 2000 Committee*, Structural Engineers Association of California, Sacramento, California.

Seismosoft, (2004). 'SeismoSignal - A Computer Program for the Processing of Strong Ground Motion Data' [online], available from URL: http//www.seismosoft.com.

Seneviratna G.D.P.K., (1995), 'Evaluation of Inelastic MDOF Effects for Seismic Design', *Ph.D. Dissertation,* Department of Civil Engineering. Stanford University.

Shome N., Bazzurro P., Comell C.A, Carballo J.E. (1998) 'Earthquakes, records, and nonlinear MDOF responses.' *Earthquake Spectra*, *Vol. 14, 469-500.*

Skokan M. J. Hart G.C. (2000) 'Reliability of Nonlinear Static Methods for the Seismic Performance Prediction of Steel Frame Buildings.' *Proceedings 12th World Conference on Earthquake Engineering, Paper No. 1972, Auckland, New Zealand.*

Somerville P.G., Smith N.F., Graves R.W., Abrahamson N.A. (1997). 'Modification of empirical strong ground motion attenuation relations to include the amplitude and duration effects of rupture directivity.', *Seismological Research Letters 68, 199-222.*

Somerville P.G., (2002). 'Characterizing Near Fault Ground Motion for the Design and Evaluation of Bridges', *Third National Conference and Workshop on Bridges and Highways, Portland, Oregon.*

Tembulkar J.M., Nau J.M. (1987), 'Inelastic Modeling and Seismic Energy Dissipation', *Journal of Structural Engineering. ASCE, Vol. 113, No. 6, 1373-1377.*

Tjhin T., Aschheim M., Hernandez-Montes E., (2005) 'Estimates of Peak Roof Displacement using "Equivalent" Single Degree of Freedom Systems.', *Technical Note, Journal of Structural Engineering. ASCE, Vol. 131(3), 517-522.*

Tjhin T., Aschheim M., Hernandez-Montes E., (2006) 'Observations on the Reliability of Alternative Multiple-Mode Pushover Analysis Methods' *Journal of Structural Engineering. ASCE, Vol. 132(3), 471-477.*

Tso W.K, Moghadam A.S. (1997) 'Seismic Response of Asymmetrical Buildings Using Pushover Analysis', In: *Fajfar P, Krawinkler, H, Editors. Seismic Design Methodologies for the Next Generation of Codes, Balkema, 311-322.*

Tso W.K., Moghadam A.S. (1998) 'Pushover procedure for seismic analysis of buildings', *Progress in Structural Engineering and Materials, Vol. 1, No.3, pp.337-344.*

Uang C.M., Bertero V.V. (1990). 'Evaluation of Seismic Energy in Structures', *Earthquake Engineering and Structural Dynamics, Vol. 19, 77-90.*

Vamvatsikos D., Cornell C.A. (2002). 'Incremental dynamic analysis.' *Earthquake Engineering and Structural Dynamics, Vol. 31(3), 491-514.*

Veletsos A.S., Newmark N.M., (1960) 'Effects of Inelastic Behavior on the Response of Simple Systems to Earthquake Ground Motions.' *Proceedings of 2nd World Conference Earthquake Engineering, Japan, Vol. II, 895-912.*

Veletsos A.S., Newmark N.M., Chelapati C.V., (1965) 'Deformation Spectra for Elastic and Elastoplastic Systems Subjected to Ground Shock and Earthquake Motions.' *Proceedings 3rd World Conference Earthquake Engineering, Wellington, New Zealand, Vol. 2, 663-680.*

Vian M.D., Bruneau M.M., (2003), 'Tests to Structural Collapse of Single Degree of Freedom Frames Subjected to Earthquake Excitations' *Journal of Structural Engineering. ASCE, Vol. 129(12), 1676-1685.*

Vidic T., Fajfar P., Fischinger M. (1994) 'Consistent inelastic design spectra: strength and displacement.' *Earthquake Engineering and Structural Dynamics, Vol. 23, 502-521.*

Wen Y.K. (1976), 'Method for Random Vibration of Hysteretic Systems', *J. Eng. Mech. Div., ASCE, 102(2), 249-263.*

Whittaker A., Constantinou M., Tsopelas P., (1998), 'Displacement estimates for performance-based seismic design'. *Journal of Structural Engineering, ASCE, 124, 905-912.*

Wight J.K., Burak B., Canbolat B.A., Liang X., (1997) 'Modelling and Software Issues for Pushover Analysis of RC Structures', *Seismic design methodologies for the next generation of codes, Proc. of the International Workshop, P. Fajfar and H. Krawinkler, eds., Bled, Slovenia.*

Williams M.S., Albermani F. (2003) 'Evaluation of Displacement-Based Analysis and Design Methods for Steel Frames with Passive Energy Dissipators.' *Civil Engineering Research Bulletin No. 24, Department of Civil Engineering, University of Queensland.*

Yang P., Wang Y., (2000) 'A Study on Improvement of Pushover Analysis' *Proceedings of the 12th World Conference on Earthquake Engineering Auckland, Paper 1940, New Zealand Society for Earthquake Engineering.*

Zahrah T.F., Hall W.J. (1984). 'Earthquake Energy Absorption in SDOF Structures', *Journal of Structural Division, Proc. ASCE, Vol. 110, No. ST8, pp. 1757-1772.*

Zou X.-K., Chan C.-M., (2004) 'Optimal seismic performance-based design of reinforced concrete buildings using nonlinear pushover analysis.', *Engineering Structures, Vol. 27, pp 1289-1302.*

APPENDIX A.

CONSTANT-DUCTILITY SPECTRA (CHOPRA, 1995)

The governing equation of an inelastic SDOF system is as follows:

$$m\ddot{u} + c\dot{u} + f_s(u,\dot{u}) = -m\ddot{u}_g(t) \quad \text{(A-1)}$$

where m is the mass, c is the viscous damping constant, and $f_s(u,\dot{u})$ is the resisting force of an elastoplastic SDOF system as shown in Figure A-1.

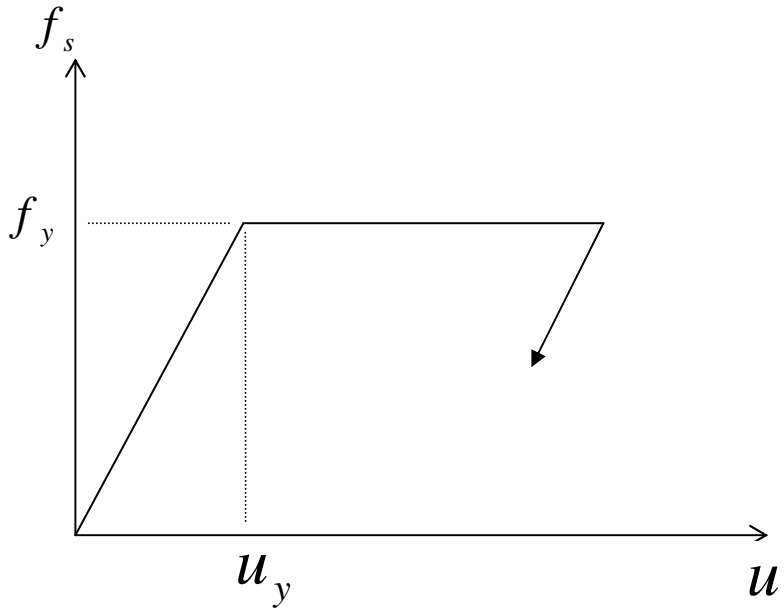

Figure A - 1 Typical elastoplastic system

In general for a given $\ddot{u}_g(t)$, $u(t)$ depends on ω_n, ζ, u_y and the form of the force-deformation relation. If eq. (A-1) is divided by *m* one can obtain:

$$\ddot{u} + 2\zeta\omega_n\dot{u} + \omega_n^2 u_y \tilde{f}_s(u,\dot{u}) = -\ddot{u}_g(t) \quad \text{(A-2)}$$

where $\omega_n = \sqrt{\frac{k}{m}}$, $\zeta = \frac{c}{2m\omega_n}$ and $\tilde{f}_s(u,\dot{u}) = \frac{f_s(u,\dot{u})}{f_y}$ (A-3)

The function $\tilde{f}_s(u,\dot{u})$ describes the force-deformation relation in a partially dimensionless form as shown in Figure A-2.

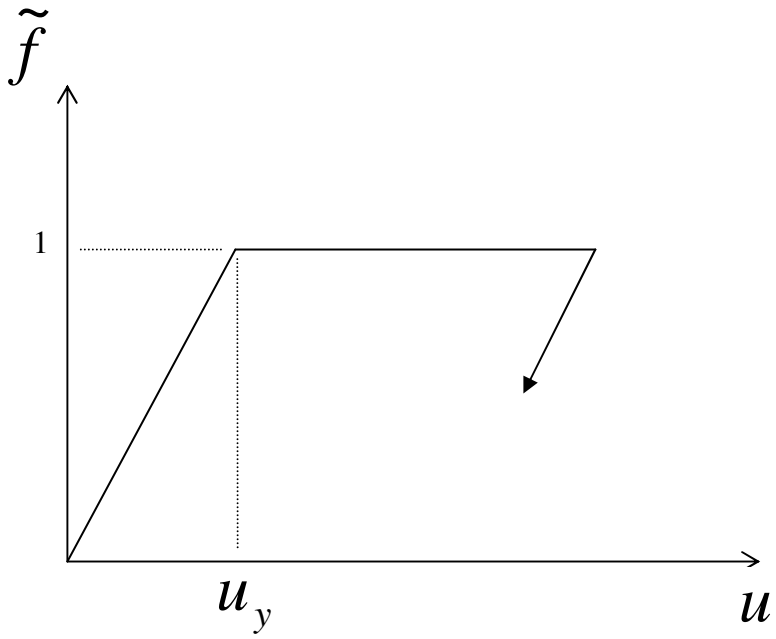

Figure A - 2 Force deformation relation in normalised form

Furthermore, for a given $\ddot{u}_g(t)$, the ductility factor μ depends on ω_n, ζ, $\bar{f}_y$ where $\bar{f}_y$ is the normalised yield strength of the elastoplastic system defined as:

$$\bar{f}_y = \frac{f_y}{f_e} = \frac{u_y}{u_e} \quad \text{(A-4)}$$

where f_e and u_e are the are the elastic strength and displacement of the corresponding linear SDOF system. The procedure for this proof is as follows. Equation (A-2) is rewritten

in terms of $\mu(t) = \frac{u(t)}{u_y}$. Therefore substituting for $u(t) = u_y \mu(t)$ $, \dot{u}(t) = u_y \dot{\mu}(t)$ and $, \ddot{u}(t) = u_y \ddot{\mu}(t)$ into equation (A-2) and dividing by u_y, yields:

$$\ddot{\mu} + 2\zeta\omega_n \dot{\mu} + \omega_n^2 \tilde{f}_s(\mu, \dot{\mu}) = -\omega_n^2 \frac{\ddot{u}_g(t)}{a_y} \quad \text{(A-5)}$$

where, $a_y = \frac{f_y}{m}$ can be interpreted as the acceleration of the mass necessary to produce the yield force f_y, *and* $\tilde{f}_s(\mu, \dot{\mu})$ is the force-deformation relationship in dimensionless form (Figure B-3).

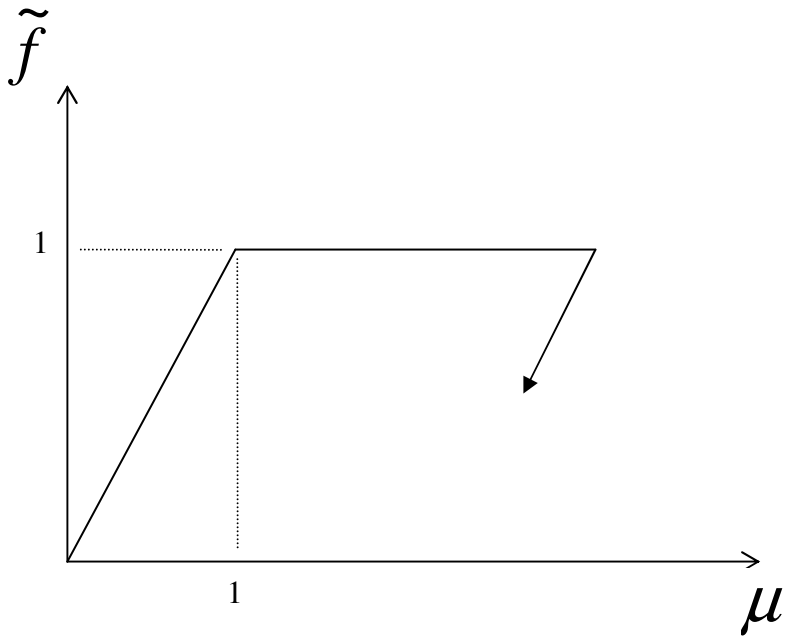

Figure A - 3 Force deformation relation in normalised form

Equation A-5 shows that for a given $\ddot{u}_g(t)$ and for a given $\tilde{f}_s(\mu, \dot{\mu})$ relationship, $\mu(t)$ depends on ω_n, ζ, a_y. In turn a_y depends on ω_n, ζ.

APPENDIX B

SDOF STUDY -DISPLACEMENT TIME-HISTORIES

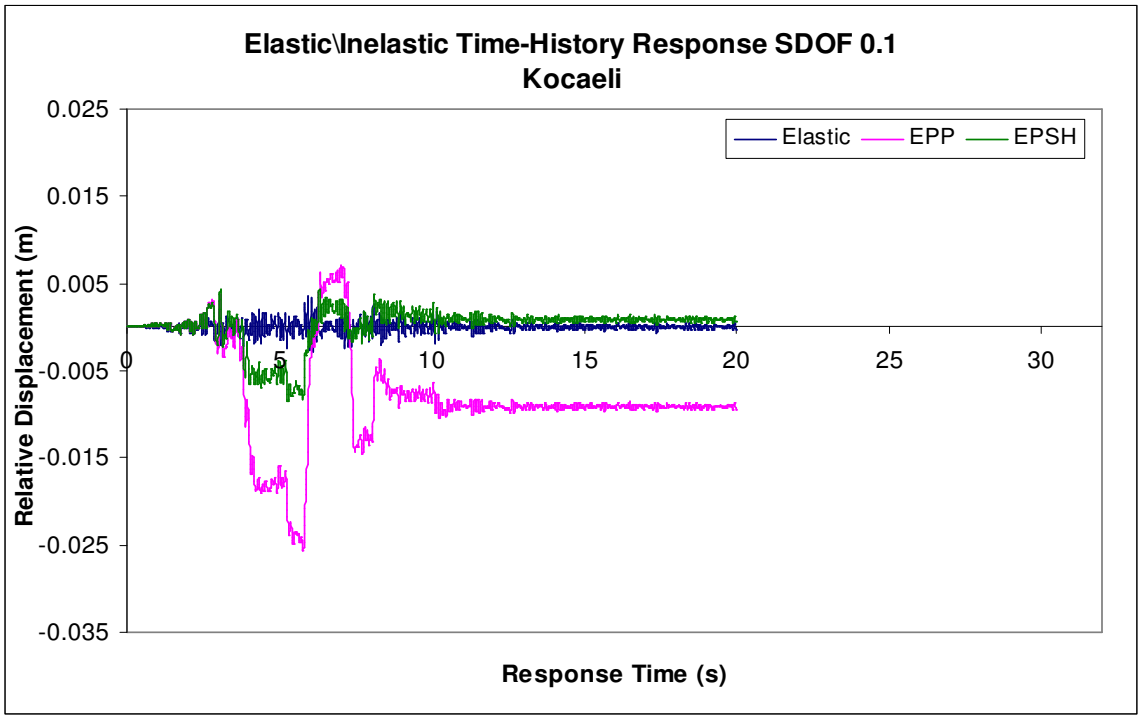

Figure B - 1 Displacement Time-Histories of SDOF 0.1 for the Kocaeli ground motion

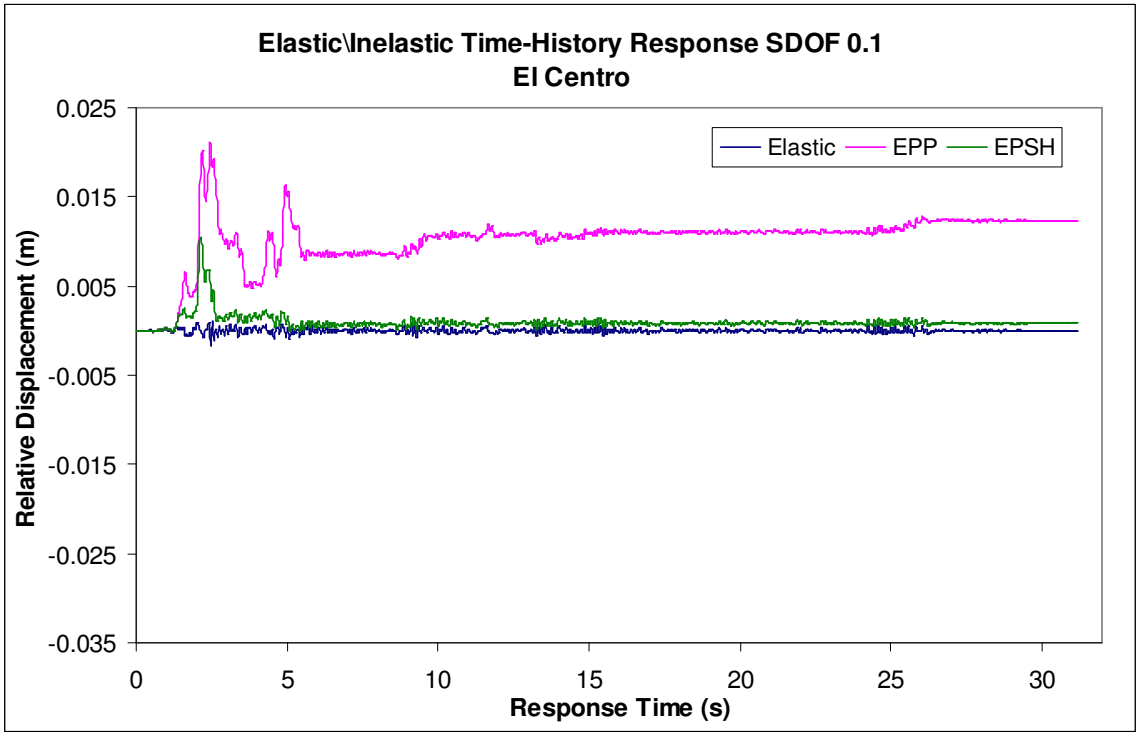

Figure B - 2 Displacement Time-Histories of SDOF 0.1 for the Kocaeli ground motion

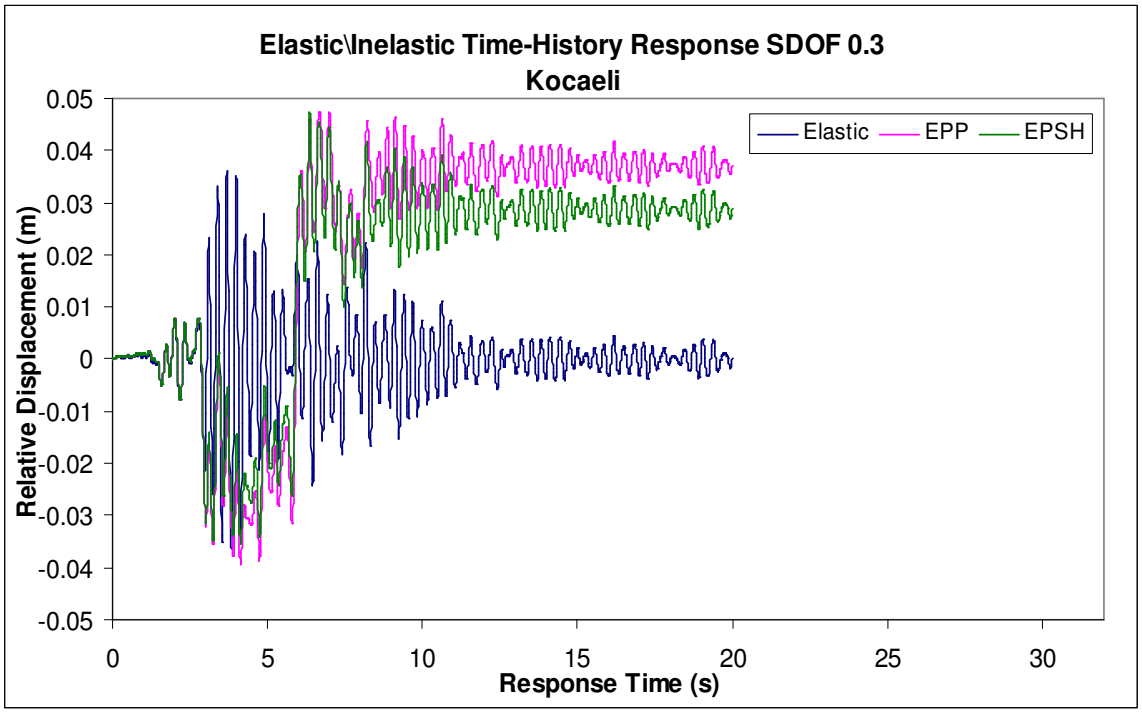

Figure B - 3 Displacement Time-Histories of SDOF 0.3 for the Kocaeli ground motion

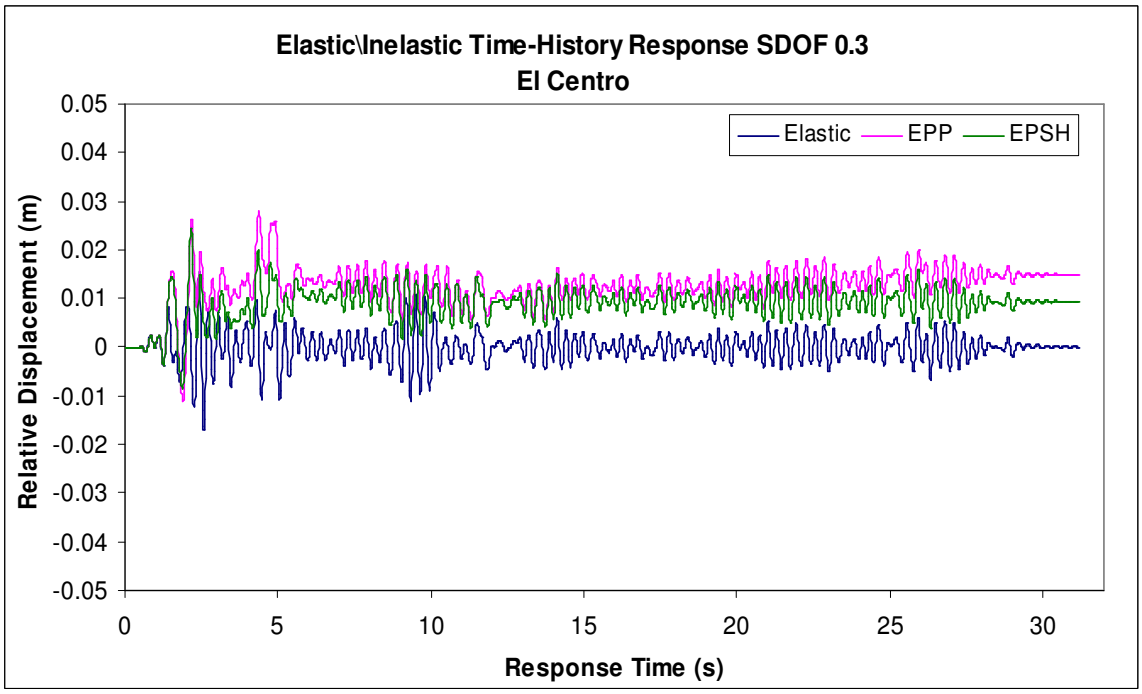

Figure B - 4 Displacement Time-Histories of SDOF 0.3 for the El Centro ground motion

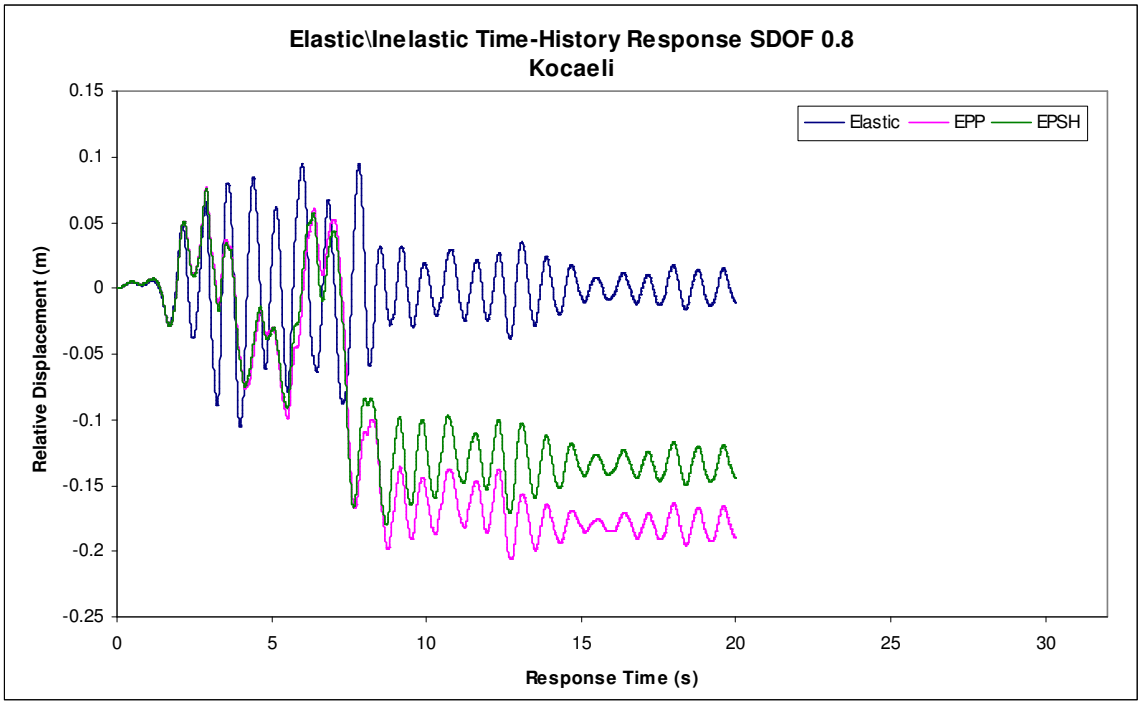

Figure B - 5 Displacement Time-Histories of SDOF 0.8 for the Kocaeli ground motion

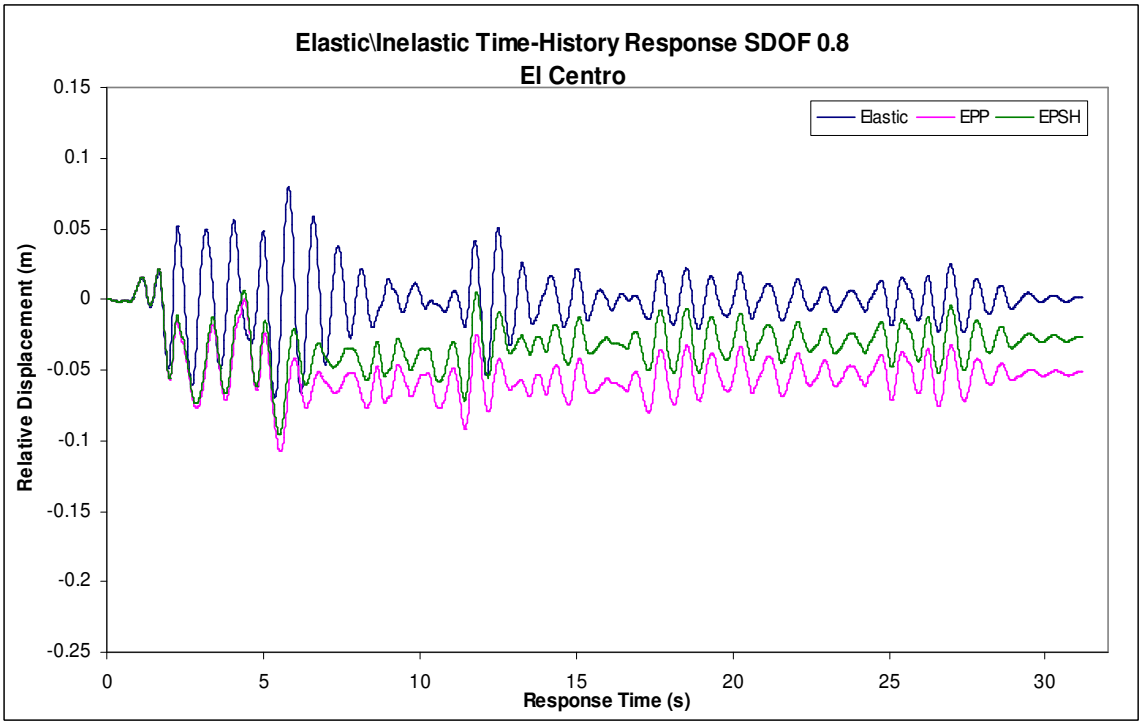

Figure B - 6 Displacement Time-Histories of SDOF 0.8 for the El Centro ground motion

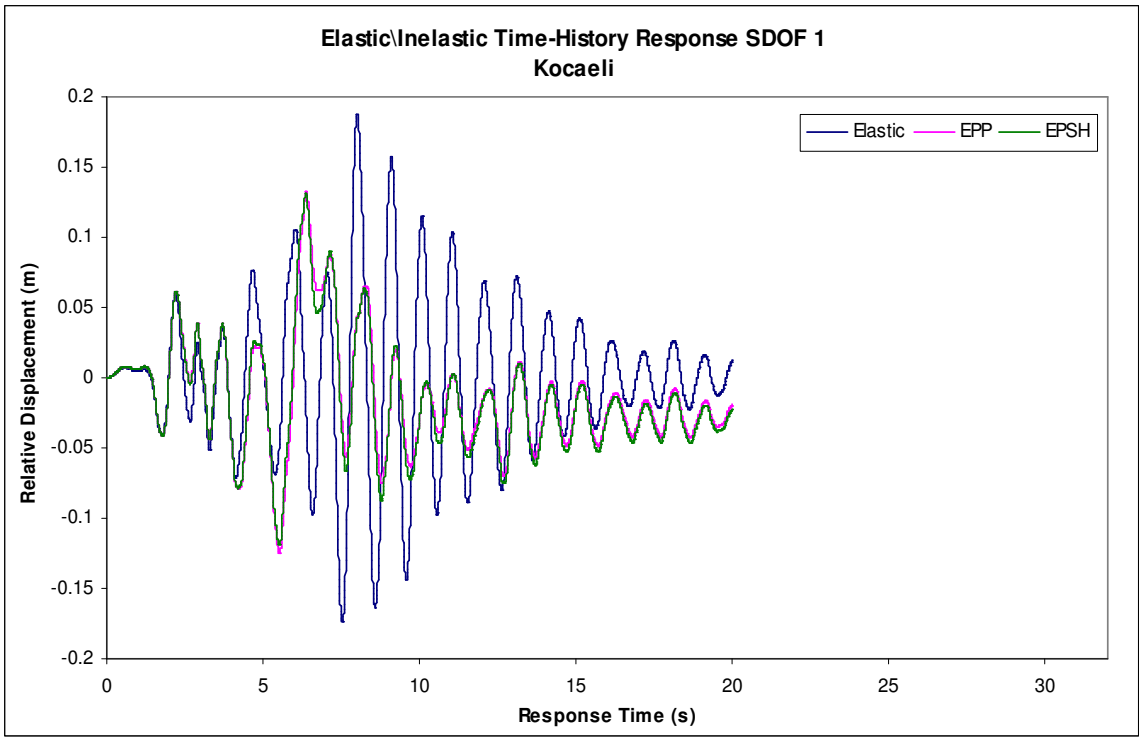

Figure B - 7 Displacement Time-Histories of SDOF 1 for the Kocaeli ground motion

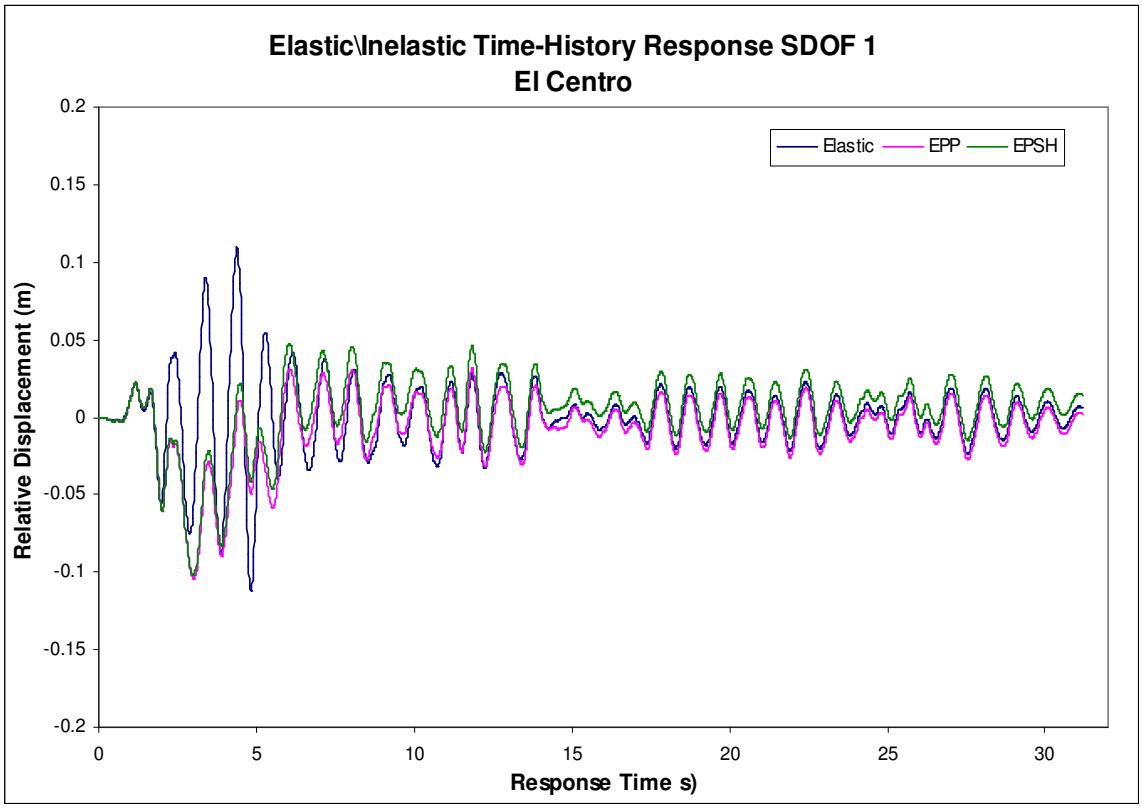

Figure B - 8 Displacement Time-Histories of SDOF 1 for the El Centro ground motion

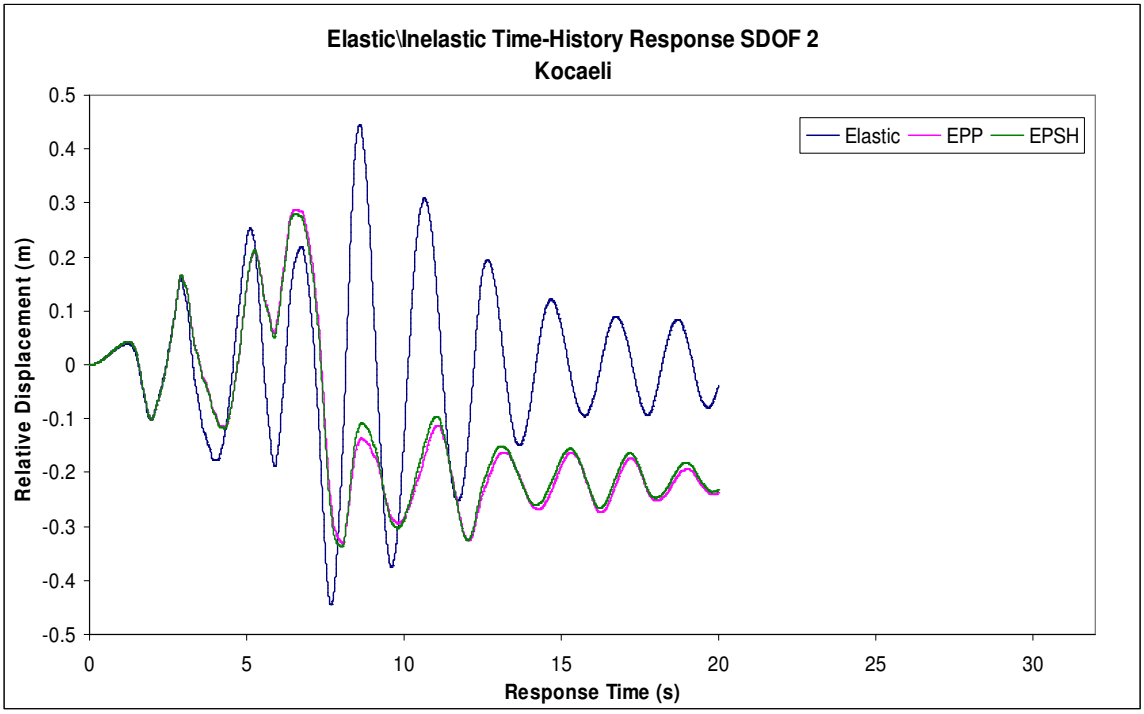

Figure B - 9 Displacement Time-Histories of SDOF 2 for the Kocaeli ground motion

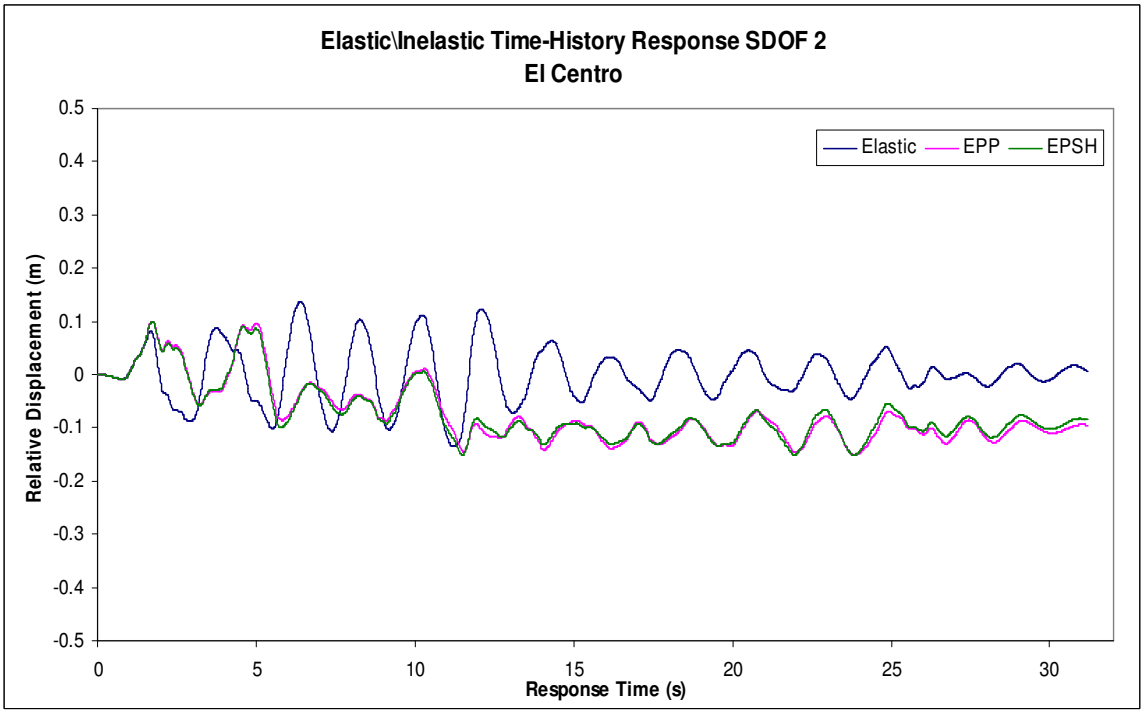

Figure B - 10 Displacement Time-Histories of SDOF 2 for the El Centro ground motion

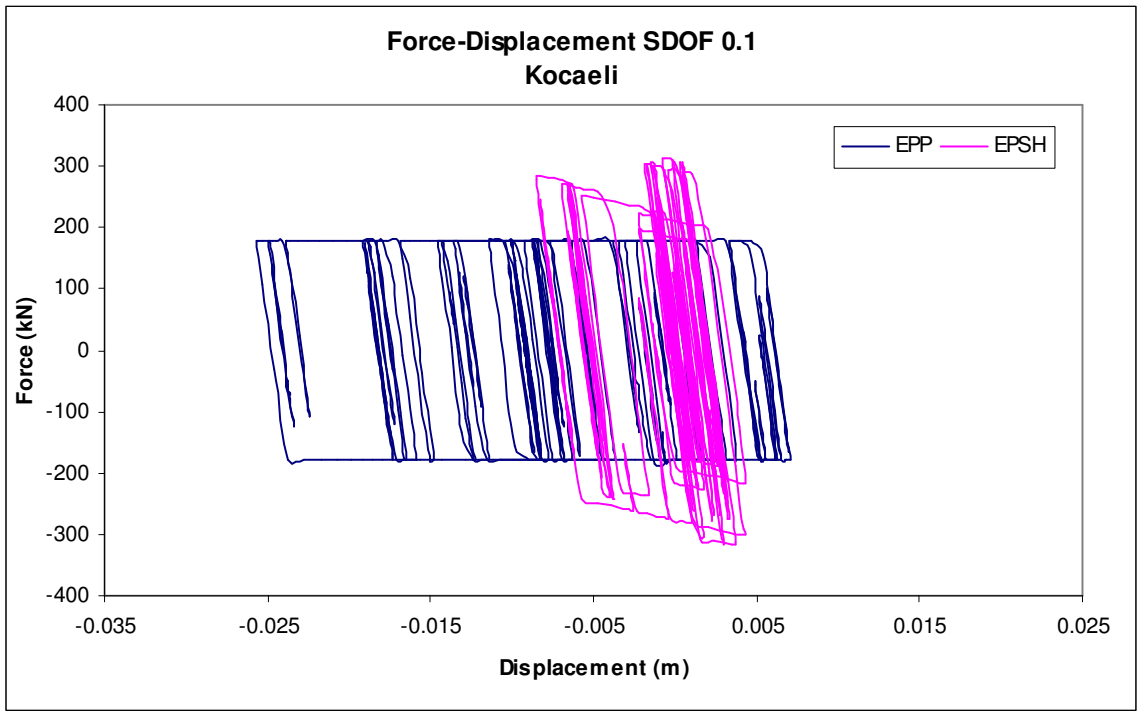

Figure B - 11 Force - Displacement Response of SDOF 0.1 system for the Kocaeli ground motion

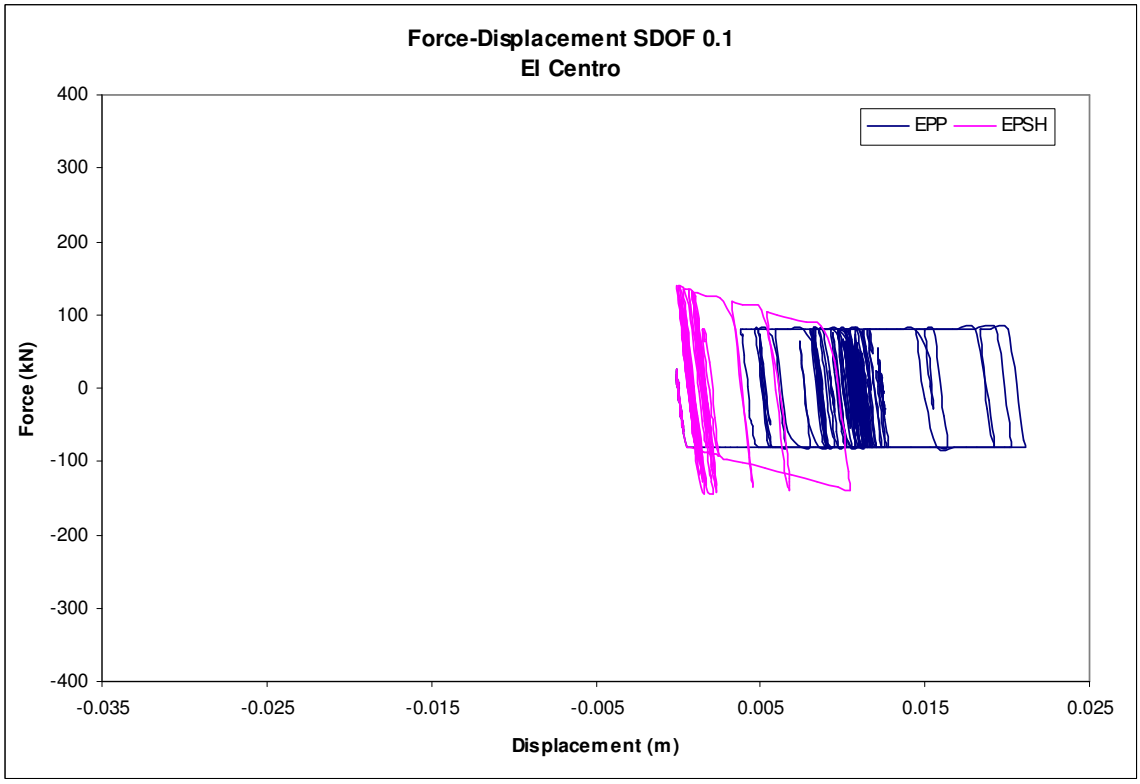

Figure B - 12 Force - Displacement Response of SDOF 0.5 system for the El Centro ground motio

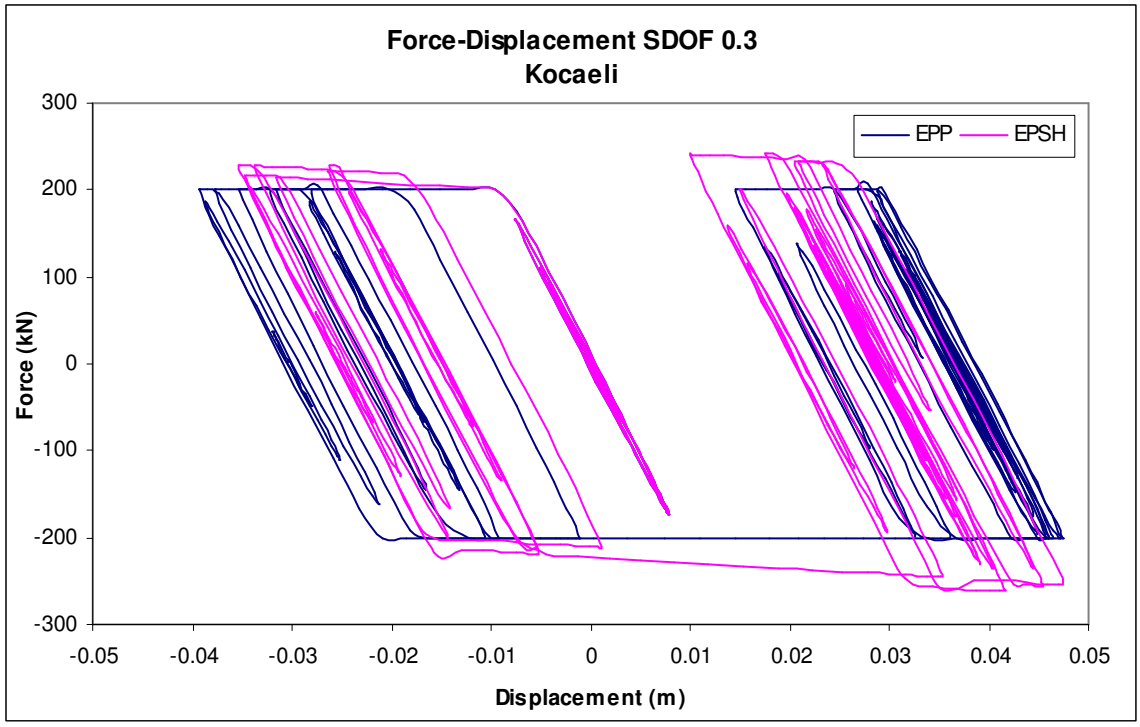

Figure B - 13 Force - Displacement Response of SDOF 0.3 system for the Kocaeli ground motion

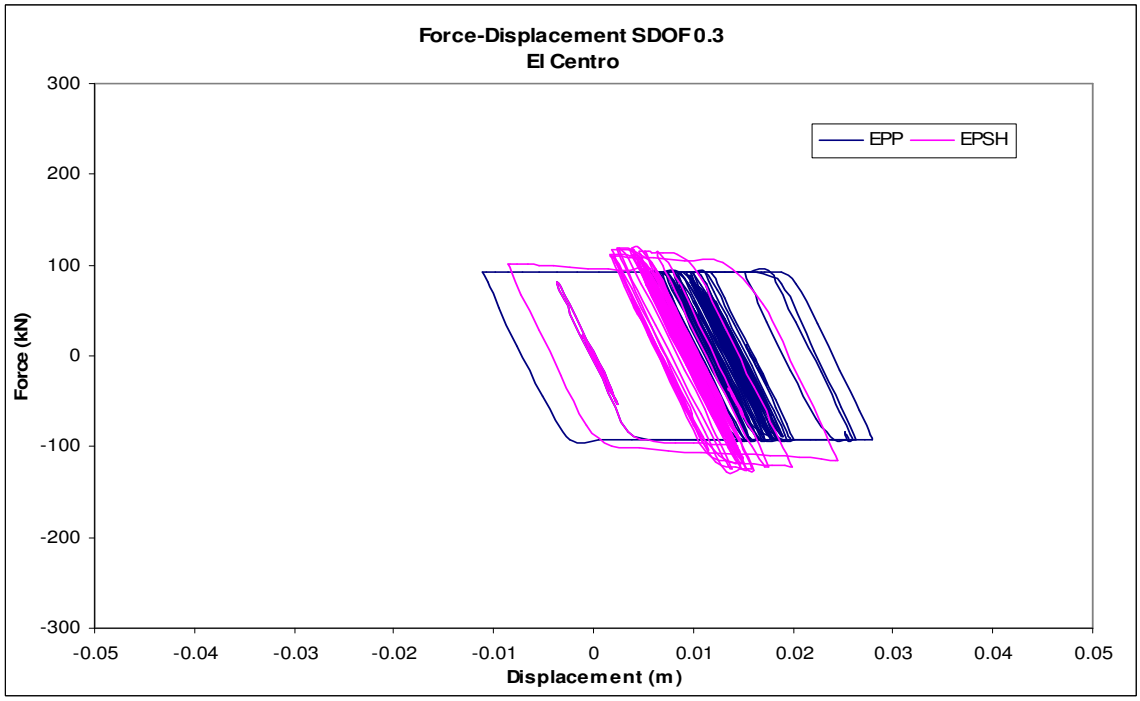

Figure B - 14 Force - Displacement Response of SDOF 0.3 system for the El Centro ground motion

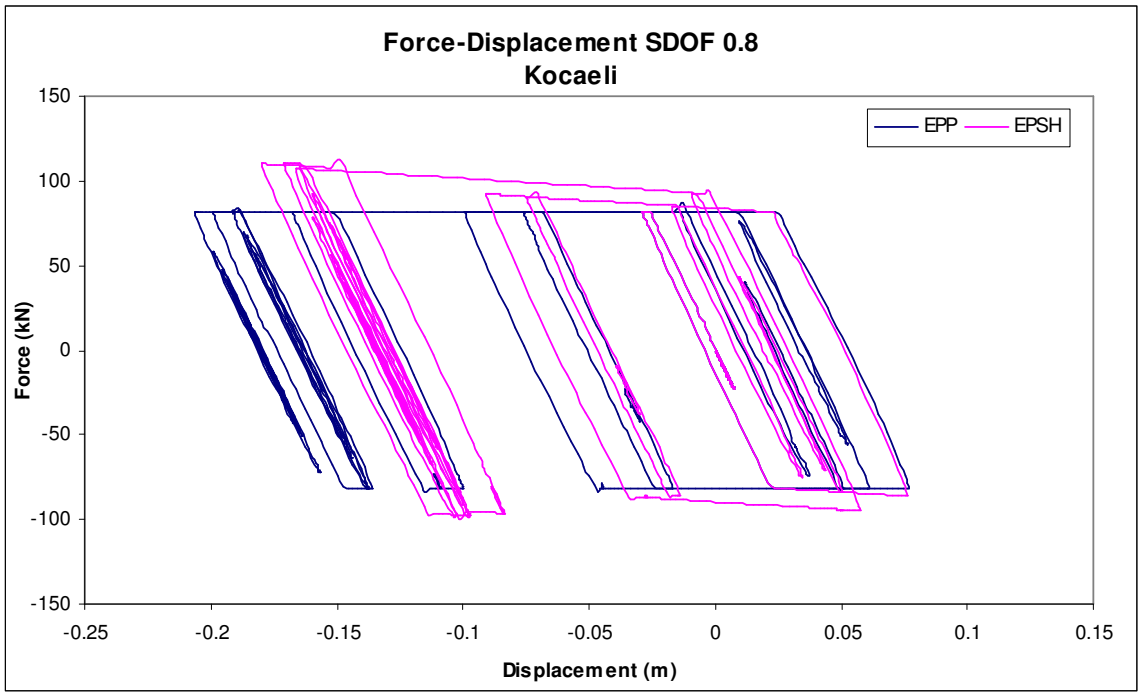

Figure B - 15 Force - Displacement Response of SDOF 0.8 system for the Kocaeli ground motion

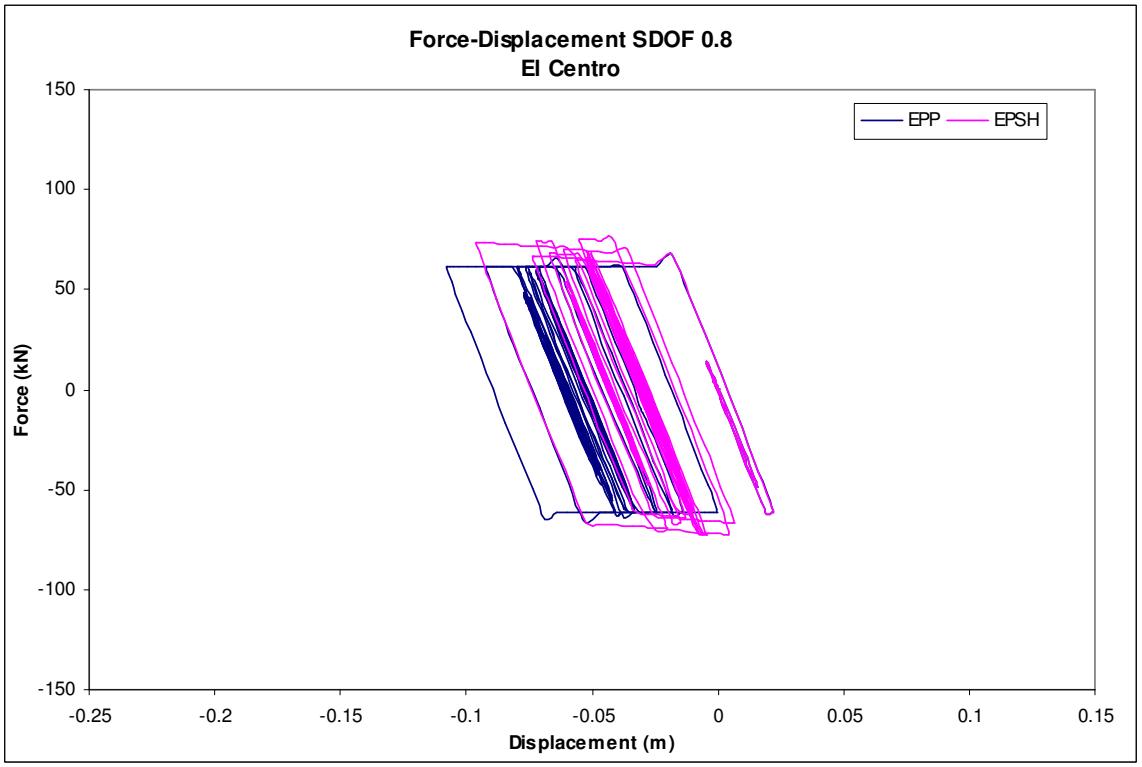

Figure B - 16 Force - Displacement Response of SDOF 0.8 system for the El Centro ground motion

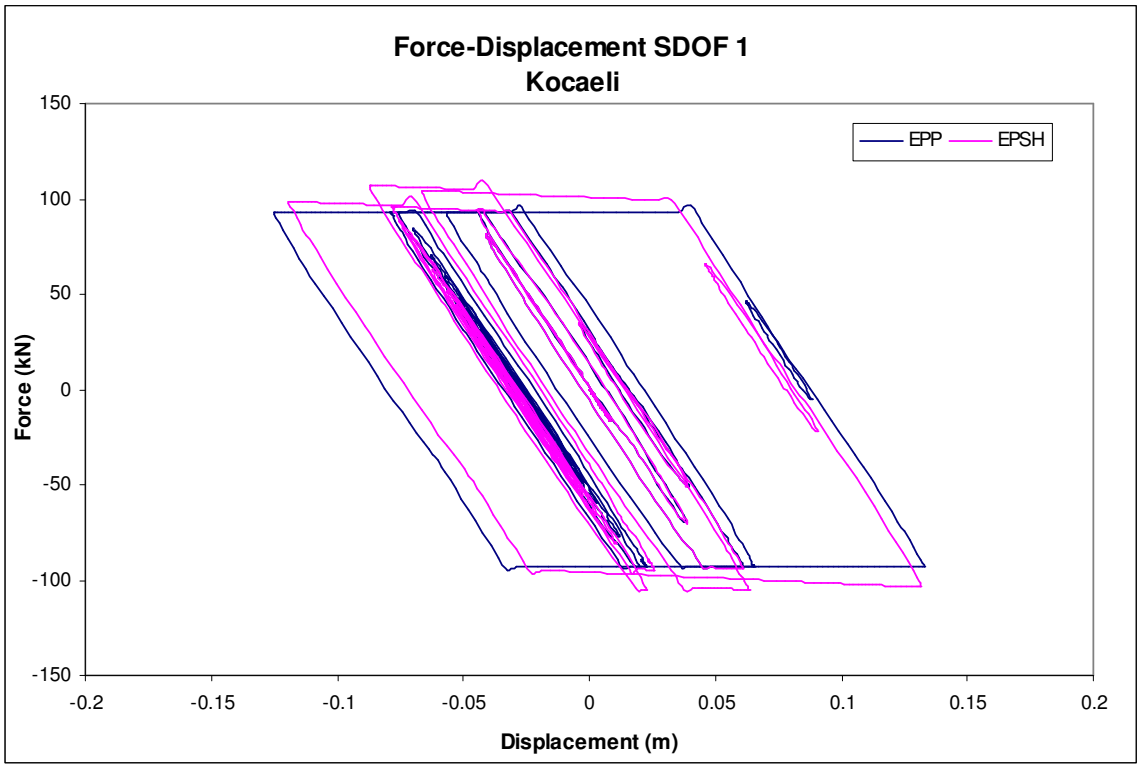

Figure B - 17 Force - Displacement Response of SDOF 1 system for the Kocaeli ground motion

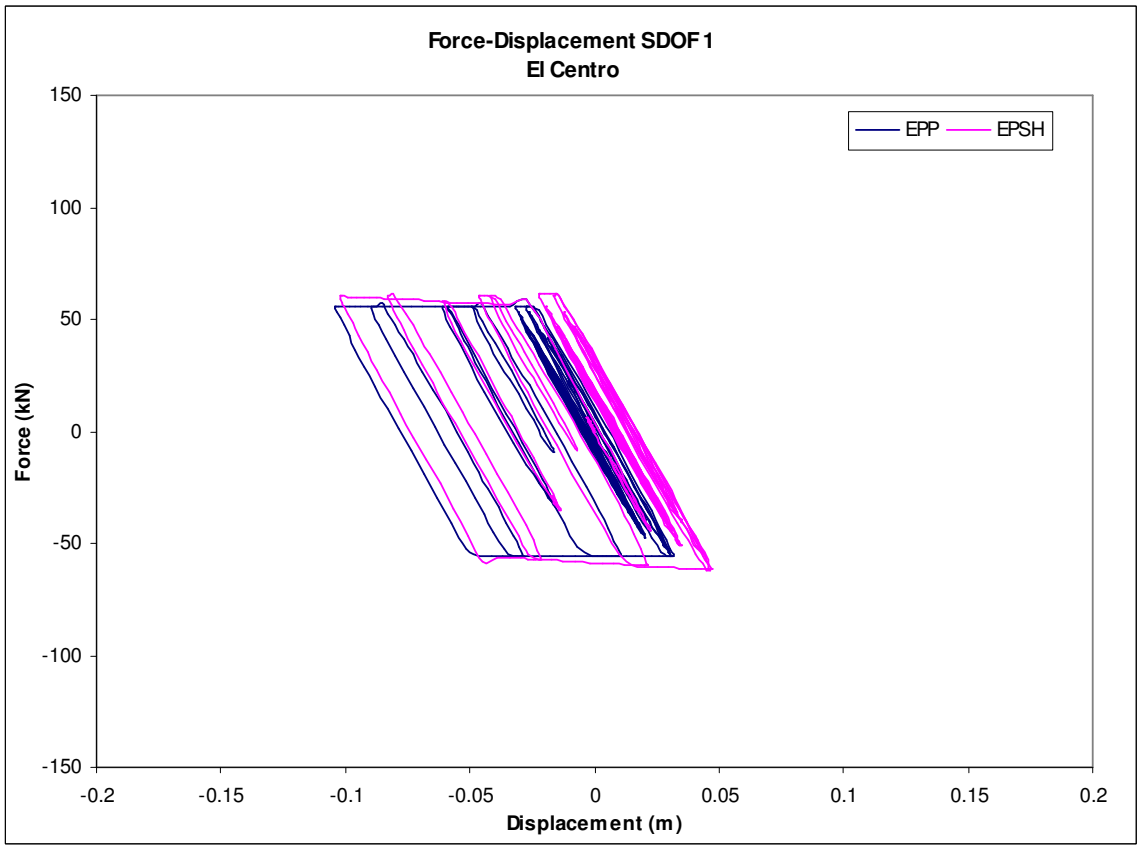

Figure B - 18 Force - Displacement Response of SDOF 1 system for the El Centro ground motion

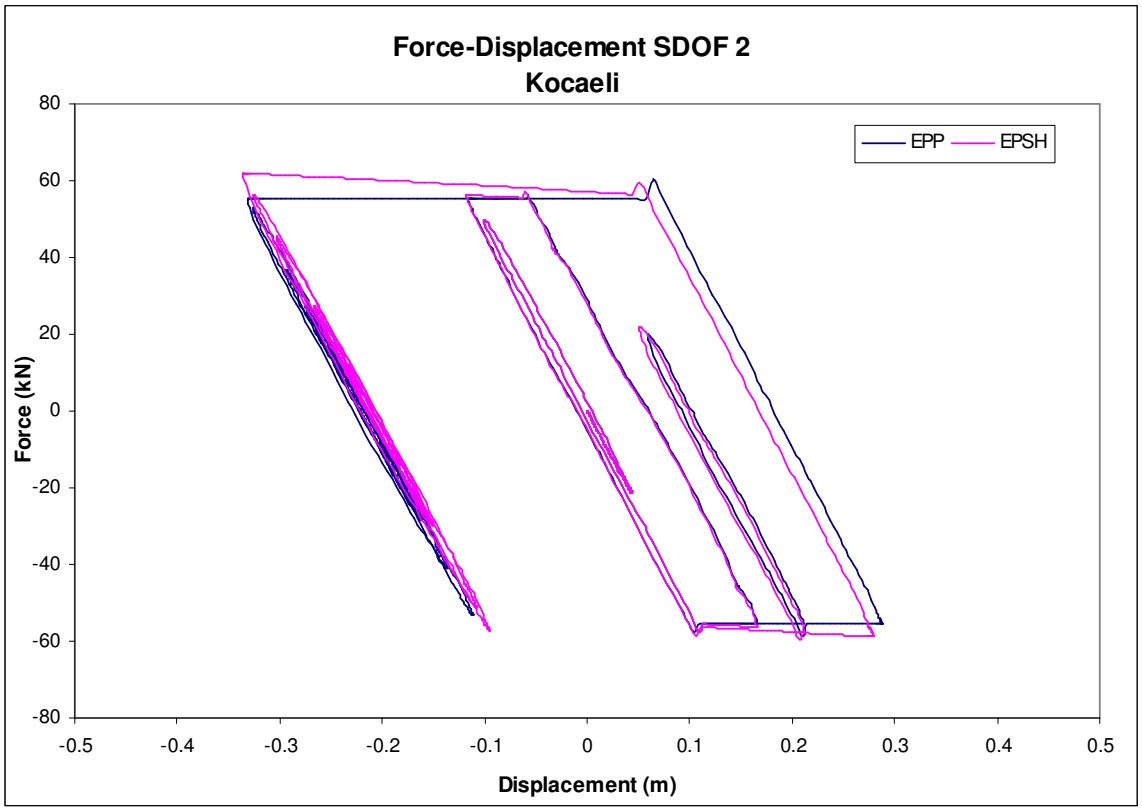

Figure B - 19 Force - Displacement Response of SDOF 2 system for the Kocaeli ground motion

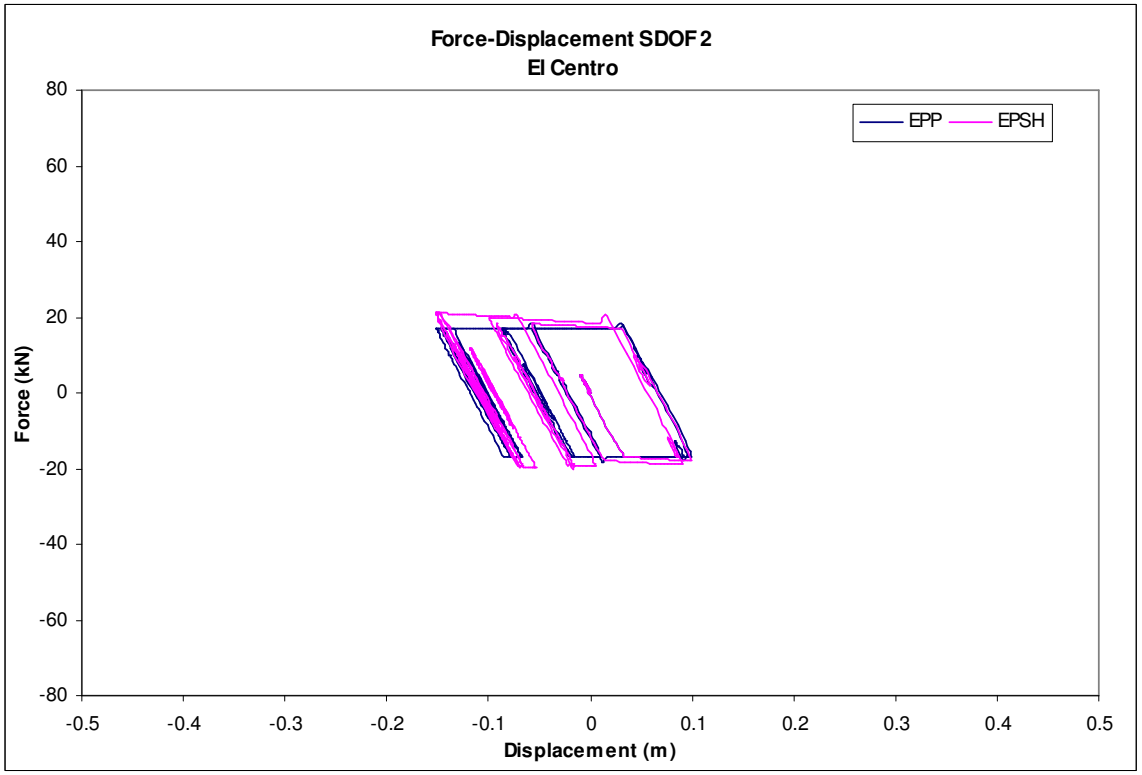

Figure B - 20 Force - Displacement Response of SDOF 2 system for the El Centro ground motion

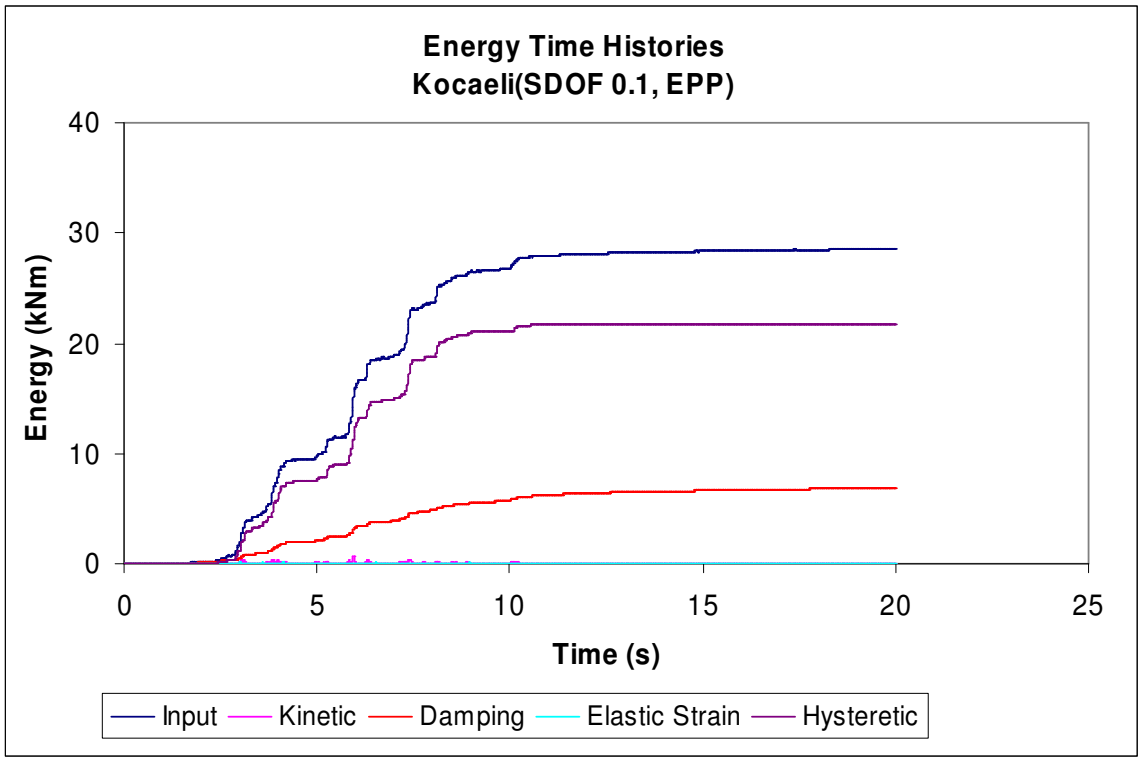

Figure B - 21 Energy Time-Histories SDOF 0.1, EPP, Kocaeli ground motion

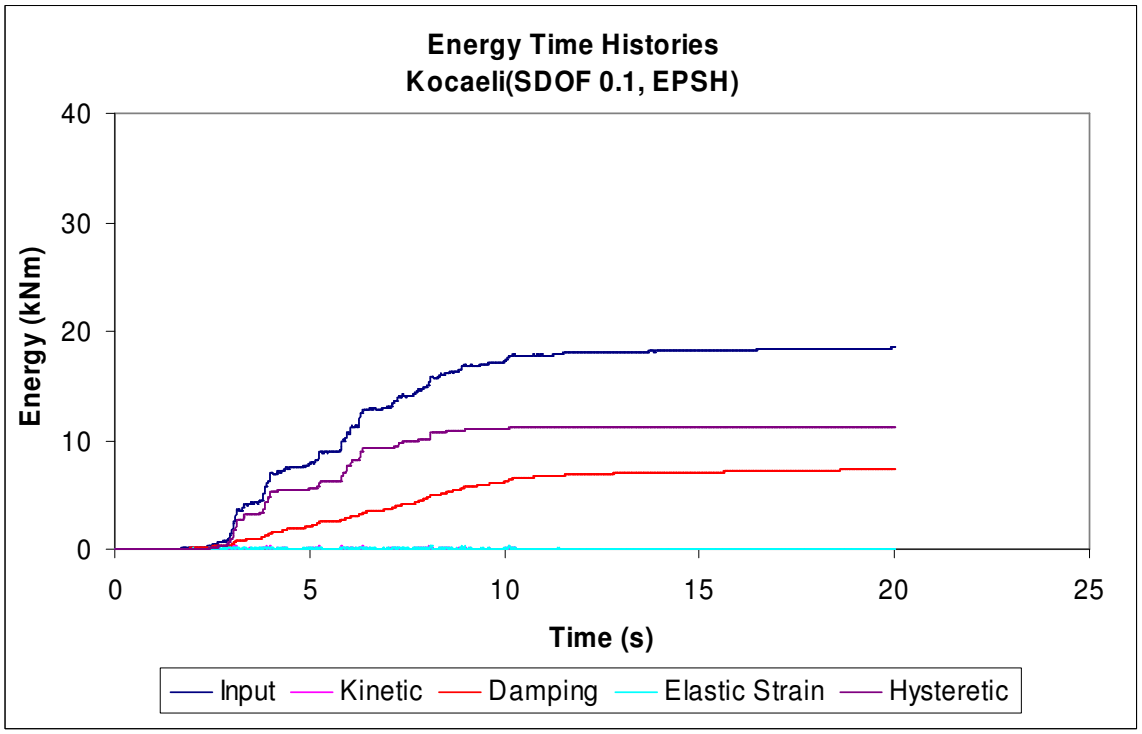

Figure B - 22 Energy Time-Histories SDOF 0.1, EPSH, Kocaeli ground motion

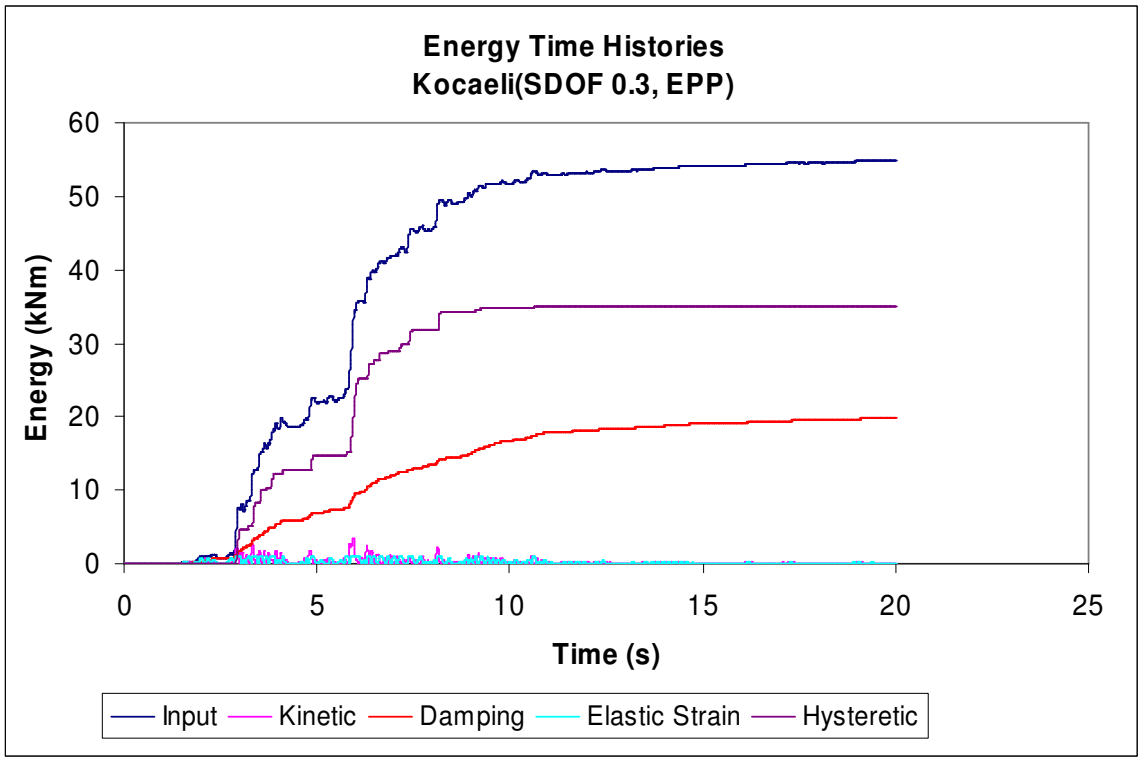

Figure B - 23 Energy Time-Histories SDOF 0.3, EPP, Kocaeli ground motion

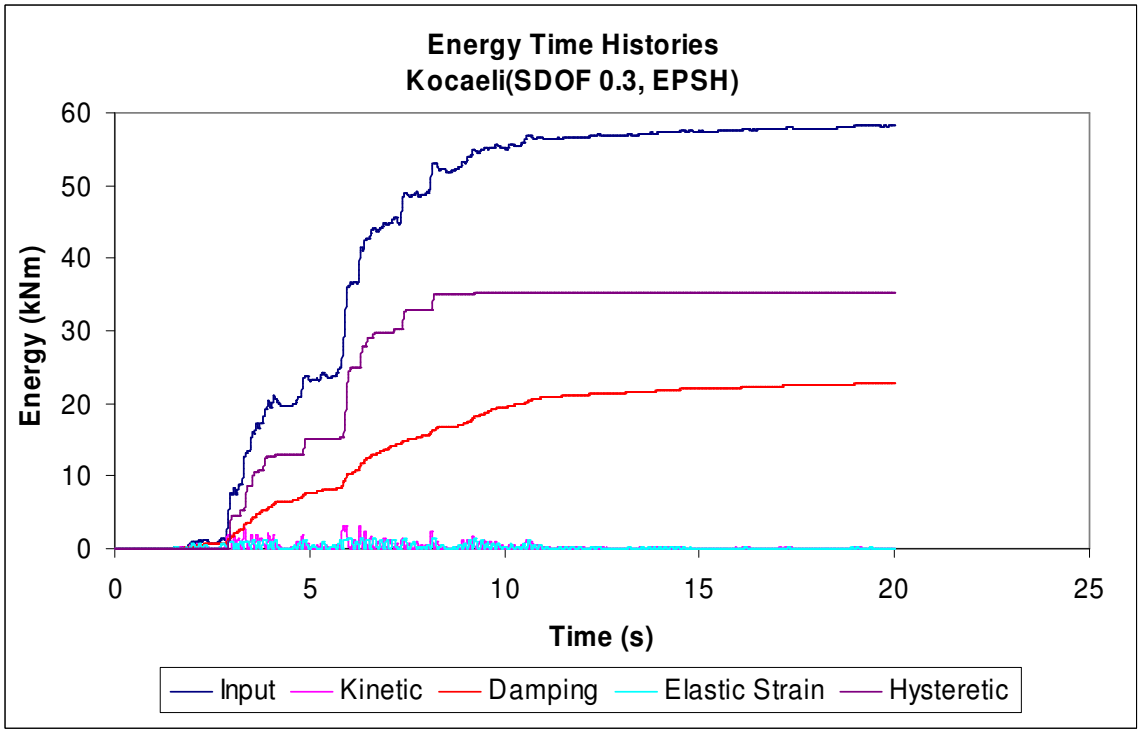

Figure B - 24 Energy Time-Histories SDOF 0.3, EPSH, Kocaeli ground motion

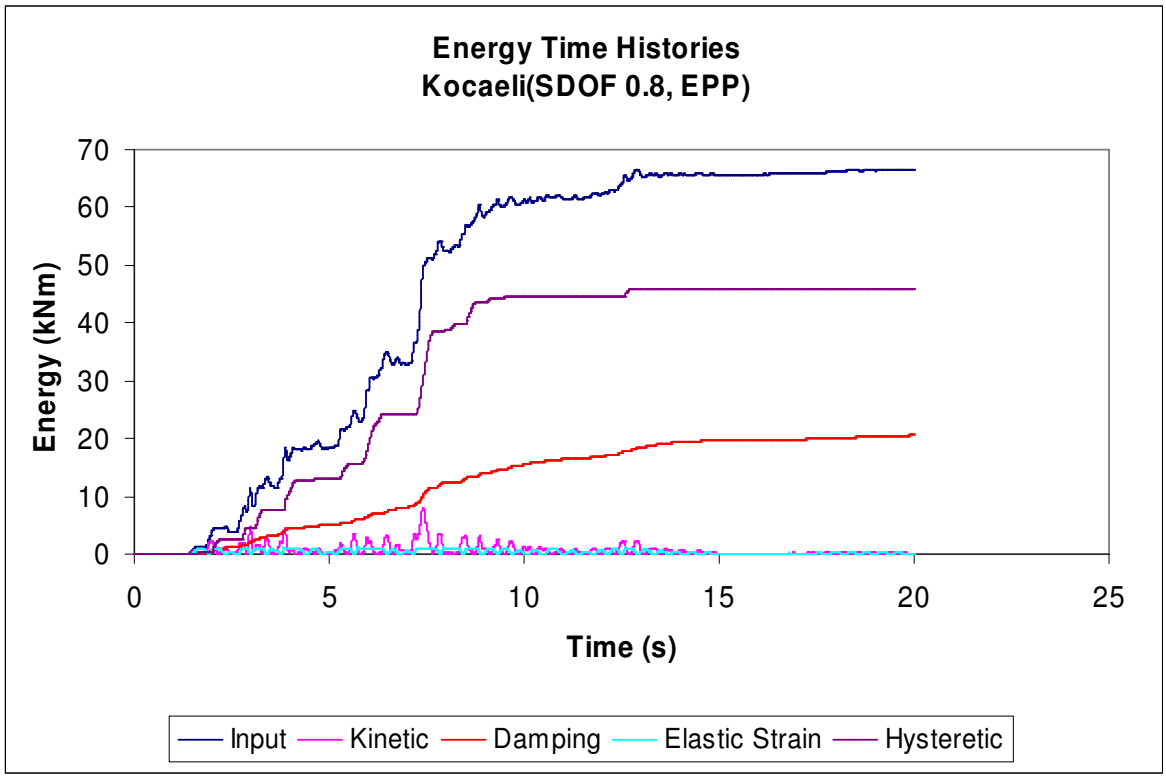

Figure B - 25 Energy Time-Histories SDOF 0.8, EPP, Kocaeli ground motion

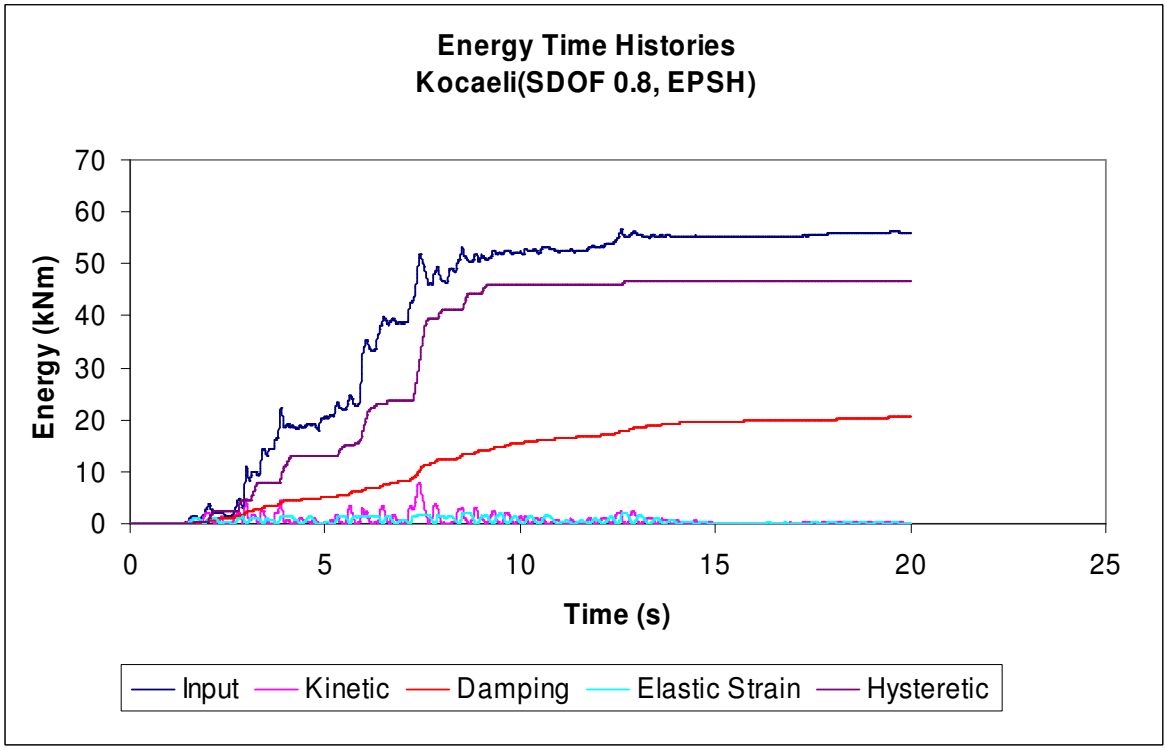

Figure B - 26 Energy Time-Histories SDOF 0.8, EPSH, Kocaeli ground motion

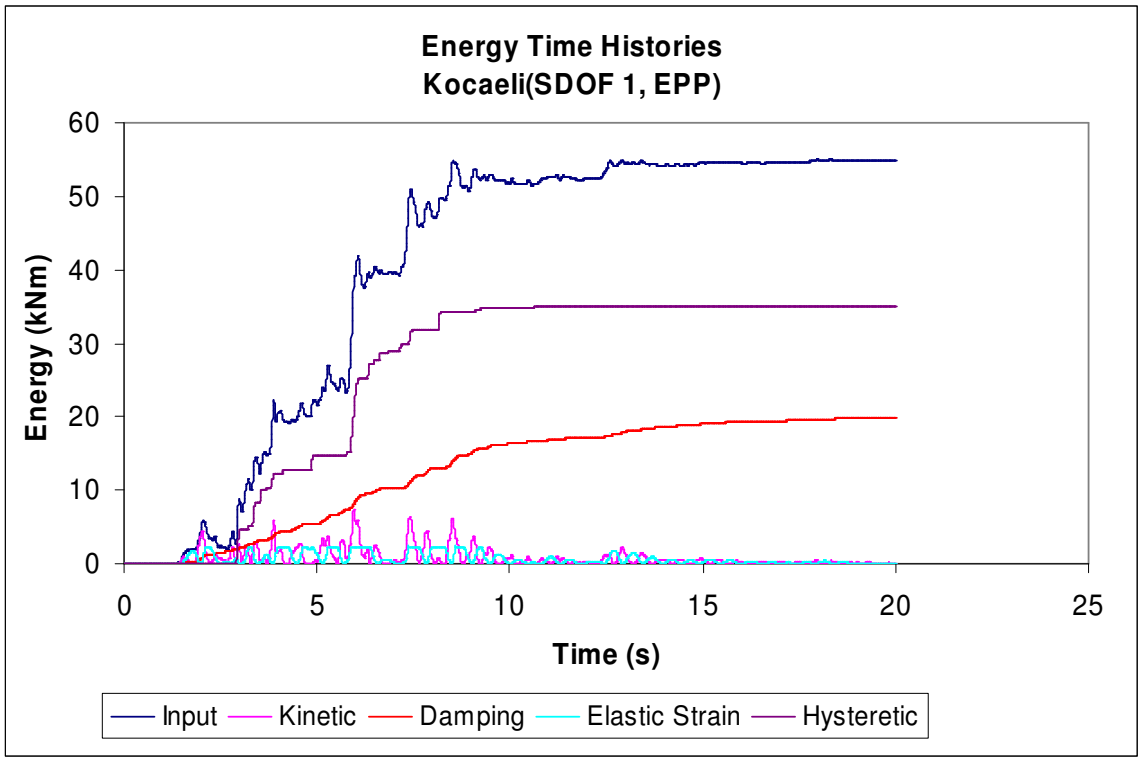

Figure B - 27 Energy Time-Histories SDOF 1, EPP, Kocaeli ground motion

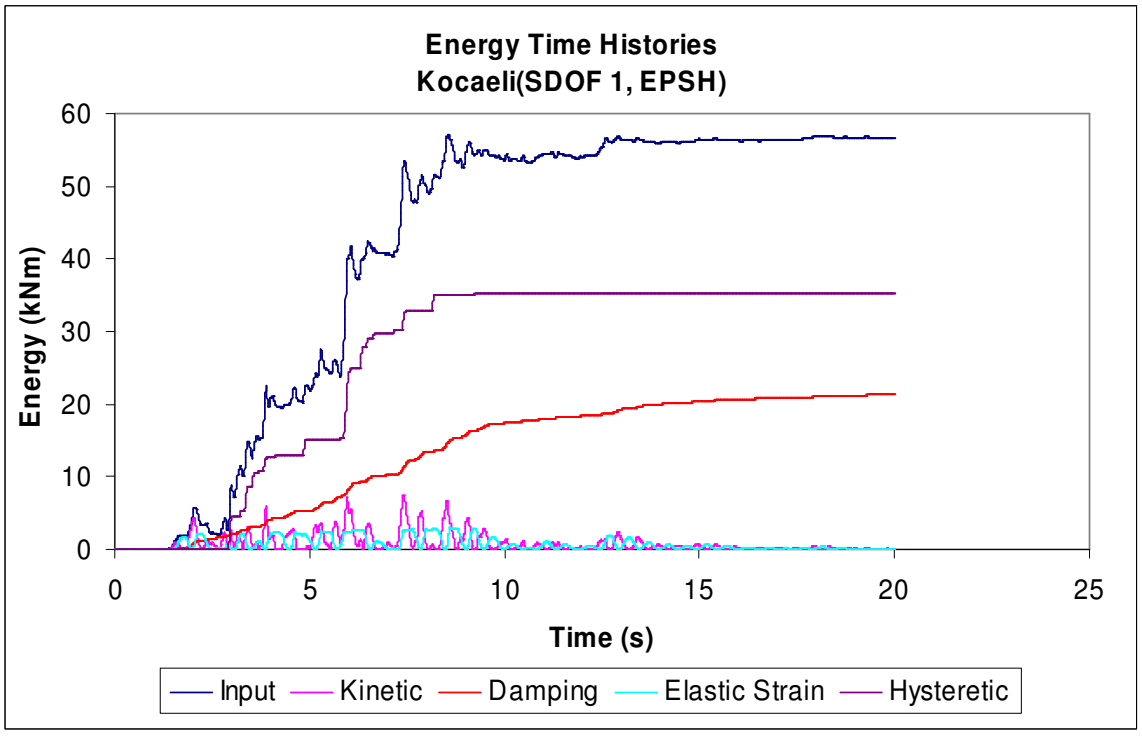

Figure B - 28 Energy Time-Histories SDOF 1, EPSH, Kocaeli ground motion

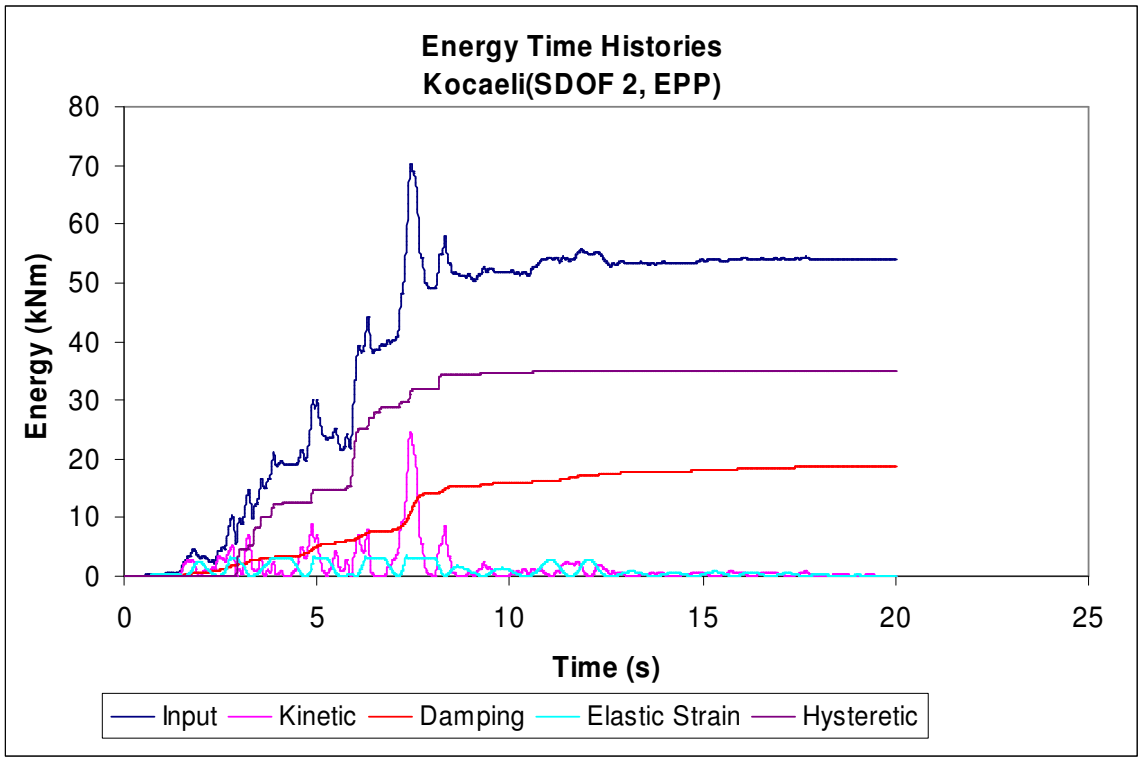

Figure B - 29 Energy Time-Histories SDOF 2, EPP, Kocaeli ground motion

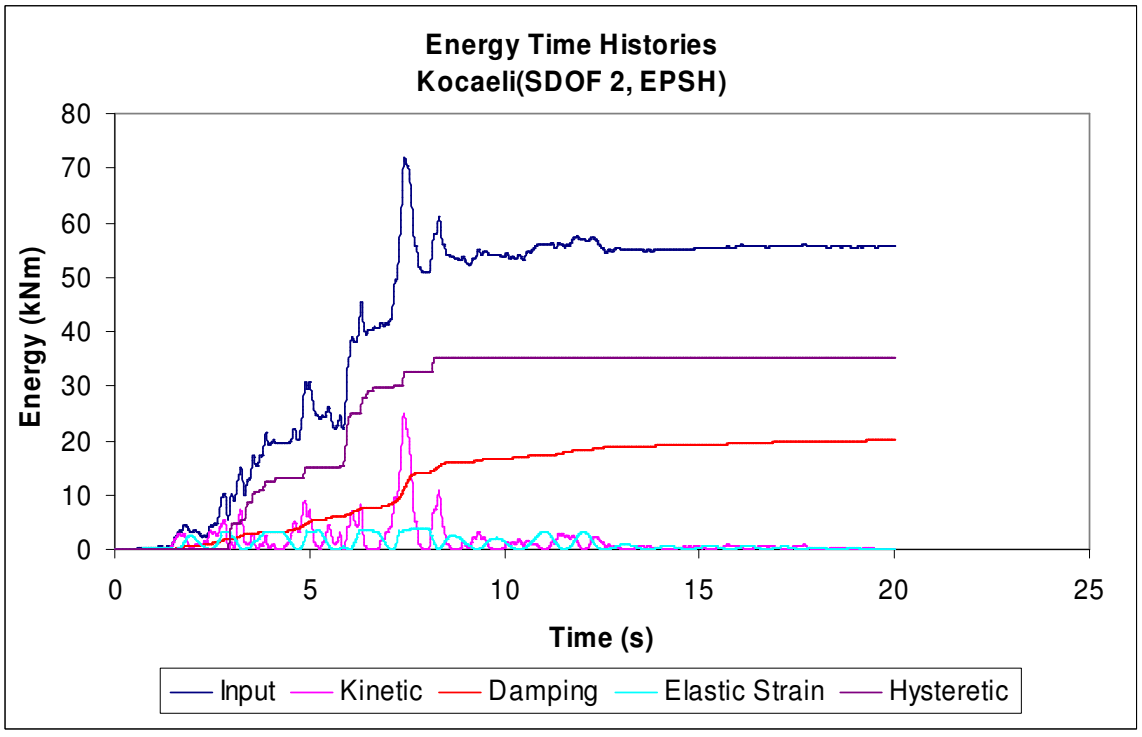

Figure B - 30 Energy Time-Histories SDOF 2, EPSH, Kocaeli ground motion

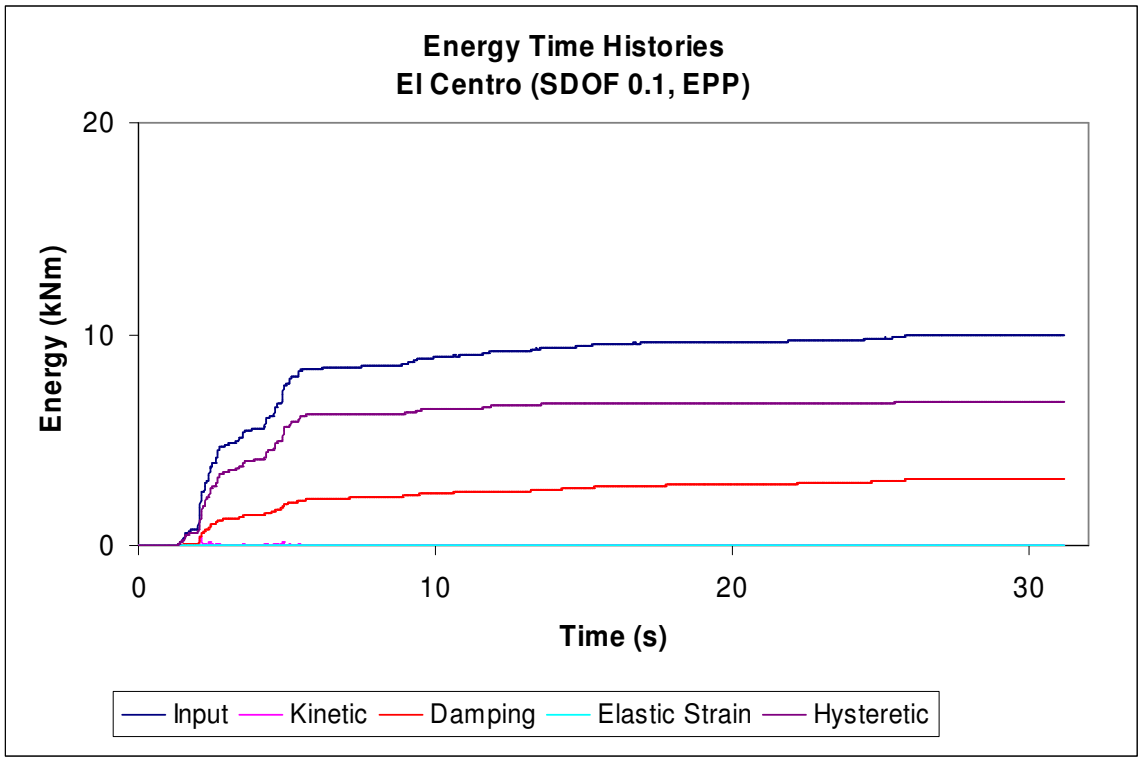

Figure B - 31 Energy Time-Histories SDOF 0.1, EPP, El Centro ground motion

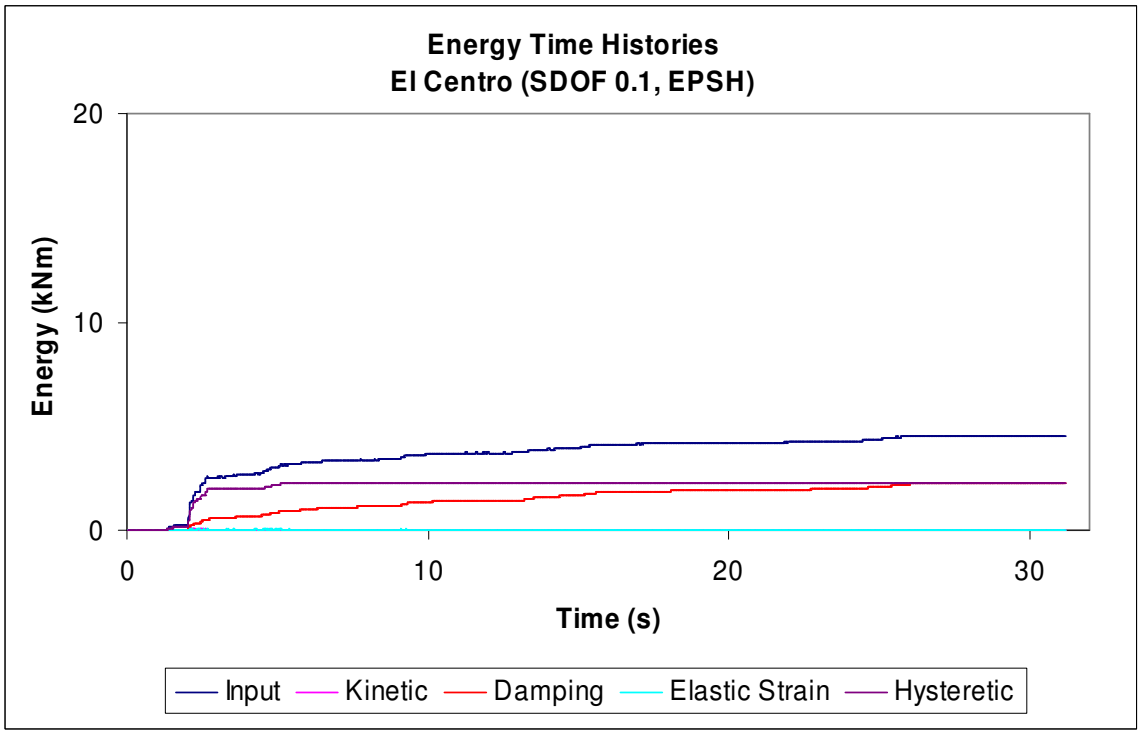

Figure B - 32 Energy Time-Histories SDOF 0.1, EPSH, El Centro ground motion

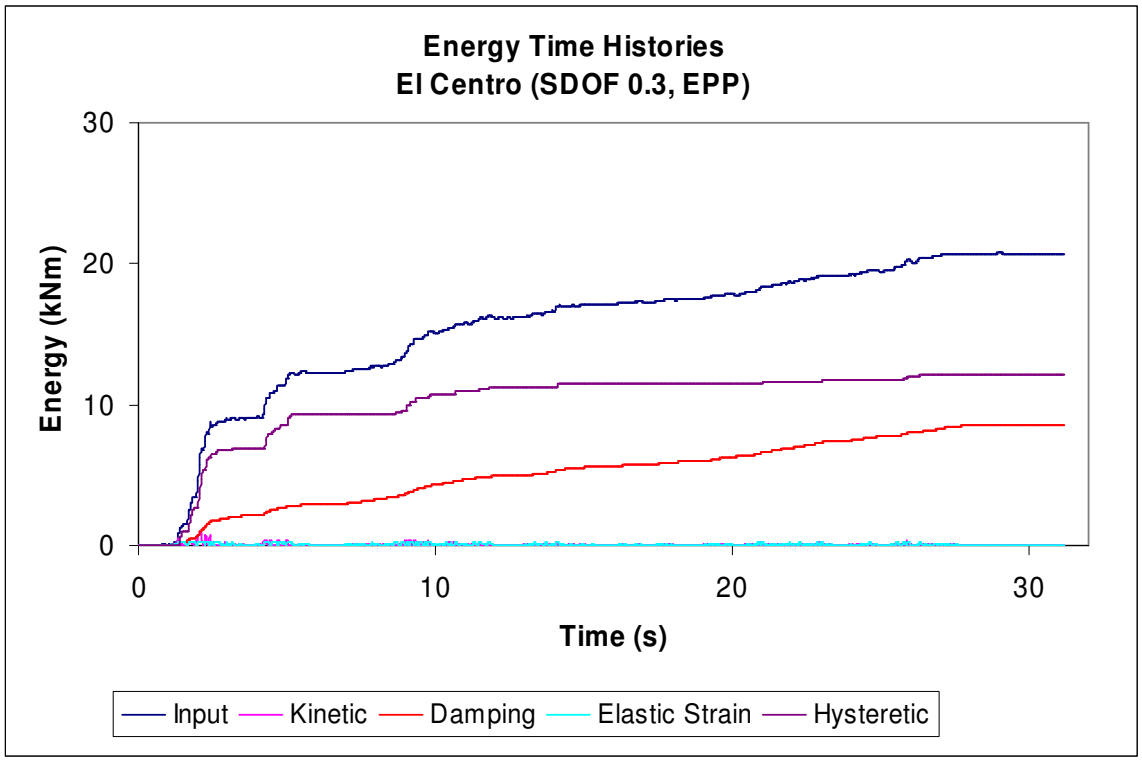

Figure B - 33 Energy Time-Histories SDOF 0.3, EPP, El Centro ground motion

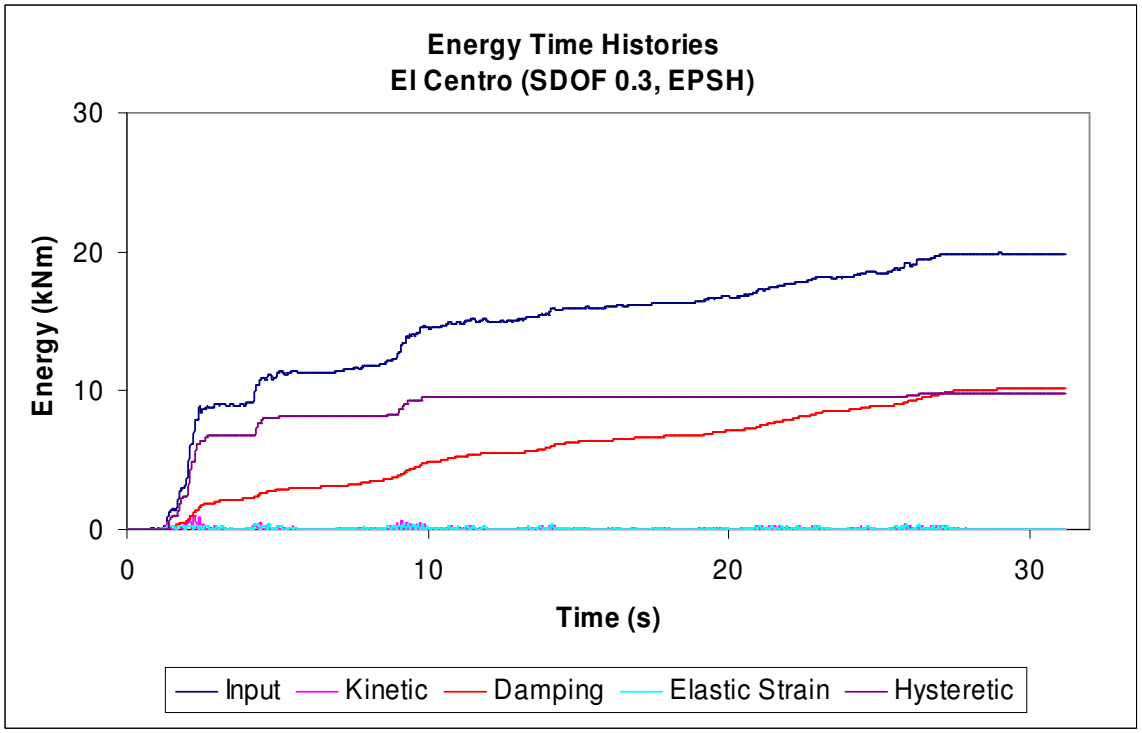

Figure B - 34 Energy Time-Histories SDOF 0.3, EPSH, El Centro ground motion

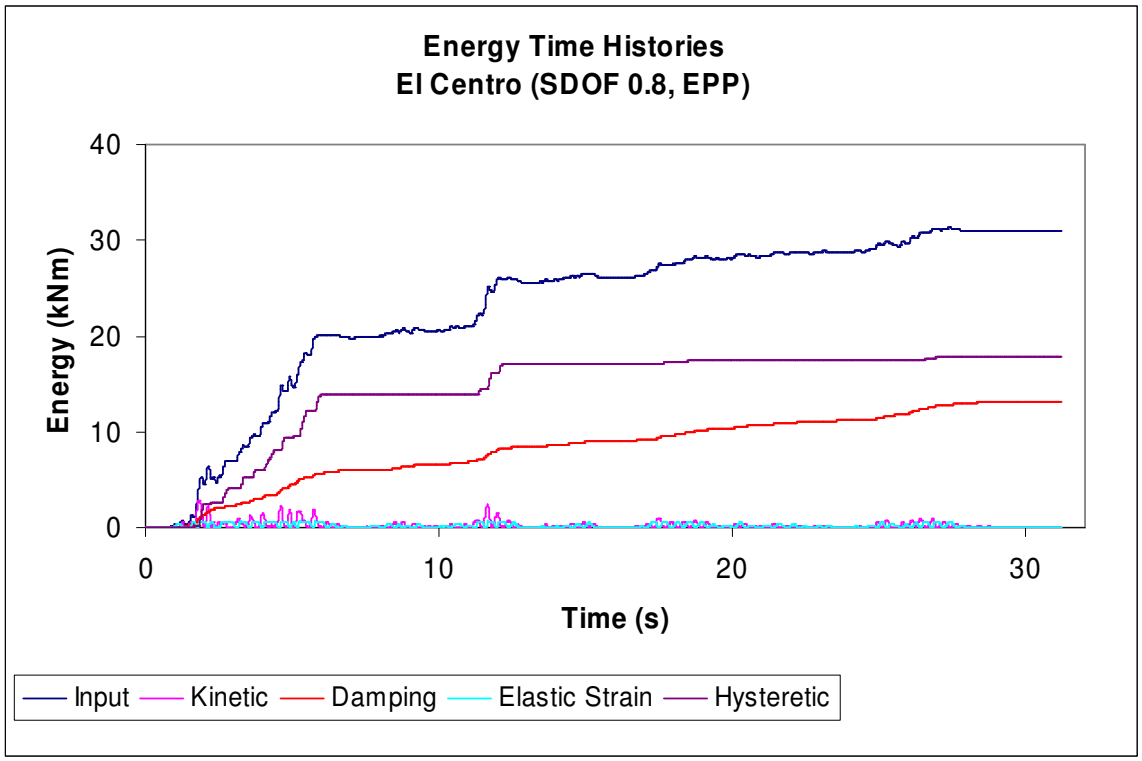

Figure B - 35 Energy Time-Histories SDOF 0.8, EPP, El Centro ground motion

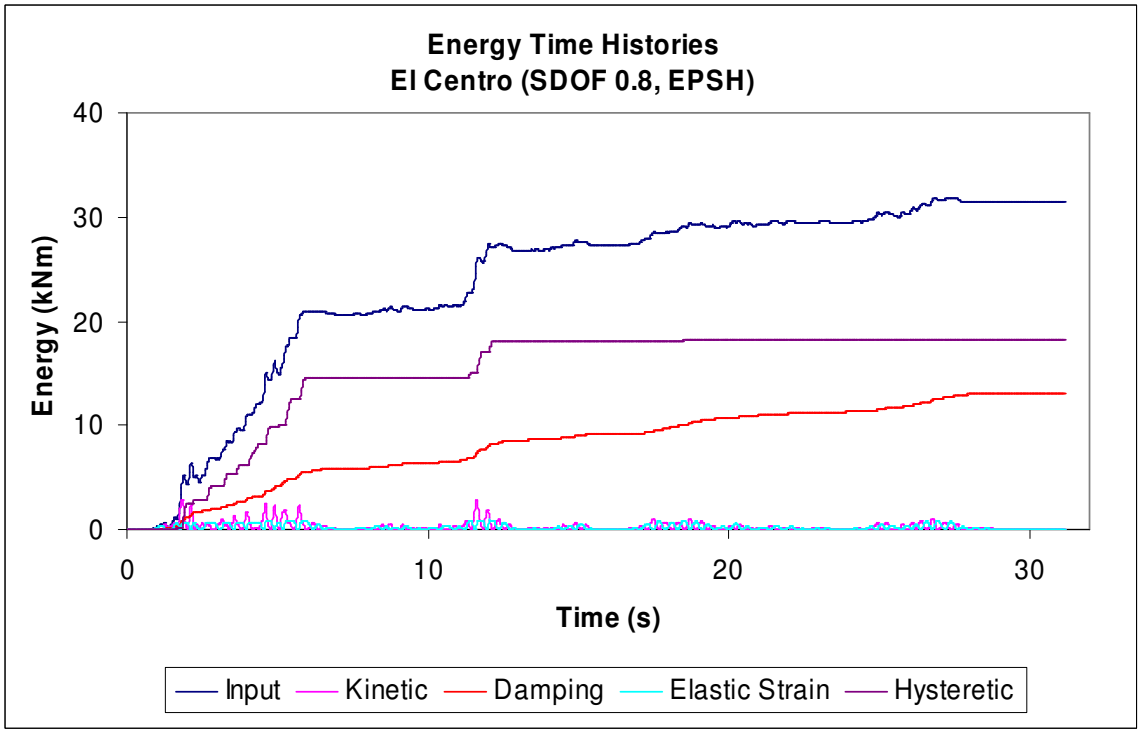

Figure B - 36 Energy Time-Histories SDOF 0.8, EPSH, El Centro ground motion

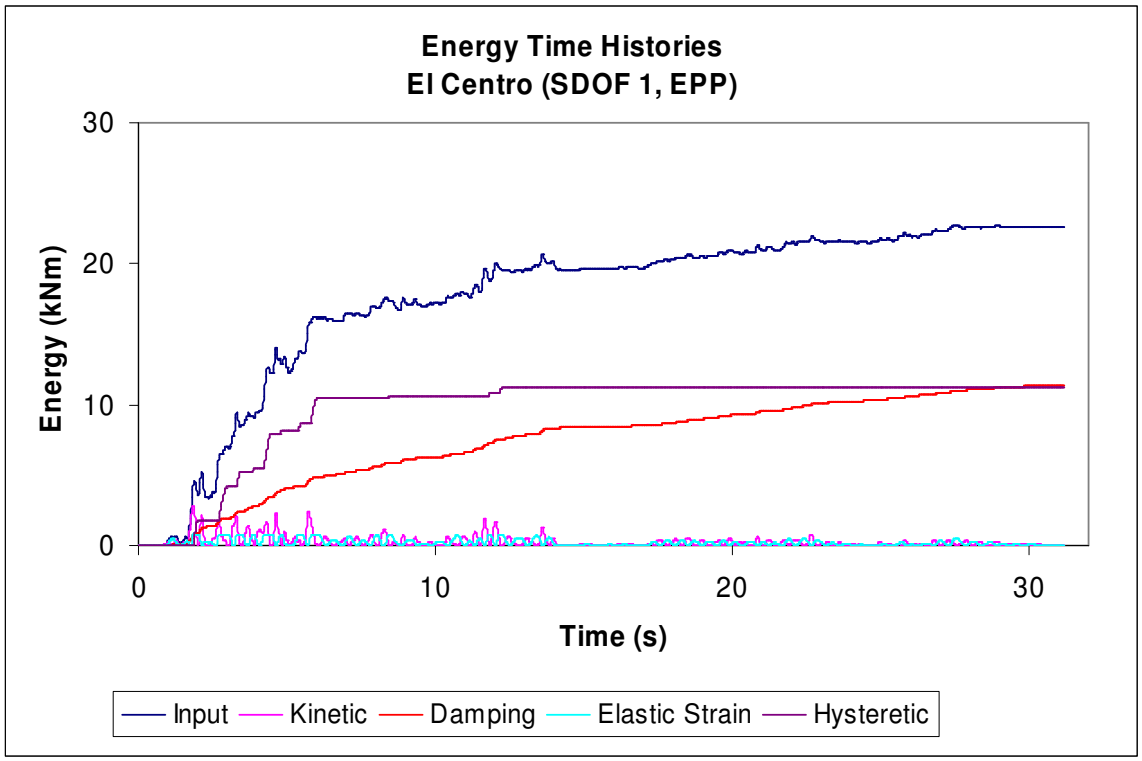

Figure B - 37 Energy Time-Histories SDOF 1, EPP, El Centro ground motion

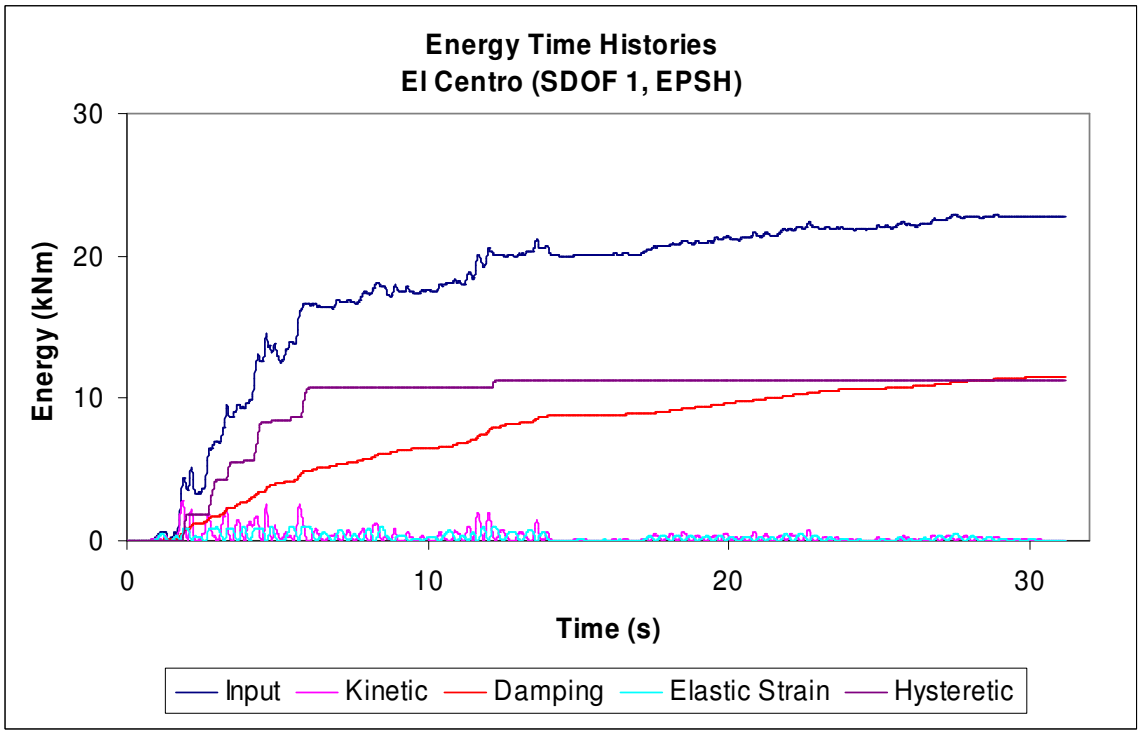

Figure B - 38 Energy Time-Histories SDOF 1, EPSH, El Centro ground motion

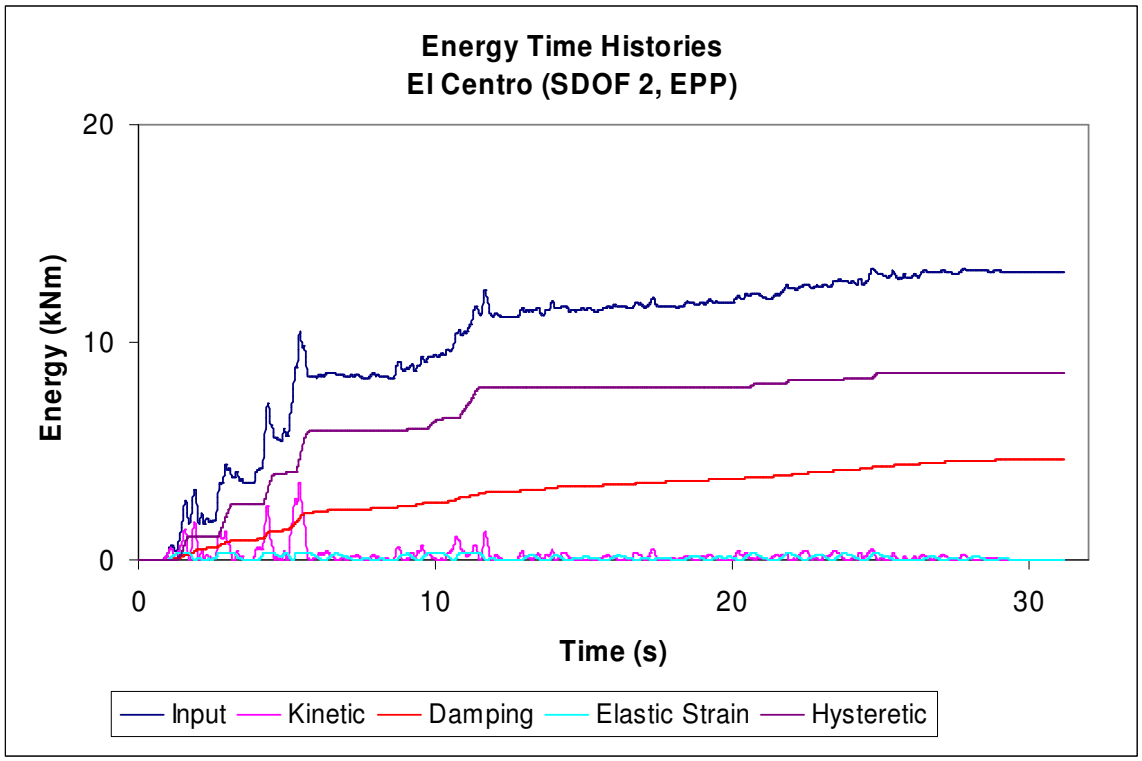

Figure B - 39 Energy Time-Histories SDOF 2, EPP, El Centro ground motion

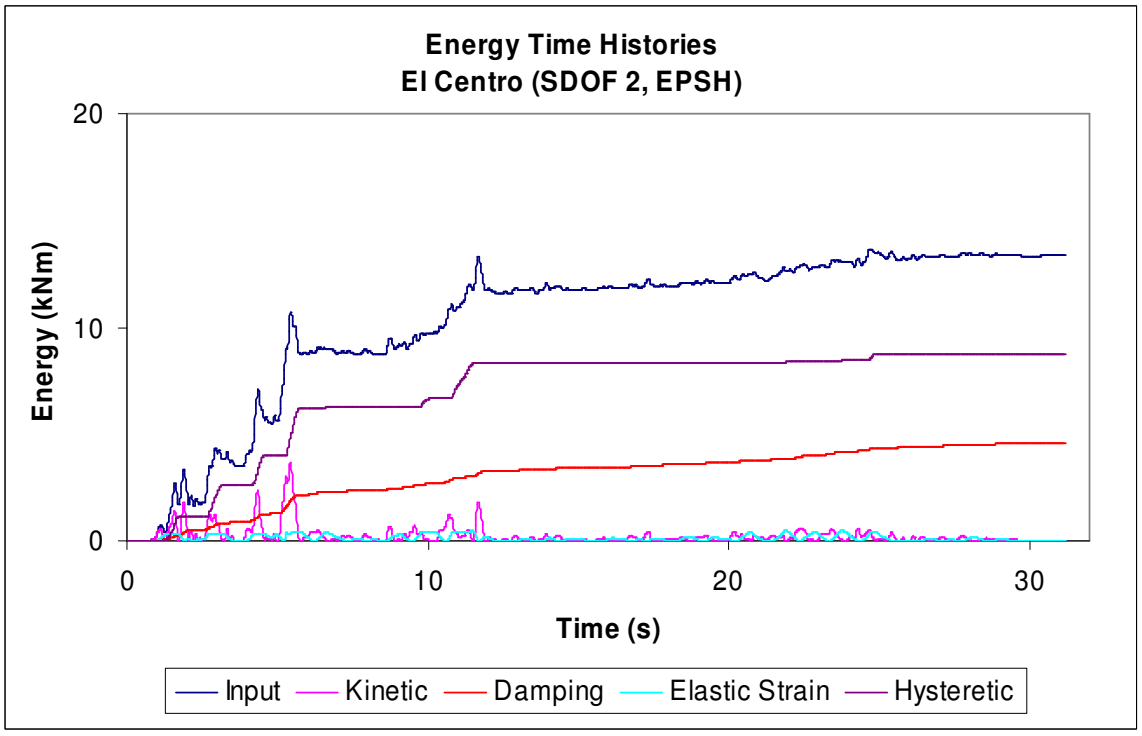

Figure B - 40 Energy Time-Histories SDOF 2, EPSH, El Centro ground motion

APPENDIX C

PUSHOVER ANALYSIS OF A SDOF SYSTEM TO KOCAELI GROUND MOTION

This appendix serves as an explanatory note on how the pushover analyses were conducted. The SDOF system presented in Chapter 4 and the Kocaeli ground motion – Chapter 3 - is going to be used. The N2 method will be utilised following the steps presented in Chapter 2 for both types of hysteretic models.

According to section 2.4.3 the nonlinear static analyses of the two hysteretic SDOF systems results in the load-deformation curves, Figure 4.10. These curves are then converted to the capacity spectrum curve, Figure C-1.

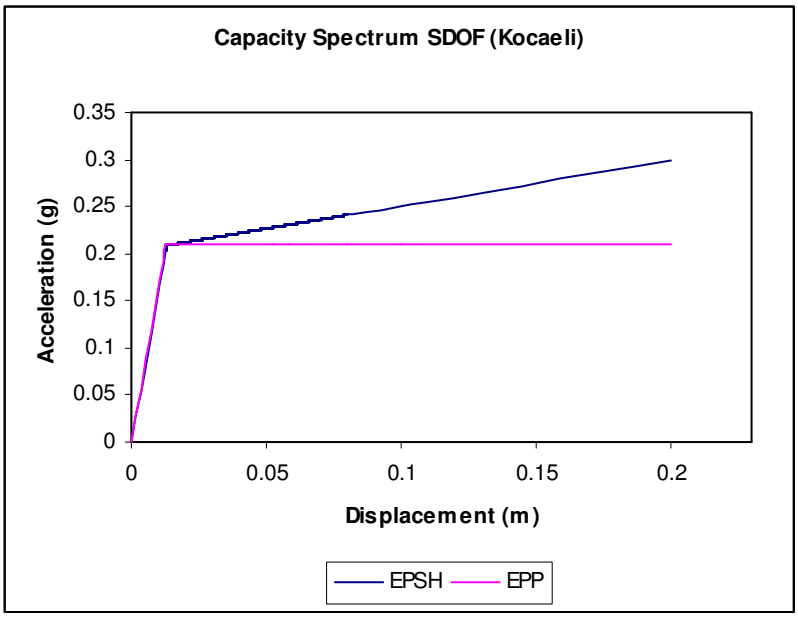

Figure C - 1 Capacity spectra for EPP and EPSH models

The results of both SDOF models are shown below in Table C.1.

	EPP	**EPSH**
Yield Displacement (m)	0.012974	0.012973
Yield Reaction Force (kN)	102.5	102.5
Yield Acceleration (g)	0.2090	0.2089

Table C.1 Nonlinear static analyses results for EPP and EPSH models.

The seismic demands for the equivalent SDOF system can now be determined as follows: The displacement can be estimated by employing eq. 2.33, and assuming that the equal displacement rule is valid. This is consistent because the characteristic period of the system being 0.5 seconds is larger than 0.40 seconds which is the characteristic period of soils with average shear velocity v_{s30} of at least 800 m/s as defined in EC8. This complies with the fact that Sakarya station can be considered that is based on rock soil - that is Type A soil –as denoted in EC8. Other possible choices could be used to define a characteristic period. These could either consider the maximum Fourier amplitude period, or the predominant period of the ground motion. In these cases also the equal displacement rule would be valid.

The ductility μ, can then be estimated through eq. 2.32. The elastic acceleration demand for the specific SDOF properties is obtained from the elastic pseudo-acceleration spectrum.

Thus for the EPP model:

$$S_d \approx 0.052 \text{ m}$$

$$R_\mu = \frac{0.8369}{0.2090} \approx 4 = \mu$$

For the EPSH model:

$$R_{\mu} = \frac{0.8369}{0.2089} \approx 4 = \mu$$

$$S_d \approx 0.052 \text{ m}$$

$$F_{max} = 111.74 \text{ kN}$$